FORSCHUNGSZENTRUM ROSSENDORF

WISSENSCHAFTLICH-TECHNISCHE BERICHTE
FZR-258
April 1999
ISSN 1437-322X

Preprint

Mini-Workshop „Electromagnetic Radiation off Colliding Hadron Systems: Dileptons and Bremsstrahlung“

Editors:
Eckart Grosse, Burkhard Kämpfer

Herausgeber:
FORSCHUNGSZENTRUM ROSSENDORF
Postfach 51 01 19
D-01314 Dresden
Telefon (03 51) 26 00
Telefax (03 51) 2 69 04 61

Als Manuskript gedruckt

FORSCHUNGSZENTRUM ROSSENDORF

WISSENSCHAFTLICH-TECHNISCHE BERICHTE

FZR-258

April 1999

Preprint

Mini-Workshop „Electromagnetic Radiation off Colliding Hadron Systems: Dileptons and Bremsstrahlung"

Editors:

Eckart Grosse, Burkhard Kämpfer

Mini-Workshop
"Electromagnetic Radiation off Colliding Hadron Systems: Dileptons and Bremsstrahlung"

Since several years various groups of the *Institute of Nuclear and Hadron Physics* at *Forschungszentrum Rossendorf (FZR)* are involved in medium energy physics projects where electromagnetic signals play a role:
(i) pp bremsstrahlung experiments at COSY-ToF have been proposed by a group from Dresden with FZR participation, and a large part of the ToF detector system has been built in Rossendorf.
(ii) The FZR is presently building one of the large wire chamber planes for the HADES detector at GSI and is also actively taking part in the HADES commissioning.
(iii) The theory group here at Rossendorf is working in the field of dilepton production and other electromagnetic processes.

To discuss the research in these fields with colleagues from other places and to coordinate the efforts this mini-workshop was organized. The idea was to discuss the results of the experiments at different accelerators, the status of the calculations and the plans for future investigations. Besides bremsstrahlung special emphasis will be on dielectron production; other processes with electromagnetic signals (like vector-meson production) have also been discussed.

E. Grosse B. Kämpfer

Electromagnetic Radiation off Colliding Hadron Systems: Dileptons & Bremsstrahlung

---

Miniworkshop at the
Forschungszentrum Rossendorf near Dresden,
Institute of Nuclear and Hadron Physics
April 16 - 17, 1999
Lecture Hall (Kleiner Hörsaal im Haus 120)

Programme

Thursday, April 15: Arrival

Friday, April 16 :

		chairman: E. Grosse
9.00 a. m.	E. Grosse (Rossendorf):	Opening
	U. Mosel (Giessen):	Hadrons in medium - overlook and perspective
	J. Bacelar (Groningen):	Virtual bremsstrahlung experiments in few-body systems at KVI
Break		
		chairman: H. Freiesleben
11.15 a.m.	J. Ritman (Giessen):	Rho, omega, phi production in pp reactions near threshold
	V. Hejny (Jülich):	Photoproduction of light mesons - results from TAPS at MAMI
Lunch (Canteen)		
		chairman: B. Kämpfer
1.45 p.m.	O. Scholten (Groningen):	pp bremsstrahlung: theory & polarization effects
	C. Fuchs (Tübingen):	Background contributions to dilepton spectra in pp collisions
	N. Kalantar (Groningen):	Bremsstrahlung experiments at KVI
Break		

		chairman: K. Möller
4.15 p.m.	S. Scherer (Mainz):	NN bremsstrahlung and Compton scattering - examples of the impossibility of measuring off-shell effects
	J. Zlomanzcuk (Uppsala/Warszawa):	Bremsstrahlung experiments at CELSIUS
	E. Kuhlmann (Dresden/Jülich):	Bremsstrahlung experiments at COSY/ToF
Buffet - Dinner		

Saturday, April 17:

		chairman: J. Friese
9.00 a.m.	J. Wambach (Darmstadt):	Dileptons and chiral symmetry restoration
	G. Wolf (Budapest)	Describing the in-medium rho & omega
Break		
		chairman: J. Stroth
10.45 a.m.	M. Krivoruchenko (Tübingen):	Deacay rates for dilepton production in HICs
	F. Dohrmann (Rossendorf):	The HADES project
	P. Tlusty (Rez):	Status of the HADES - TOF
Lunch (Haus 120)		
		chairman: P. Senger
1.00 p.m.	R. Holzmann (GSI):	First experiments with HADES: e^+e^- production in pp and AA collisions
	R. Schicker (GSI):	Dalitz decay measurements with HADES
	W. Koenig (GSI):	Omega meson spectroscopy at HADES in pi-A reactions

Departure

Participants

Who	From	Where	When
Bakelar, J.	Groningen	Pension ARCADE	15.4. - 17.4.
Bielcik, J.	Darmstadt	Pension ARCADE	15.4. - 17.4.
Brinkmann, K.	Dresden	privat	15.4. - 17.4.
Eberl, T.	München	Pension Zu den Linden	15.4. - 18.4.
Fabietti, L.	München	Pension Zu den Linden	15.4. - 18.4.
Freiesleben, H.	Dresden	privat	
Friese, J.	München	Pension Zu den Linden	15.4. - 18.4.
Fuchs, C.	Tübingen	Pension Zu den Linden	15.4. - 17.4.
Hejny, V.	Jülich	Pension ARCADE	15.4. - 17.4.
Holzmann, R.	Darmstadt	Pension ARCADE	15.4. - 17.4.
Kagarlis, M.	Darmstadt	Pension Zu den Linden	15.4. - 17.4.
Kalantar, N.	Groningen	Pension ARCADE	15.4. - 17.4.
Karsch, L.	Dresden	privat	15.4. - 17.4.
Kivoruchenko, M.	Tübingen	Pension Zu den Linden	15.4. - 17.4.
Koenig, W.	Darmstadt	Pension ARCADE	15.4. - 18.4.
Kugler, A.	Rez	Pension Rüger	15.4. - 17.4.
Kuhlmann, E.	Dresden/Jülich	Pension ARCADE	15.4. - 17.4
Mosel, U.	Giessen	Pension ARCADE	15.4. - 18.4
Münz, C.	Frankfurt	Pension Zu den Linden	15.4. - 17.4
Richter, M.	Dresden	privat	15.4. - 17.4
Ritman, J.	Giessen	Pension Zu den Linden	15.4. - 17.4
Schadmand, S.	Giessen	Pension Rüger	15.4. - 17.4
Scherer, S.	Mainz	Pension Zu den Linden	15.4. - 17.4
Schicker, R.	Darmstadt	Pension Zu den Linden	15.4. - 17.4
Schönmeier, P.	Dresden	privat	15.4. - 17.4
Scholten, O.	Groningen	Pension ARCADE	15.4. - 17.4

Schulte-Wissermann M.	Dresden	privat	15.4. - 17.4.
Senger, P.	Darmstadt	Unterkunft bei Dr. Naumann	15.4. - 17.4.
Stroht, J.	Darmstadt	Pension Becker	15.4. - 18.4.
Tlusty, P.	Rez	Pension Rüger	15.4. - 17.4.
Wambach, J.	Darmstadt	Pension Zu den Linden	16.4. - 18.4.
Wolf, G.	Budapest	Unterkunft bei Dr. Wagner	15.4. - 17.4.
Wüstenfeld, J.	Darmstadt	Pension ARCADE	15.4. - 18.4.
Zlomanzcuk, J.	Uppsala/Warzaw	Pension ARCADE	15.4. - 18.4.
Zumbruch, P.	Darmstadt	Pension Zu den Linden	15.4. - 18.4.

---

from Rossendorf:

H.W. Barz
M. Debowski
S. Dshemuchadse
K. Gallmeister
E. Grosse
B. Kämpfer
R. Kotte
K. Möller
H. Müller
L. Naumann
O. Pavlenko
C. Schneider
D. Wohlfarth

Transparencies of the Miniworkshop

Electromagnetic Radiation off Colliding Hadron Systems: Dileptons and Photons

U. Mosel:
Hadrons in medium – overlook and perspective

J. Bacelar:
Virtual bremsstrahlung experiments in few-body systems at KVI

J. Ritman:
Meson production experiments in pp reactions with the DISTO spectrometer

V. Hejny:
Photoproduction of light mesons – results from TAPS at MAMI

O. Scholten:
Proton–proton bremsstrahlung

C. Fuchs:
Background contributions to dilepton spectra in pp collisions

N. Kalantar:
Bremsstrahlung experiments at KVI

S. Scherer:
NN bremsstrahlung and Compton scattering
– examples of the impossibility of measuring off-shell effects

J. Zlomanczuk:
Bremsstrahlung in pp collisions at 310 MeV

E. Kuhlmann:
Bremsstrahlung experiments at COSY-TOF

J. Wambach:
Dileptons and chiral symmetry restoration

Gy. Wolf:
Vector mesons in nuclear matter

M. Krivoruchenko:
Decay rates for dilepton production in HICs

F. Dohrmann:
The HADES project

P. Tlusty:
Status of the HADES–ToF

R. Holzmann:
Fist experiments with HADES: e^+e^- production in pp and AA collisions

R. Schicker:
Dalitz decay measurements with HADES

W. Koenig:
Ω meson spectroscopy at HADES in πA reactions

U. Mosel:

Hadrons in medium – overlook and perspective

Justus-Liebig-Universität Giessen
Institut für Theoretische Physik

Hadrons in Medium
Introduction and Overview*

Based on work with:
E. Bratkovskaya, W. Cassing,
M. Effenberger, H. Lenske,
S. Leupold

*Supported by BMBF, DFG and GSI Darmstadt

- Motivation/Introduction
- QCD Sum Rules vs Hadronic Models
- Observables: Dileptonproduction
  - Heavy-Ion Reactions
  - Pion-Induced Reactions
  - Photoabsorption and Photodileptons
  - Effects at High Energies and Momenta
- Summary/Conclusions

Electromagnetic Formfactors

Transition rate for em process

$$\sim \left| \int d^3x \, dt \, e^{-i(\vec{p}_\gamma \vec{x} + E_\gamma t)} \, j_{em}(\vec{x}, t) \right|^2$$

- Space-like

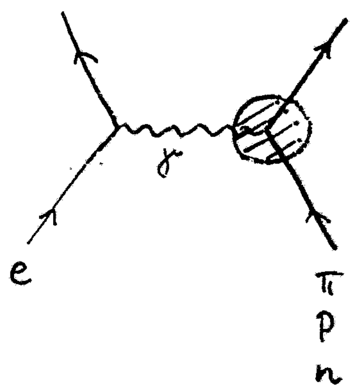

$E_\gamma^2 - \vec{p}_\gamma^2 < 0$

[illegible]

E_{γ^*} [illegible]

Spatial distribution of hadrons: $F(\vec{x})$ [illegible]

- time-like

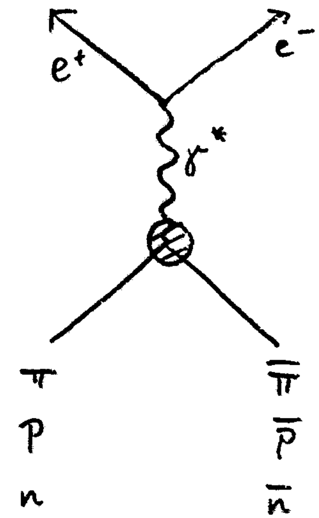

$E_\gamma^2 - \vec{p}_\gamma^2 > 0$ [illegible]

[illegible]

$M_{\gamma^*} \gtrsim 2$ GeV for $p\bar{p}$

$M_{\gamma^*} \gtrsim 0.28$ GeV for $\pi^+\pi^+$

"physical regio

$$F_\pi(q^2) = 1 + \left(\frac{g_{\rho\pi}}{g_{\rho\gamma}}\right)^{1} \frac{q^2}{m_\rho^2 - i m_\rho \Gamma_\rho(q^2) - q^2} + \left(\frac{g_{\omega\pi}}{g_{\omega\gamma}}\right)^{0.017} \frac{q^2 e^{i\varphi_{\omega\rho}}}{m_\omega^2 - i m_\omega \Gamma_\omega(q^2) - q^2}$$

ρ-ω Mixing.

constant for a measured decay widths.

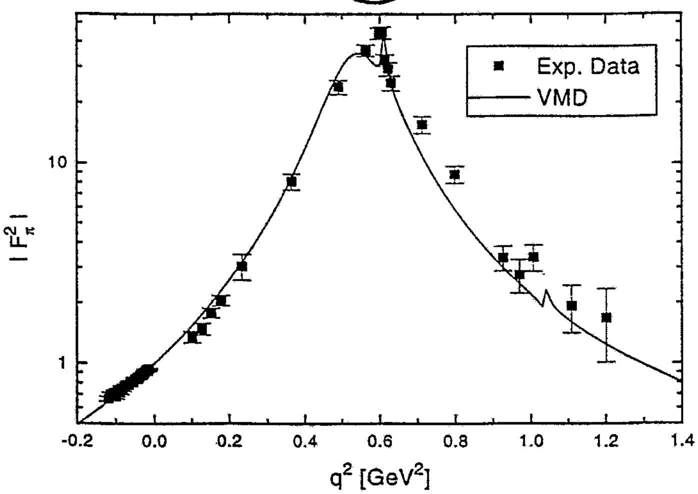

Dönges, Schäfer, Mosel PRC (1995)

"Monopole Fit"
(with q^2-dependent strengths)

VMD1

$$\mathcal{L}_{\rho A} = -\frac{e}{2 g_{\rho\gamma}} F^A_{\mu\nu} G^{\mu\nu}_\rho - e J^H_\mu A^\mu + \dots$$

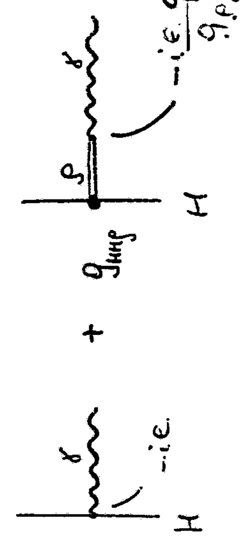

VMD2

$$\mathcal{L}_{\rho A} = -\frac{e m_\rho^2}{g_{\rho\gamma}} \rho_\mu A^\mu$$

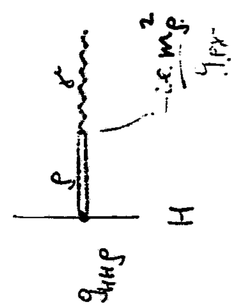

Needs: $g_{HH\rho} \overset{!}{=} g_{\rho\gamma}$!

Photonpropagator

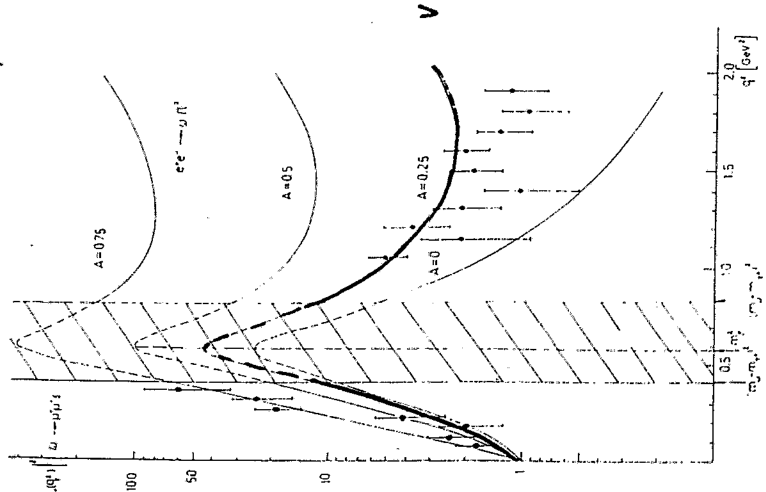

Fig. 28. Study of the transition form factor at the $\omega\pi^0$ vertex in $\omega \to \pi^0\mu^+\mu^-$ decay [?] and in the reaction $e^+e^- \to \omega\pi^0$ [70]. The curves are the prediction of the generalized vector dominance model taking into account the contribution from the $\rho(770)$ and $\rho(1600)$ mesons (see [illegible]), A = [illegible] … $(m_\omega - m_\pi)^2 \le q^2 \le (m_\omega + m_\pi)^2$ kinematically forbidden region

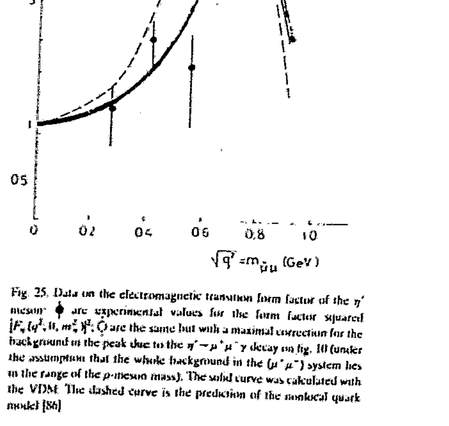

Fig. 25. Data on the electromagnetic transition form factor of the η' meson: ϕ are experimental values for the form factor squared $|F_{\eta'}(q^2, 0, m_{\eta'}^2)|^2$; ○ are the same but with a maximal correction for the background in the peak due to the $\eta' \to \mu^+\mu^-\gamma$ decay on fig. 10 (under the assumption that the whole background in the $(\mu^+\mu^-)$ system lies in the range of the ρ-meson mass). The solid curve was calculated with the VDM. The dashed curve is the prediction of the nonlocal quark model [86]

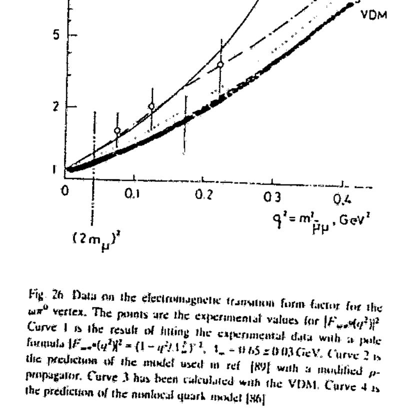

Fig. 26. Data on the electromagnetic transition form factor for the $\omega\pi^0$ vertex. The points are the experimental values for $|F_{\omega\pi^0}(q^2)|^2$. Curve 1 is the result of fitting the experimental data with a pole formula $|F_{\omega\pi^0}(q^2)|^2 = (1 - q^2/\Lambda_\omega^2)^{-2}$, $\Lambda_\omega = 0.65 \pm 0.03$ GeV. Curve 2 is the prediction of the model used in ref. [89] with a modified ρ-propagator. Curve 3 has been calculated with the VDM. Curve 4 is the prediction of the nonlocal quark model [86]

Nuovo Cimento A100 (1988) 1

$$
(39)\quad
\begin{cases}
f^{(1)}_{\omega N\bar N}/f_\omega = 0.91 \pm 0.04\,, & f^{(1)}_{\rho N\bar N}/f_\rho = 0.22 \pm 0.03\,,\\
f^{(1)}_{\phi N\bar N}/f_\phi = -0.59 \pm 0.06\,, & f^{(1)}_{\rho' N\bar N}/f_{\rho'} = -1.84 \pm 0.18\,,\\
f^{(2)}_{\omega N\bar N}/f_\omega = -1.08 \pm 0.02\,, & f^{(2)}_{\rho N\bar N}/f_\rho = 1.90 \pm 0.03\,,\\
f^{(2)}_{\phi N\bar N}/f_\phi = 2.09 \pm 0.04\,, & f^{(2)}_{\rho' N\bar N}/f_{\rho'} = 0.63 \pm 0.22\,,
\end{cases}
$$

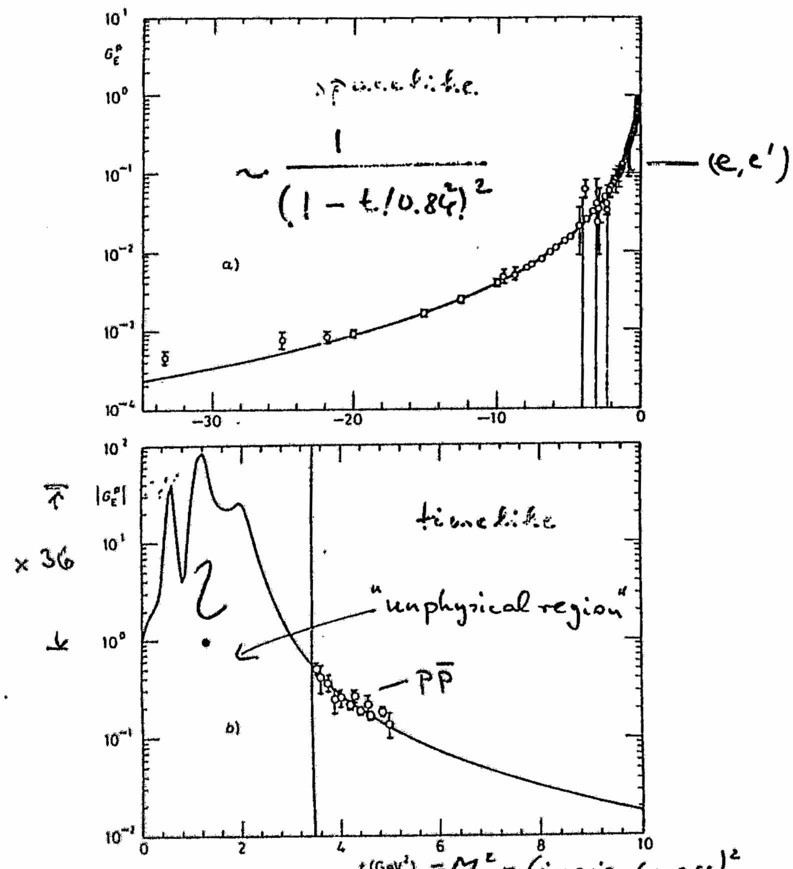

Fig. 1. – *a*) Comparison of electric proton form factor with the data in the spacelike region. *b*) The behaviour of electric proton form factor in the timelike region and its comparison with the data obtained from $e^+e^- \to p\bar p$ and $p\bar p \to e^+e^-$.

How well does VDM work?

- Pions good within ~ 20%.
  Form factor measured, peak at ..., other mesons (ω e.g.) don't work.
- Nucleon couplings within factors of 2

Form factor cannot be measured in pole region → "unphysical region"

Ways out

- Dispersion theoretical analysis [illegible]
- [illegible]

Clean Experiment

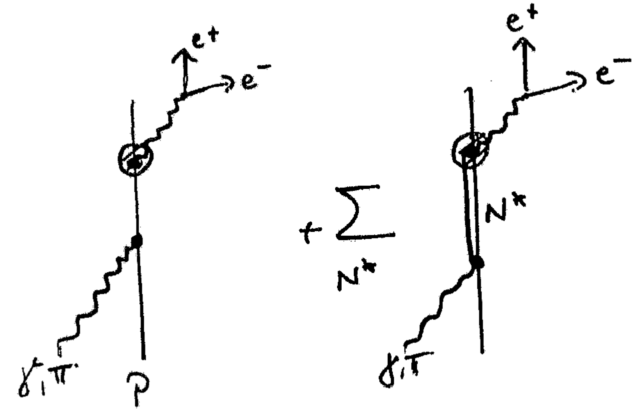

+ crossed diagrams + t-channel

+ Bethe Heitler contribution

"Compton Scattering with Time-like Photon"

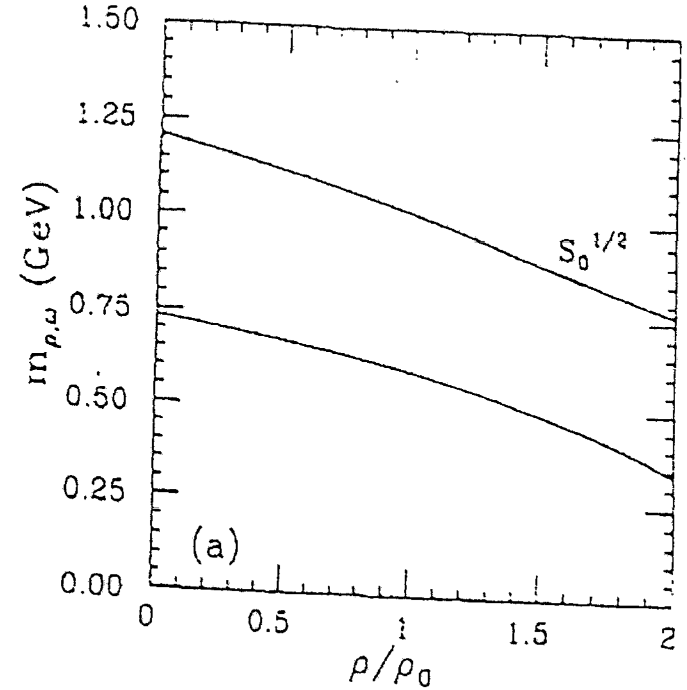

QCD SUM RULE Result

Hatsuda & Lee 1992

$$\sigma(e^+e^- \to \text{hadrons}) = -\frac{4\pi\alpha}{s}\, \text{Im}\, \Pi(q^2)$$

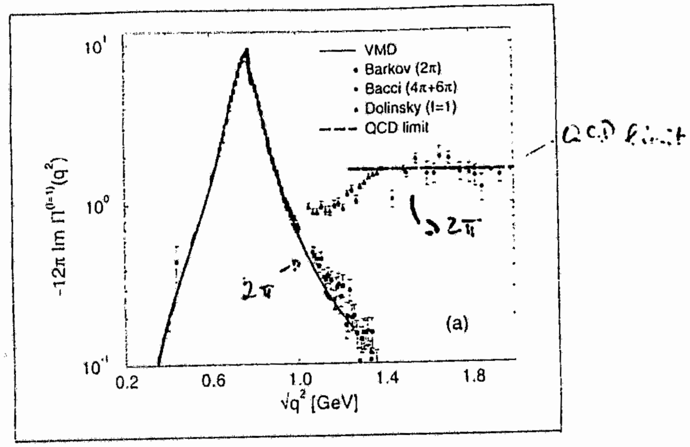

from: Klingl, Weise 1997

Current-Current Correlator

$$\Pi^{\mu\nu}(q) = \int d^4x\, e^{iqx} \langle 0 | T[j^\mu(x) j^\nu(0)] | 0 \rangle$$

$$= (q^2 g^{\mu\nu} - q^\mu q^\nu)\, \Pi(q^2)$$

Simple VMD:

$$j^\mu = \frac{m_V^{o\,2}}{g_V} V^\mu$$

$$\Pi(q^2) = \frac{m_V^{o\,4}}{g_V^2} D_V(q^2)$$

Vector Meson Propagator

$$D_V(q^2) = \frac{1}{q^2 - m_V^{o\,2} - \Pi_V(q^2)}$$

$$\text{Im}\, \Pi(q^2) = \frac{m_V^{o\,4}}{g_V^2} |D_V|^2\, \text{Im}\, \Pi_V(q^2)$$

$$\equiv \frac{\text{Im}\, \Pi_V(q^2)}{g_V^2} F_V(q^2)$$

VM Selfenergy $\leftrightarrow$ $\text{Im}\, \Pi$

Spectral Function of Vector Mesons

$$A(q^2) = -\frac{1}{\pi}\Im D_V(q^2) = -\frac{1}{\pi}\frac{g_V^2}{m_V^{0\,4}}\Im\Pi(q^2) \quad (1)$$

$$\int_0^\infty dq_0^2\, A(q_0, \vec{q}) = 1 \qquad \text{Prob. Distr.} \quad (2)$$

2 Strategies to determine A:

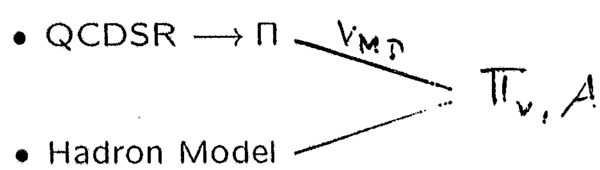

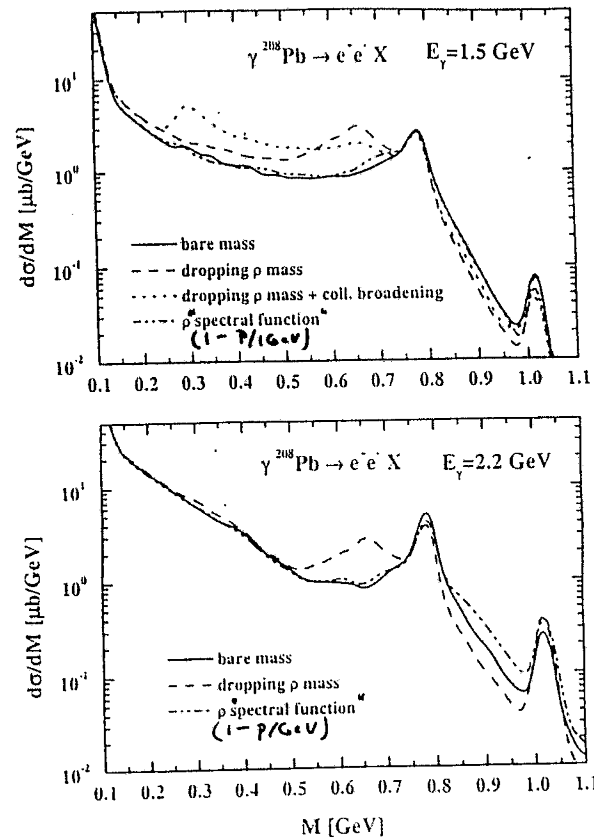

QCD Sum Rule

Compare OPE of current-current correlator for space-like distances with spectral function in time-like region.

Use Dispersion Relation to connect both regions ($Q^2 = -q^2 = -s$)

$$
\begin{aligned}
\frac{Q^2}{\pi}\int_0^\infty ds \frac{\Im\Pi(s)}{s\left(s+Q^2\right)}
&= -\frac{1}{8\pi^2}\left(1+\frac{\alpha_s}{\pi}\right)\ln\frac{Q^2}{\Lambda^2} \\
&\quad + \frac{m_q\langle\bar{q}q\rangle}{Q^4} + \frac{1}{24}\frac{\langle\frac{\alpha_s}{\pi}G^2\rangle}{Q^4} \\
&\quad + \frac{\langle(\bar{q}q)^2\rangle}{Q^6} + \ldots
\end{aligned}
$$

Lhs dominated by soft scale ($\sim m_\rho$), rhs (OPE) separates hard, perturbative from soft, non-perturbative scale (condensates). Parametrize $\Im\Pi$ in terms of few parameters, to be extracted from Sum Rule.

In-medium OPE

$$
\begin{aligned}
\langle\bar{q}q\rangle_\rho &= \langle\bar{q}q\rangle_0 + \frac{\sigma_N}{2m_q}\rho \\
\langle\frac{\alpha_s}{\pi}G^2\rangle &= \langle\frac{\alpha_s}{\pi}G^2\rangle_0 - \frac{8}{9}m_N^0\rho_N \\
\langle(\bar{q}q)^2\rangle &\sim \kappa\langle\bar{q}q\rangle^2
\end{aligned}
$$

Mean Field Approximation

QCD SR PREDICTION FOR ρ-MESON:

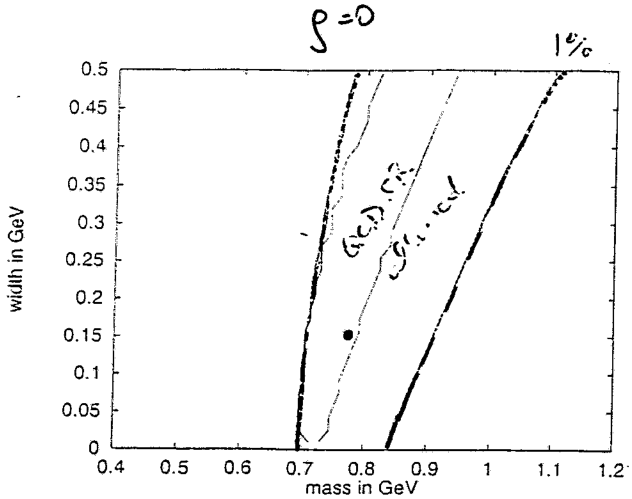

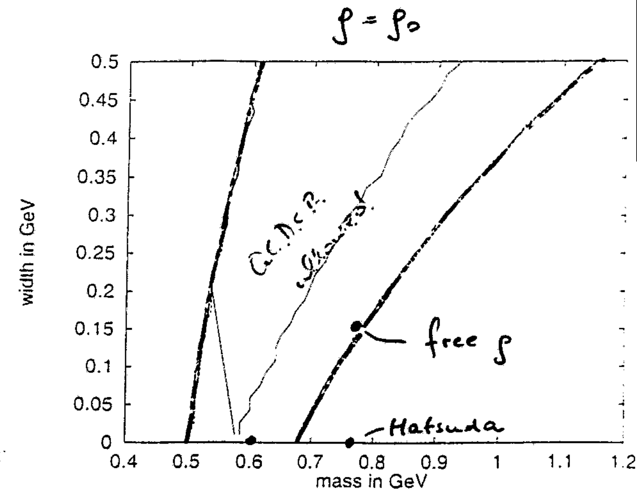

systematic errors due to uncertainties in condensates included

Leupold, Peters, Mosel, NPA (98) · A 628 (1998) 311

Ansatz for Spectral Function of ρ

$$\Im\Pi(s) = \pi F \frac{S(s)}{s}\Theta(s_0 - s) + \frac{1}{8\pi}\left(1 + \frac{\alpha_s}{\pi}\right)\Theta(s - s_0)$$

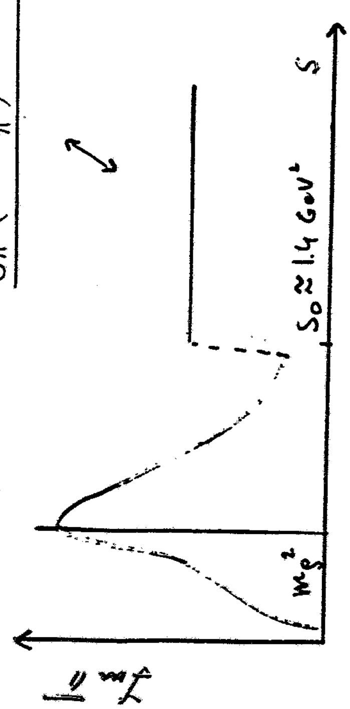

- Hatsuda, Lee Ansatz (1992):

  $$S(s) = \delta(s - m_\rho^2)$$

  Determine F, m_ρ, s_0 from QCDSR

- Leupold, Peters, Mosel (NPA (1998):

  $$S(s) = \frac{1}{\pi}\frac{\sqrt{(s)}\Gamma(s)}{\left(s - m_f^2\right)^2 + s\Gamma(s)^2}.$$

  Determine (m_ρ, Γ_ρ) from QCDSR!
  $+F, s_0$

Hadron properties in Medium:

- masses
- widths
- coupling strengths

all linked by "$t\rho$" approximation:

\# $$\Pi_V = -4\pi f_{VN}(0)\,\rho \qquad \text{(for meson)}$$

good for [illegible] and for low densities

- mass: [illegible]

  with [illegible] $= \dfrac{\mathrm{Re}\,f[illegible]}{\mathrm{Im}\,f[illegible]}$

- width: [illegible]

Is there more than \# ?

Hadron Model

$$\Pi_V = -4\pi f_{VN}(0)\,\rho_N$$

in lowest order in nuclear density

$\Rightarrow$ Need VN Scattering Amplitude

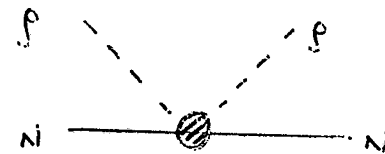

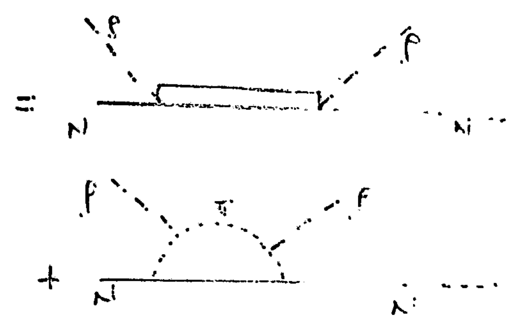

N* Resonance Graphs

Meson Cloud Graphs

Models of In-Medium ρ

- *Hermann, Friman, Noerenberg (1993)*

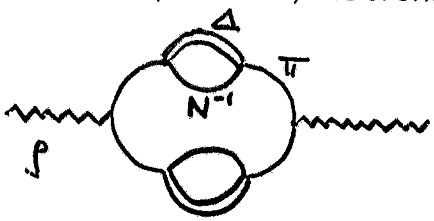

broadens ρ, shifts strength down

- *Asakawa, Ko (1993)*
  combine HFN model with QCDSR, ρ pole moves down, broadens

- *Klingl, Weise (1997)*
  method similar to AK, but much more refined hadronic model

- *Rapp, Wambach (1997)*
  N^*N^{-1} + 'state of the art' pion dynamics, significant broadening of ρ

- *Friman, Pirner (1997)*
  2 p-wave resonances with ρ-decay widths: $N(1720)$, $\Delta(1905)$, broadens and weakens free ρ pole, moves strength down to new N^*N^{-1} peak.

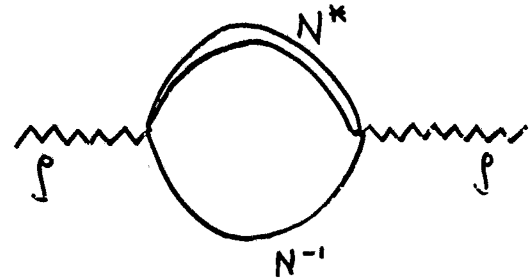

- *Peters, Post, Lenske, Leupold, Mosel, (NPA (1998) in press)*

  ALL p-wave resonances up to 1.9 GeV

  \+ s-wave resonances, in particular N(1520) with $\Gamma_\rho = 20\% \, \Gamma_{tot} \approx 25$ MeV

  \+ Selfconsistent feedback of ρ spectral function on N^* width.

Spectral function

$$A = -\frac{1}{\pi} \, \mathrm{Im} \, \Pi$$

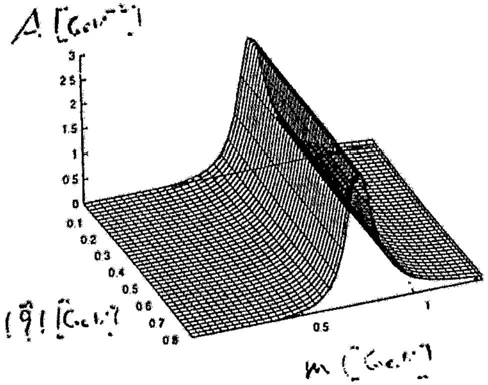

Free ρ

ρ - spectral function

$\rho = \rho_0$

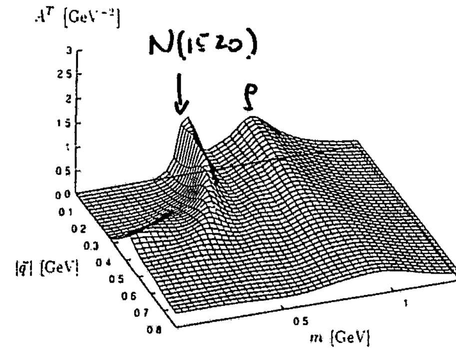

transverse

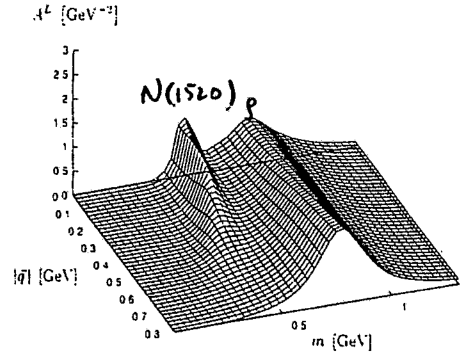

longitudinal

$\Pi \sim \rho$: non-selfconsistent

$$\Pi^{\mu\nu} \sim \left(-\omega^2 P_T^{\mu\nu} - q^2 P_L^{\mu\nu}\right) F(\vec{q}^{\,2})$$

$$\times \rho_N \frac{E^* - m_N}{\omega^2 - (E^* + m_N)^2}$$

(for small ρ

Selfconsistent calculation

L

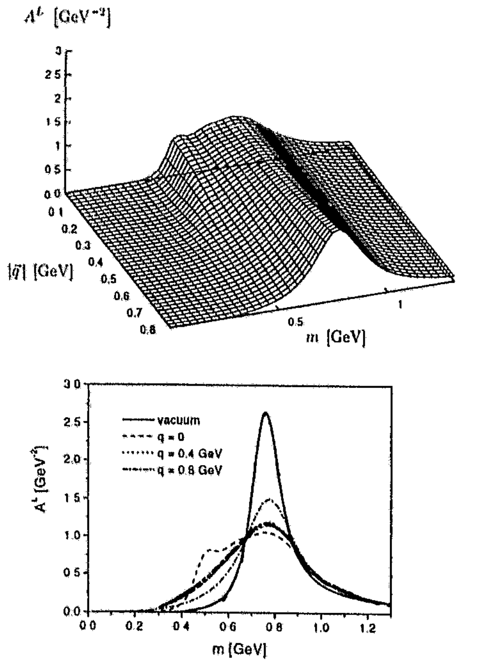

Figure 7: Same as Fig. 6, but for the longitudinal spectral function.

Selfconsistent Calculation

ρ + N^* changed

T

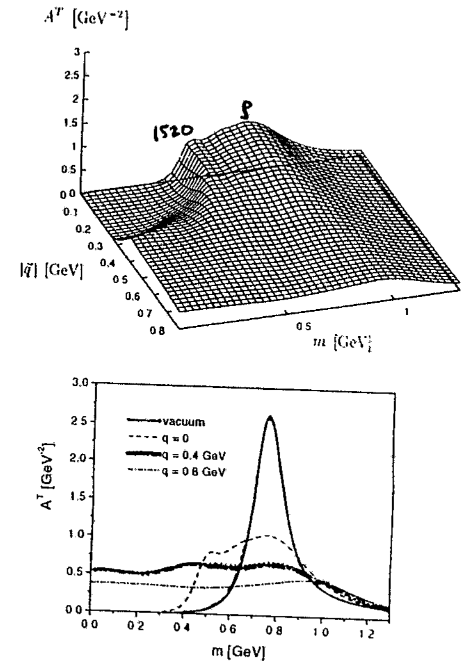

Figure 6: Self-consistent transverse spectral function of the rho meson for $\rho_N = \rho_0$. Lower part: Cuts through the upper part for different three-momenta together with the vacuum spectral function.

Transport Calculations

→ Secondaries (ππ→ρ) taken into account

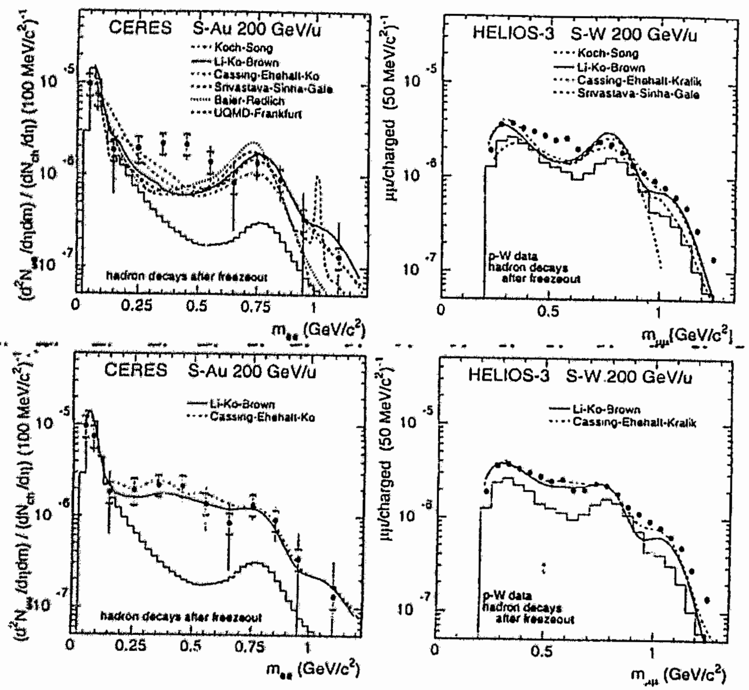

in-medium corrections
hoped

"Sensitivity ... "

V. Koch

Pb + Pb

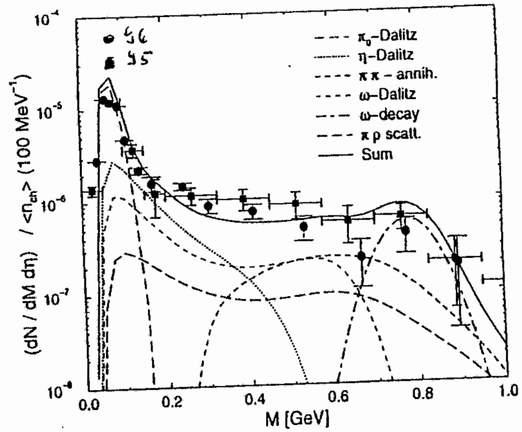

Koch et al.
Prediction
PRC54(96)
1903

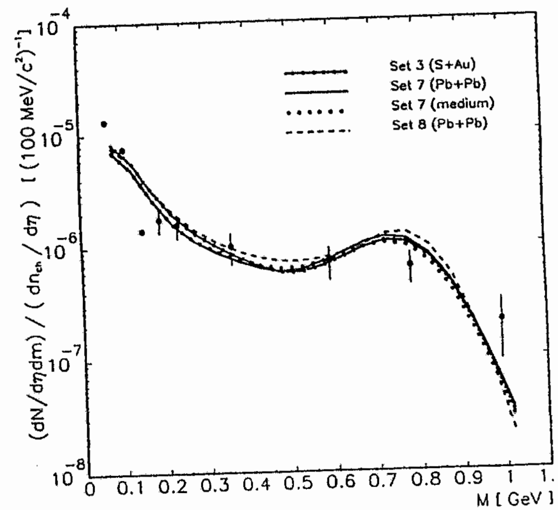

central Pb + Pb

Elena Bratkovskaya 98
HSD

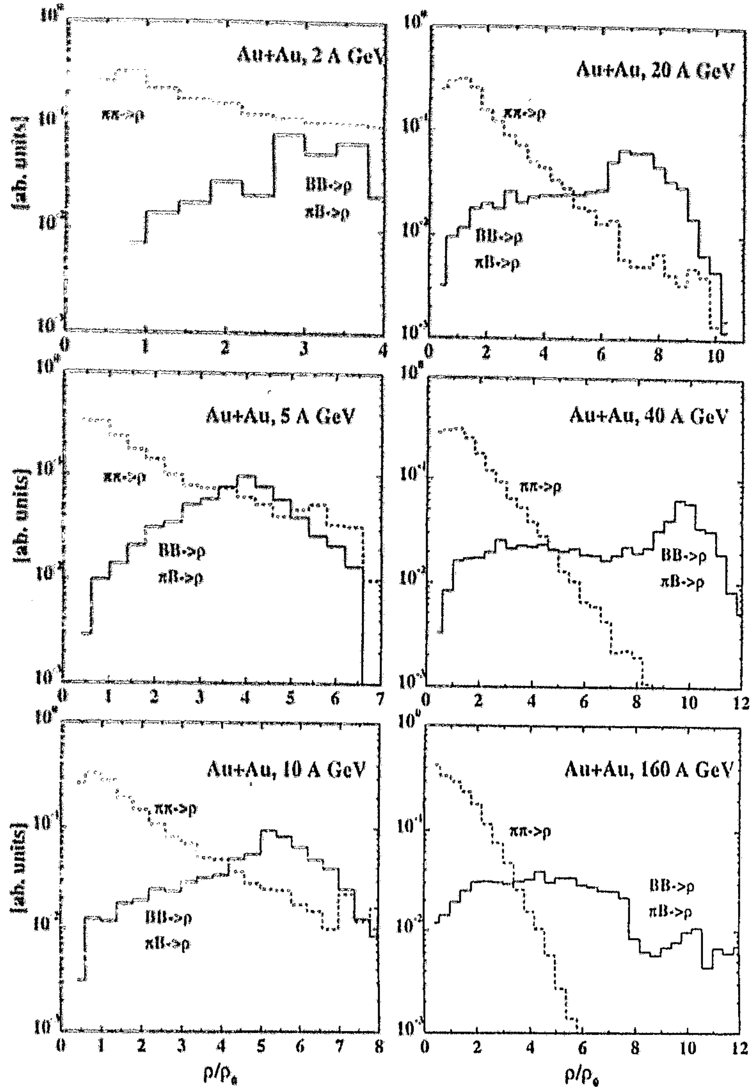

Coupled Channel BUU

$$(\frac{\partial}{\partial t} + \frac{\partial H_i}{\partial \vec{p}}\frac{\partial}{\partial \vec{r}} - \frac{\partial H_i}{\partial \vec{r}}\frac{\partial}{\partial \vec{p}})F_i = G_i\mathcal{A}_i - L_iF_i$$

Gain ↗ (on $G_i\mathcal{A}_i$) Loss ↖ (on L_iF_i)

Take into account all resonances rated at least 2 stars in Manley et al.:

CC - Space

$P_{33}(1232)$, $P_{11}(1440)$, $D_{13}(1520)$, $S_{11}(1535)$, $P_{33}(1600)$, $S_{31}(1620)$, $S_{11}(1650)$, $D_{15}(1675)$, $F_{15}(1680)$, $P_{13}(1879)$, $S_{31}(1900)$, $F_{35}(1905)$, $P_{31}(1910)$, $D_{35}(1930)$, $F_{37}(1950)$, $F_{17}(1990)$, $G_{17}(2190)$, $D_{35}(2350)$.

CC Space

Resonances couple to:

$N\pi$, $N\eta$, $N\omega$, ΛK, $\Delta(1232)\pi$, $N\rho$, $N\sigma$, $N(1440)\pi$, $\Delta(1232)\rho$.

$$\begin{array}{lcl}
\pi N & \leftrightarrow & \rho N \\
\pi N & \leftrightarrow & \omega N \\
\pi N & \rightarrow & \omega\pi N \\
\omega N & \rightarrow & \pi\pi N \\
\omega N & \rightarrow & \omega N \\
\pi N & \leftrightarrow & \phi N \\
\pi N & \rightarrow & \phi\pi N \\
\phi N & \rightarrow & \pi\pi N \\
\phi N & \rightarrow & \phi N
\end{array}$$

+ String fragmentation for $\sqrt{s} > 2.1$ GeV

The "How" of Transport

CCBUU

$$\left(\frac{\partial}{\partial t} + \frac{\partial H_i}{\partial \vec{p}}\frac{\partial}{\partial \vec{r}} - \frac{\partial H_i}{\partial \vec{r}}\frac{\partial}{\partial \vec{p}}\right)F_i = G_i \mathcal{A}_i - L_i F_i$$

$$H_i = \sqrt{(\mu + S_i)^2 + \vec{p}^2}$$

↑ scalar selfenergy

"spectral ps density" →

$$f_i(\vec{r},\vec{p},\mu,t) = \frac{F_i(\vec{r},\vec{p},\mu,t)}{\mathcal{A}_i(\vec{r},\vec{p},\mu,t)}$$ ps-density

Spectral function

$$\mathcal{A}_i(\mu) = \frac{2}{\pi}\frac{\mu^2\Gamma_{tot}(\mu,\vec{x},t,\vec{p})}{(\mu^2 - M_i^2)^2 + \mu^2\Gamma_{tot}^2(\mu,\vec{x},t,\vec{p})}$$

$$\Gamma(\vec{r},t,\vec{p},\mu) \rightarrow \Gamma(\rho(\vec{r},t),|\vec{p}|,\mu)$$

Consistency condition

$$\Gamma_{tot,\rho} = \gamma L_\rho \quad !$$

earlier only for Δ's, now also for ρ's

PROPAGATION OF BROAD RESONANCES

First in Ehehalt et al. for Δ (1993)

Gain and Loss Terms illustrated for $\rho + N \leftrightarrow R$

Gain term:

$$G_\rho = \frac{1}{A_\rho}\int \frac{d^3p_R}{(2\pi)^3} d\mu_R \times F_R(\vec{r},\vec{p}_R,\mu_R,t)\frac{d\Gamma_{R\to N\rho}}{d^3p_\rho d\mu_\rho}(1 - f_n(\vec{r},\vec{p}_n,t))$$

Loss term:

$$L_\rho = \Gamma_{\rho\to\pi\pi} + \int \frac{d^3p_n}{(2\pi)^3} f_n(\vec{r},\vec{p}_n,t) v_{n\rho}\sigma_{\rho n\to R}$$

Dileptons through strict VMD

$$\Gamma_{V\to e^+e^-}(M) = C_V \frac{m_V^4}{M^3}$$

Testparticle Ansatz for "Spectral Phase Space Density"

$$F(\vec{x},t,\vec{p},\mu) = \sum_i \delta(\vec{x}-\vec{x}_i(t))(\vec{p}-\vec{p}_i(t)) \times \delta(\mu-\mu_i)$$

μ_i : mass of testparticle i

Propagate testparticles in scalar pot:

$$s_i(\rho_i(t)) = (\mu_i^{med} - \mu_i^{vac})\frac{\rho_i(t)}{\rho_i^{cr}}$$

$$\mu_i^*(\rho_i(t)) = \mu_i^{vac} + s_i(\rho(t))$$

correct asymptotics!

Cross section for production of resonance R in collision of meson m with baryon B:

$$\sigma_{mB\to R} = \frac{2J_R}{(2J_m+1)(2J_B+1)} \times \frac{4\pi}{k^2}\frac{s\Gamma^{in}_{mB}\Gamma^{out}_{tot}}{(s-M_R^2)^2+s\Gamma^{out\,2}_{tot}}$$

$$\Gamma^{out}_{mB} = \Gamma^0_{mB}\frac{\rho_{mB}(s)}{\rho_{mB}(M_R)}$$

$$\rho_{mB}(s) = \int d\mu_m d\mu_B \times \mathcal{A}_m(\mu_m)\mathcal{A}_B(\mu_B)\frac{q(s,\mu_m,\mu_B)}{s}B^2_{l_{mB}}(qR)$$

$$\mathcal{A}_i(\mu) = \frac{2}{\pi}\frac{\mu^2\Gamma_{tot}(\mu)}{(\mu^2-M_i^2)^2+\mu^2\Gamma^2_{tot}(\mu)}$$

$$\Gamma^{in}_{mB} = C^{J_R}_{mB}\Gamma^0_{mB}\frac{kB^2_{l_{mB}}(kR)}{s\rho_{mB}(M_R)}$$

5

Elementary $\pi^- + N \to e^+e^- + X$

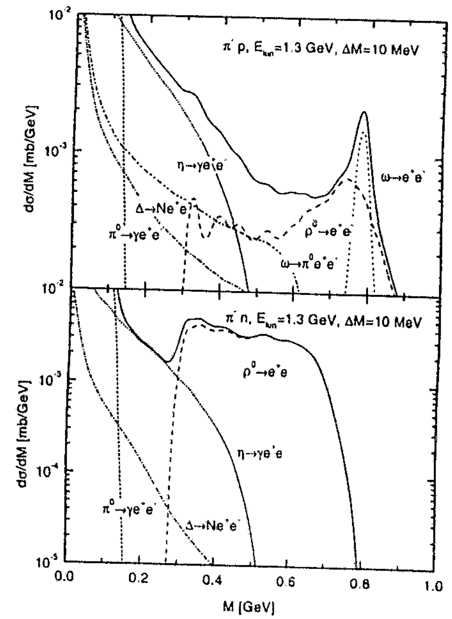

Large contributions from

$N^* \to \Delta + \rho \to e^+e^-$, $\hookrightarrow \Delta + \pi$

Uncertain!

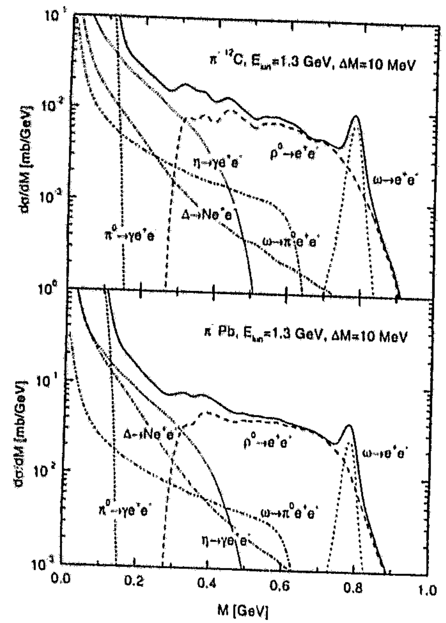

Collisional Broadening

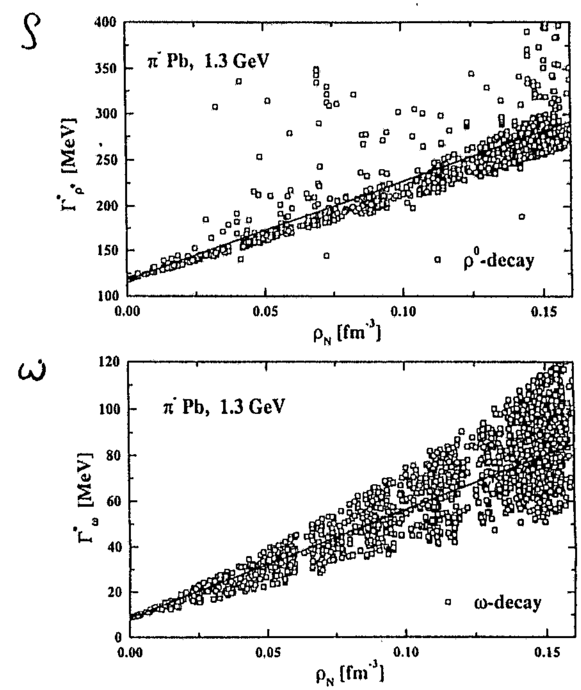

$$\Gamma_V = \Gamma_{vac} + \delta\Gamma_V$$

$$\delta\Gamma_V = \ldots$$

$$= \ldots \frac{\rho_N}{\rho_0} \ldots$$

$$\ldots \frac{\rho_N}{\rho_0} \ldots$$

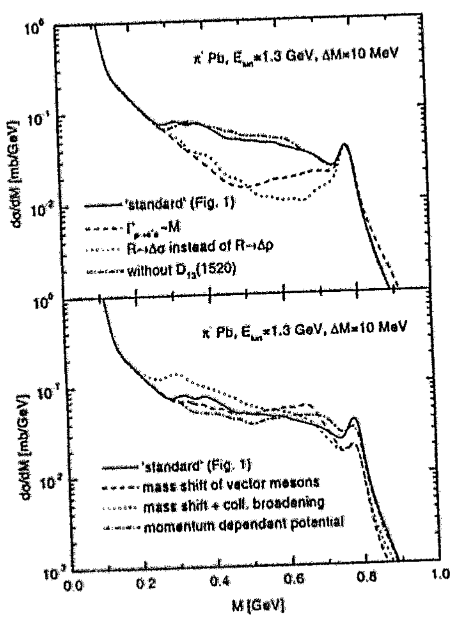

π⁻ Pb, E_kin=1.3 GeV, ΔM=10 MeV
'standard' (Fig. 1)
R→Δσ instead of R→Δρ
without D13(1520)
π⁻ Pb, E_kin=1.3 GeV, ΔM=10 MeV
'standard' (Fig. 1)
mass shift of vector mesons
mass shift + coll. broadening
momentum dependent potential
dσ/dM [mb/GeV]
M [GeV]

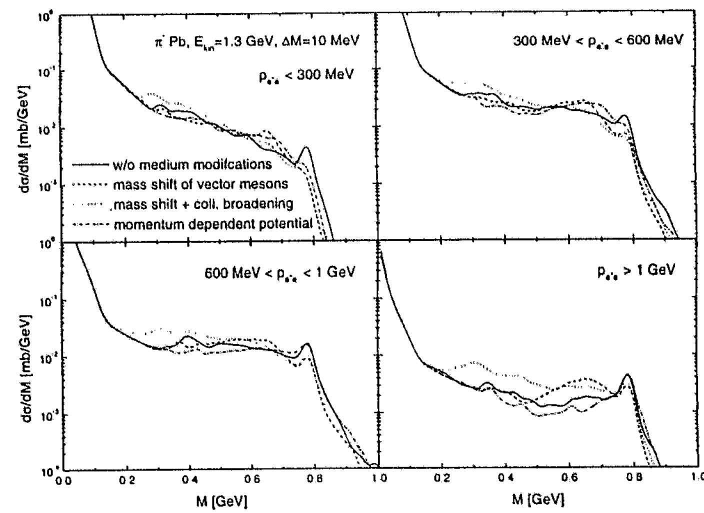

π⁻ Pb, E_kin=1.3 GeV, ΔM=10 MeV
p_e+e- < 300 MeV
300 MeV < p_e+e- < 600 MeV
600 MeV < p_e+e- < 1 GeV
p_e+e- > 1 GeV
w/o medium modifcations
mass shift of vector mesons
mass shift + coll. broadening
momentum dependent potential
dσ/dM [mb/GeV]
M [GeV]

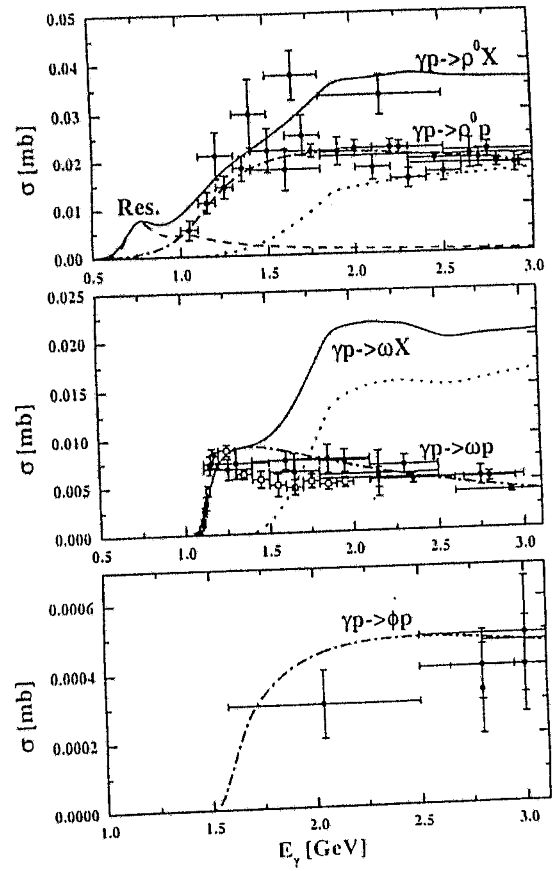

N. Bianchi et al., PL B325 (94) 333

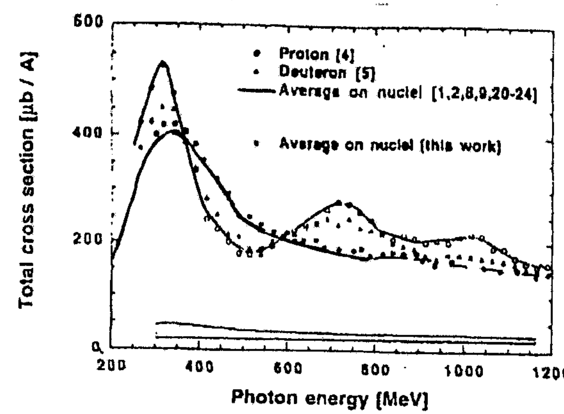

Photonuclear In-medium Effect

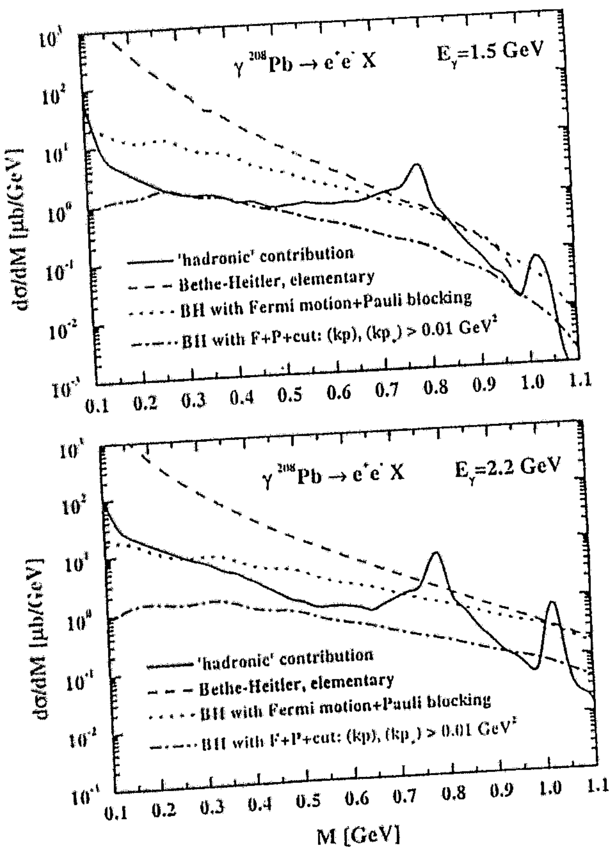
γ ^{208}Pb → e⁺e⁻ X
E$_γ$=1.5 GeV
E$_γ$=2.2 GeV
'hadronic' contribution
Bethe-Heitler, elementary
BH with Fermi motion+Pauli blocking
BH with F+P+cut: (kp), (kp$_+$) > 0.01 GeV^2
dσ/dM [μb/GeV]
M [GeV]

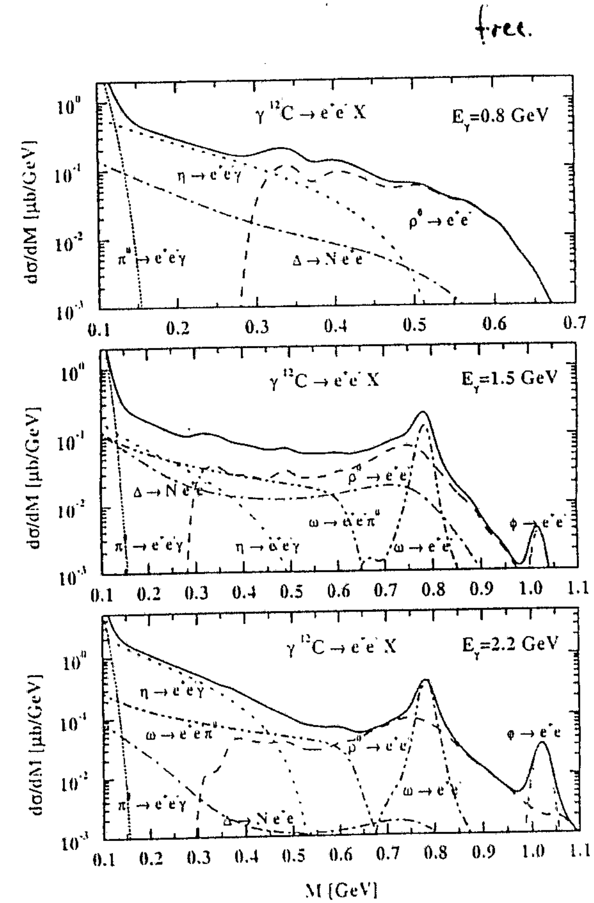
free.
γ ^{12}C → e⁺e⁻ X
E$_γ$=0.8 GeV
E$_γ$=1.5 GeV
E$_γ$=2.2 GeV
η → e⁺e⁻γ
π^0 → e⁺e⁻γ
Δ → N e⁺e⁻
ρ^0 → e⁺e⁻
ω → e⁺e⁻π^0
ω → e⁺e⁻
φ → e⁺e⁻
dσ/dM [μb/GeV]
M [GeV]

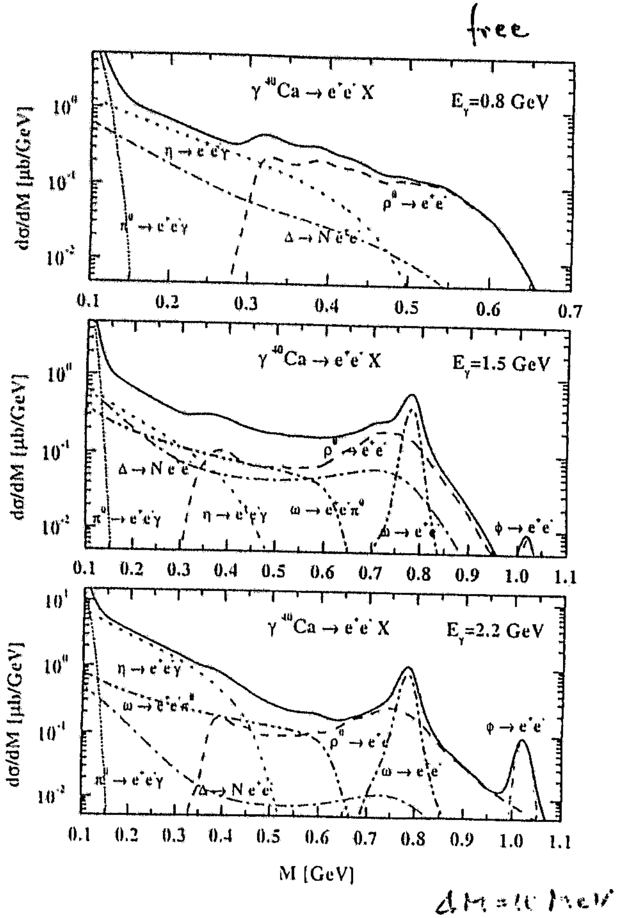

free
$\gamma\,^{40}Ca \rightarrow e^+e^- X$
E_γ=0.8 GeV
E_γ=1.5 GeV
E_γ=2.2 GeV
$\eta \rightarrow e^+e^-\gamma$
$\rho^0 \rightarrow e^+e^-$
$\pi^0 \rightarrow e^+e^-\gamma$
$\Delta \rightarrow N e^+e^-$
$\omega \rightarrow e^+e^-\pi^0$
$\omega \rightarrow e^+e^-$
$\phi \rightarrow e^+e^-$
dσ/dM [μb/GeV]
M [GeV]

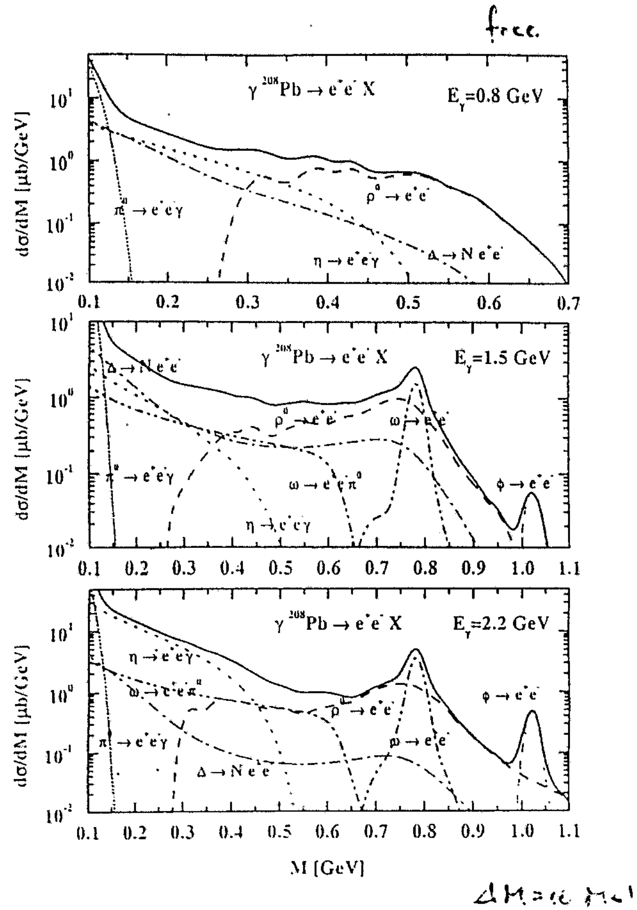

free
$\gamma\,^{208}Pb \rightarrow e^+e^- X$
E_γ=0.8 GeV
E_γ=1.5 GeV
E_γ=2.2 GeV
$\eta \rightarrow e^+e^-\gamma$
$\rho^0 \rightarrow e^+e^-$
$\pi^0 \rightarrow e^+e^-\gamma$
$\Delta \rightarrow N e^+e^-$
$\omega \rightarrow e^+e^-\pi^0$
$\omega \rightarrow e^+e^-$
$\phi \rightarrow e^+e^-$
dσ/dM [μb/GeV]
M [GeV]

Collision widths $\Gamma_{coll} = X \rho \langle v \sigma^{tot}_{VN} \rangle$

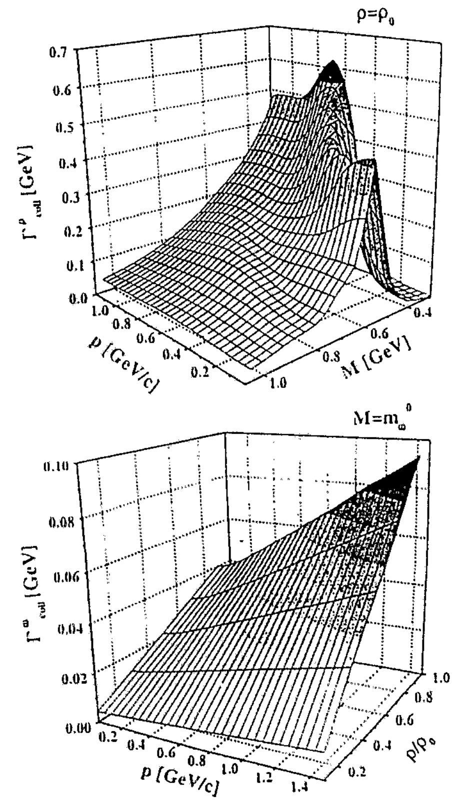

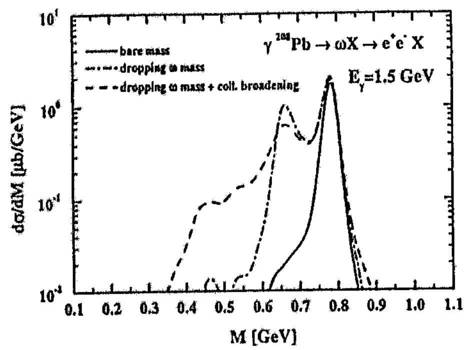

FIG. 15. The dilepton yield from ω mesons for γPb at 1.5 GeV. The solid line indicates the bare mass case, the dot-dashed line is the result with in-medium masses, the dashed line shows the effect of collisional broadening together with the dropping mass.

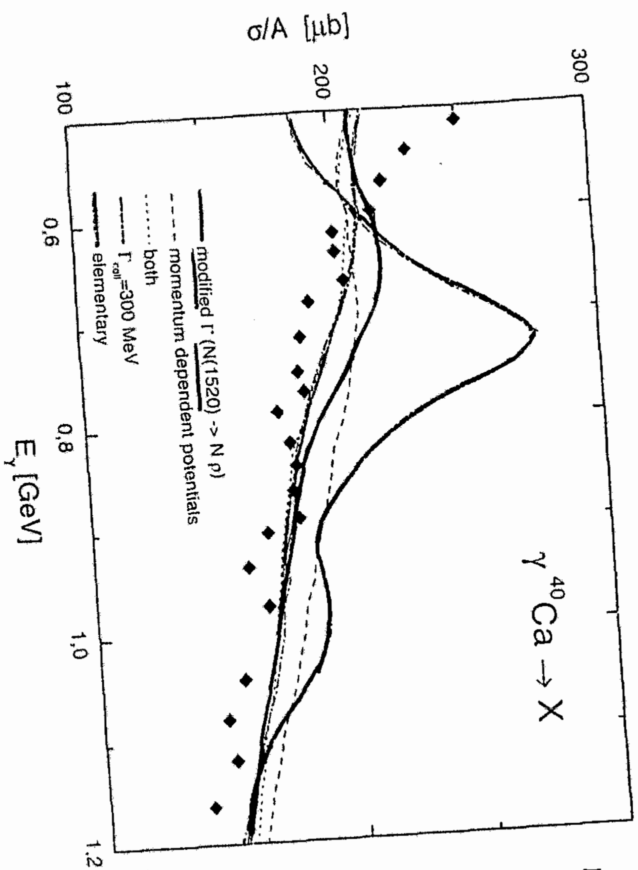

Conclusions

- QCD Sum Rules give only wide constraints for in-medium properties of hadrons → Original expectation of QCD mandated lowering of mass too naive.

- All realistic hadronic models give significant broadening up to dissolution of ρ meson. Mass shift meaningless.

- Transverse and longitudinal ρ spectral functions differ significantly. → Check in polarization measurements.

- In-medium changes of ρ also affect nucleon resonance widths ⟶ photoabsorption cross section.

- Heavy-Ion Collisions achieve large peak densities and thus large sensitivity to in-medium ρ spectral function. But: smear over time (density, temperature), average over polarization.

- Pion- and Photon-induced reactions give equally strong signal, cleaner, should enable to differentiate between longitudinal and transverse ρ's.

- At high energies collision broadening of ρ mesons remarkably constant: $\delta\Gamma_\rho \approx 100$ MeV. Initial State Shadowing only effective if $\lambda_\rho \approx 2\, fm \leq l_{\mathrm{coh}}$.

J. Bacelar:

Virtual bremsstrahlung experiments in few-body systems at KVI

Workshop on E.M. Radiation off colliding hadron systems: Dileptons and Bremsstrahlung

Virtual Bremsstrahlung experiments in few-body systems at KVI

J. Bacelar - April 1999

- Introd. to virtual bremsstrahlung in NN
- Experimental techniques
- The proton-proton system: ppe^+e^-
- The p-d capture: $^3He\gamma$, $^3Hee^+e^-$
- Future plans

Below pion threshold

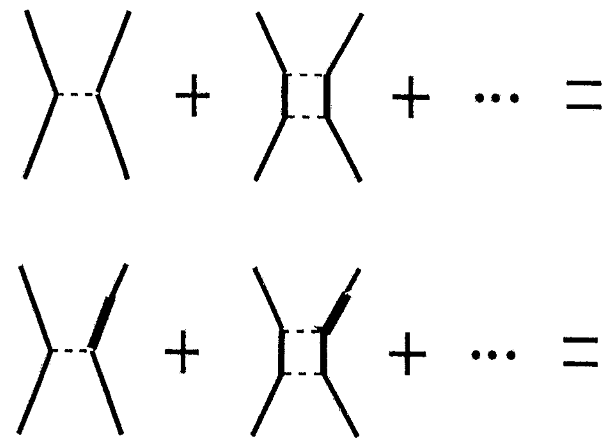

$$\sigma^{el.} \rightarrow T^{on-shell} = < on|V + VGV + ...|on >$$

$$\sigma^{\gamma} \rightarrow T^{\frac{1}{2}off-shell} = < off|V + VGV + ...|on >$$

Below pion threshold

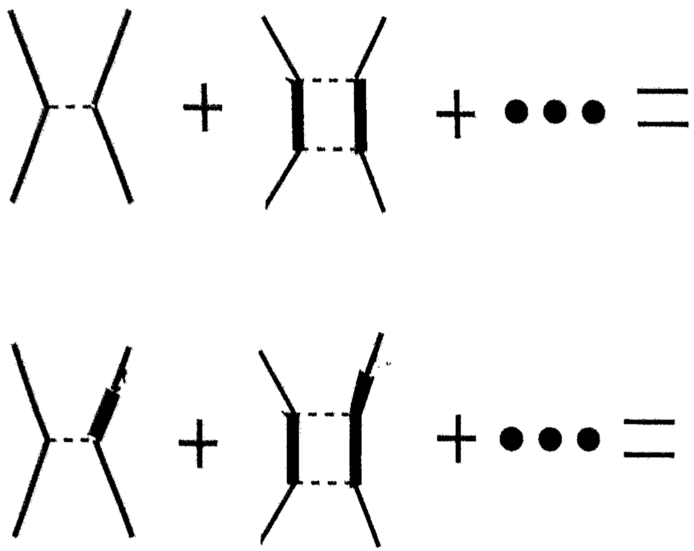

$\sigma^{el.} \rightarrow T^{on-shell} = < on|V + VGV + ...|on >$

$\sigma^{\gamma} \rightarrow T^{\frac{1}{2} off-shell} = < off|V + VGV + ...|on >$

Virtual photon has a mass

Transverse as well as longitudinal polarizations.

Decays into electron-positron pair

Nucleon-nucleon interactie

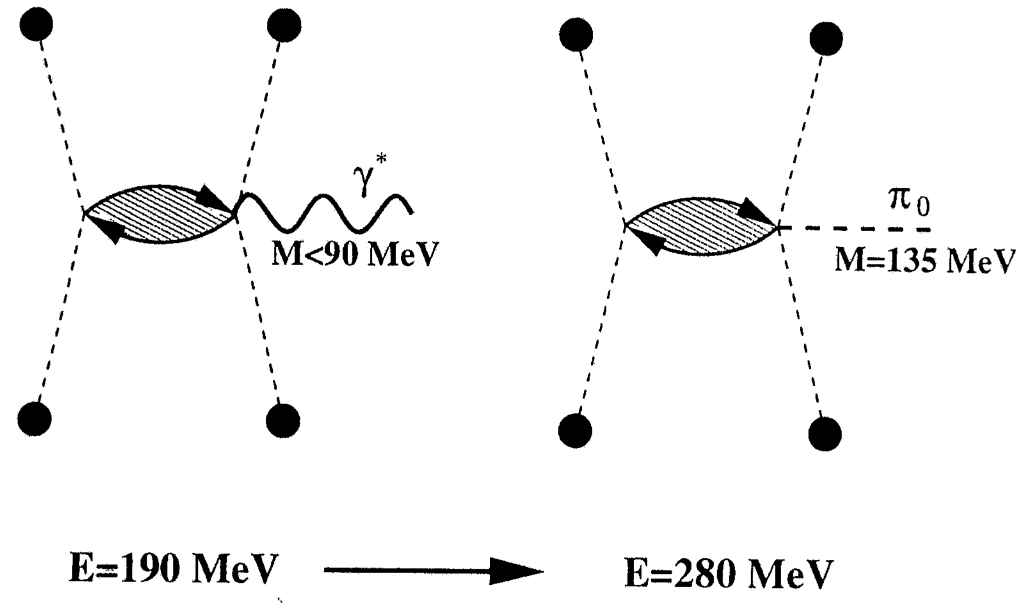

Nucleon-Nucleon Bremsstrahlung

Relevant Feynman Diagrams

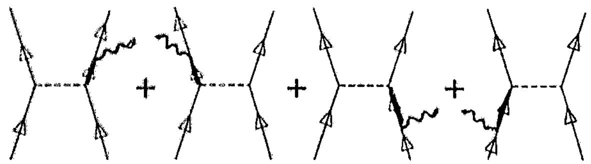

a)

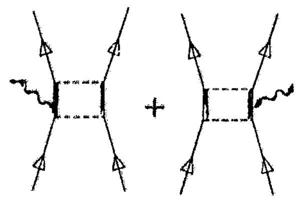

b)

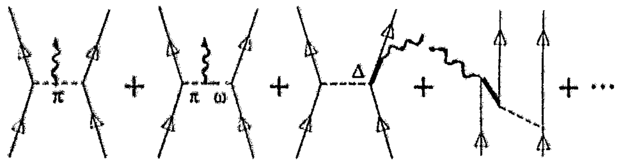

c)

a) External Bremsstrahlung (Single Scattering)

b) Internal Bremsstrahlung (Double Scattering)

c) MEC + Δ + $N\bar{N}$ + ...

LT-decomposition

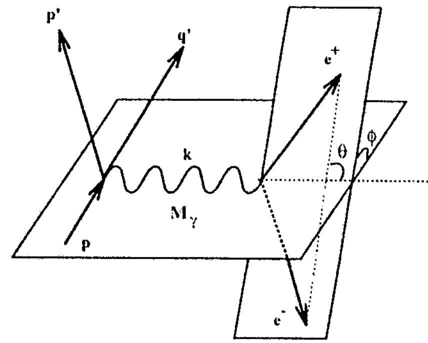

$$A \sim \frac{e^2}{{M_\gamma}^2} J^\mu M_\mu$$

$$|A|^2 \sim \frac{W_T}{{M_\gamma}^2}\left(1 - \frac{2l^2}{{M_\gamma}^2} sin^2\theta\right) + \frac{W_L}{{M_\gamma}^2}\left(1 - \frac{4l^2}{k_0^2} cos^2\theta\right) + \frac{2l^2}{{M_\gamma}^4} sin^2\theta (W_{TT} cos2\phi + W_{TT'} sin2\phi) + \frac{2l^2}{{M_\gamma}^3 k_o} sin2\theta (W_{LT} cos\phi + W_{LT'} sin\phi)$$

Experimentele opzet

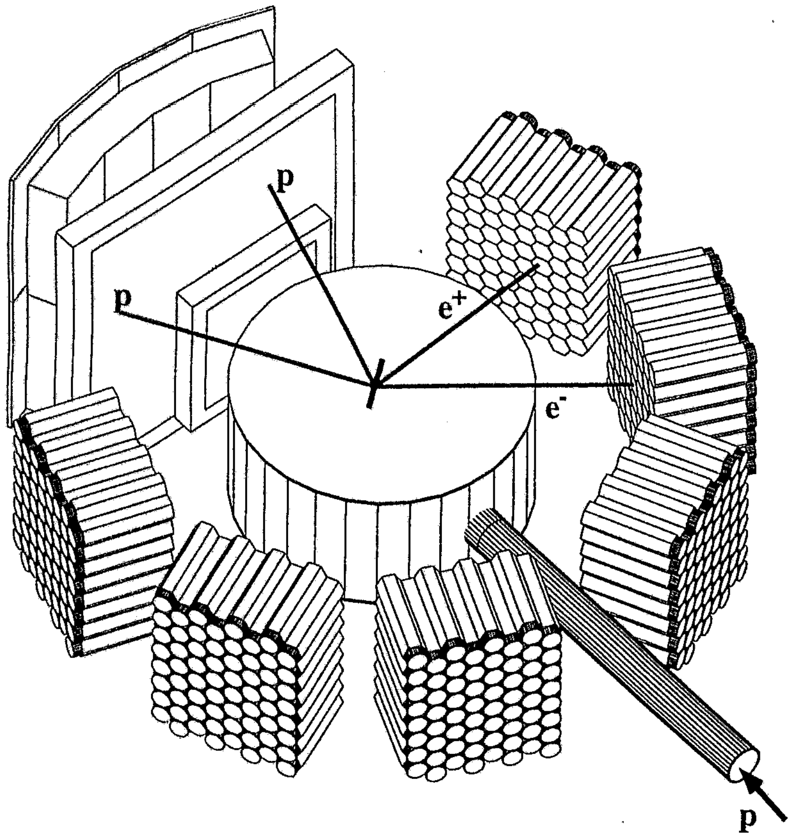

Dif. X-section $ppe^{+}e^{-}$

Absolute scale: systematical error ±15%

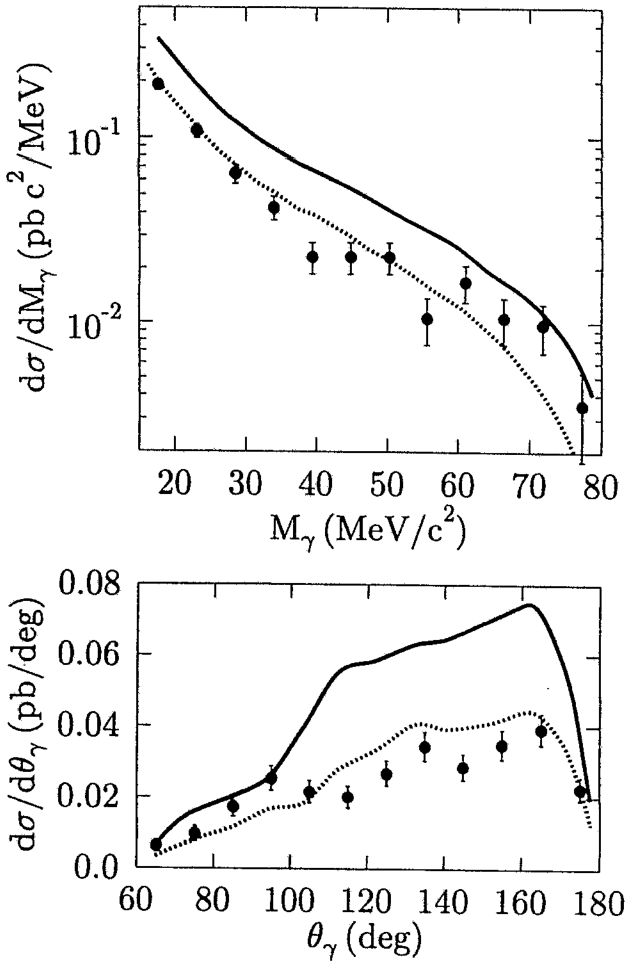

published in: J. Messchendorp et al. PRL 82 (99) 2645

Results pp → pp e⁺e⁻

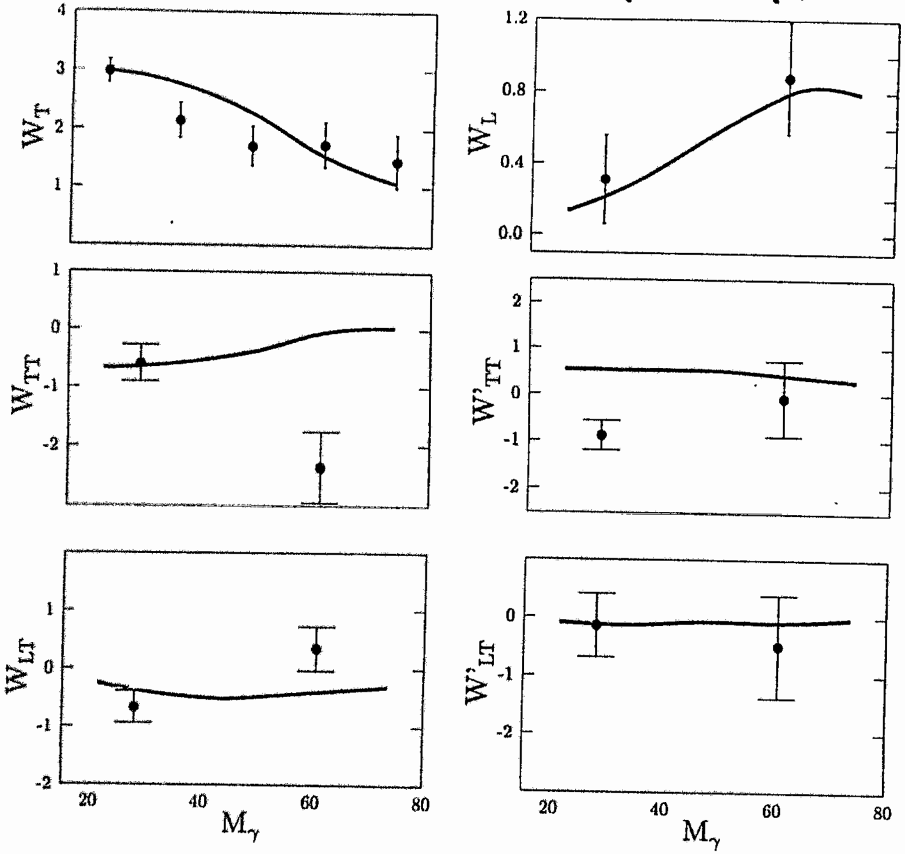

$$W_T \sim |J_x|^2 + |J_y|^2$$
$$W_{TT} \sim |J_y|^2 - |J_x|^2$$
$$W_{LT} \sim J_z J_x^*$$

$$W_L \sim |J_z|^2$$
$$W'_{TT} \sim J_x J_y^*$$
$$W'_{LT} \sim J_z J_y^*$$

Calculations by G. Martinus, O. Scholten, J.A. Tjon.

Resultaten

$p + p \rightarrow p + p + \gamma + \gamma$
Measured cross-sections

ppe^+e^- data BLOCK exp.

e^+e^- contribution subtracted

Preliminary data: J. Messchendorp

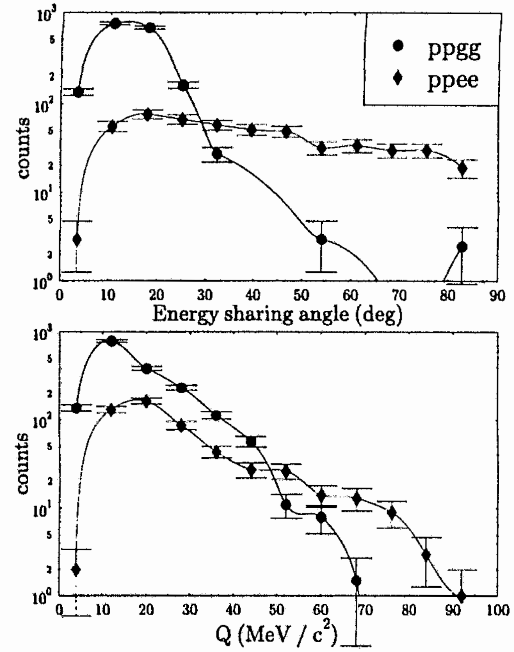

Calculations

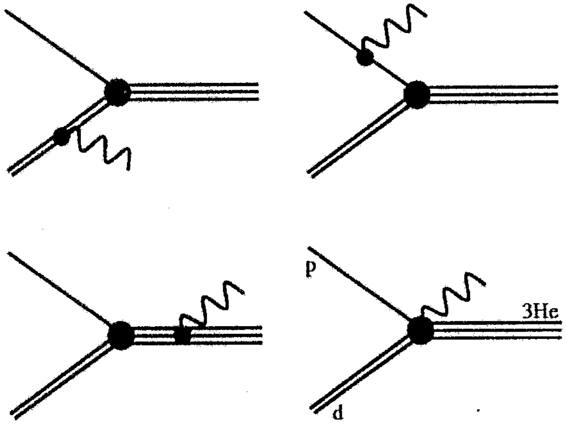

- Calculation by A. Korchin, O. Scholten and D. van Neck
  - Wave function ^{3}He with Argonne V18
  - Contact term ⇒ Current conservation

Experimental setup

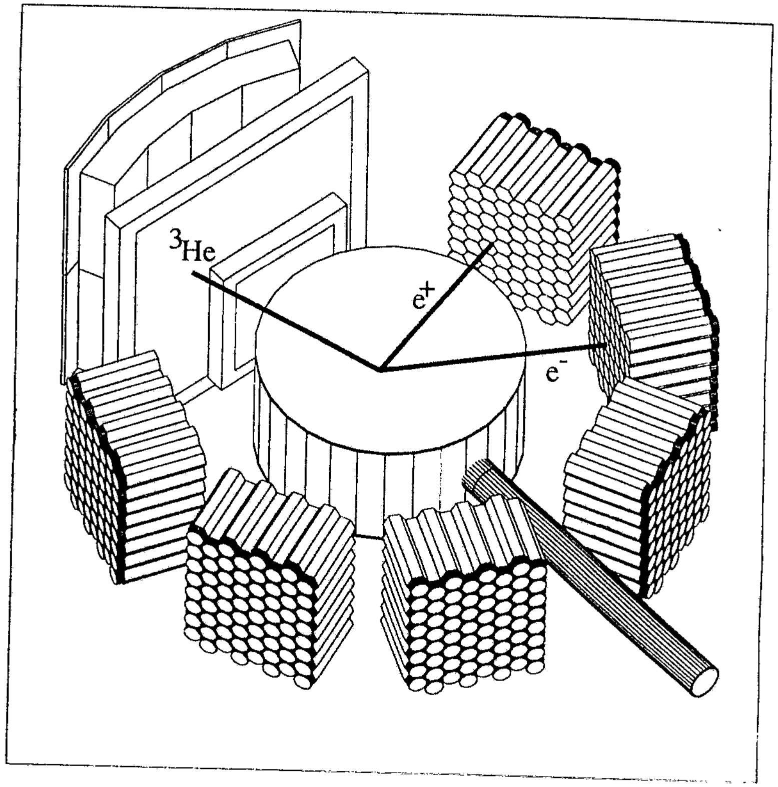

- 190 MeV polarized proton beam, LH_2/LD_2

Channel selection

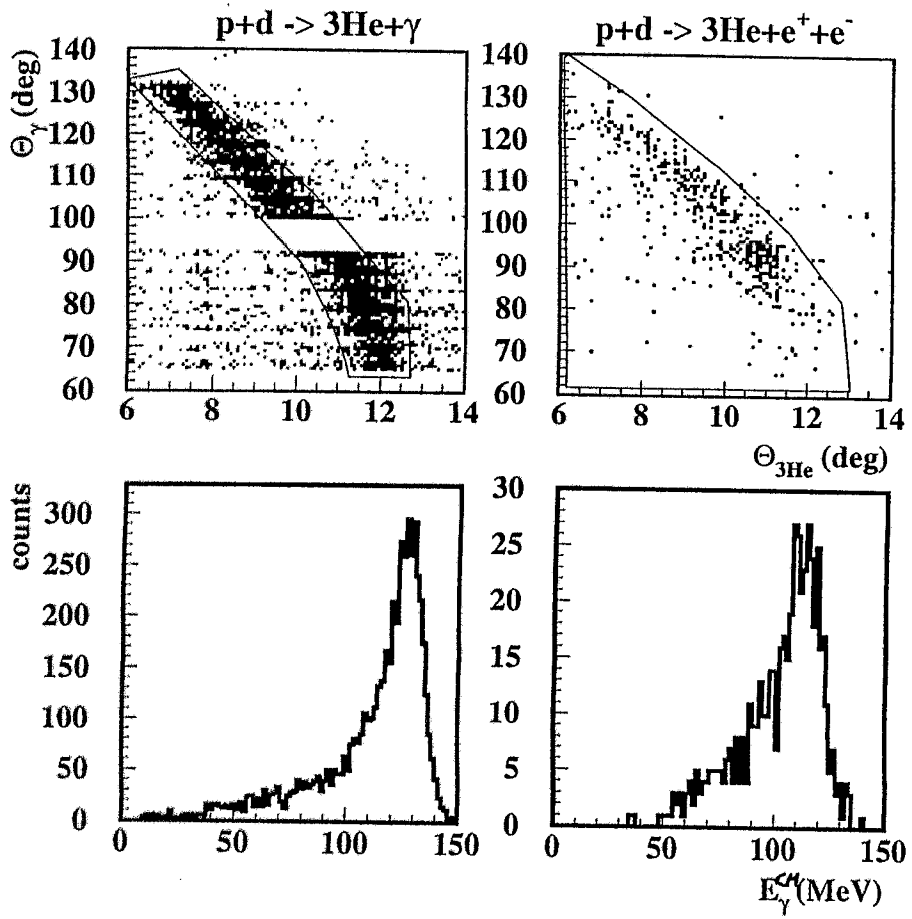

Results pd

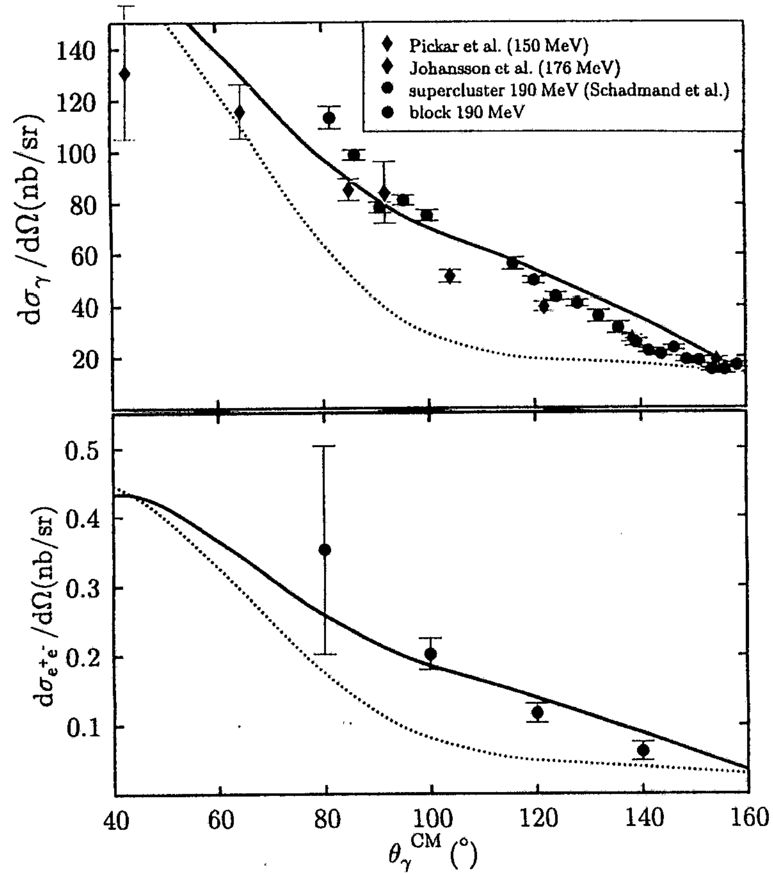

Calculations by A. Yu. Korchin et al.

Results pd

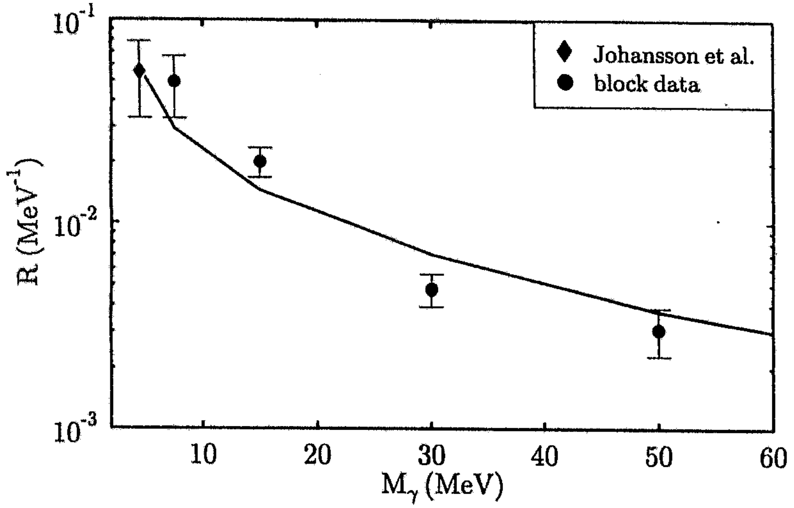

Calculations by A. Yu. Korchin et al.

Results $p+d \rightarrow {}^3He+e^+e^-$

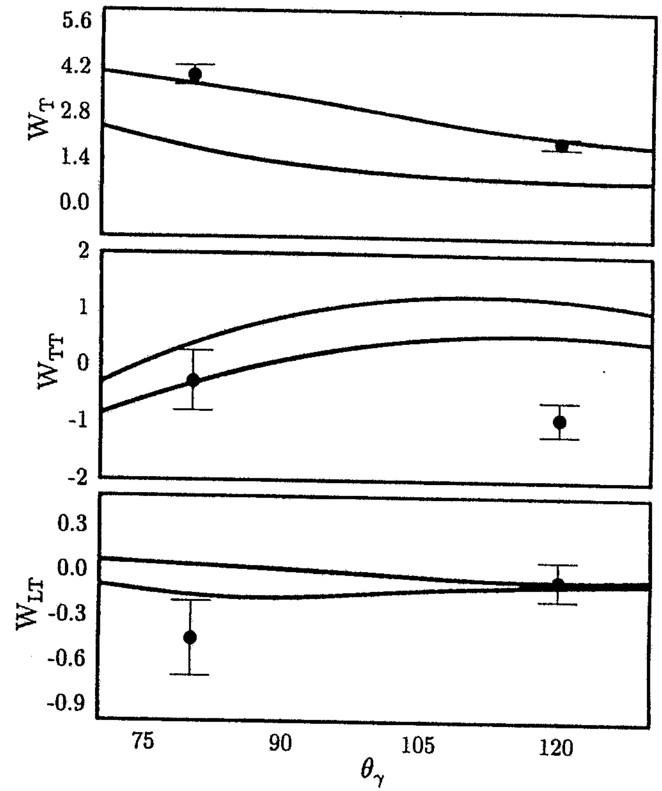

Calculations by A. Yu. Korchin et al.

— α=1.2

— α=0

104 elements removed

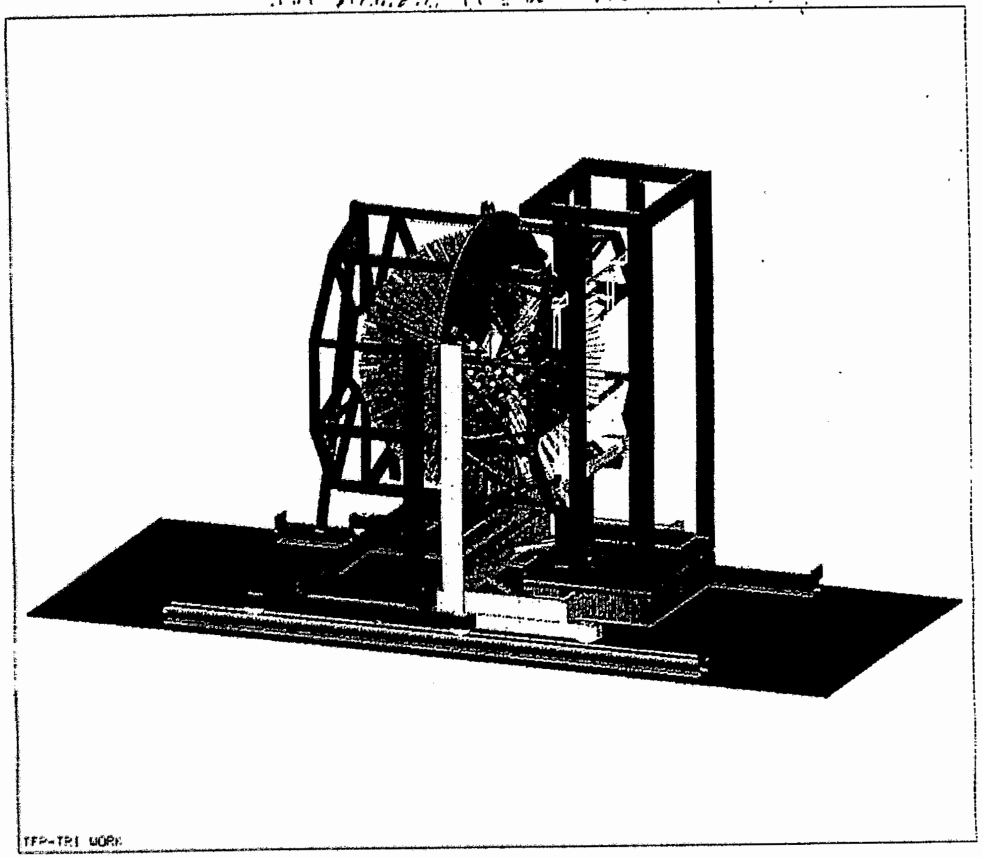

Conclusions

- $p + p \rightarrow p + p + e^+e^-$
  - First experiment success: $W_T, W_L, W_{TT}, W_{TL}, W'_{TT}, W'_{TL}$ obtained
  - Exp. Plastic Ball 1999.
- $p + p \rightarrow p + p + \gamma + \gamma$
  - First experimental results
  - Interferometer methods, virtual π^0 with Plastic Ball
- $p + d \rightarrow ^3 He + e^+e^-$
  - Real and virtual capture measured
  - Model calc. explain data
  - High accuracy with Plastic Ball

Collaborators

- KVI:
  - J.B.
  - M.J. van Goethem
  - M.N. Harakeh
  - M. Hoefman
  - H. Huisman
  - N. Kalantar-Nayestanaki
  - H. Löhner
  - J.G. Messchendorp
  - R. Ostendorf
  - S. Schadmand
  - R. Turissi
  - M. Volkerts
  - H.W. Wilschut
  - A. van der Woude
- GSI:
  - R. Holzmann
  - R. Simon
- NPI, Prague:
  - A. Kugler
  - K. Tcherkashenko
  - V. Wagner

KVI

J. Ritman:

Meson production experiments in pp reactions with the DISTO spectrometer

James Ritman II. Phys. Inst. Giessen

Meson Production Experiments in pp Reactions with the DISTO Spectrometer

- *DISTO Spectrometer*
- ϕ/ω *Production: Results at 2.85 GeV*
- *Total* K^- *Cross section*
- ρ *Meson Production*
- $\eta - \eta'$ *and the* $U_A(1)$ *Anomaly in QCD*
- *Summary and Outlook*

DISTO Spectrometer

$\vec{p}p \rightarrow pK\vec{\Lambda}(\vec{\Sigma}^o)$ *and* $\vec{p}p \rightarrow pp(\phi,\omega,\rho,\eta,\eta')$

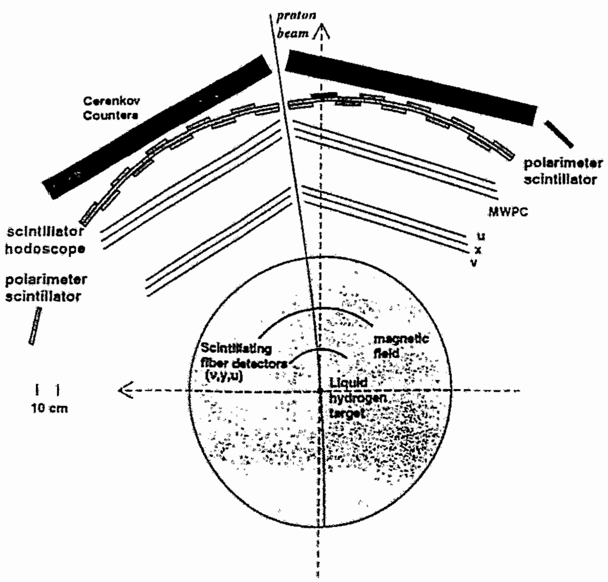

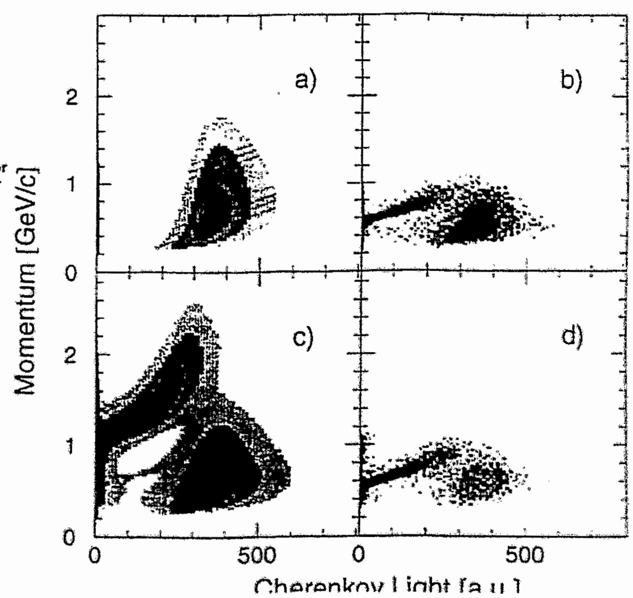

Experimental Method

- 4 Charged Particles in Final State

  Momentum determination via tracking in dipole B-field

  Particle Identification with:

  - Water Cherenkov detectors
  - Plastic Hodoscopes

- Kinematically complete/overdetermined measurement

  $pp \rightarrow pp\,\phi \rightarrow pp\,K^+ K^-$ (BR = 50%)

  Missing Mass (pp) = Invariant Mass (KK)

  $pp \rightarrow pp\,\omega \rightarrow pp\,\pi^+ \pi^- \pi^o$ $(\pi^o \rightarrow \gamma\gamma)$ (BR = 89%*99%)

  Missing Mass (pp) = $Mass_{\omega}$

  Missing Mass ($pp\pi^+\pi^-$) = $Mass_{\pi^o}$

ϕ/ω Data

Strong deviation from OZI by up to Factor 100 for $\phi\gamma$

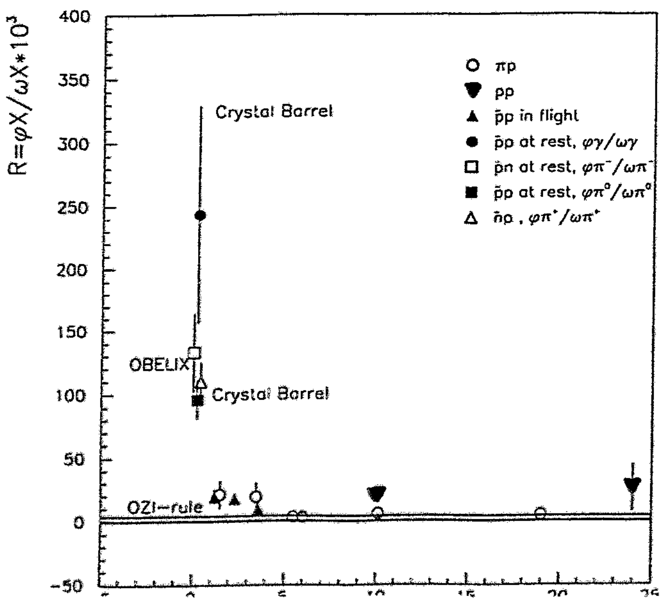

S-Wave component dominant

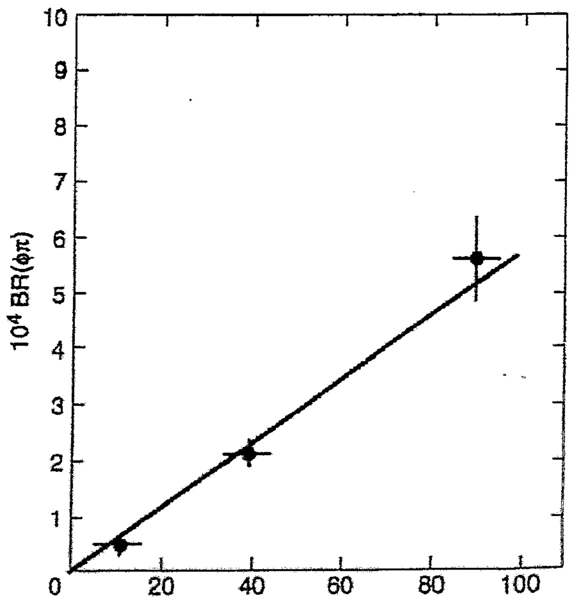

Okubo - Zweig - Iizuka

Strangeness in the Nucleon and the OZI rule

OZI rule: Diagrams with disconnected quark lines are strongly suppressed

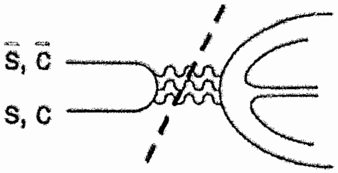

OZI-forbidden

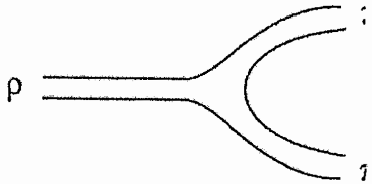

OZI-allowed

$|\phi\rangle = \cos\delta\ |s\bar{s}\rangle + \sin\delta\ |q\bar{q}\rangle \sim |s\bar{s}\rangle$

$|\omega\rangle = \sin\delta\ |s\bar{s}\rangle - \cos\delta\ |q\bar{q}\rangle \sim |q\bar{q}\rangle$

If $|p\rangle = |uud\rangle$:

$\phi / \omega \sim 0.0043$

Near Threshold pp Reactions

φ / ω Production Ratio is OZI suppressed

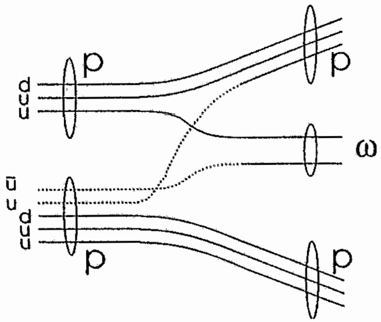

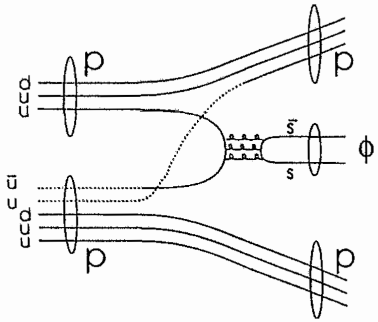

Near Threshold (large S-wave contribution)

DISTO Collaboration

(Dubna, Indiana, Saclay, Torino, Cracow, Giessen, GSI, FFM)

pp reactions at 83 MeV above threshold

(lowest previously 1730 MeV)

Identification of ω-meson

$pp \to pp\,\omega \to pp\,\pi^+\pi^-\pi^0$

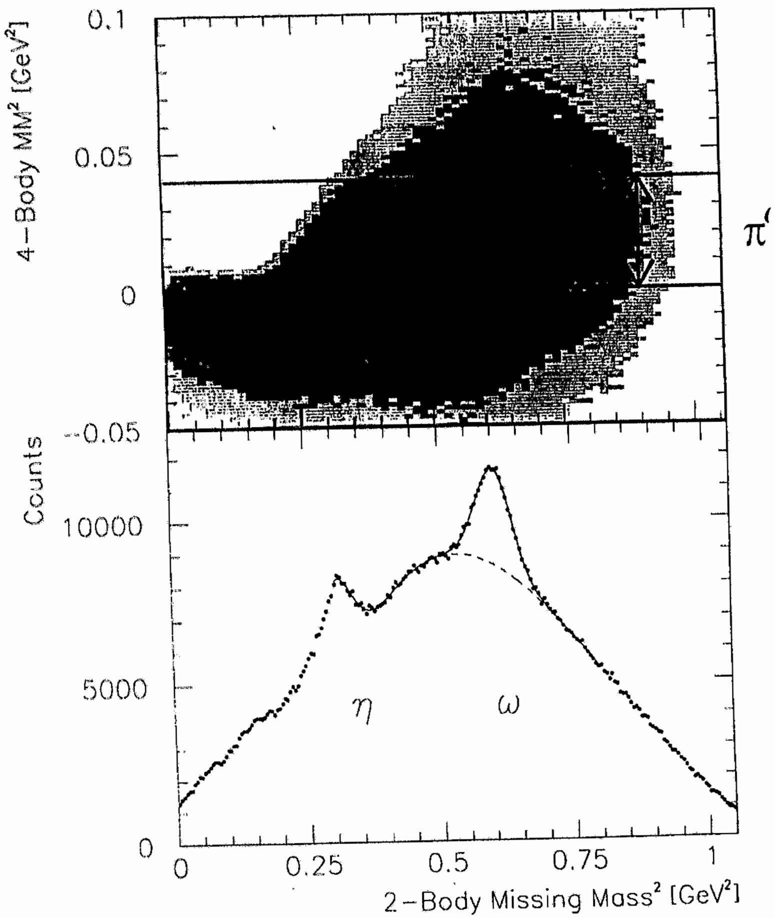

OZI Violation?

Dramatic in $p\bar{p}$ annihilation:

$s\bar{s}$ in the nucleon?

or 2-step processes?

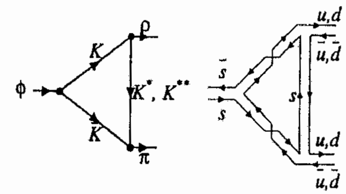

figure by V.E.Markushin

non-Dramatic:

pp high energies (factor 3-6)

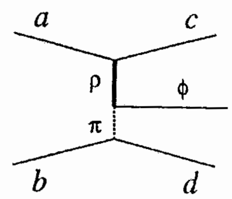

figure by A.I.Titov et al.

pp low energies (factor ~12)

2-step processes?

ϕ / ω - Ratio (Phys Rev Lett 81, 4572 (1998))

Ph.D. Thesis, A.Brenschede Giessen 1997

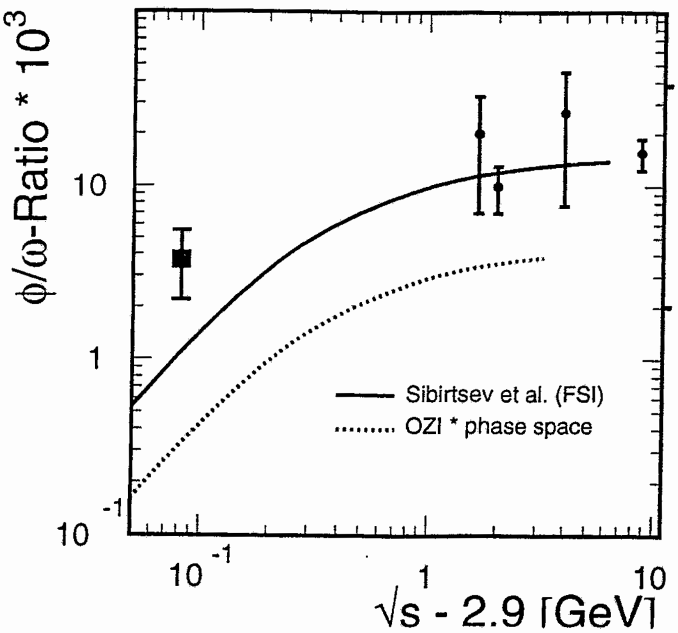

Factor 12 enhancement to OZI similar to higher energy pp-data
but LEAR up to 100

Sibertsev et al.: reasonable description with OME-Model

Data:
Arenton et al.: PRD 25 (82) 2241
Baldi et al.: PLB68 (77)
Blobel et al.: PLB59 (75)
S.V.Golovkin et al., ZPA359 (97)
Theory:

ϕ, ω Absolute Cross Section Ratio

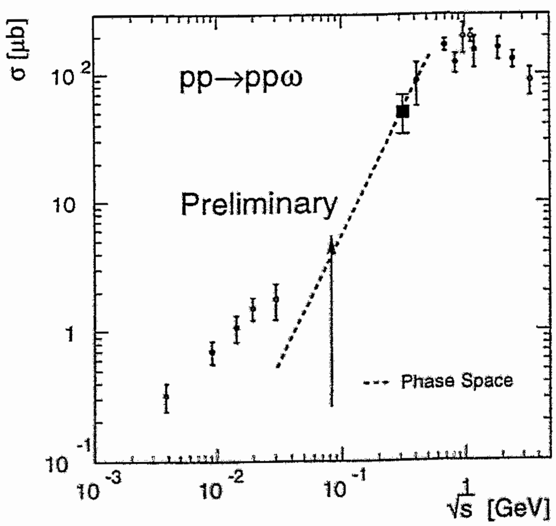

Preliminary

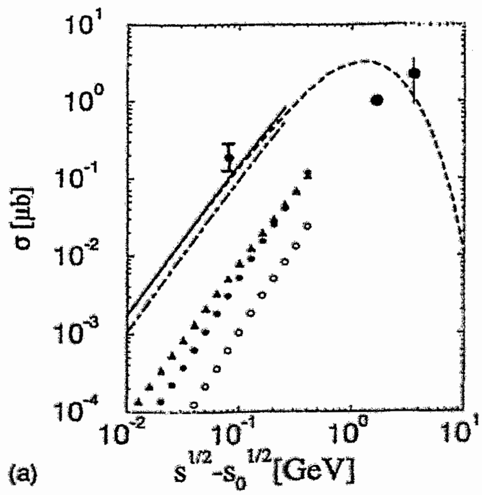

A.Titov, B. Kämpfer & V.Shklyar, PRC 59, 999 (99).

$\phi/\omega \sim 0.19/6 \sim 0.03$

OZI = 0.0043

ϕ / ω - *Angular Distributions*

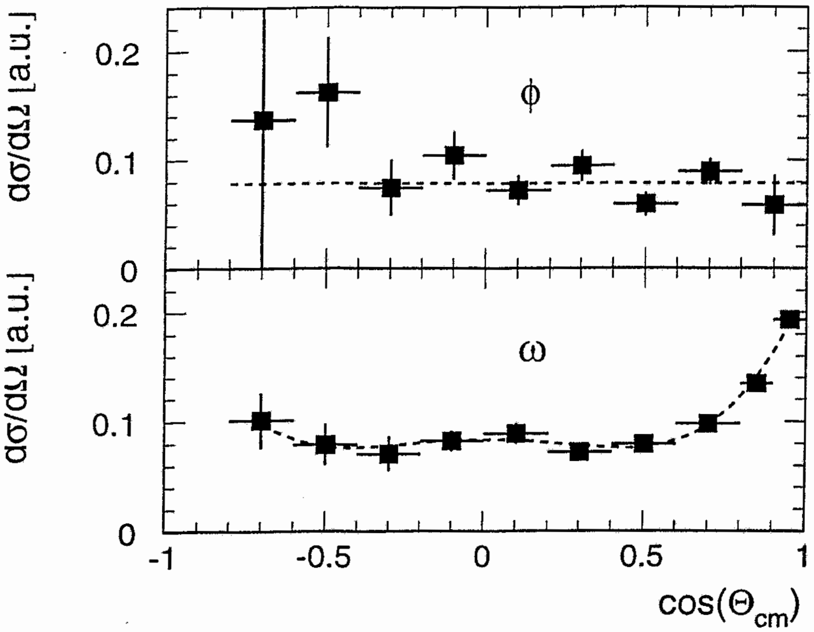

ϕ – mostly S-wave relative to pp system

ω – strongly peaked

Inclusive K⁻ Production

(No other channel Available)

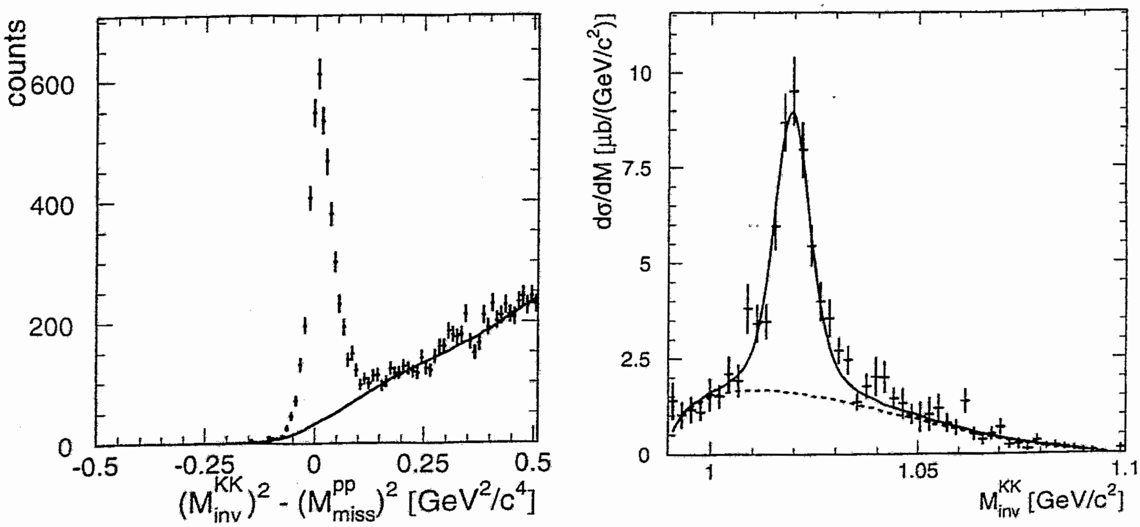

K^+K^- Absolute Cross Sections

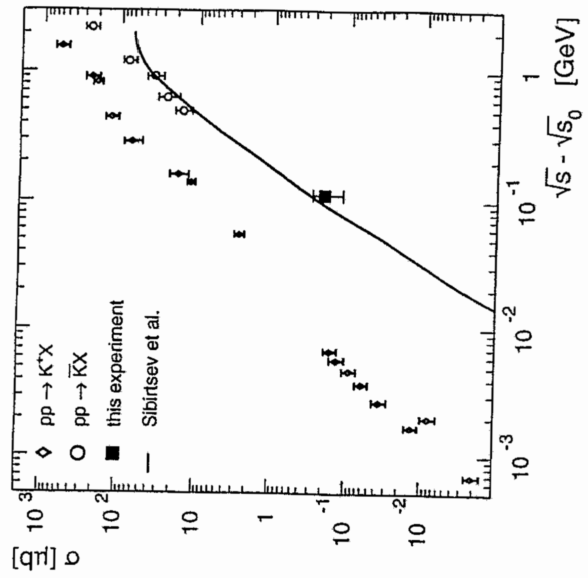

K^+K^- Production in pp and HI Reactions

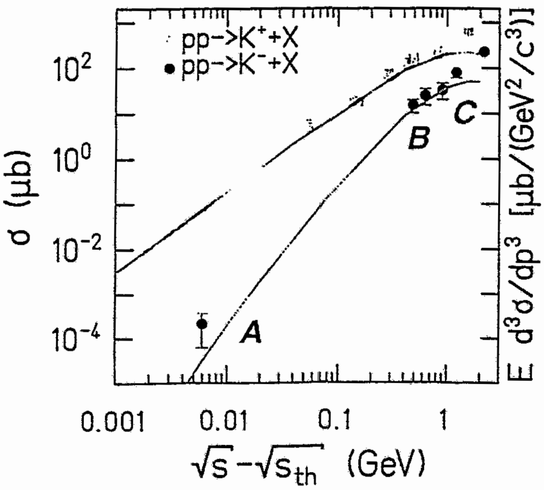

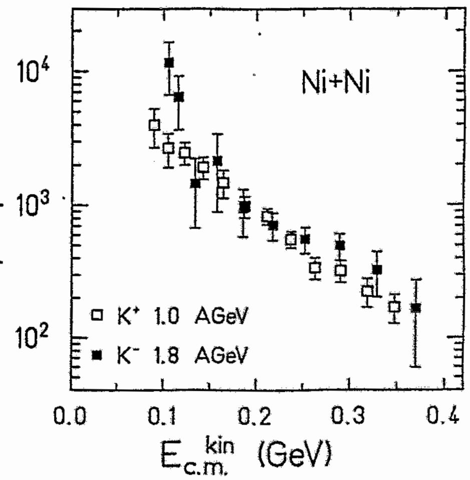

A Not Published

B Data from $ppK^0\bar{K}^0$

C Sum of Some Exclusive Channels

KaoS, PRL 78, 4007 (1997).

$Y\pi$ -> NK^- not sufficient

Cassing et al., NPA 614, 415 (1997)

Calculations: Sibirtsev et al ZPA351, 333(1995) & ZPA358, 101(1997)

Structure of the η' Meson

- ***By far heaviest member of PS nonet***
  958 MeV >> 135 MeV

- ***QCD fluctuations ($U_A(1)$ anomaly) allows***
  η' to gain mass from PS gluon states

- ***What is $g_{NN\eta'}$?***

- ***Coupling to baryon resonances?***

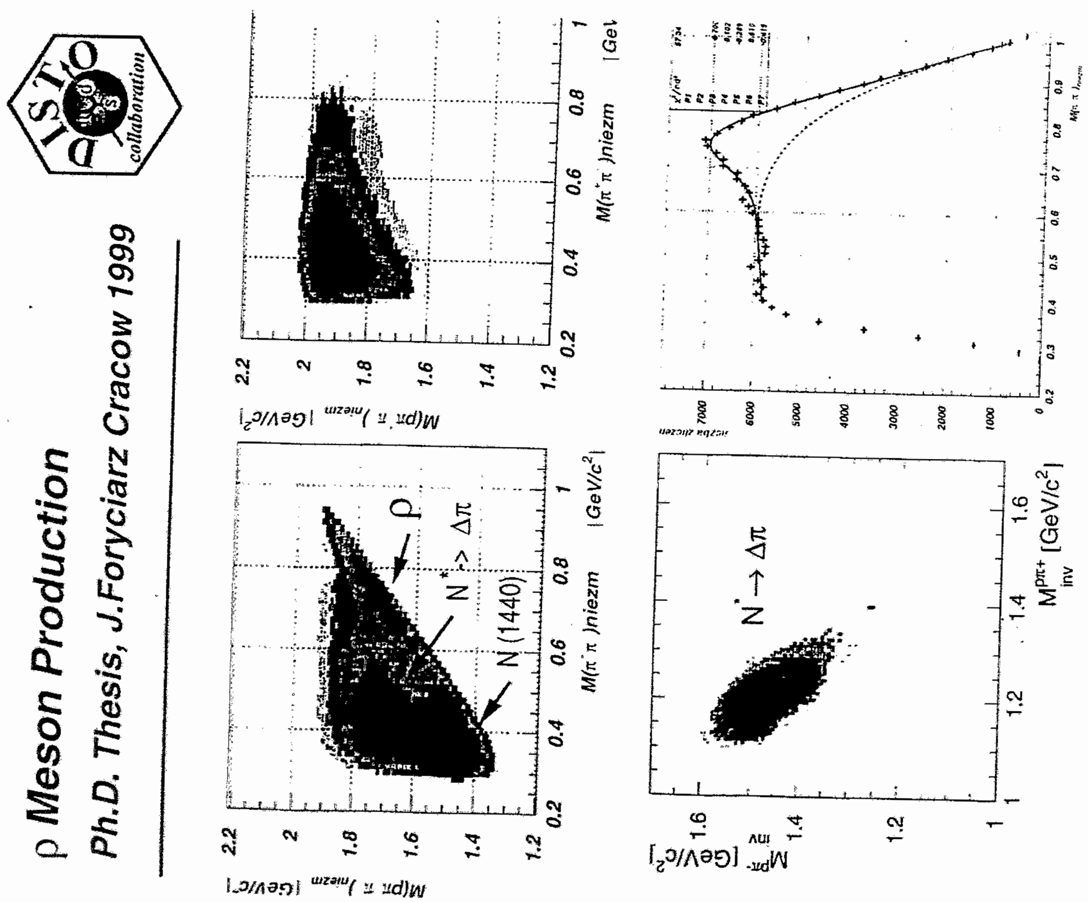

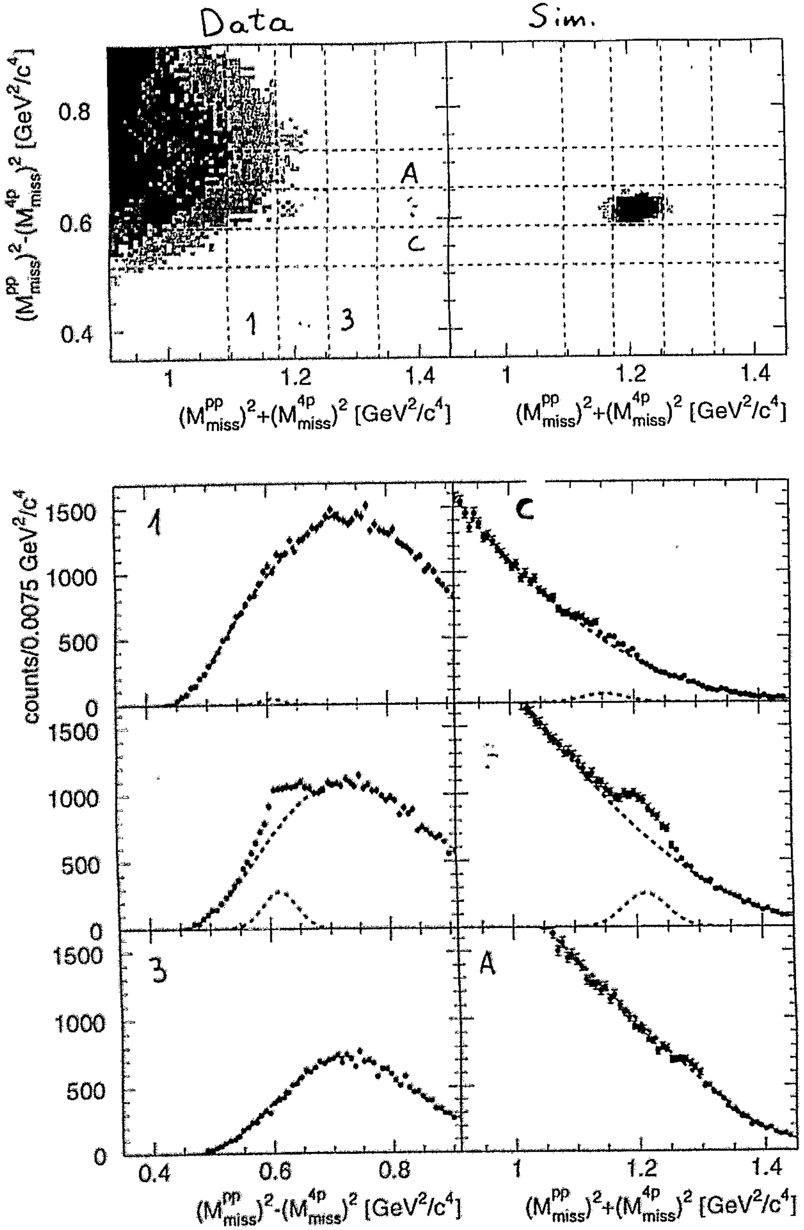

η' Production Cross Section

Ph.D. Thesis, H-W Pfaff Giessen 1999

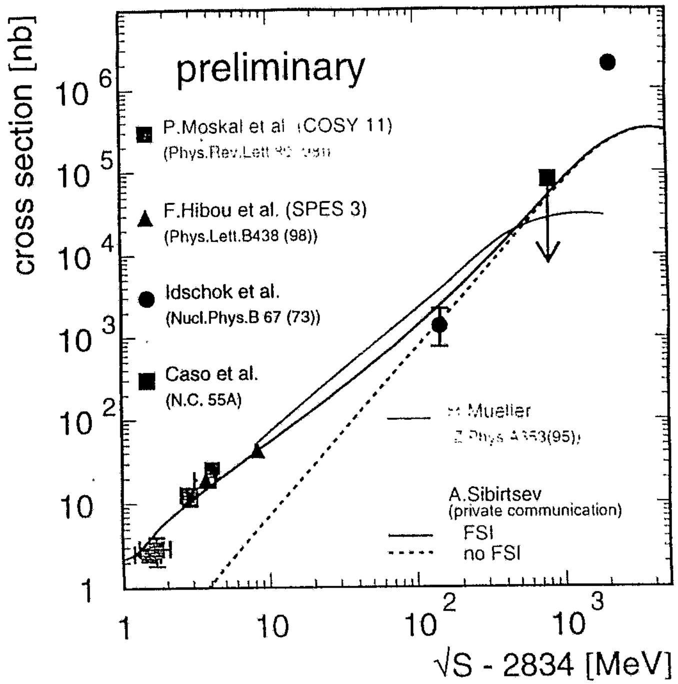

Production of ϕ and ω Mesons in Near-Threshold pp Reactions

F. Balestra,[4] Y. Bedfer,[3] R. Bertini,[3,4] L. C. Bland,[2] A. Brenschede,[8,*] F. Brochard,[3] M. P. Bussa,[4] V. Chalyshev,[1] Seonho Choi,[2] M. Debowski,[6] M. Dzemidzic,[2] I. V. Falomkin,[1] J.-Cl. Faivre,[3] L. Fava,[4] L. Ferrero,[4] J. Foryciarz,[6,7] V. Frolov,[1] R. Garfagnini,[4] D. Gill,[10] A. Grasso,[4] E. Grosse,[5,†] S. Heinz,[3] V. V. Ivanov,[1] W. W. Jacobs,[2] W. Kühn,[8] A. Maggiora,[4] M. Maggiora,[4] A. Manara,[3,4] D. Panzieri,[4] H.-W. Pfaff,[8] G. Piragino,[4] G. B. Pontecorvo,[1] A. Popov,[1] J. Ritman,[8] P. Salabura,[6] P. Senger,[5] J. Stroth,[9] F. Tosello,[4] S. E. Vigdor,[2] and G. Zosi[4]

(DISTO Collaboration)

[1]*JINR, Dubna, Russia*
[2]*Indiana University Cyclotron Facility, Bloomington, Indiana*
[3]*Laboratoire National Saturne, CEA Saclay, France*
[4]*Dipartimento di Fisica "A. Avogadro" and INFN, Torino, Italy*
[5]*Gesellschaft für Schwerionenforschung, Darmstadt, Germany*
[6]*M. Smoluchowski Institute of Physics, Jagellonian University, Kraków, Poland*
[7]*H. Niewodniczanski Institute of Nuclear Physics, Kraków, Poland*
[8]*II. Physikalisches Institut, University of Gießen, Gießen, Germany*
[9]*Institut für Kernphysik, University of Frankfurt, Frankfurt, Germany*
[10]*TRIUMF, Vancouver, Canada*
(Received 26 August 1998)

The ratio of the exclusive production cross sections for ϕ and ω mesons has been measured in pp reactions at $T_{\mathrm{beam}} = 2.85$ GeV. The observed ϕ/ω ratio is $(3.7 \pm 0.7^{+1.2}_{-0.9}) \times 10^{-3}$. After phase space corrections, this ratio is about a factor of 10 enhanced relative to naive predictions based upon the Okubo-Zweig-Iizuka rule, in comparison to an enhancement by a factor of ~3 previously observed at higher energies. The modest increase of this enhancement near the production threshold is compared to the much larger increase of the ϕ/ω ratio observed in specific channels of $\bar{p}p$ annihilation experiments.
[S0031-9007(98)07664-9]

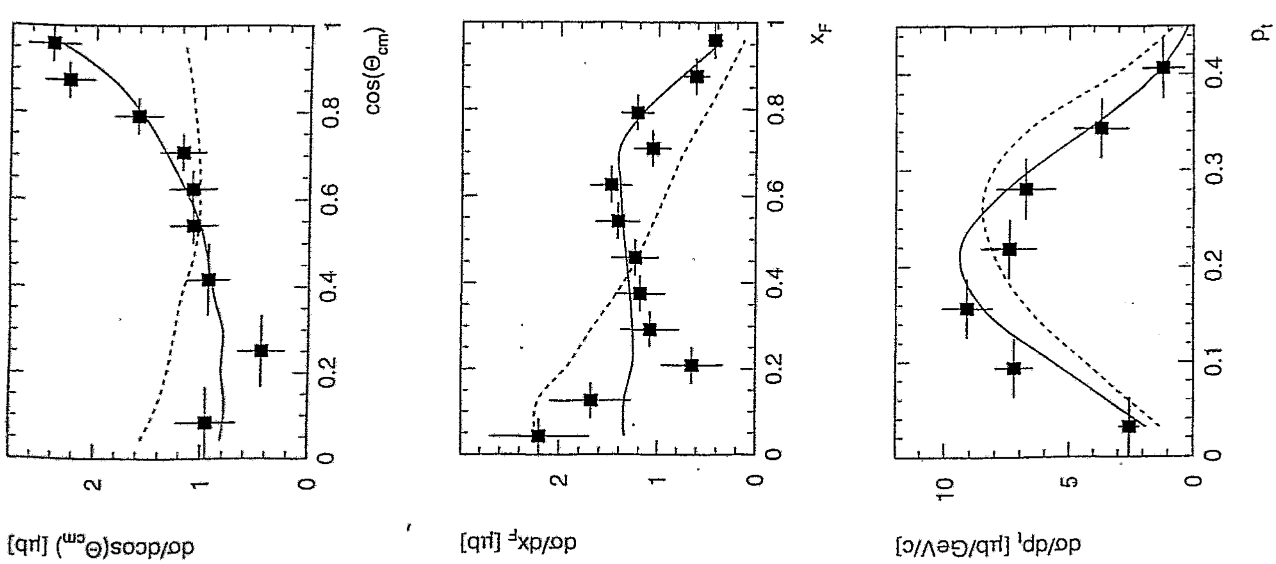

Summary & Outlook

- *First measurement of* ϕ *meson near threshold* in pp
- ϕ/ω *Ratio rises slightly at threshold*
- *What is Strangeness content of protons?*
- *Higher statistics -> polarization observables?*
- *First measurement of inclusive* K^- *yield*
- ρ *Meson identifcation*
- η*'NN Measured with small FSI*
- *2.1 & 2.5 GeV Data:* ω,η' *Excitation function*

V. Hejny:

Photoproduction of light mesons – results from TAPS at MAMI

Photoproduction of light mesons with TAPS at MAMI

V. Hejny
II. Physikalisches Institut, Universität Gießen *
for the
TAPS - Collaboration
and the
A2 - Collaboration

- ☐ Introduction
- ☐ Experimental Setup
- ☐ Particle Identification
- ☐ Results
  - π^0, 2π and η production from p,n and nuclei
- ☐ Summary

* present address: Institut für Kernphysik, Forschungszentrum Jülich

Introduction

goal: investigations on the **nucleon** by **photoexcitation** and observation of the decay into **mesons**

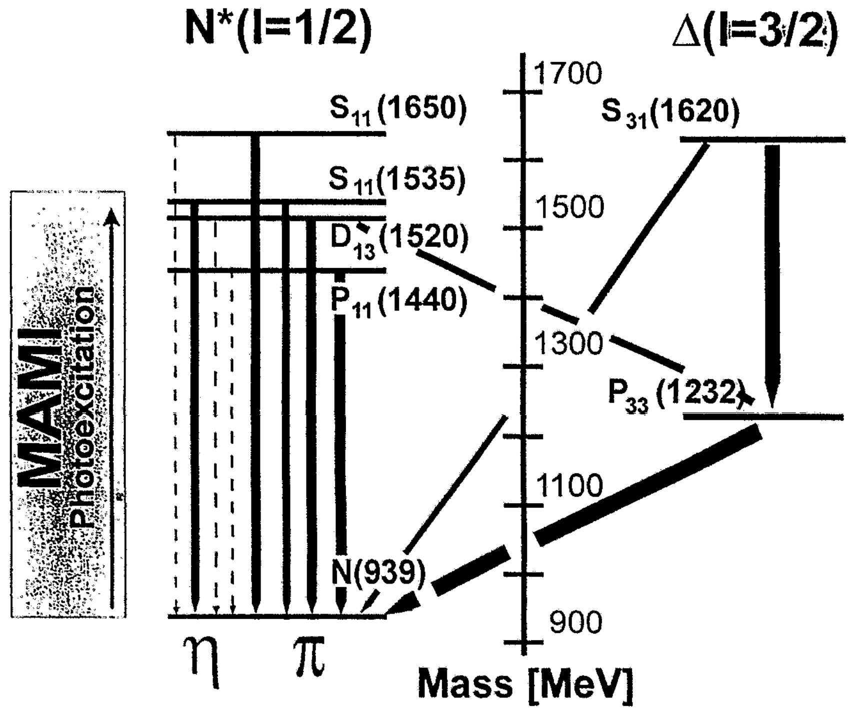

p,d,^{4}He	cross sections and resonance properties on proton and neutron
d,^{4}He,C, Ca,Nb,Pb	e.g. medium modifications of resonances

Experimental Setup

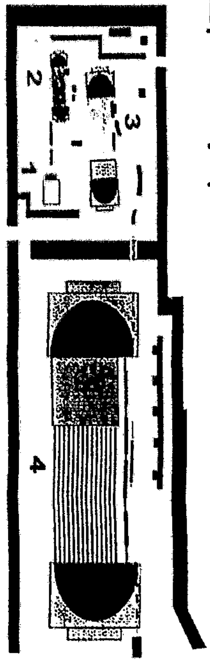

MAMI: High Quality cw-Beam

$E_{electron}$ = 180 - 880 MeV
Duty Factor = 100 %

TAGGER: Tagged Photons

ΔE = 2 MeV (at E = 880 MeV)

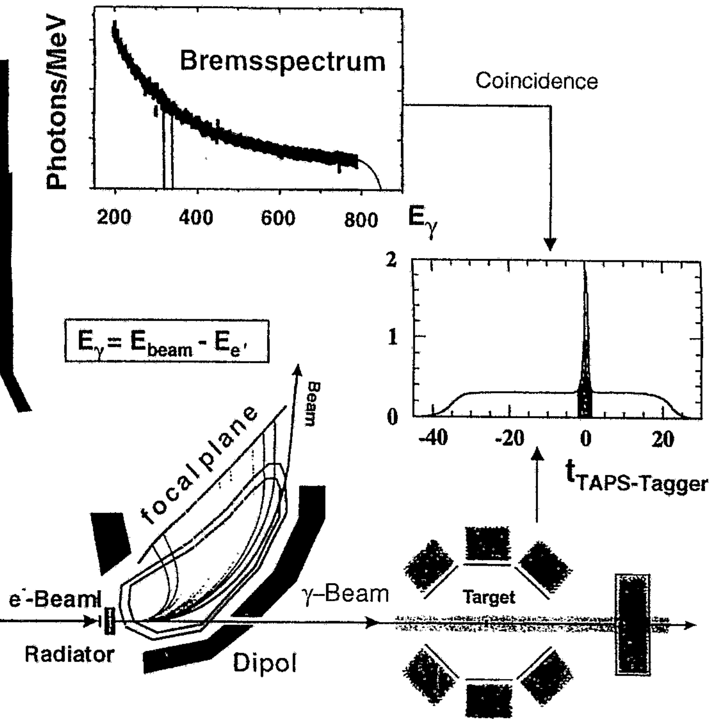

TAPS: BaF_2-Photon-Spectrometer

TAPS setup

detector setup:

6 BaF_2 blocks

- 64 crystals
- 64 individual veto detectors

forward wall:

- 120 plastic-BaF_2 phoswich-moduls

scattering chamber with liquid helium or deuterium target

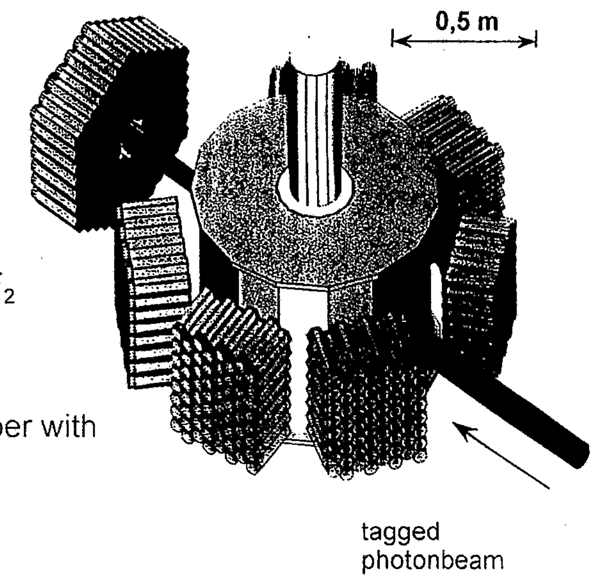

standard TAPS modul:

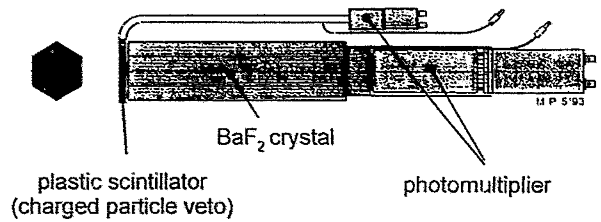

Identification of mesons

decay channel $\eta,\pi^0 \rightarrow 2\gamma$

→ photon identification

- charged particle identification using **veto counters**
- particle discrimination exploiting BaF_2 **pulse shape**
- **photon-photon coincidence** within BaF_2 time resolution ($\sigma \sim 150$ps)

→ invariant mass analysis

$$m_{\gamma\gamma} = \sqrt{(E_1+E_2)^2-(\vec{p}_1+\vec{p}_2)^2} = \sqrt{2E_1E_2(1-\cos\vartheta_{12})}$$

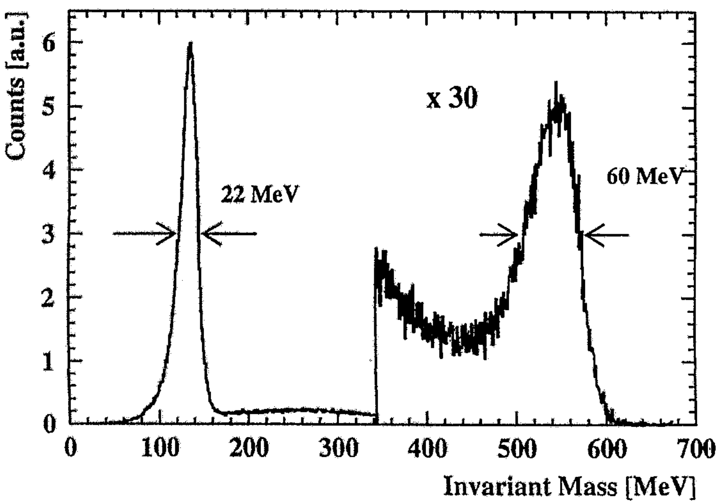

pulse shape analysis

→ intrinsic feature of BaF_2

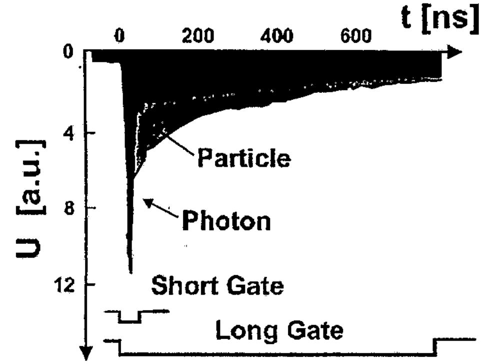

→ puls shape spectra
(forward wall and standard BaF_2)

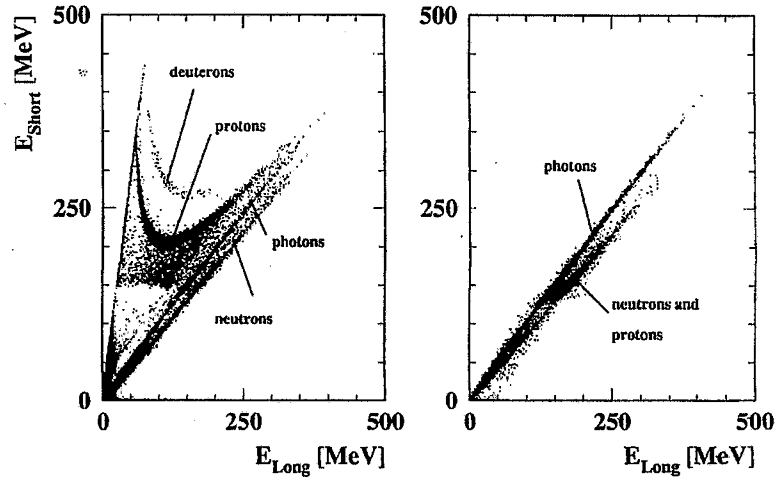

Photoabsorption on Nuclei

Biachi et al.,
Phys. Lett. B 325
(1994)

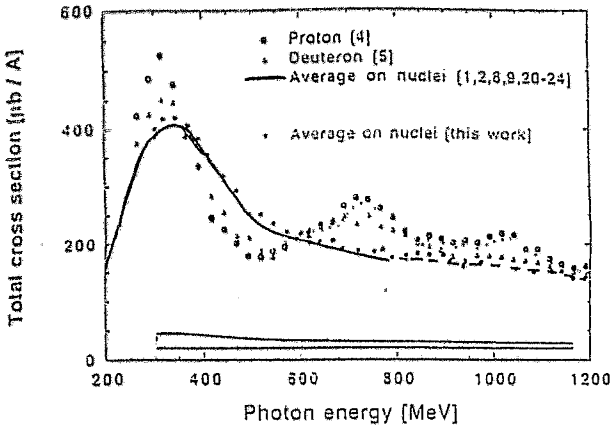

Different Channels on Proton:

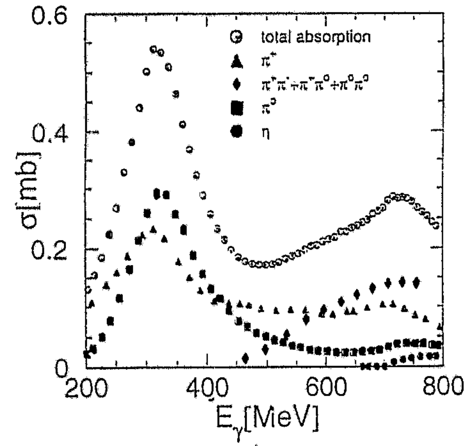

η production fom p and n

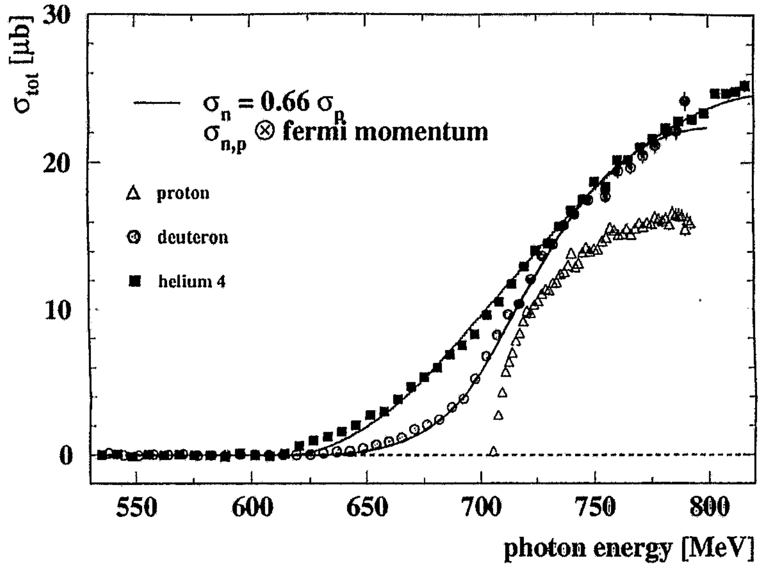

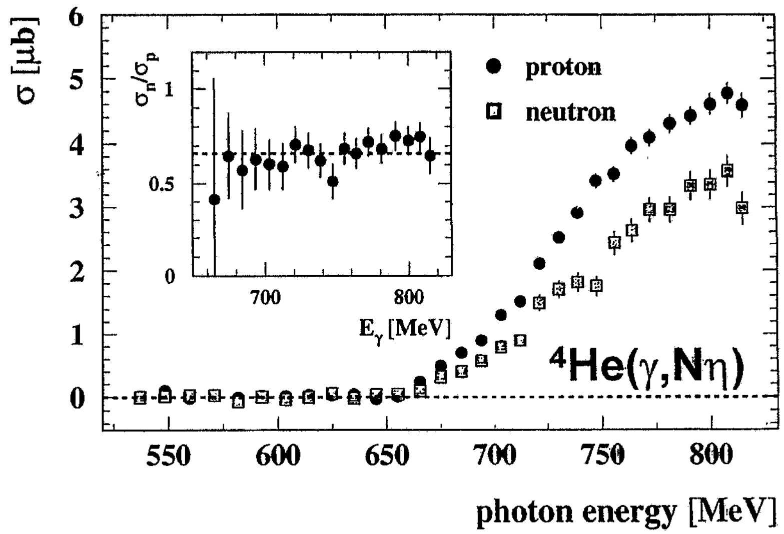

$\sigma_n/\sigma_p = 2/3$

A(γ,η)X: data <-> models

Input: processes p(γ,η)p, n(γ,η)n
fermi motion
η, N* propagation in nuclei
Pauli blocking of final states
collision broadening

R.C. Carrasco (Valencia) Phys. Rev. C 48 (1993) — A. Hombach et al. (Gießen) Z. Phys. A (1995)

η mean free path Monte Carlo — η,N* propagation as in heavy ion collisions

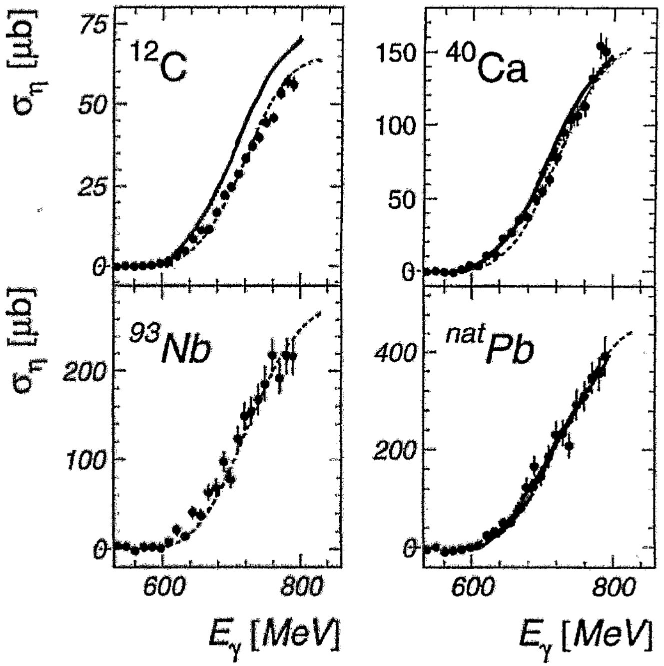

π^0 production from p and d

total cross section:

sp ⊗ fermi momentum

η: fermi motion dominant effect on d (and ^{4}He)

π^0: additional ´deuteron effects´
no theoretical description yet available

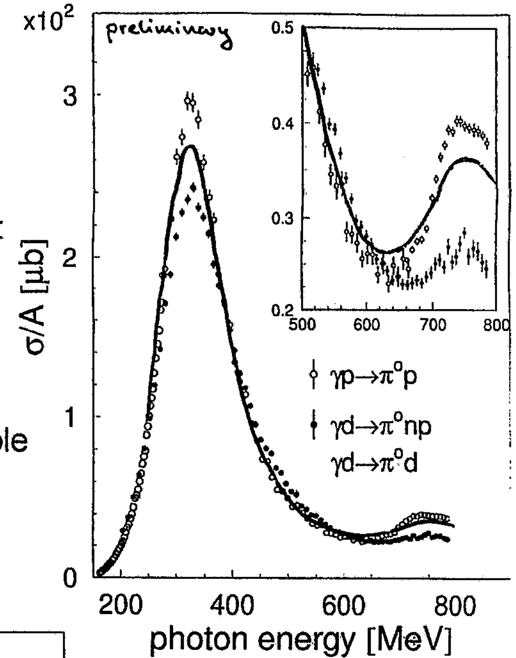

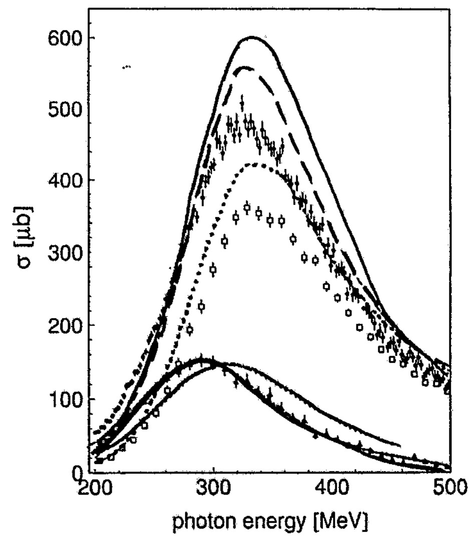

deconı... and quas...

Laget et al.:
coherent
breakup without FSI
breakup with pn-FSI

Kamalov et al.
Wilhelm et al.
Schmidt et al.

$A(\gamma,\pi^0)X$: total cross sections

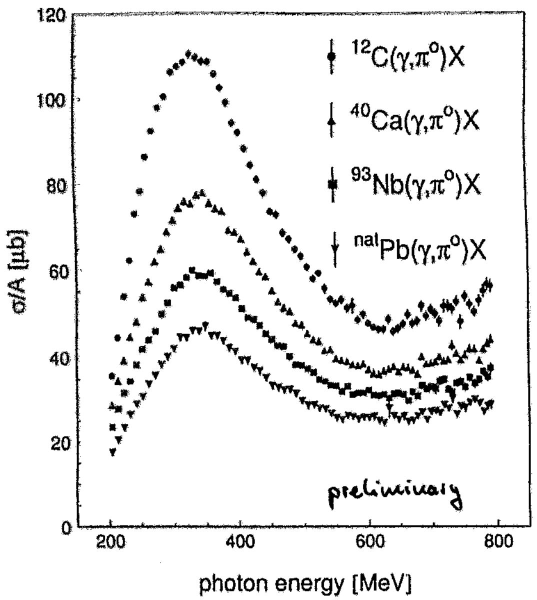

mass number dependence

$\sigma(A) \sim A^{\alpha}$

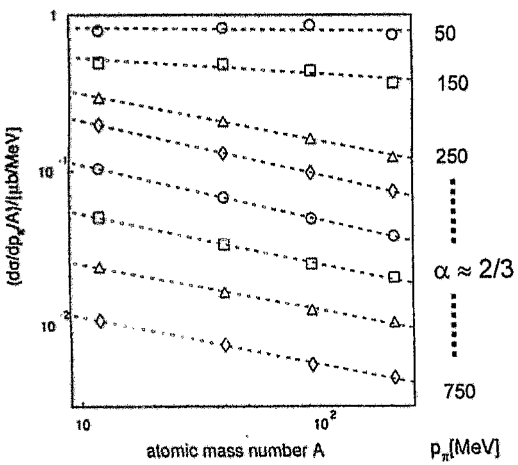

$(\sigma/A^{2/3})/(\sigma(^{12}C)/12^{2/3})$

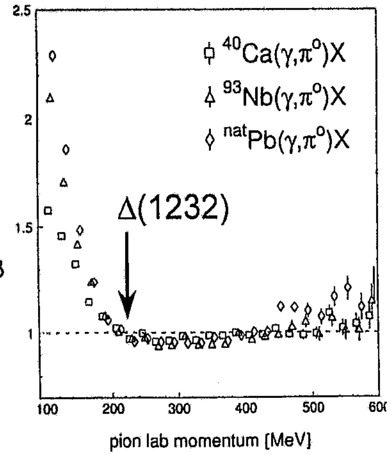

$A(\gamma,\pi^0)X$: models

Model:
(Effenberger et al.)

standard BUU

Δ absorption from Δ-hole models

additional medium modification for ρ meson:

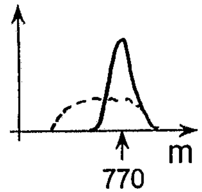

$m_\rho \downarrow \;\Rightarrow\; \Gamma_{N\rho}(D_{13})\uparrow$

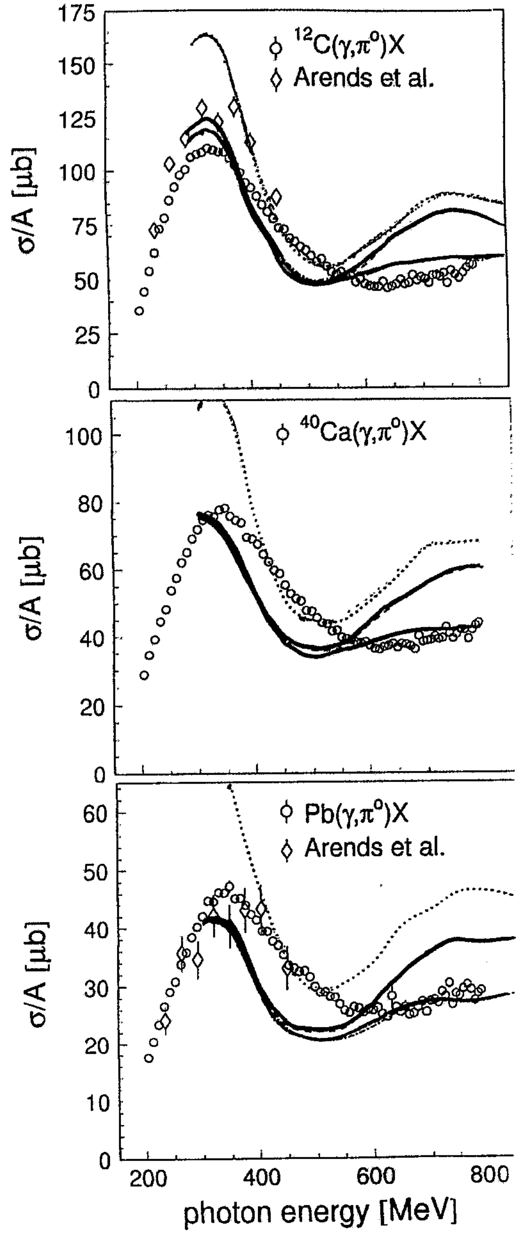

$Pb(\gamma,\pi^0)Pb$: Identification

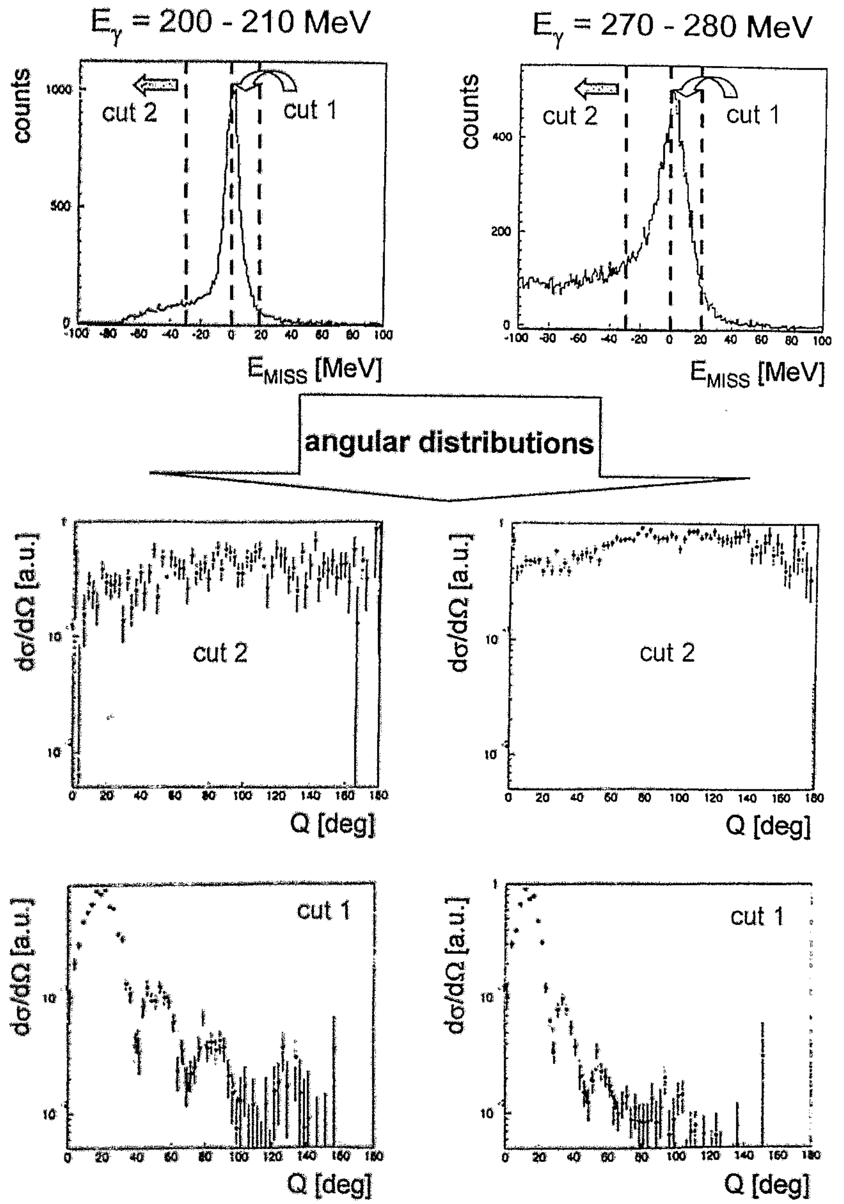

$A(\gamma,\pi^0)A$: Δ resonance modification ?

model: (Peters et al.)

relativistic, non-local DWIA

- ······ free production operator
- – – full nucleon prop. + δm_Δ = -30 MeV
- —— full nucleon prop. + δm_Δ = -30 MeV + $\delta\Gamma_\Delta$ = 20 MeV

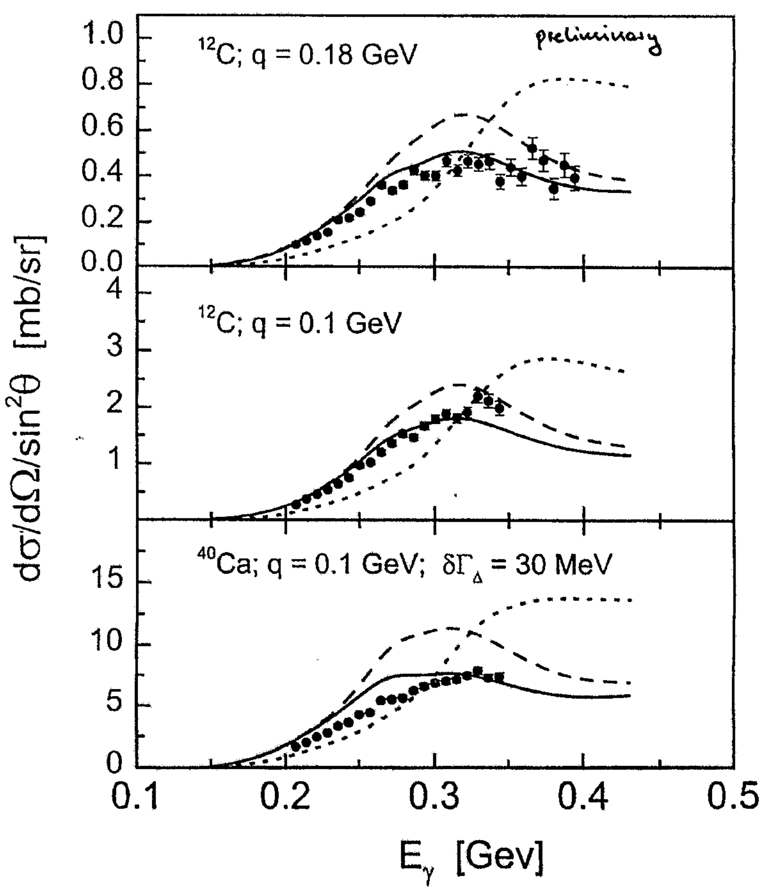

$p(\gamma,\pi^0\pi^0)p$

Total Cross Section:

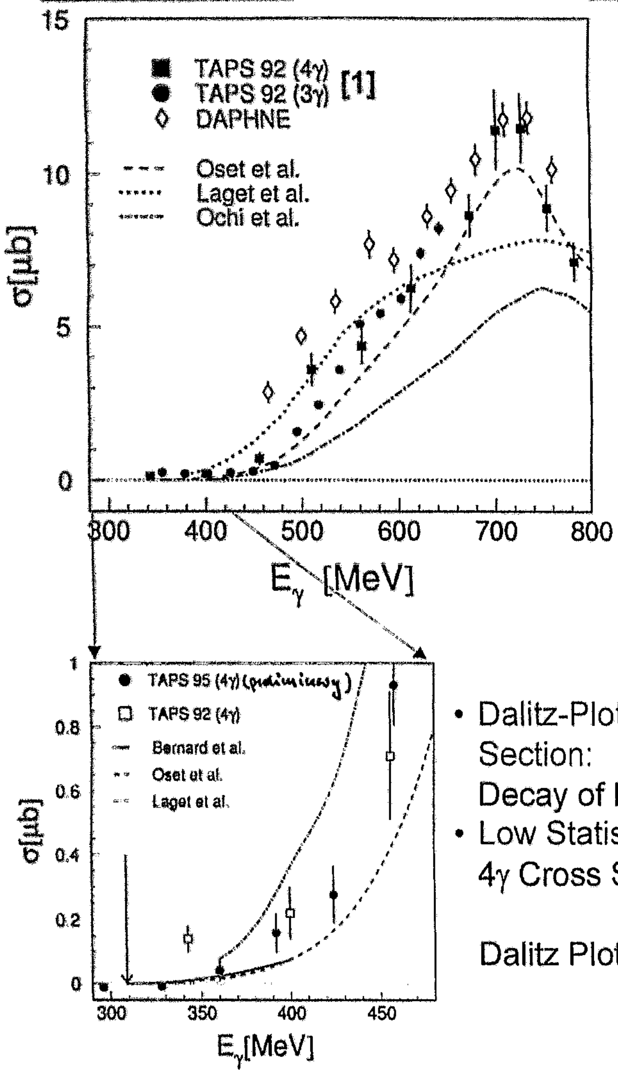

Dalitz Plots (4γ-Events):

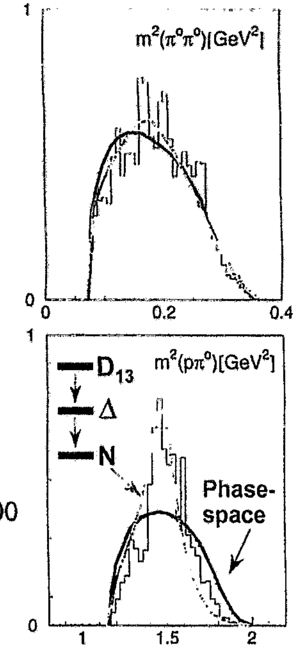

- Dalitz-Plots & Total Cross Section:
  Decay of D_{13} via Δ
- Low Statistics at Threshold:
  4γ Cross Section
  ⇒ Exp. 1995
  Dalitz Plots
  ⇒ New Proposal

[1] Härter et al.,
Phys.Rev. C55 (1997) 359

$d(\gamma,\pi^0\pi^0)X$: $n(\gamma,\pi^0\pi^0)n$

total cross sections
on proton and
deuteron

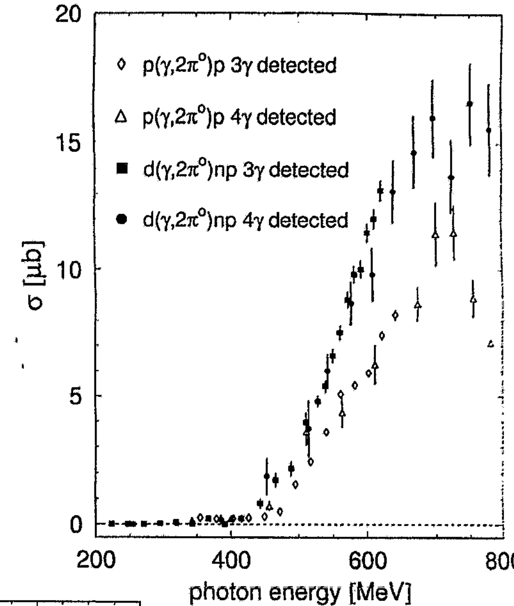

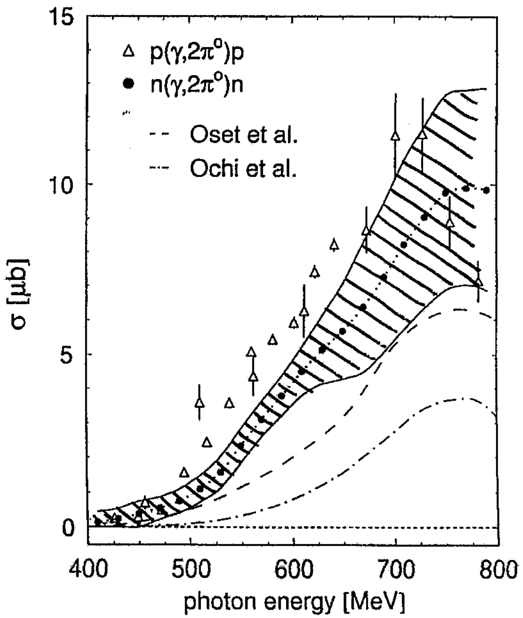

extracted cross
section on the

same model used as
in η photoproduction

$A(\gamma,\pi^0\pi^0)X$: total cross sections

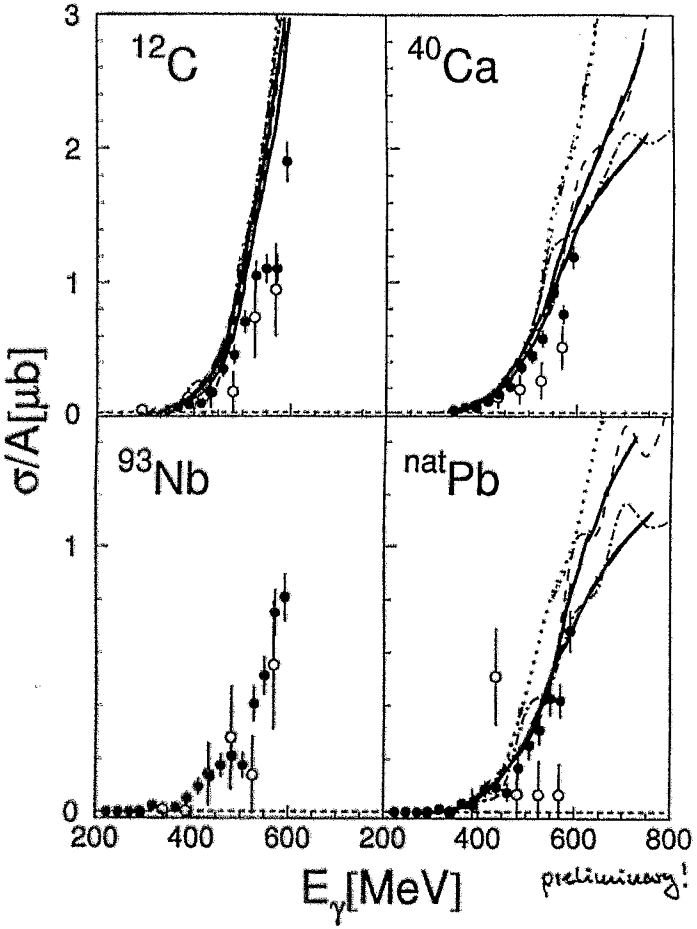

(Effenberger et al.)

- standard BUU
- Δ-absorpt. from Δ-hole models
- D_{13} medium effekt ($D_{13} \rightarrow N\rho$)

Summary

- photoproduction of π^0, 2π and η mesons measured on proton, deuteron and complex nuclei

  ⇨ medium modifactions ?

- no effects seen for $S_{11}(1535)$ resonance using η photoproduction

- coherent π^0 data can be described assuming \ modifications: δm_Δ = -30 MeV, $\delta\Gamma_\Delta$ = 20 MeV (Peters et al.)

- calculations of π^0 and $2\pi^0$ channel on nuclei give better descriptions assuming modifications of the ρ meson (smaller mass, larger width) (Effenberger et al.)

- no models available for missing strength in π^0 production from d in the second resonance region (FSI seems very important)

O. Scholten:

Proton–proton bremsstrahlung

Proton - proton bremsstrahlung

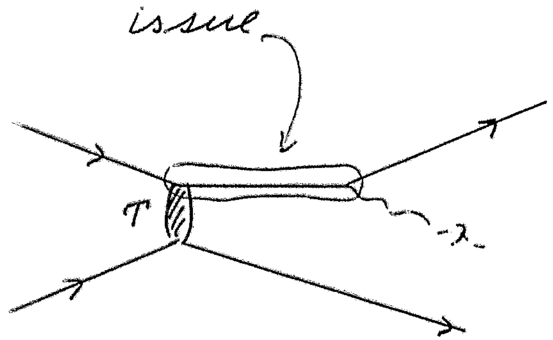

Olaf Scholten

Groningen

Proton - proton bremsstrahlung

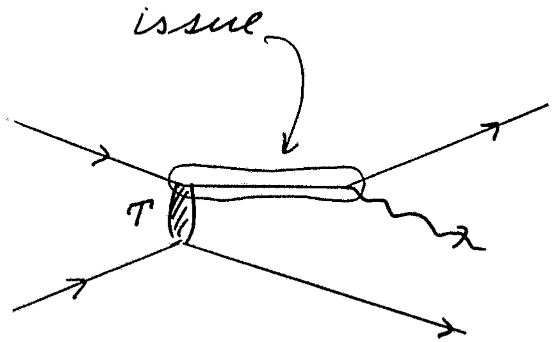

Full calculation of off-shell effects

G. Martinus

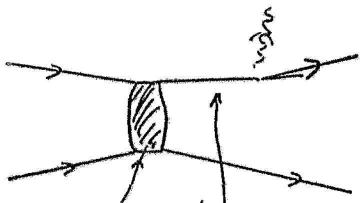

Fleischer, Tjon

T-matrix, full relativity

Blankenbecler - Sugar

full propagator $\frac{\not p - m}{p^2 - m^2}$

- Positive energy states (nucleon)
- Negative energy states ("anti-nucleon")

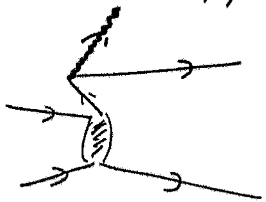

Z-graphs

Important ?!

	pos E	neg E
Propagator : $\frac{1}{\Delta E}$	$\simeq \frac{1}{q}$	$\simeq 1/M$
$\langle \Gamma_\gamma \rangle$:	$\sim \lvert\vec{p}\rvert / M$	~ 1
×	$\frac{\lvert\vec{p}\rvert}{q} \frac{1}{M}$	$\frac{1}{M}$

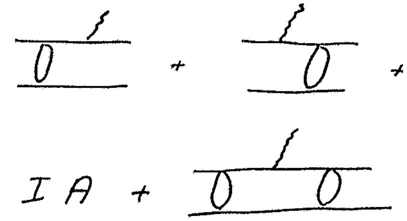

+ : Project on positive energy states in intermediate propagators

+/− : keep Dirac propagators

IA : Impuls Approx ≡ Born terms

Full : include rescattering

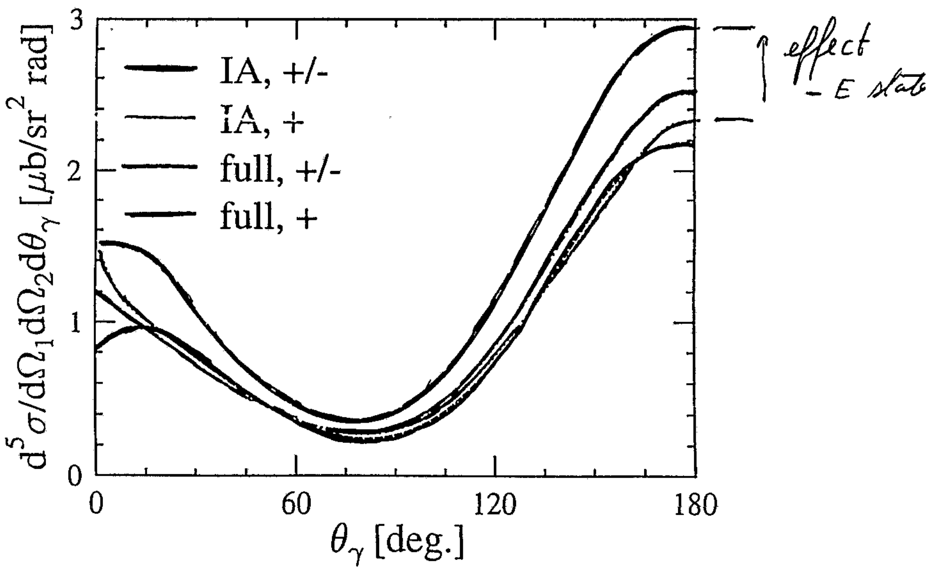

E = 280 MeV , $\theta_1 = 12°$, $\theta_2 = 12.4°$

N-N Potential

Fleischer-Tjon

Blankenbecler-Sugar

3 D reduction of Bethe-Salpeter
Evaluate kernel at $\mathcal{E} = 0$

V : O B E

cutoff : $\frac{\Lambda^2}{\Lambda^2 - p^2}$; $\Lambda^2 = 1.5\, M^2$

in bremsstrahlung :

equal-time approx.

effect approx. : few percent decrease of σ

Meson Exchange Currents

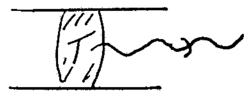

mechanism :

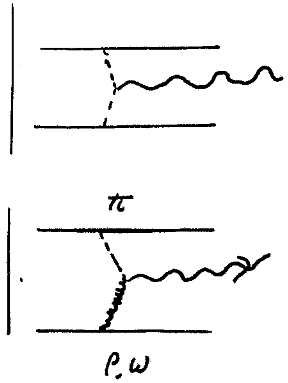

large for pn

$\simeq 0$ for pp

add to $pp\gamma$

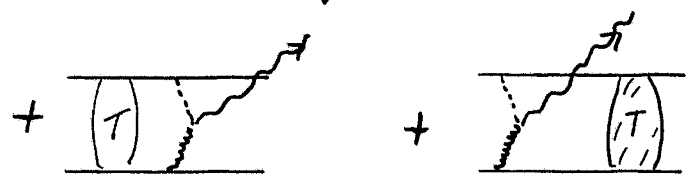

Microscopic Model Calculations

G. Martinus

- Relativistic T-matrix
  Fleischer-Tjon OBE potential
  Blankenbecler-Sugar
- Full relativity
  negative energy states
  "Z-graphs"
- Rescattering

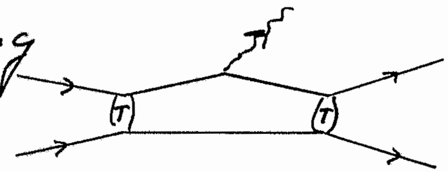

- Meson exchange currents

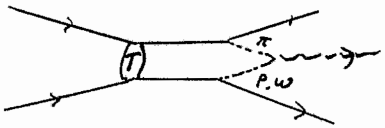

- Δ-isobar currents

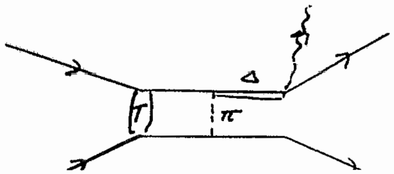

190 MeV

Proton-Proton Bremsstrahlung

$\vec{p} + p \rightarrow p + p + \gamma$

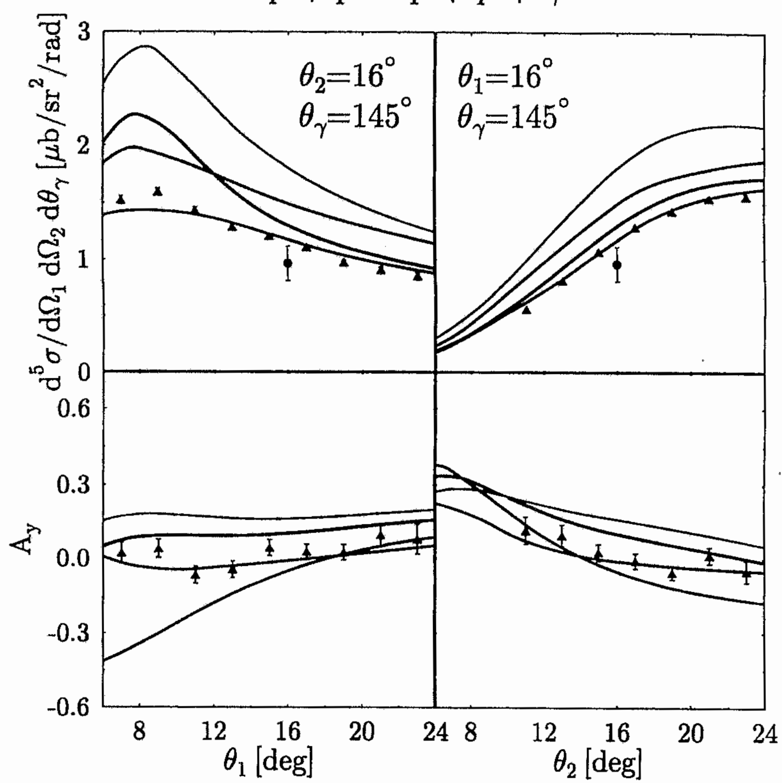

- SPA by Timmermans, Gibson and Liou
- Full calculation by K. Nakayama
- Full calculation by Martinus et al.
- Full calculation by J. Eden et al.
- Data point: Rogers et al. PRC **22** 2512 (1980)

Data by Harry Huisman

KVI

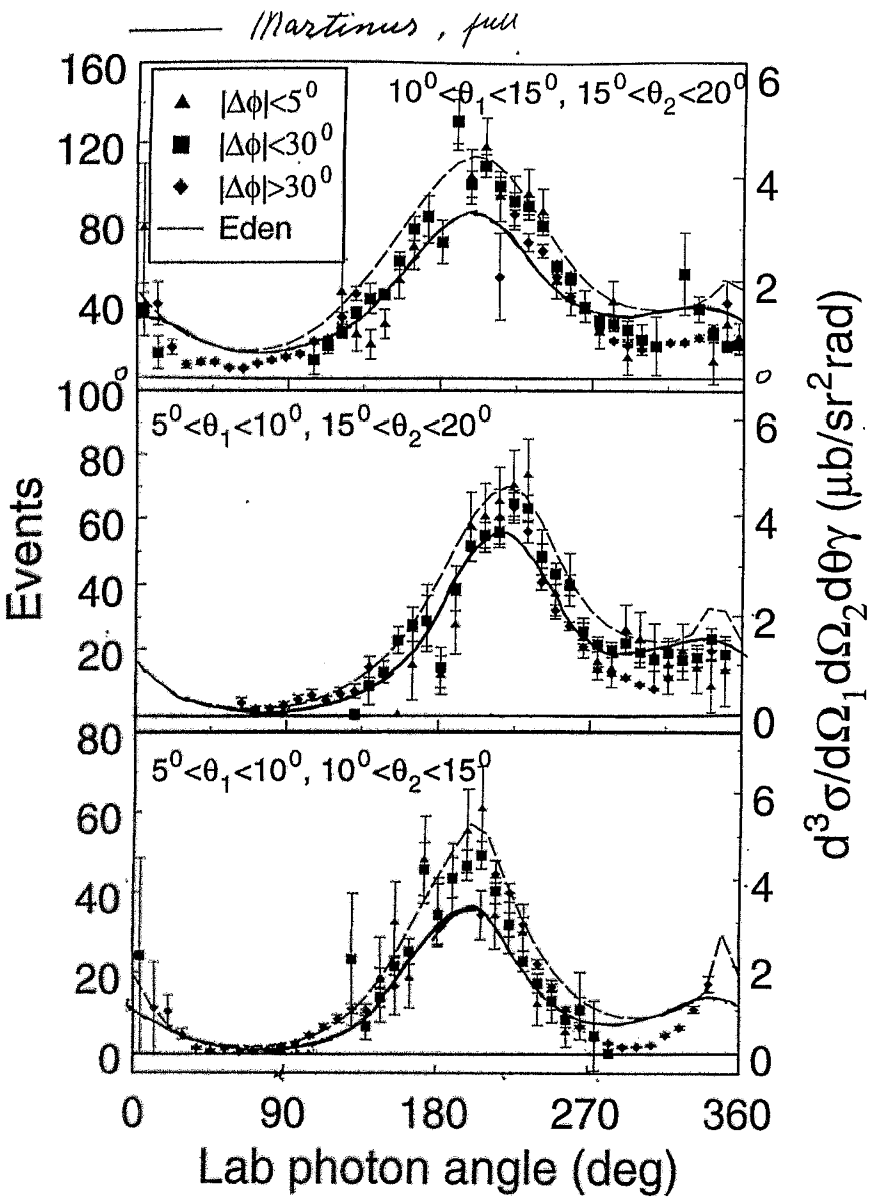

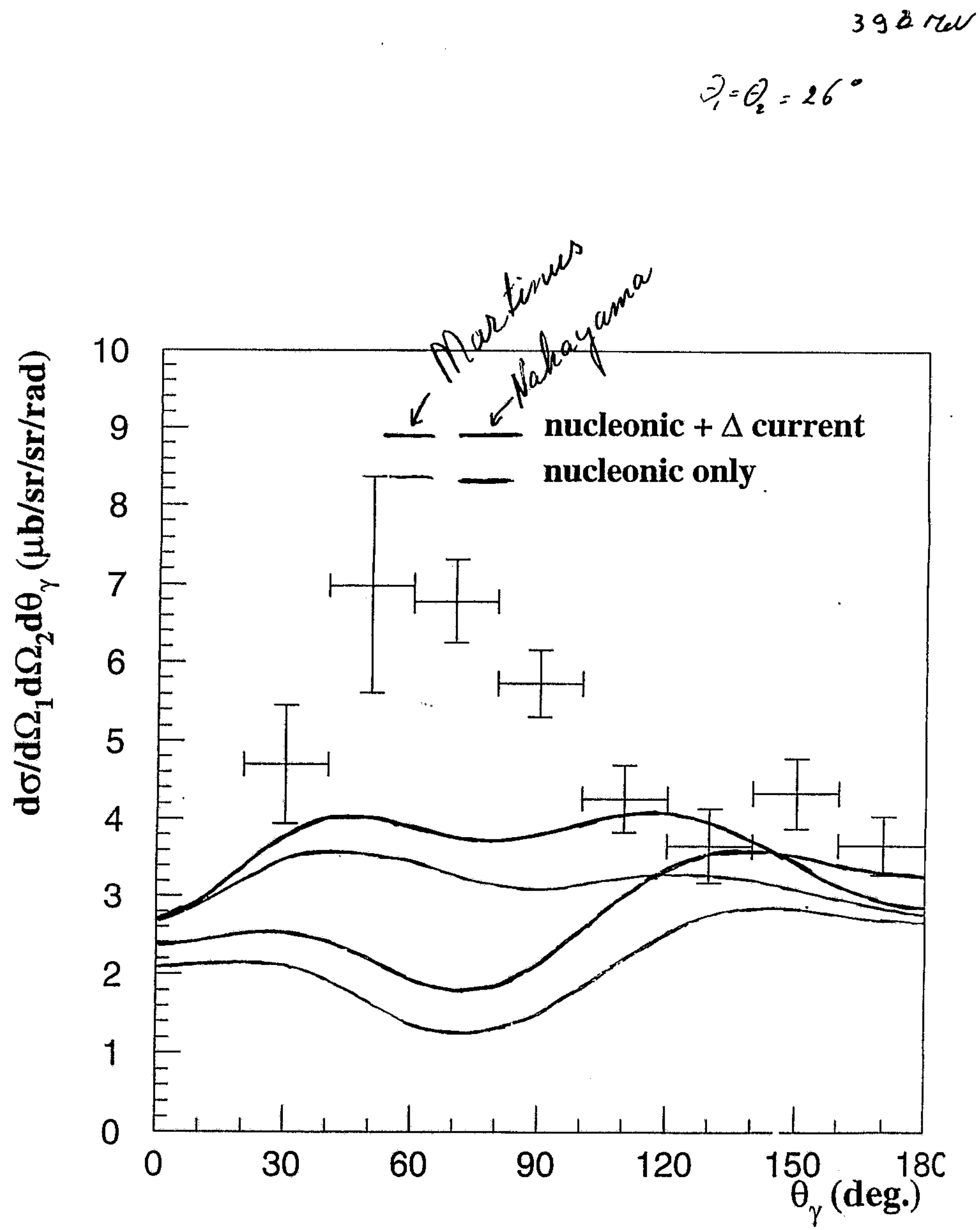

Figures from Jozef Zlomanczuk, Uppsala, 310MeV

~~Preliminary Data~~

Present day calculations

Include:

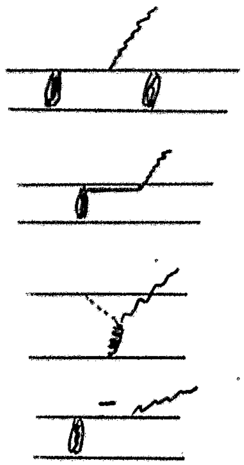

Very advanced ;

disagreement with (some) data

KVI	190 MeV	norm
COSY	280	~ OK
Uppsala	320	~ OK
Osaka	392	shape

Additional

Off - shell effects

or equivalently

Dynamics of interacting N

or equivalently

meson loop corrections to
- N - self energy
- NN - vertices

in progress

What can we learn?

missing ingredients

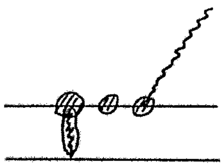

- T-matrix
  - Coupling to neg E states
  - structure intermediate 2 nucleon prop.
- Propagator: $\frac{1}{\not p - m + \Sigma(P)}$ 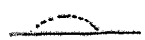
- γ-vertex: $\gamma^\mu + \frac{i\kappa}{2m} F(p^2)\, \sigma^{\mu\nu} q_\nu$
- Contact terms:

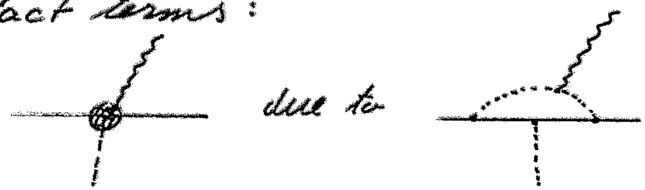

Different effects indistinguishable from each other

J. Kondratiuk

Off-shell form factors

Speculative

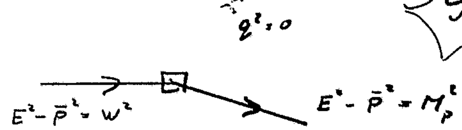

$$\Gamma^\mu(W^2) = e\left[\tilde F_1(W^2)\,\gamma^\mu + i\tilde F_2(W)\,\sigma^{\mu\nu} q_\nu / 2M\right]$$

Current conservation: $F_1(w) \equiv 1$

$$\tilde F_2(W) = F_2^+(W^2)\Lambda^+ + F_2^-(W^2)\Lambda^-$$

$$F_2^+(W^2) = \kappa + \kappa\, k\, \frac{W^2 - m^2}{m^2} + \dots$$

κ: Proton magn. moment; k: free parameter; χPT: $k \simeq 2$

$$F_2^-(W^2) = \kappa^- + \dots$$

κ^-: free parameter

1 loop calculations:

$$-5\kappa < \kappa^- < 20\kappa$$

Model:

$k^- = 0$ $k = 2$

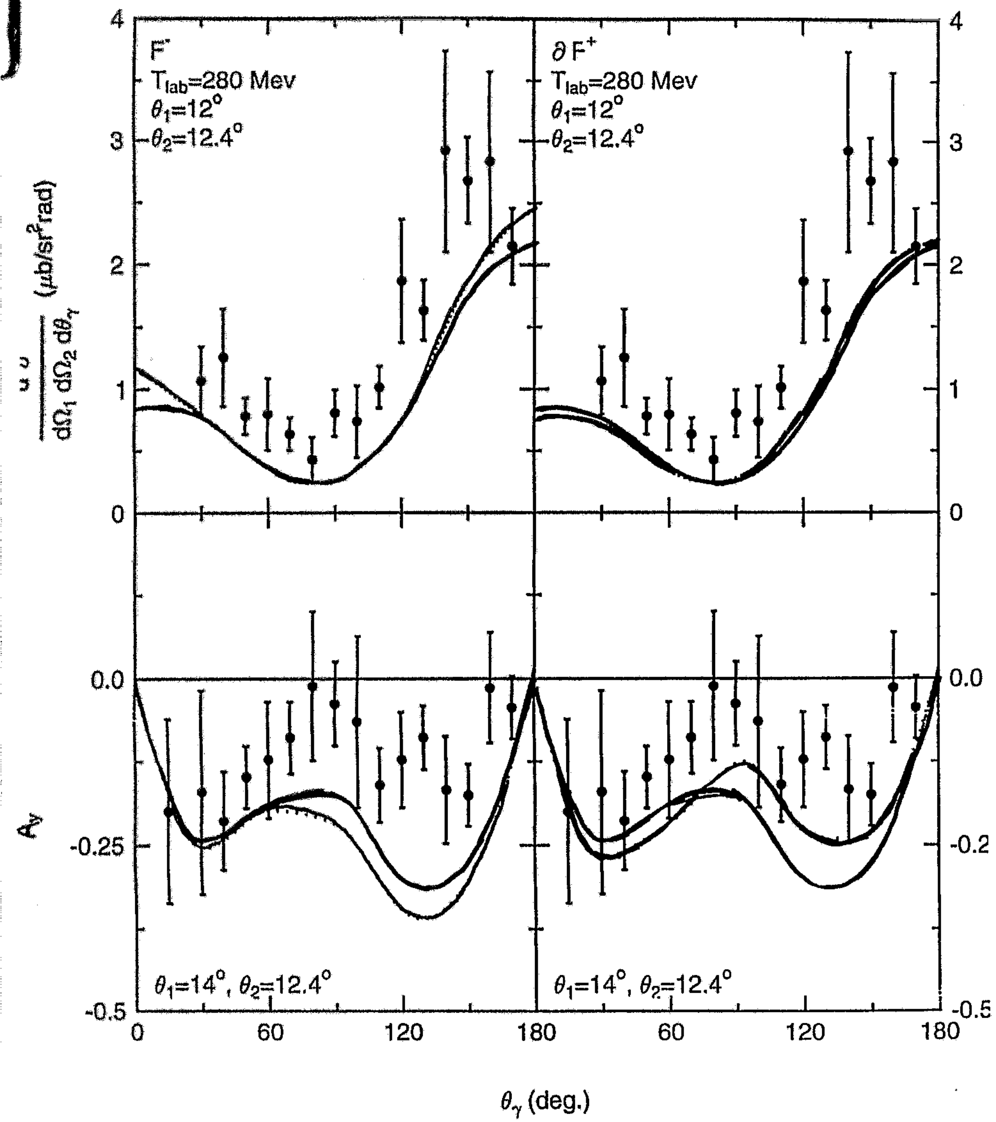

Virtual Bremsstrahlung

$(e^+ + e^-)$ pair production

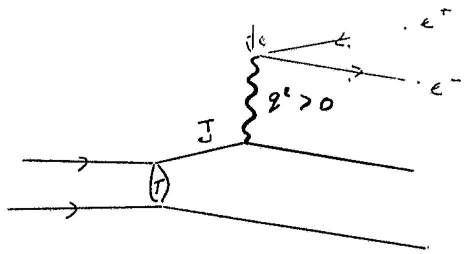

Similar to electron scattering

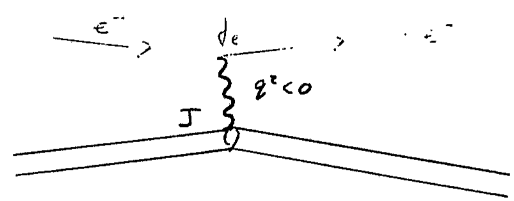

Both: structure functions

Matrix element $\mathcal{M} = J_\mu j_e^\mu$

Observables $|\mathcal{M}|^2 = (J_\mu j_e^\mu)(J_\nu j_e^\nu)^*$

$= (J_\mu J_\nu^*)\ (j_e^\mu j_e^{\nu *})$

structure functions (Hadronic tensor)   leptonic tensor

Differences:

(e, e') : charge densities

$(e^+ e^-)$: current density

Virtual Bremsstrahlung

$p + p \to p + p + e^+ + e^-$

KVITS003

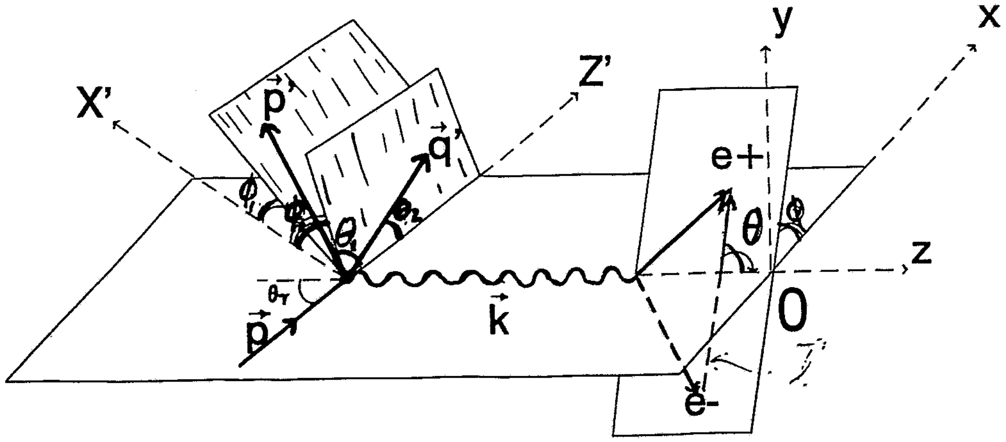

$$|M|^2 = \frac{e^4}{2 m_e^2 m_\gamma^2} W_s \Big[V_T \Big(1 - 2\frac{\ell^2}{m_\gamma^2} \sin^2\theta\Big) + V_L \Big(1 - 4\frac{\ell^2}{k_0^2} \cos^2\theta\Big) + $$
$$+ 2\frac{\ell^2}{m_\gamma^2} \sin^2\theta \big(V_{TT} \cos 2\Phi + V'_{TT} \sin 2\Phi\big) + $$
$$+ 2\frac{\ell^2}{k_0 m_\gamma} \sin 2\theta \big(V_{LT} \cos\Phi + V'_{LT} \sin\Phi\big)\Big]$$

Classical Response

– Electron Scattering (on bound state)

Hadronic Currents:

$$\text{charge} = J^0 = \int\Big(\int \rho(x,t)\, \overbrace{e^{i\omega t}}^{=1}\, dt\Big) e^{iqx} d^3x =$$
$$\overset{\omega=0}{\simeq} \int \bar{\rho}(x)\, e^{iqx}\, d^3x =$$

$$\text{currents} = \vec{J} = \int \underbrace{\Big(\int \vec{j}(x,t)\, e^{i\omega t}\, dt\Big)}_{=0 \text{ for } \omega = 0} e^{iqx} d^3x$$

time-averaged current = 0 if init. state = fin. state ($\omega = 0$)

alternative:

$$q_\mu \cdot J^\mu = 0 = \omega J^0 - \vec{q} \cdot \vec{J}$$

$$\therefore \quad J_L = \frac{\omega}{|q|} J^0 \to 0 \text{ for } \omega \to 0$$

Electron scattering measures charge density

Classical Response

– Bremsstrahlung (from continuum state)

Virtual

Hadronic Currents:

(ch)arge = $J^0 = \int \left(\int \rho(x,t)\, e^{iqx}\, d^3x \right) e^{i\omega t}\, dt$

= total charge Z for $\vec{q} \to 0$
time in-dependent $\therefore \int Z e^{i\omega t} dt = 0$ for $\omega \neq 0$

(c)urrents: $\vec{J} = \int \left(\int \vec{j}(x,t)\, d^3x \right) e^{i\omega t}\, dt$

for $\vec{q} \to 0 \simeq J_L = \int \bar{\vec{j}}_{\hat{q}}(t)\, e^{i\omega t}\, dt$

fourier components of - space averaged - radial current density

alternative: $q_\mu J^\mu = 0 \Rightarrow \omega J^0 - \vec{q} \cdot \vec{J} = 0$

$\therefore J^0 = \frac{\vec{q} \cdot \vec{J}}{\omega} = \frac{|q|\, J_L}{\omega} = 0$

Numerics:

$J^0 \to 0$ for $\vec{q} \to 0$

due to several orders of magnitude cancellations.

↳ numerical inaccuracies.

↳ "safe procedure":

$J^0 = \frac{\vec{q} \cdot \vec{J}}{\omega}$ $\vec{J}$ calculated

Conclusions:

- although 'simple' ppγ is non-trivial Exp & Th
- Discrepancy between Exp & Th
  - non-nucleonic degrees
  - off-shell form factors

Should be Consistent with

πN → πN
γN ⇔ πN
γN → γN

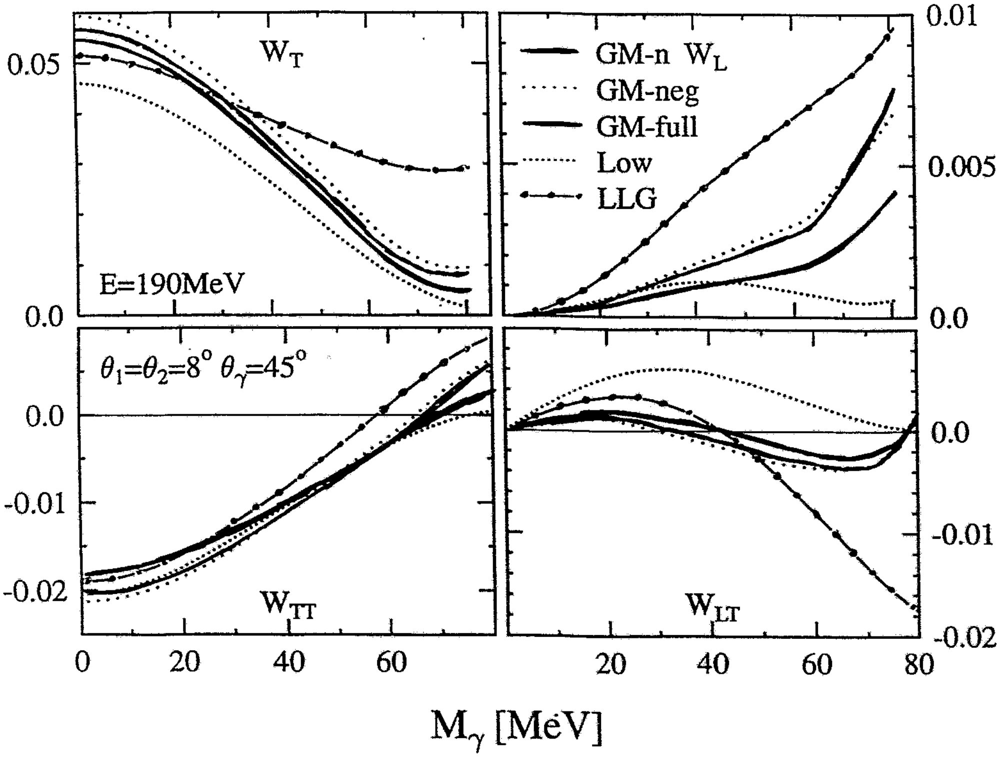

C. Fuchs:

Background contributions to dilepton spectra in pp collisions

Background contributions to the dilepton production in pp and $\bar{p}p$ collisions

C. Fuchs, M. Krivoruchenko, A. Fäßler

Tübingen

Fig. 4 Ernst et al. ...

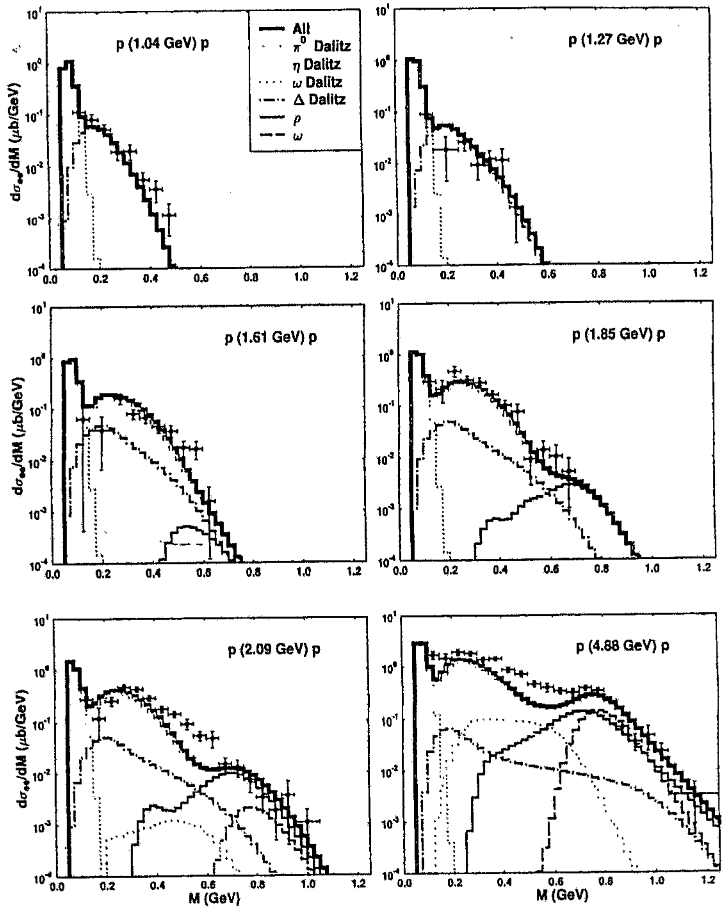

Importance of e^+e^- decays which contribute to the background?

⇒ M. Krivoruchenko

⇒ nucl-th/9904024

Decay mode	$B^{th}_{e^+e^-}$	$B^{exp}_{e^+e^-}$	$B^{th}_{\mu^+\mu^-}$	$B^{exp}_{\mu^+\mu^-}$
• $\rho^0 \to \ell^+\ell^-$	input	$(4.48 \pm 0.22) \times 10^{-5}$	4.5×10^{-5}	$(4.60 \pm 0.28) \times 10^{-5}$
$\rho \to \pi\ell^+\ell^-$	4.1×10^{-6}		4.6×10^{-7}	
$\rho^0 \to \eta\ell^+\ell^-$	2.7×10^{-6}		7.0×10^{-11}	
$\rho^\pm \to \pi^\pm\pi^0\ell^+\ell^-$	5.4×10^{-5}		1.8×10^{-7}	
$\rho^0 \to \pi^+\pi^-\ell^+\ell^-$	1.7×10^{-4}		6.7×10^{-7}	
$\rho^0 \to \pi^0\pi^0\ell^+\ell^-$	7.5×10^{-8}		2.4×10^{-9}	
$\rho \to \pi\eta\ell^+\ell^-$	1.9×10^{-12}			
• $\omega \to \ell^+\ell^-$	input	$(7.15 \pm 0.19) \times 10^{-5}$	7.1×10^{-5}	$< 1.8 \times 10^{-4}$
• $\omega \to \pi^0\ell^+\ell^-$	7.9×10^{-4}	$(5.9 \pm 1.9) \times 10^{-4}$	9.2×10^{-5}	$(9.6 \pm 2.3) \times 10^{-5}$
$\omega \to \eta\ell^+\ell^-$	6.0×10^{-6}		1.8×10^{-9}	
$\omega \to \pi^+\pi^-\ell^+\ell^-$	3.9×10^{-6}		2.9×10^{-8}	
$\omega \to \pi^0\pi^0\ell^+\ell^-$	2.0×10^{-7}		7.4×10^{-9}	
$\omega \to \pi^0\eta\ell^+\ell^-$	8.7×10^{-10}			
• $\phi \to \ell^+\ell^-$	input	$(3.00 \pm 0.06) \times 10^{-4}$	3.0×10^{-4}	$(2.48 \pm 0.34) \times 10^{-4}$
$\phi \to \pi^0\ell^+\ell^-$	1.6×10^{-5}	$< 1.2 \times 10^{-4}$	4.8×10^{-6}	
$\phi \to \eta\ell^+\ell^-$	1.1×10^{-4}	$(1.3 ^{+0.8}_{-0.6}) \times 10^{-4}$	6.8×10^{-6}	
• $\eta \to \gamma\ell^+\ell^-$	6.5×10^{-3}	$(4.9 \pm 1.1) \times 10^{-3}$	3.0×10^{-4}	$(3.1 \pm 0.4) \times 10^{-4}$
$\eta \to \pi^+\pi^-\ell^+\ell^-$	3.6×10^{-4}	$(1.3 ^{+1.2}_{-0.8}) \times 10^{-3}$	1.2×10^{-8}	
• $\eta' \to \gamma\ell^+\ell^-$	4.2×10^{-4}		8.1×10^{-5}	$(1.04 \pm 0.26) \times 10^{-4}$
$\eta' \to \omega\ell^+\ell^-$	2.0×10^{-4}			
$\eta' \to \pi^+\pi^-\ell^+\ell^-$	1.8×10^{-3}		2.0×10^{-5}	
• $f_0 \to \gamma\ell^+\ell^-$	2.2×10^{-7}		2.8×10^{-8}	
$f_0 \to \pi^+\pi^-\ell^+\ell^-$	1.4×10^{-4}		4.1×10^{-7}	
• $a_0^0 \to \gamma\ell^+\ell^-$	6.0×10^{-8}		7.4×10^{-9}	

• usually taken into account

Production Cross Sections, p+p Reactions

Measured (COSY):

$pp \to pp\rho^0$	parameterizations:
$pp \to pp\omega$	Sibirtsev / Cassing
$pp \to pp\phi$	
$pp \to pp\eta$	

Isospin-relations for ρ-production:

$$|NN\rho\rangle = [illegible]\,|\rho \otimes (NN)\rangle + [illegible]\,|N \otimes (\rho N)\rangle$$

[illegible]

$$\Rightarrow \quad \sigma(pp \to pp\rho^0) = \sigma(pp \to pn\rho^+) = \sigma(nn \to nn\rho^0) = \sigma(nn \to pn\rho^-)$$

$$\sigma(pn \to pn\rho^0) = \sigma(pn \to nn\rho^+) = \sigma(pn \to pp\rho^-) = 4\,\sigma(pp \to pp\rho^0)$$

Production Cross Sections, π+p Reactions

Known:

$\pi^- p \to \omega n$

$\pi^- p \to \omega \Delta^0$

$\pi^- p \to \eta n$

$\pi^- p \to \rho^0 n$

Isospin relations:

Assumption: $\sigma(\pi^- p \to \omega\Delta^0) = \sigma(\pi^- p \to \rho^0\Delta^0)$

about 20 % accuracy!

➡	$N\pi \to \Delta\rho$	16 channels
	$N\pi \to N\rho$	10 channels
	$N\pi \to N\omega$	4 "
	$N\pi \to \Delta\omega$	12 "
	⋮	⋮

Direct Decays of Vectormesons

$$\Gamma(V \to e^+e^-) = \frac{3\pi\alpha^2}{3g_V^2}\frac{m_V^4}{M^4}\left(1+2\frac{m_e^2}{M^2}\right) p^*(M, m_e, m_e)$$

$$p^*(\sqrt{s}, m_1, m_2) = \frac{\sqrt{(s-(m_1+m_2)^2)(s-(m_1-m_2)^2)}}{2\sqrt{s}}$$

Mass distribution (Breit Wigner):

$$f(M) = \frac{1}{\pi}\frac{2M m_V \Gamma_V(M)}{(M^2-m_V^2)^2 + m_V^2\Gamma_V^2(M)}$$

$$\frac{dB}{dM} = f(M)\frac{\Gamma(V\to e^+e^-)}{\Gamma_V(M)}$$

$\Rightarrow$ No 2π threshold for $\rho_0 \to e^+e^-$ decay

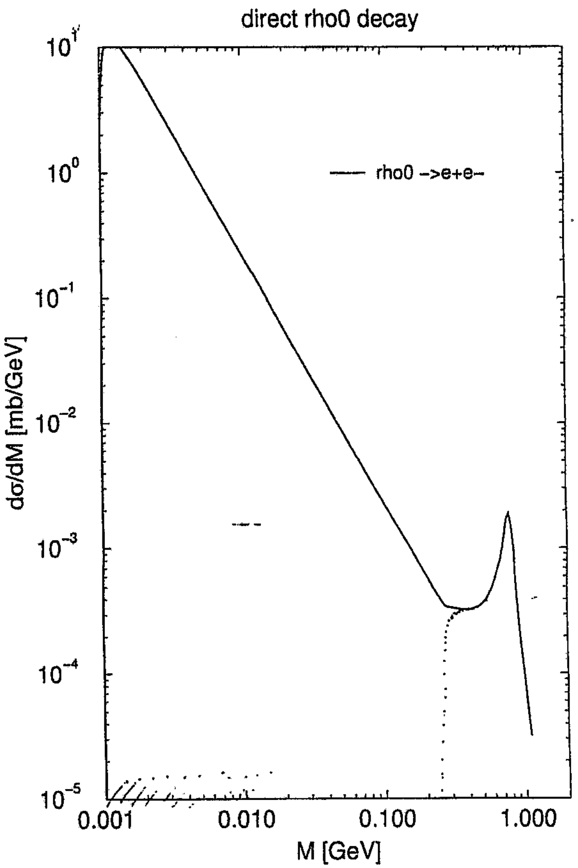

Bremsstrahlung region

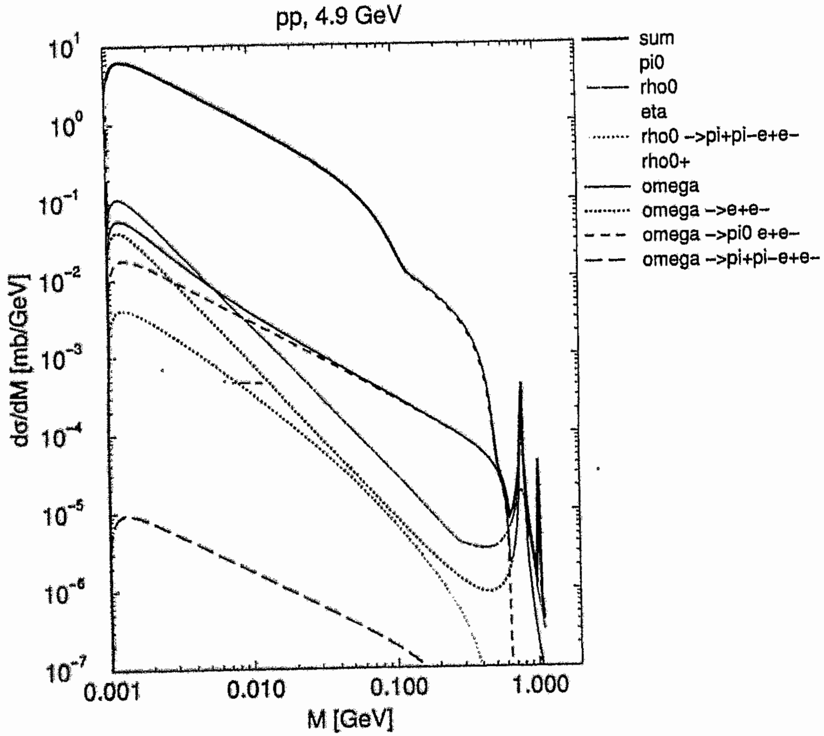

pp, 4.9 GeV
dσ/dM [mb/GeV]
M [GeV]
sum
pi0
rho0
eta
rho0 ->pi+pi-e+e-
rho0+
omega
omega ->e+e-
omega ->pi0 e+e-
omega ->pi+pi-e+e-

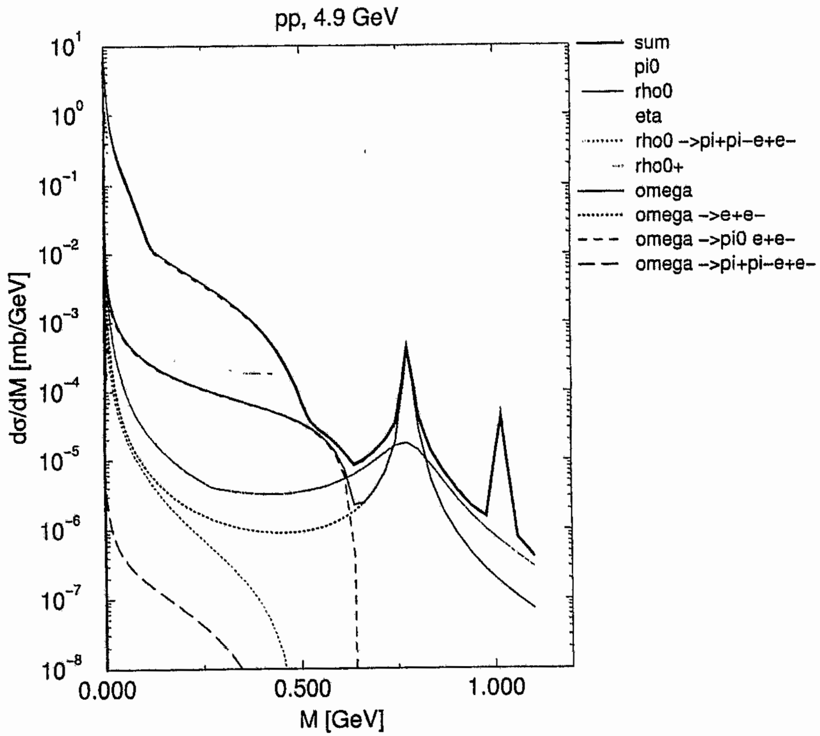

pp, 4.9 GeV
dσ/dM [mb/GeV]
M [GeV]
sum
pi0
rho0
eta
rho0 ->pi+pi-e+e-
rho0+
omega
omega ->e+e-
omega ->pi0 e+e-
omega ->pi+pi-e+e-

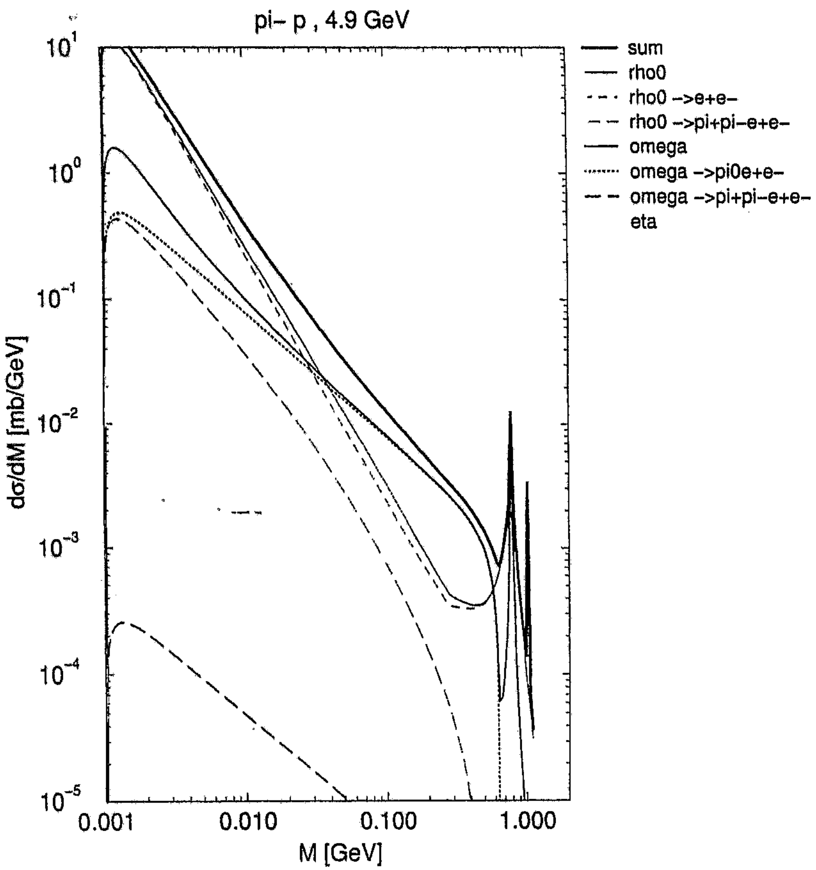
pi− p , 4.9 GeV
dσ/dM [mb/GeV]
M [GeV]
sum
rho0
rho0 −>e+e−
rho0 −>pi+pi−e+e−
omega
omega −>pi0e+e−
omega −>pi+pi−e+e−
eta

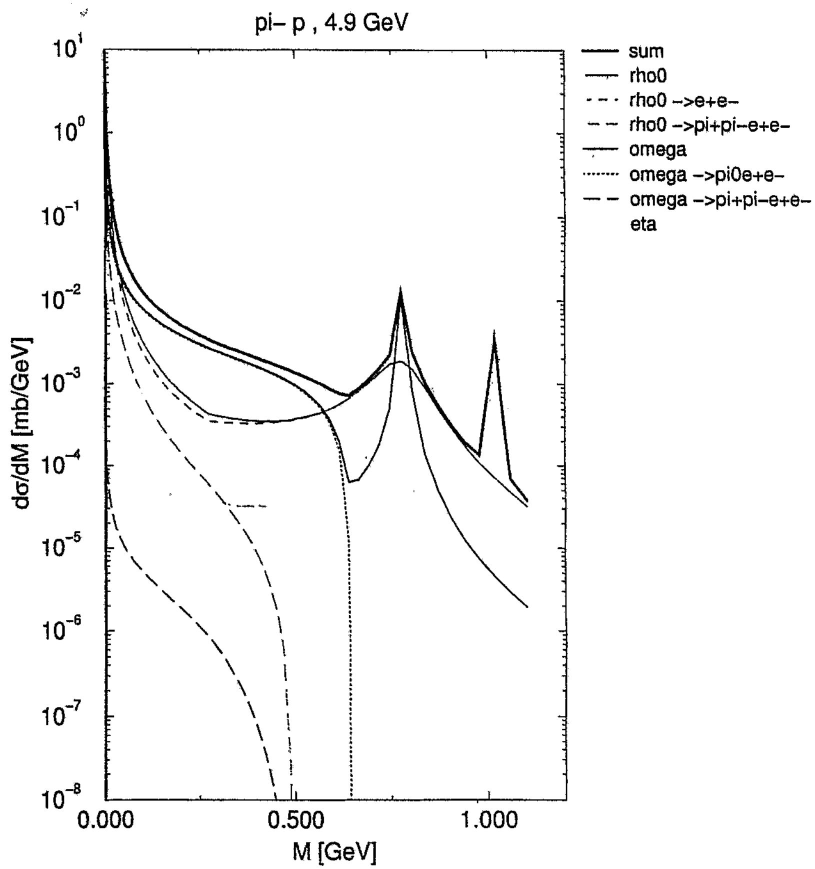
pi− p , 4.9 GeV
dσ/dM [mb/GeV]
M [GeV]
sum
rho0
rho0 −>e+e−
rho0 −>pi+pi−e+e−
omega
omega −>pi0e+e−
omega −>pi+pi−e+e−
eta

Summary

- Four body decays ([illegible] $\pi^+\pi^- e^+e^-$) give in some cases important contributions to the total dilepton decay

  but mainly in the low energy region
  $\Rightarrow$ difficult to observe
- similar for $\eta' \to \pi^+\pi^0 e^+ e^-$
- 2π – threshold disappears in the direct $\rho^0 \to e^+e^-$ decay

  $\Rightarrow$ large contribution at small $M_{e^+e^-}$
  $\Rightarrow$ should match with the Bremsstrahlung contribution
- πp reactions are appropriate to study ρ, ω decays at $M_{e^+e^-} \leq 0.5$ GeV

N. Kalantar:

Bremsstrahlung experiments at KVI

Probing Few-Body Systems
with
Bremsstrahlung

Nasser Kalantar

Mini-workshop on
Electromagnetic Radiation off Colliding
Hadron Systems:
Dileptons & Bremsstrahlung
Dresden, Germany
April 16, 1999

Outline

– Nucleon-Nucleon Bremsstrahlung

- General remarks
- Review of some experimental work on $pp\gamma$ and $pd\gamma$ at other laboratories

– KVI experiments on pp and pd systems

- Detection system
- Preliminary bremsstrahlung results

– Summary and outlook

****

J.C.S. Bacelar[a], M.J. van Goethem[a], M.N. Harakeh[a], M. Hoefman[a], H. Huisman[a], N. Kalantar[a], A. Kugler[c], H. Löhner[a], J.G. Messchendorp[a], R.W. Ostendorf[a], S. Schadmand[a], R. Simon[b], R. Turrisi[a], M. Volkerts[a], V. Wagner[c], H.W. Wilschut[a]

[a] KVI, Groningen; [b] GSI, Darmstadt;
[c] NPI, Řež u Prahy;

Nucleon-Nucleon Bremsstrahlung

Relevant Feynman Diagrams

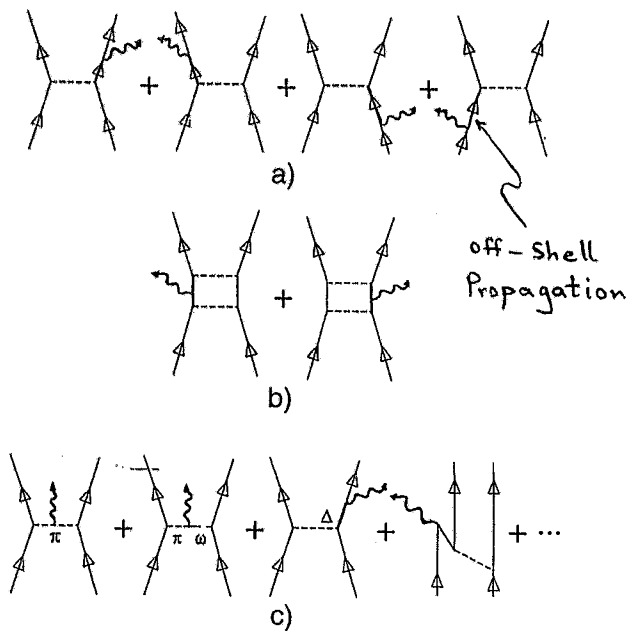

a) External Bremsstrahlung (Single Scattering)

b) Internal Bremsstrahlung (Double Scattering)

c) MEC + Δ + $N\bar{N}$ + ...

Soft-Photon

$$\lim_{\hbar\omega\to 0} \frac{d^3N}{(d^3k/k_0)} = \frac{z^2\alpha}{4\pi^2}\left|\frac{\epsilon^*\cdot p'}{k\cdot p'} - \frac{\epsilon^*\cdot p}{k\cdot p}\right|^2$$

For pn:

$\lim_{\hbar\omega\to 0} \frac{d^3N}{(d^3k/k_0)} \propto$ $\Rightarrow$ Dipole

For pp:

$\lim_{\hbar\omega\to 0} \frac{d^3N}{(d^3k/k_0)} \propto$ $=0 \Rightarrow$ Quadrupole

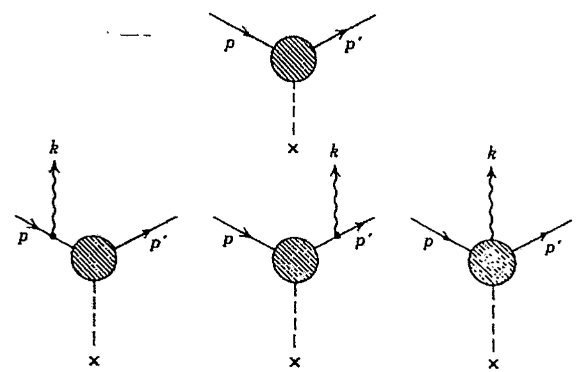

OESA   Exact calc.

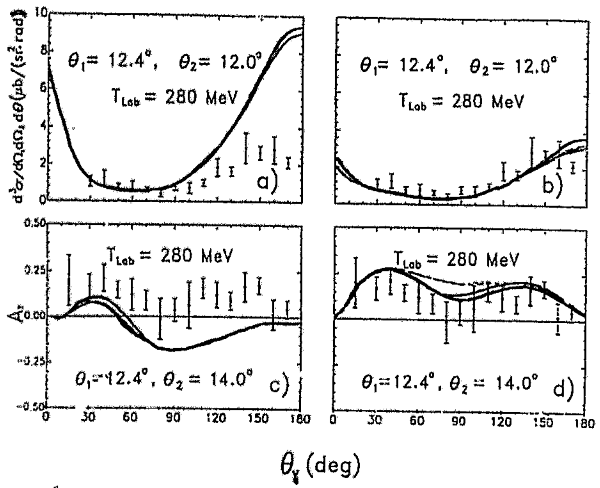

— OBEPQ

-- OBEPT

— Paris

Herrmann, Nakayama

Data not normalized.

(K. Michaelian et al., Phys. Rev. D41 (1990) 2689)

- It is obvious from both cross section data and analyzing power that 'off-shell' effects must be taken into account.
- Small differences between potentials.

IUCF Data

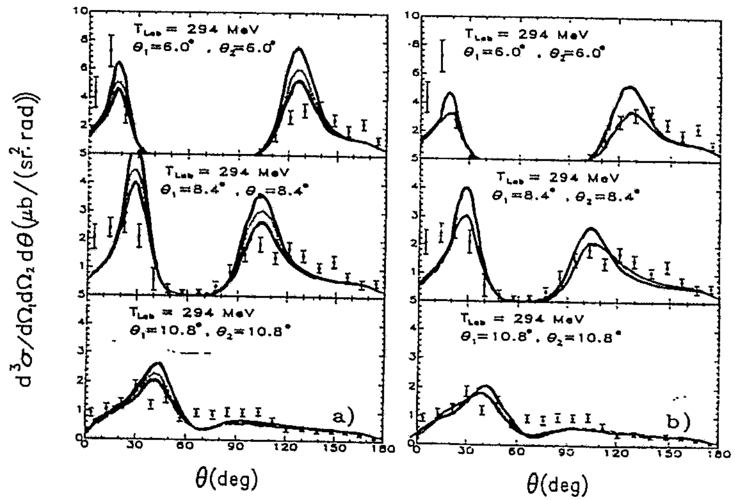

— OBEPQ   — Paris (no Coulomb correction)

OBEPQ-pp   — Paris (with Coulomb correction)

Calculations: Herrmann et al., Nucl. Phys. A582, 568 (1995)

Data: B.V. Przewoski et al., Phys. Rev. C45, 2001 (1992)

Available $pp\gamma$ data (Modern):

- TRIUMF: coplanar, small θ_p
  but NORMALIZATION problems
- IUCF: integrated, small θ_p
  but DIFFICULT to calculate

Recent and Proposed $NN\gamma$ Experiments:

- KVI: coplanar, non-coplanar, small θ_p, large Ω_p and Ω_γ
- CELSIUS: 4π detector, ring experiment
- COSY: 4π detector, high energies, low luminosity
- LANSCE: $np\gamma$ measurement (n beam)
- IUCF: small θ_p, C_{yy}, ring experiment
- RCNP: coplanar, large θ_p, high energies

KVI Experiments

- High precision absolute cross-section measurements on $pp\gamma$ to compare to "complete" calculations.
- Absolute cross-section measurements and channel selection of the $pd\gamma$ reactions.
- Use of polarized beam for high-precision measurements of the analyzing power of $\vec{p}p\gamma$ and $\vec{p}d\gamma$.
- p-Nucleus bremsstrahlung measurements to look at A-dependence.
- αp-bremsstrahlung measurement.

Note: All measurements involve real and virtual photons.
All measurements are exclusive.
All measurements are ingredients for reaction-mechanism studies in heavy-ion collisions.

Following exit channels exist for $p + d$ bremsstrahlung:

1. $p + d \longrightarrow {}^3\mathrm{He} + \gamma$

2. $p + d \longrightarrow p + d + \gamma$

3. $p + d \longrightarrow p + n + p_{spec} + \gamma$

(1) and (2) are energetically distinguished from (3) and .

Cross section of the Cyclotron AGOR

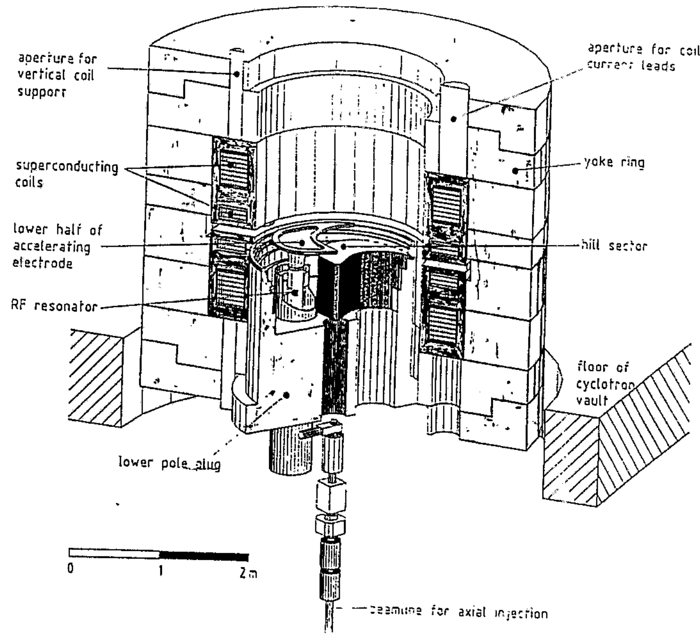

Detection System for $NN\gamma$ Experiments

SALAD (Small Angle Large Acceptance Detector)

- Detection of hadrons
- Two wire chambers for tracking:
  - Wire spacing 2 mm
  - Cathode-Anode spacing 4 mm
- Two stacks of Scintillators:
  - 24 thick elements for energy
  - 26 thin elements for veto

TAPS (Two Arm Photon Spectrometer)

- Detection of photons
- $\approx$ 400 crystals
- $\approx$ 25% of 4π for BLOCK geometry
- $\approx$ 20% of 4π for SUPERCLUSTER geometry

KVI

Schematic Top View of SALAD and TAPS

(supercluster geometry)

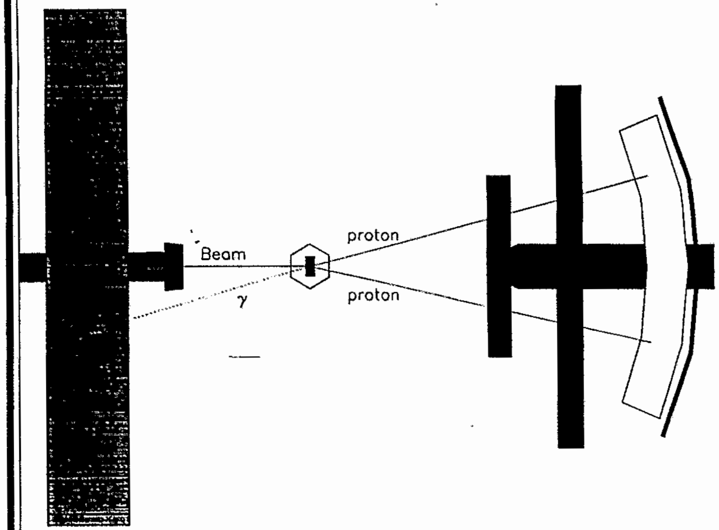

KVI

Elastic pp Cross Sections

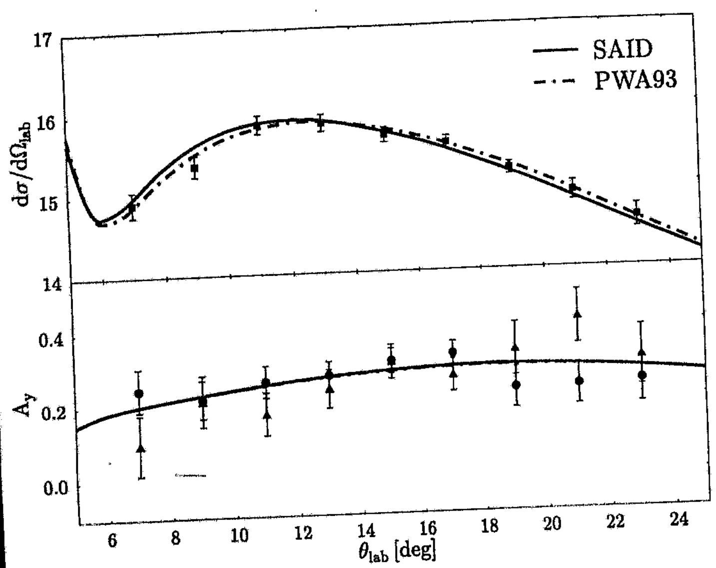

Data: H. Huisman

The calculations are from Virginia and Nijmegen

Event Reconstruction

Measure: $\underbrace{\theta_1, \phi_1, \theta_2, \phi_2, \theta_\gamma}$ ϕ_γ^M, E_1^M, E_2^M, E_γ^M

Reconstruction $\Rightarrow$ ϕ_γ^R, E_1^R, E_2^R, E_γ^R

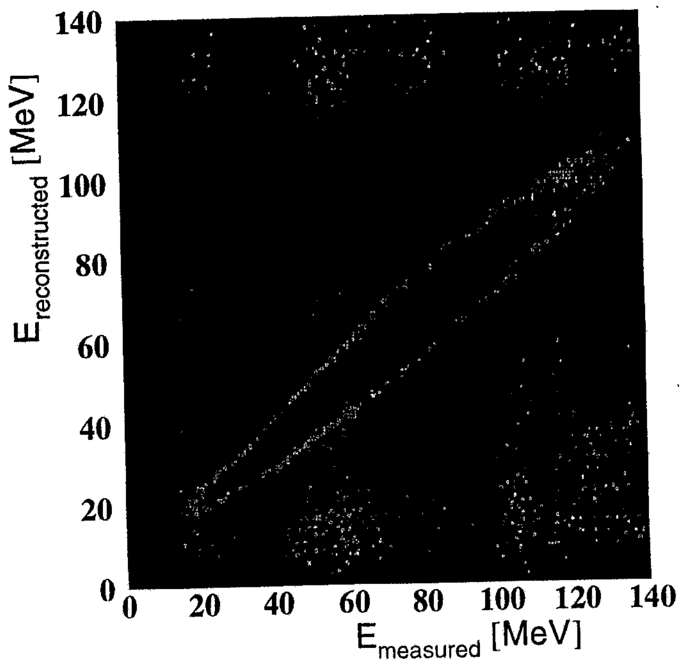

Proton-Proton Bremsstrahlung

$\vec{p} + p \rightarrow p + p + \gamma$

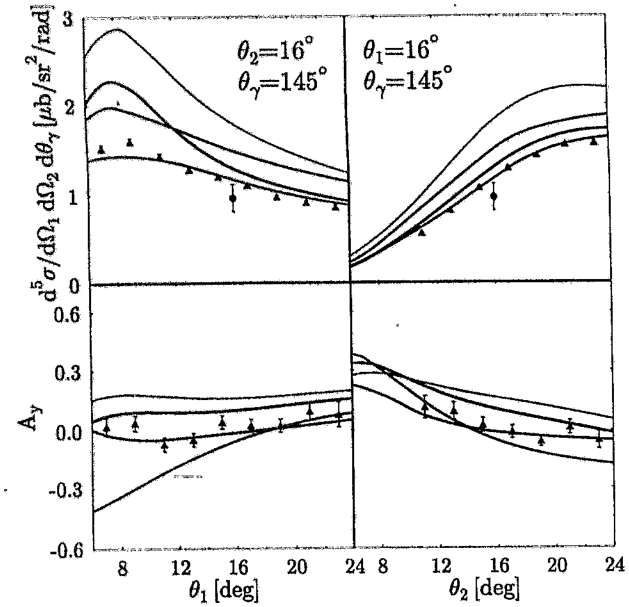

[redacted] Data: H. Huisman

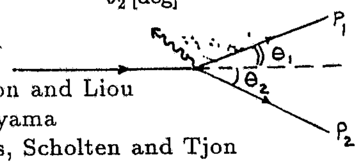

sub. P.R.L.

- SPA by Timmermans, Gibson and Liou
- Full calculation by K. Nakayama
- Full calculation by Martinus, Scholten and Tjon
- Full calculation by J. Eden
- Data point: Rogers et al. PRC **22** 2512 (1980)

Schematic Top View of SALAD and TAPS

(block geometry)

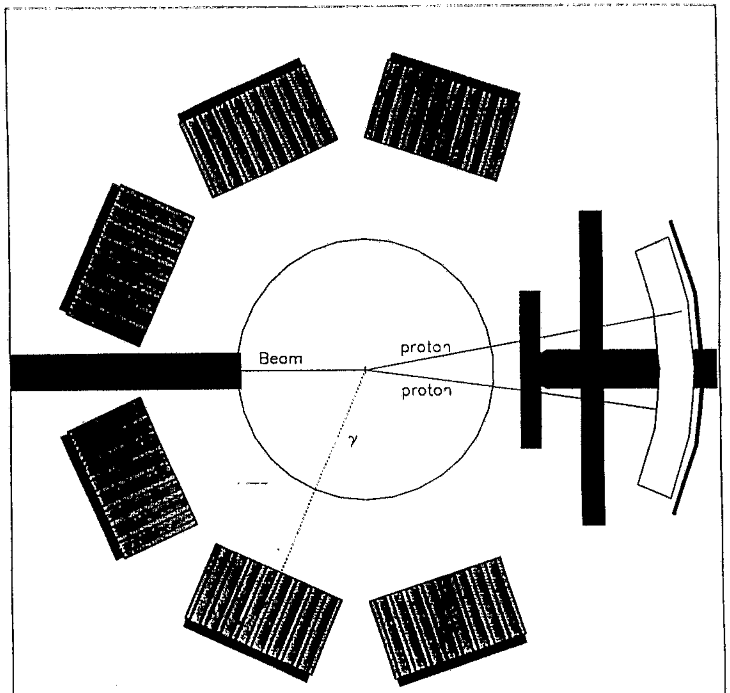

Figure 2

Proton-Proton Bremsstrahlung

$\vec{p} + p \rightarrow p + p + \gamma$

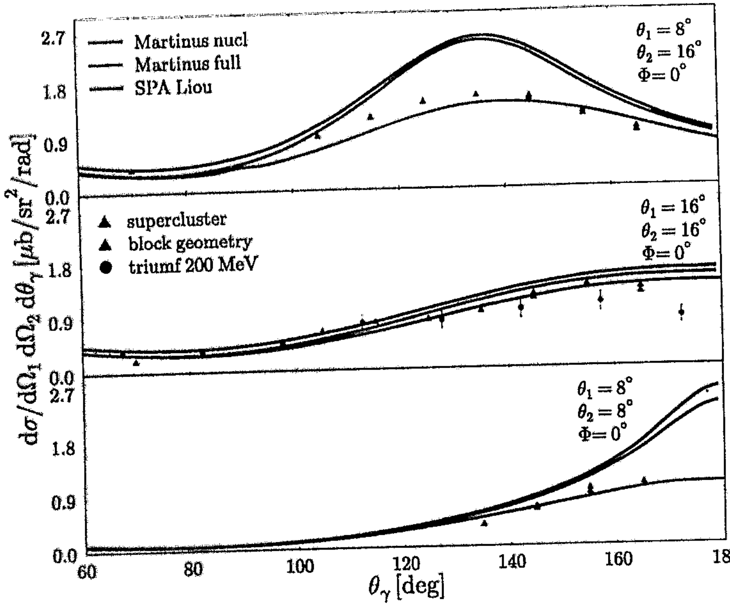

Data: H. Huisman
- SPA by Timmermans, Gibson and Liou
- Full calculation by Martinus, Scholten and Tjon
- calculation by Martinus, Scholten and Tjon
- Data points: Rogers et al. PRC 22 2512 (1980)

Various parameters as a function of TIME

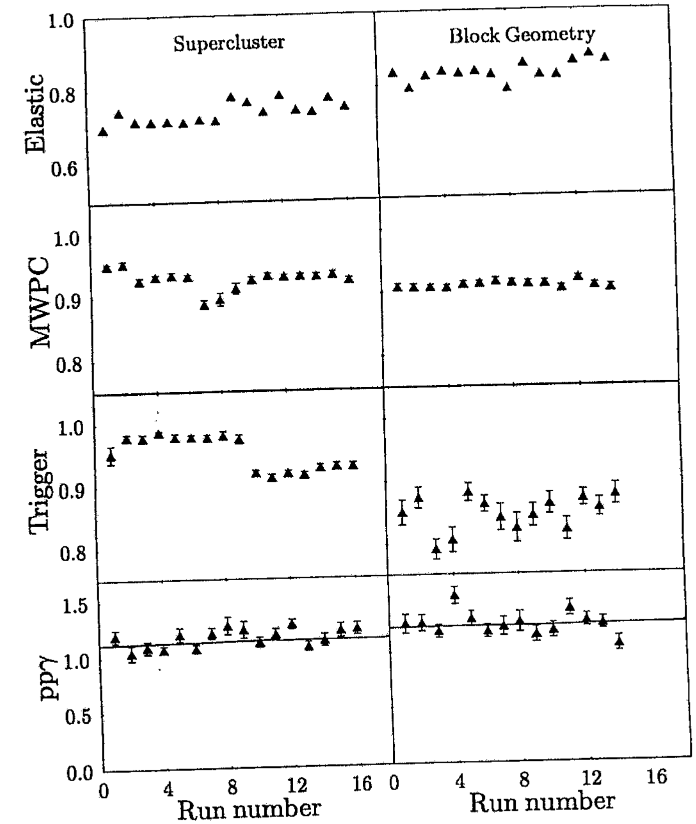

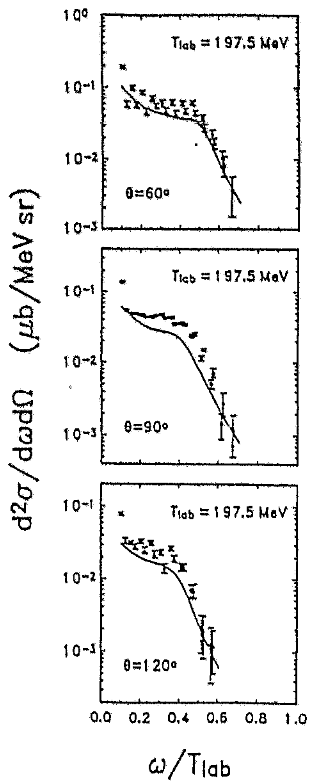

J.A. Pinston et al., P.L. B249, 402 (1990)

J. Clayton et al., P.R. C45, 1810 (1992)

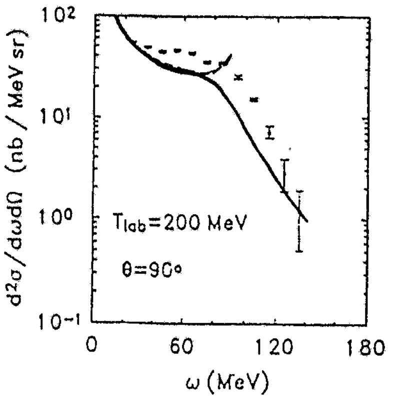

— Elementary np process

— np process "folded"

K. Nakayma, P.R. C45, 2039 (1992)

Channel Selection

Following exit channels exist for $p + d$ bremsstrahlung:

1. $p + d \longrightarrow p + d + \gamma$
2. $p + d \longrightarrow {}^3\text{He} + \gamma$
3. $p + d \longrightarrow p + n + p_{spec} + \gamma$
4. $p + d \longrightarrow$ [illegible]

(1) and (2) are energetically distinguished from (3) and [illegible].

“Coherent” $pd\gamma$: Diagnostics

Reconstructed versus Measured Energies

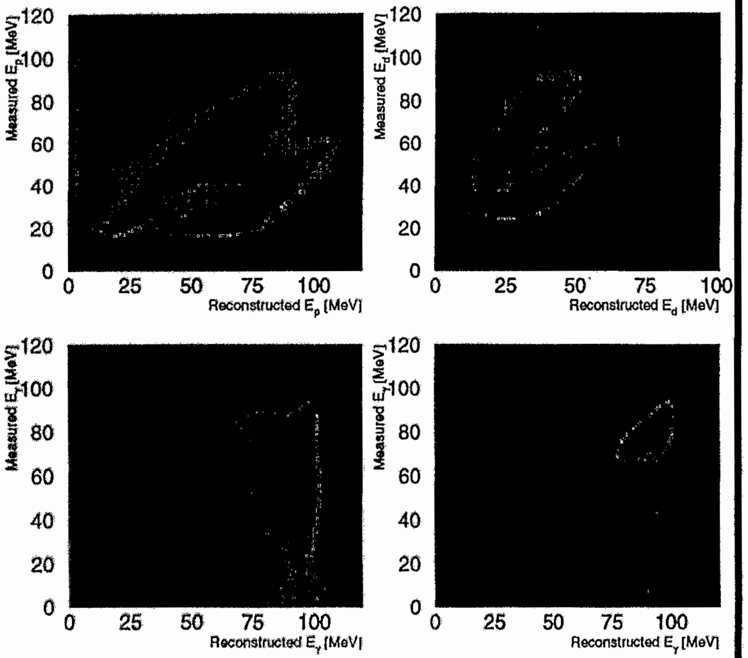

“Coherent” $pd\gamma$: Cross Sections

$$\vec{p} + d \rightarrow p + d + \gamma$$

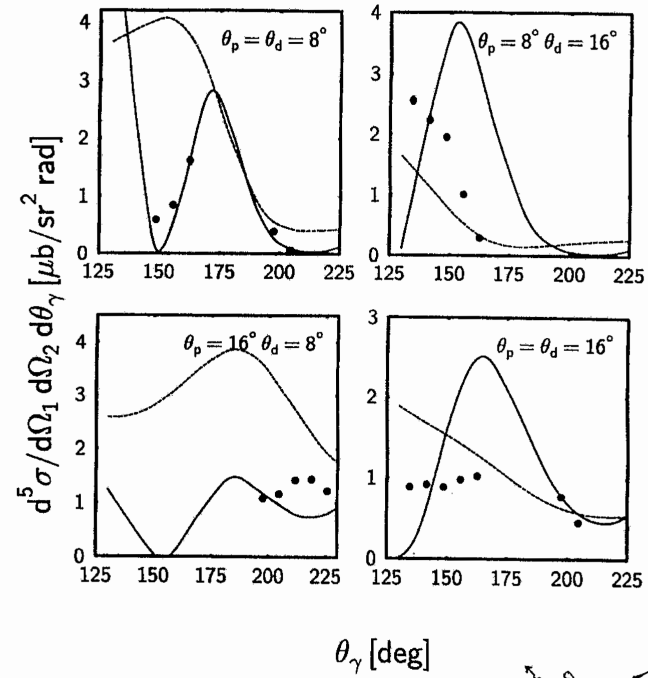

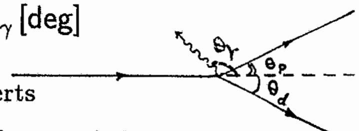

Preliminary Data: M. Volkerts

— SPA Calculation for pn downscaled by a factor of 3

— *Classical* calculation for pd on arbitrary scale

Summary

- New results emerging for cross sections and analyzing powers for *pp* and *pd* bremsstrahlung, improved in phase-space coverage as well as statistics;
- Spin observables are immune to large normalization uncertainties;
- Still disagreements between the most modern calculations and the data!

Outlook

- Other regions of phase space are being analyzed for possible hints to theorists;
- For the first time, large non-coplanar geometries with high accuracies have been measured yielding new observables;
- Study underway to measure **large** proton angles moving towards SPA;
- 4π detection for γ^* studies.

KVI

S. Scherer:

NN bremsstrahlung and Compton scattering
– examples of the impossibility of measuring off-shell effects

Nucleon Nucleon Bremsstrahlung and Compton Scattering: Examples of the Impossibility of Measuring Off-shell Effects

S. Scherer
Institut für Kernphysik, Mainz

Dresden, 16 April 1999

1. Motivation
2. Toy model Lagrangian for pn bremsstrahlung and Compton scattering off p
3. Conclusions

in collaboration with H. W. Fearing

http://www.kph.uni-mainz.de/T/lecture.html

1) Motivation

- What is the electromagnetic interaction of a *bound, off-mass-shell* nucleon in e.g. $(e, e'p)$
- Medium modifications, swollen nucleon
- Simple example

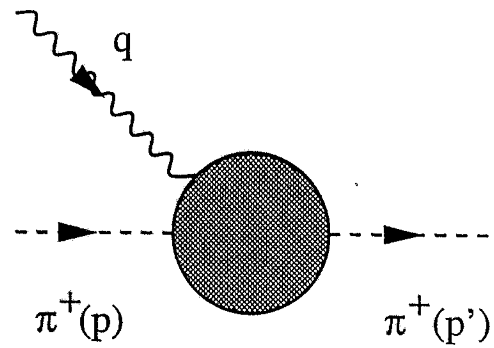

p+q=p'

$$\Gamma^\mu(p',p) = (p'+p)^\mu F(q^2,p'^2,p^2) + (p'-p)^\mu G(q^2,p'^2,p^2)$$

- Two form functions F and G of three scalar variables:

$$q^2, p'^2, p^2$$

- Is it possible to experimentally test and uniquely identify contributions from off-shell electromagnetic form functions?

- Example: pole terms of $\gamma^* \pi \to \gamma\pi$

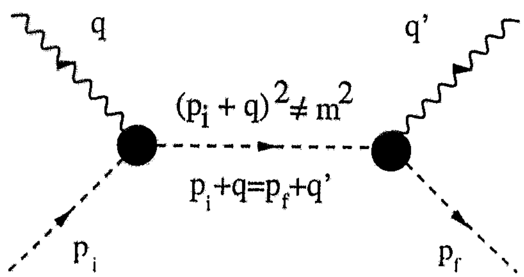

- Observable: form factor

$$F(q^2) = F(q^2, m_\pi^2, m_\pi^2)$$

- Analogy in NN bremsstrahlung: NN off shell, e.m. vertex off shell

Example

[Simplified version of H. W. Fearing, Phys. Rev. Lett. **81**, 758 (1998)]

- Simple example: $\pi^+ + \pi^0 \to \pi^+ + \pi^0 + \gamma$

- Nonlinear σ model describes pion interactions at low energies

$$\mathcal{L} = \frac{F^2}{4}\mathrm{Tr}\left[D_\mu U (D^\mu U)^\dagger\right] + \frac{F^2 m_\pi^2}{4}\mathrm{Tr}(U + U^\dagger)$$

$$F = 93\,\mathrm{MeV}$$

- U is an SU(2) matrix containing the pion fields

- Covariant derivative generates interaction with e.m. field

$$D_\mu U = \partial_\mu U + ieA_\mu [Q, U], \quad Q = \begin{pmatrix} \frac{2}{3} & 0 \\ 0 & -\frac{1}{3} \end{pmatrix}$$

- Alternative parametrizations of U:

$$U(x) = \frac{1}{F}\left[\sqrt{F^2-\vec{\pi}^2}+i\vec{\tau}\cdot\vec{\pi}(x)\right] = \exp\left[i\frac{\vec{\tau}\cdot\vec{\pi}\,'(x)}{F}\right]$$

correspond to a field transformation

$$\frac{\vec{\pi}}{F} = \hat{\pi}\,'\sin\left(\frac{\pi\,'}{F}\right) = \frac{\vec{\pi}\,'}{F}\left(1-\frac{1}{6}\frac{\vec{\pi}\,'^2}{F^2}+\cdots\right)$$

- Analogy

$$\vec{x} = (x,y,z) = (r\sin(\theta)\cos(\phi), r\sin(\theta)\sin(\phi), r\cos(\theta))$$

change of variables from cartesian to spherical coordinates

Feynman rule for the $\pi^+\pi^0$ scattering amplitude

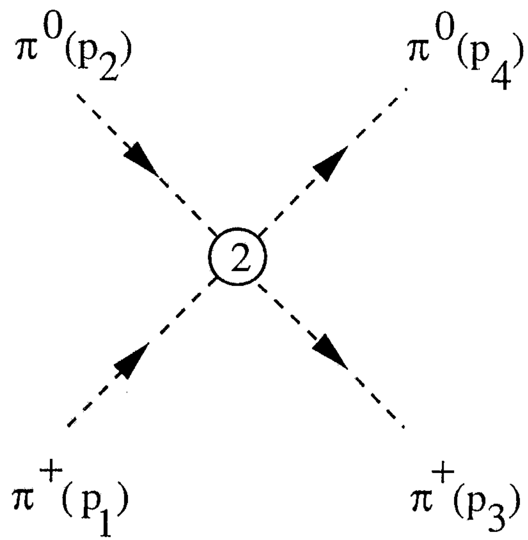

$$\mathcal{M}_1 = \frac{i}{F^2}T_0(p_1,p_3)$$

$$\mathcal{M}_2 = \frac{i}{F^2}\left[T_0(p_1,p_3)-\frac{1}{3}(\Lambda_1+\Lambda_2+\Lambda_3+\Lambda_4)\right]$$

$$T_0(p_1,p_3) = (p_3-p_1)^2-m_\pi^2$$

$$\Lambda_i = p_i^2-m_\pi^2$$

The same on-shell scattering amplitude but different off-mass-shell behavior!

Apply to $\pi^+(p_1) + \pi^0(p_2) \to \pi^+(p_3) + \pi^0(p_4) + \gamma(k)$

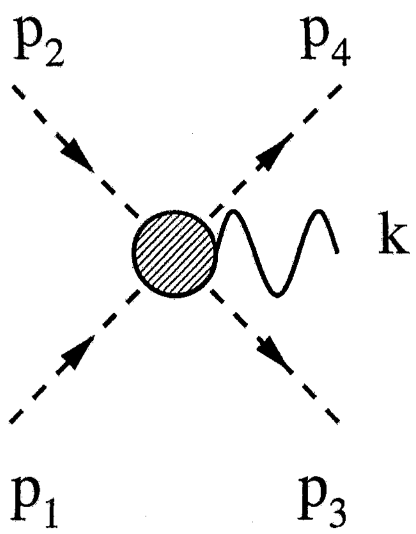

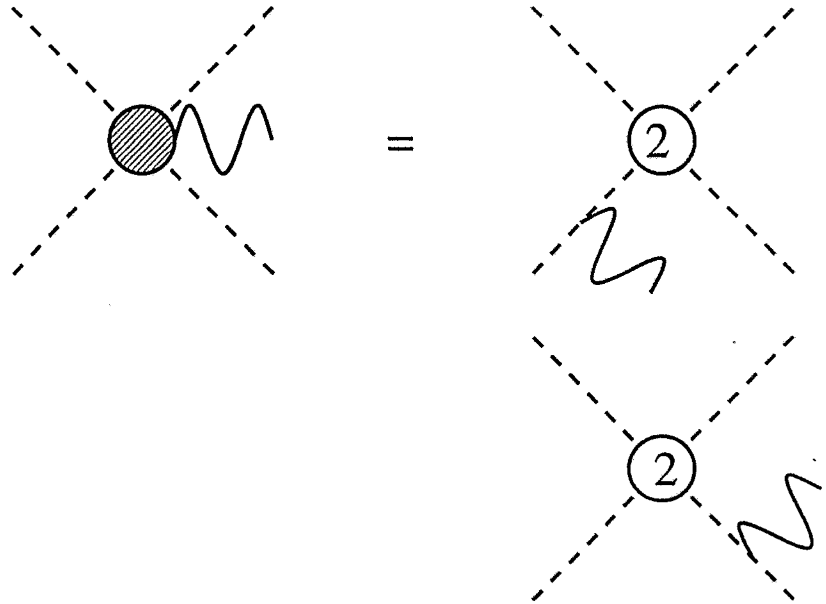

$$\mathcal{M}_1 = \frac{i}{F^2} T_0(p_1 - k, p_3) \frac{i}{(p_1-k)^2 - m_\pi^2} (-2iep_1 \cdot \epsilon)$$
$$-2iep_3 \cdot \epsilon \frac{i}{(p_3+k)^2 - m_\pi^2} \frac{i}{F^2} T_0(p_1, p_3 + k)$$
$$= \left(\frac{p_3 \cdot \epsilon}{p_3 \cdot k} - \frac{p_1 \cdot \epsilon}{p_1 \cdot k} \right) \frac{ie}{F^2} [T_0(p_1, p_3) - 2(p_1 - p_3) \cdot k]$$

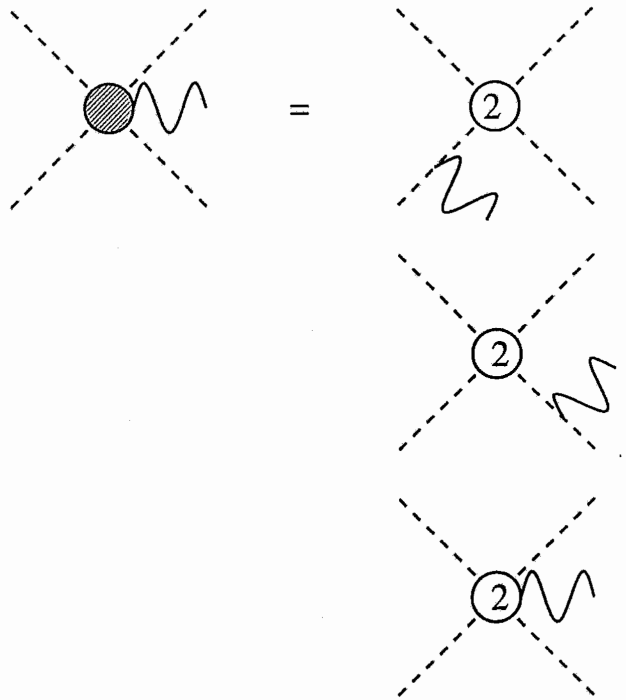

$$
\begin{aligned}
\mathcal{M}_2 &= \frac{i}{F^2}\left\{T_0(p_1-k,p_3)\boxed{-\frac{1}{3}\left[(p_1-k)^2-m_\pi^2\right]}\right\} \\
&\quad\times\frac{i}{(p_1-k)^2-m_\pi^2}(-2iep_1\cdot\epsilon) \\
&\quad -2iep_3\cdot\epsilon\frac{i}{(p_3+k)^2-m_\pi^2} \\
&\quad\times\frac{i}{F^2}\left\{T_0(p_1,p_3+k)\boxed{-\frac{1}{3}\left[(p_3+k)^2-m_\pi^2\right]}\right\} \\
&\quad +\frac{2ie}{3F^2}\epsilon\cdot(p_1+p_3) \\
&= \mathcal{M}_1
\end{aligned}
$$

- Here: Complete cancellation of "off-shell" effects and contact interactions
- In general: Two mechanisms are indistinguishable
- Manifestation of the "equivalence theorem" of field theory:
  Lagrangians which are related by field transformations generate the same on-shell S-matrix elements and thus the same observables.
- Off-shell form functions not only model dependent but also representation dependent

2) Toy model Lagrangian for pn bremsstrahlung and Compton scattering off p

- Question: Is it possible to uniquely associate observable effects with off-mass-shell behavior of the np amplitude or of the electromagnetic vertex?

Toy model Lagrangian:

$$\mathcal{L} = \bar{p}(i\not{D} - M)p - \frac{e\kappa}{4M} F_{\mu\nu}\bar{p}\sigma^{\mu\nu}p + \bar{n}(i\not{\partial} - M)n + g\bar{p}p\bar{n}n$$

- – p: proton field
  – n: neutron field (for simplicity no anomalous magnetic moment)
  – Covariant derivative: $i\not{D}p = (i\not{\partial} - e\not{A})p$
  – Field strength tensor: $F_{\mu\nu} = \partial_\mu A_\nu - \partial_\nu A_\mu$

Result for $p(p_1) + n(p_2) \to p(p_3) + n(p_4) + \gamma(q)$ with toy model:

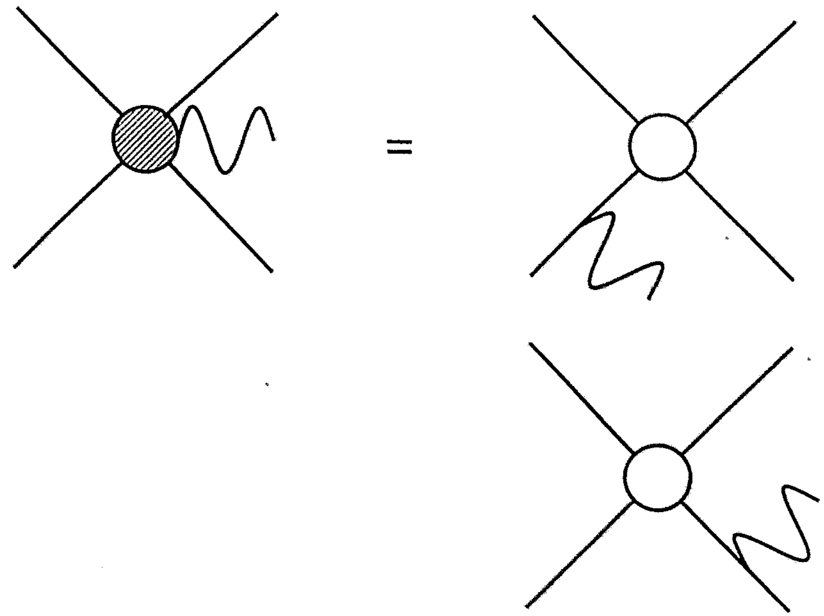

$$\mathcal{M} = ieg\bar{u}_n u_n \bar{u}_p \left\{ \frac{1}{\not{p}_1 - \not{q} - M}\left(\not{\epsilon} - \frac{\kappa}{4M}[\not{q}, \not{\epsilon}]\right) + \left(\not{\epsilon} - \frac{\kappa}{4M}[\not{q}, \not{\epsilon}]\right)\frac{1}{\not{p}_3 + \not{q} - M} \right\} u_p$$

- Consider field transformation

$$p = p' + \delta p' = (1 + \alpha \bar{n} n + \beta \sigma_{\mu\nu} F^{\mu\nu}) p'$$

- α and β arbitrary real parameters

- α generates different off-mass-shell np amplitude

- β generates different off-mass-shell e.m. vertex

$$\mathcal{L}(p,n) \;=\; \mathcal{L}(p' + \delta p', n) = \mathcal{L}'(p', n)$$

- Different functional forms of $\mathcal{L}$ and $\mathcal{L}'$

- Off-mass-shell modifications of "old" vertices

$$\begin{aligned}\Delta\mathcal{M}_{pn} &= i\alpha 1_n \left[(\not{p}_3 - M) + (\not{p}_1 - M)\right]_p \\ \Delta\mathcal{M}_{pp\gamma} &= -i\beta\left\{(\not{p}_f - M)[\not{q}, \not{\epsilon}] + [\not{q}, \not{\epsilon}](\not{p}_i - M)\right\}\end{aligned}$$

- Illustration for e.m. vertex:

$$\begin{aligned}\Gamma^\mu(p_f, p_i) &= \sum_{\alpha,\beta=+,-} \Lambda_\alpha(p_f)\Big(\gamma^\mu F_1^{\alpha\beta} \\ &\quad + i\frac{\sigma^{\mu\nu} q_\nu}{2M} F_2^{\alpha\beta} + \frac{q^\mu}{M} F_3^{\alpha\beta}\Big)\Lambda_\beta(p_i)\end{aligned}$$

$$\begin{aligned}F_i^{\alpha\beta} &= F_i^{\alpha\beta}(q^2, p_f^2, p_i^2), \qquad q = p_f - p_i \\ \Lambda_\pm(p) &= \frac{M \pm \not{p}}{2M}\end{aligned}$$

- Before field transformation:

$$\begin{aligned}F_1^{\alpha\beta} &= 1 \\ F_2^{\alpha\beta} &= \kappa \\ F_3^{\alpha\beta} &= 0\end{aligned}$$

  - no q^2 dependence
  - no p_i^2 and p_f^2 dependence

- After field transformation

$$
\begin{aligned}
F_2^{++} &= \kappa \\
F_2^{+-} &= F_2^{-+} = \kappa + \tilde{\beta} \quad \text{(sometimes } \kappa^-\text{)} \\
F_2^{--} &= \kappa + 2\tilde{\beta}
\end{aligned}
$$

where

$$\beta = \frac{e}{8M^2}\tilde{\beta}$$

- Of course, more realistic starting point possible:

$$
\begin{aligned}
\mathcal{L}_{pp\gamma} &= \bar{p}(i\not{D} - M)p - \frac{e\kappa}{4M} F_{\mu\nu}\bar{p}\sigma^{\mu\nu}p \\
&\quad - e\sum_{n=1}^{\infty}((-\partial^2)^{n-1}\partial^\nu F_{\mu\nu})F_{1n}\bar{p}\gamma^\mu p \\
&\quad - \frac{e}{4M}\sum_{n=1}^{\infty}((-\partial^2)^n F_{\mu\nu})F_{2n}\bar{p}\sigma^{\mu\nu}p \\
F_1(q^2) &= 1 + \sum_{n=1}^{\infty}(q^2)^n F_{1n} \\
F_2(q^2) &= \kappa + \sum_{n=1}^{\infty}(q^2)^n F_{2n}
\end{aligned}
$$

- Also, more complicated field transformations possible

- Additional vertices relevant to bremsstrahlung and Compton scattering $p(p_i) + \gamma(q) \to p(p_f) + \gamma(q')$:

$$
\begin{aligned}
\Delta\mathcal{M}_{pn\gamma} &= -i\alpha\beta 1_n \{(\not{p}_1 - \not{q} - M)[\not{q}, \not{\epsilon}] \\
&\qquad + [\not{q}, \not{\epsilon}](\not{p}_3 + \not{q} - M)\}_p \\
\Delta\mathcal{M}_{pp\gamma\gamma} &= -i\beta^2 \{[\not{q}, \not{\epsilon}](\not{p}_i - \not{q}' - M)[\not{q}', \not{\epsilon}'] \\
&\qquad + [\not{q}', \not{\epsilon}'](\not{p}_i + \not{q} - M)[\not{q}, \not{\epsilon}]\}
\end{aligned}
$$

- Amplitude for pn bremsstrahlung the same as with original Lagrangian

- Cancellation of off-mass-shell effects and contact interactions

- Different off-mass-shell behavior of Green's functions

- Observable results identical

Phenomenological Lagrangian to generate κ^- off-shell effects (popular in NN bremsstrahlung)

$$\begin{aligned}\mathcal{L} &= \bar{p}(i\not{\partial} - M)p - \frac{e\kappa}{4M}F_{\mu\nu}\bar{p}\sigma^{\mu\nu}p \\ &+\beta\bar{p}(-i\overleftarrow{\not{\partial}} - e\not{A} - M)\sigma^{\mu\nu}pF_{\mu\nu} \\ &+\beta F_{\mu\nu}\bar{p}\sigma^{\mu\nu}(i\not{\partial} - e\not{A} - M)p\end{aligned}$$

- Off-shell effects in the pole terms

- Contact interaction to preserve gauge invariance

- Field transformation

$$p = (1 - \beta\sigma_{\mu\nu}F^{\mu\nu})p'$$

eliminates κ^- off-shell effects by generating new contact interaction

- Consider Compton scattering

$$\begin{aligned}\mathcal{M} &= \mathcal{M}_{Born} + \mathcal{M}_{struc} \\ \mathcal{M}_{struc} &= i[4\pi\bar{\alpha}\omega\omega'\vec{\epsilon}\cdot\vec{\epsilon}\,' + 4\pi\bar{\beta}\vec{q}\times\vec{\epsilon}\cdot\vec{q}\,'\times\vec{\epsilon}\,'] + \cdots\end{aligned}$$

Results from the above Lagrangian:

$$\bar{\alpha} = -\frac{e^2}{4\pi}\frac{\bar{\beta}^2 + 2\bar{\beta}\kappa}{4M^3}, \quad \bar{\beta} = \frac{e^2}{4\pi}\frac{\kappa\bar{\beta}}{2M^3}$$

where

$$\frac{e^2}{4\pi} \approx \frac{1}{137}$$

- Problem:

Given empirical numbers

$$\begin{aligned}\bar{\alpha} &= (12.1 \pm 0.8 \pm 0.5) \times 10^{-4}\,\mathrm{fm}^3 \\ \kappa &= 1.79 \\ M &= 938\,\mathrm{MeV}\end{aligned}$$

no solution to

$$\bar{\beta}_{1/2} = -\kappa \pm \underbrace{\sqrt{\kappa^2 - \frac{4\pi}{e^2}4M^3\bar{\alpha}}}_{>0}$$

$$3.20 > 71.6$$

- Conclusion

Check consistency of "phenomenological off-shell effects" with other reactions!

3) Conclusions

- Off-shell effects in e.m. and strong vertices using pn bremsstrahlung and Compton scattering off p
- Concept of field transformations
- Equivalence theorem
- Same results for observables
- Differences in off-shell behavior of Green's functions
- Cannot uniquely distinguish between off-mass-shell contributions and contact terms
- Electromagnetic polarizabilities as consistency check of phenomenological "off-shell" Lagrangian

J. Zlomanczuk:

Bremsstrahlung in pp collisions at 310 MeV

J. Złomanczuk

Bremsstrahlung in pp Collisions at 310 MeV

H. Calén, J. Dyring, K. Fransson, L. Gustafsson, S. Häggström, B. Höistad, A. Johansson, T. Johansson, S. Kullander, A. Mörtsell, R.J.M.Y. Ruber, U. Schuberth, J. Zlomanczuk
Department of Radiation Sciences, Uppsala University, S-75121 Uppsala, Sweden

C. Ekström
The Svedberg Laboratory, S-75121 Uppsala, Sweden

K. Kilian, W. Oelert, V. Renken,
IKP, Forschungszentrum Jülich GmbH, D-52425 Jülich, Germany

R. Bilger, W. Brodowski, H. Clement, G.Kurz, G.J. Wagner
Physikalisches Institut, Tübingen University

B. Shwartz,
Budker Institute of Nuclear Physics, Novosibirsk 630 090, Russia

B. Morosov, A. Sukhanov, A.Zernov
Joint Institute for Nuclear Research, Dubna, 101000 Moscow, Russia

A. Kupsc, P. Marciniewski, J. Stepaniak
Institute for Nuclear Studies, PL-00681 Warsaw, Poland

J. Zabierowski
Institute for Nuclear Studies, PL-90137 Lodz, Poland

A. Turowiecki, Z. Wilhelmi
Institute of Experimental Physics, Warsaw University, PL-0061 Warsaw, Poland

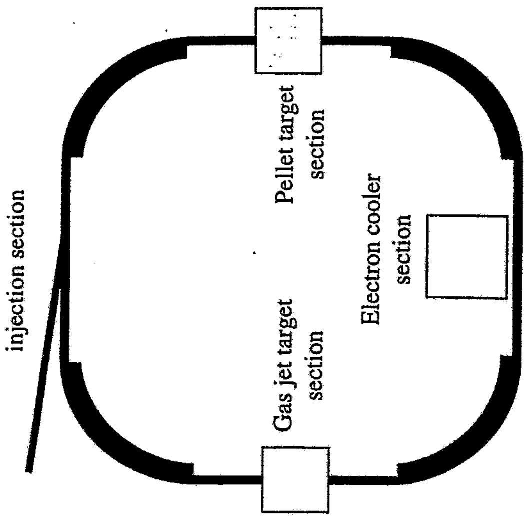

Some parameters of the CELSIUS ring

Circumference	82 m
Max. magnetic field	1.0 T (1.2 planned)
Max. Momentum	2.1xZ GeV/c (at present)
Max. energy (Z/A=1/2)	470xA MeV (at present)
Electron beam current	0-3 A
Electron beam diameter	2 cm

Achieved intensities

Proton intensity	2×10^{11}
Deuteron intensity	4×10^{10}
α-particle intensity	1×10^{10}
^{16}O intensity	3×10^{8}

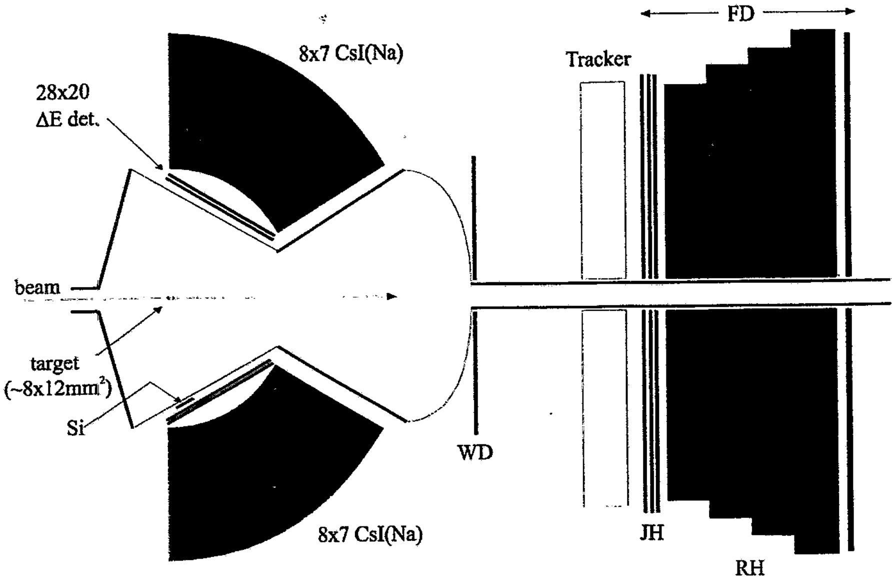

WASA-PROMICE experimental set-up

A view of the CELSIUS storage ring

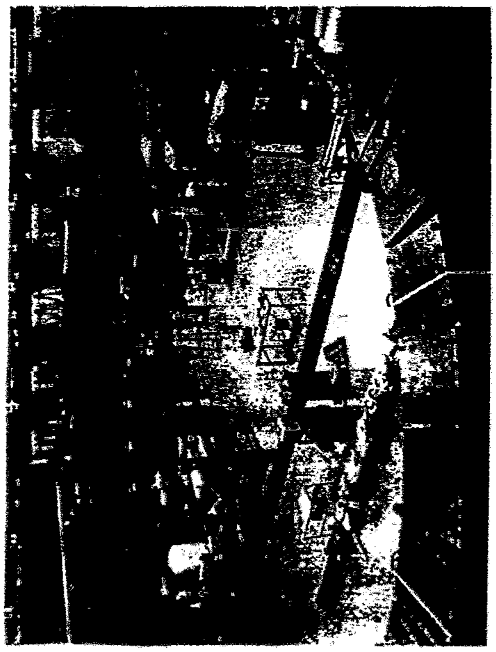

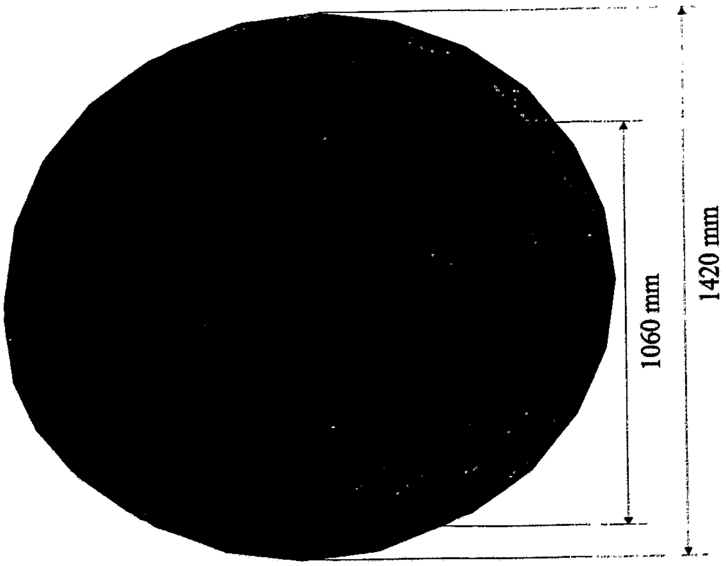

Range Hodoscope

Material: plastic scintillator

Thickness: 44 cm (proton maximum energy ~ 280 MeV)

Angular range: 4 - 21 deg

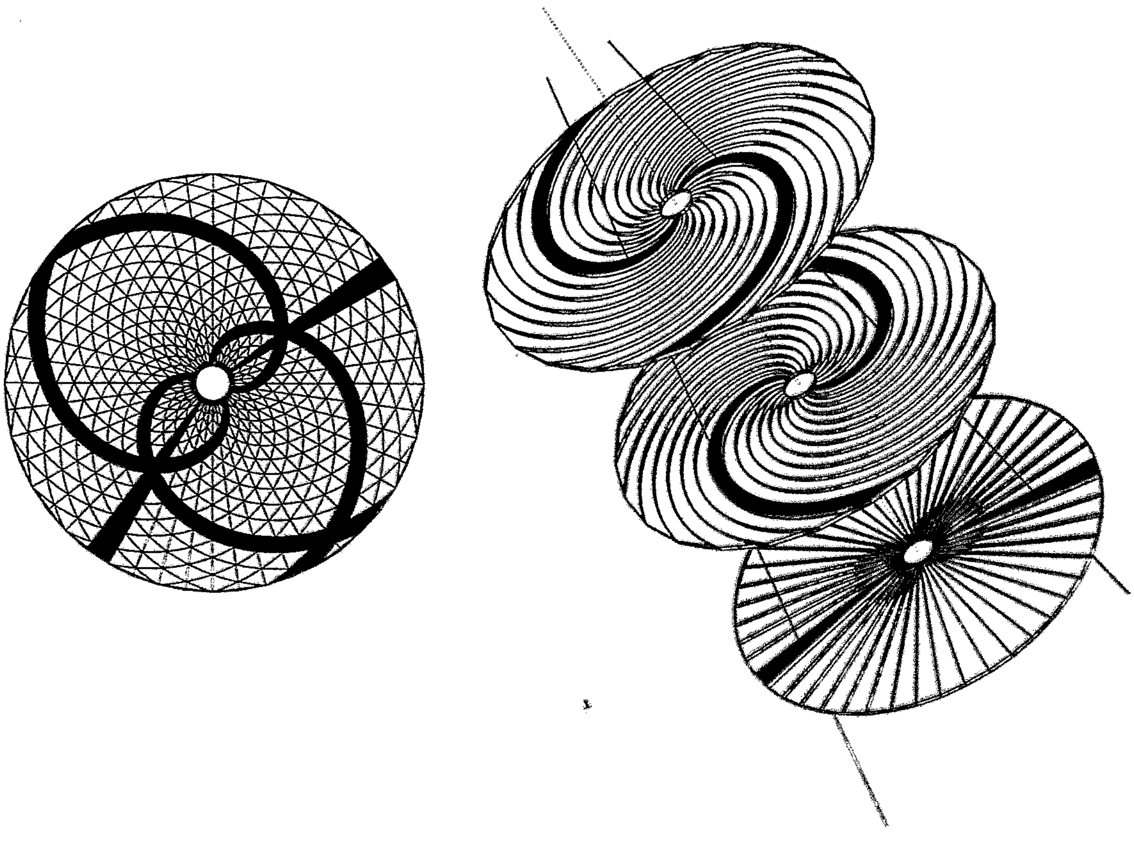

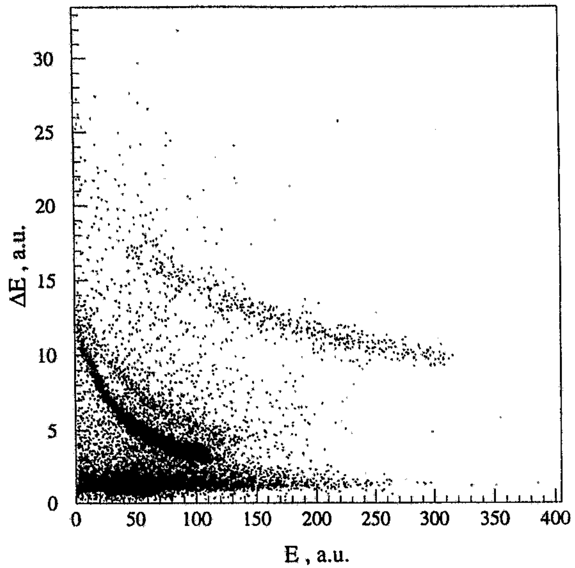

ΔE-E plot obtained for the third layer of the FHD and the first layer of the FRH

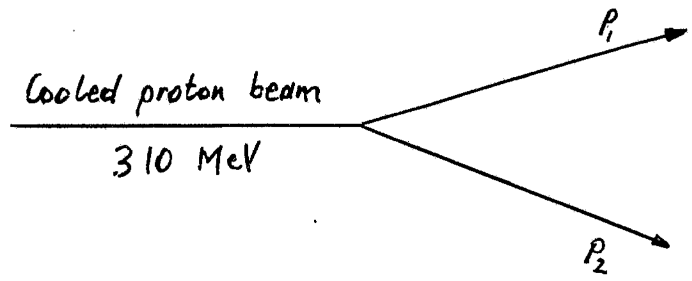

$4^\circ < \theta_p < 21^\circ$

$38\,MeV < T_p < 280\,MeV$

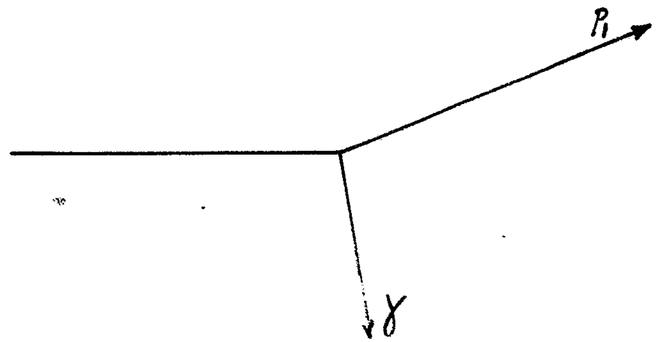

$30^\circ < \theta_\gamma < 90^\circ$

$\Delta\phi_\gamma \approx 50^\circ$

$T_\gamma \geqslant 10\,MeV$

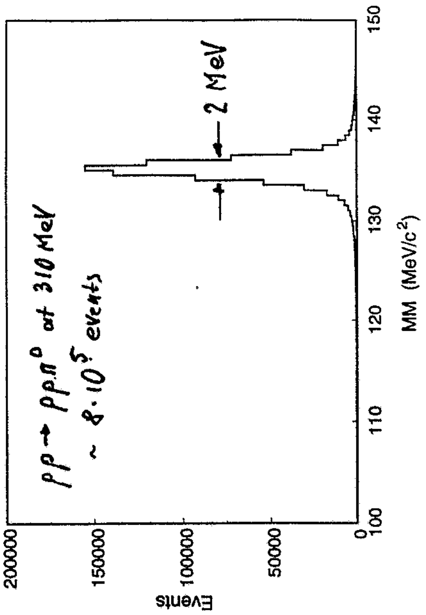
pp → ppπ⁰ at 310 MeV
~ 8·10⁵ events
2 MeV
Events
MM (MeV/c²)

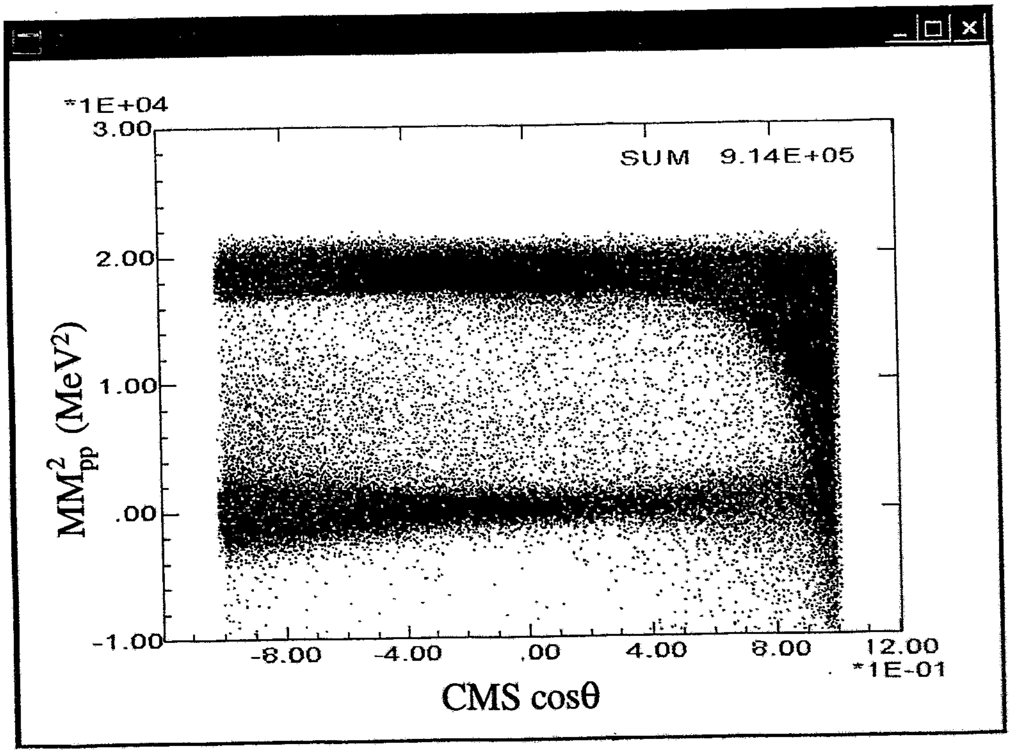
*1E+04
SUM 9.14E+05
MM²pp (MeV²)
CMS cosθ
*1E-01

Monte Carlo simulation of the pp→ppγ reaction at 310 MeV

V. Herrmann, J. Speth and K. Nakayama, Phys. Rev. **C43** (1991) 394.
...The genearal feature of the angular distributions can be understood by examining the contribution arising from the external current (one-body current excluding the rescattering term)...

$$d^2\sigma_{conv}/d\omega d\Omega = \alpha/(2\pi)^2/\omega\cdot[p'/p]\cdot[\varepsilon(p')\cdot\varepsilon(p)\cdot T^2_{pp}]\cdot (8/15\cdot\upsilon'^4 + \upsilon^4\cdot \sin^2 2\theta),$$

$$d^2\sigma_{magn}/d\omega d\Omega = \alpha/(2\pi)^2\cdot\omega/m^2\cdot[p'/p]\cdot[\varepsilon(p')\cdot\varepsilon(p)\cdot T^2_{pp}]\cdot\mu^2_p\cdot [(g-d)^2+1/3\cdot g^2\cdot\upsilon'^2 + d^2\cdot\upsilon^2\cdot \cos^2\theta],$$

where ω and θ are the photon energy and angle in CMS, υ and υ' stand for the proton velocities in the pp CM systems (before and after the scattering), d and g are constants and μ_p is the proton magnetic moment.

Since for the phase space $d^2\sigma/d\omega d\Omega \propto \omega\cdot p'/p$ the event weight W given by the phase space Monte Carlo program has been replaced with:

$$W' = W\cdot W_{pp\gamma}$$

where

$$W_{pp\gamma} = 1/\omega\cdot(8/15\cdot\upsilon'^4 + \upsilon^4\cdot \sin^2 2\theta)\cdot(1/\omega) + \omega/m^2\cdot[(g-d)^2+1/3\cdot g^2\cdot\upsilon'^2 + d^2\cdot\upsilon^2\cdot \cos^2\theta]\cdot\mu^2_p\cdot(1/\omega) .$$

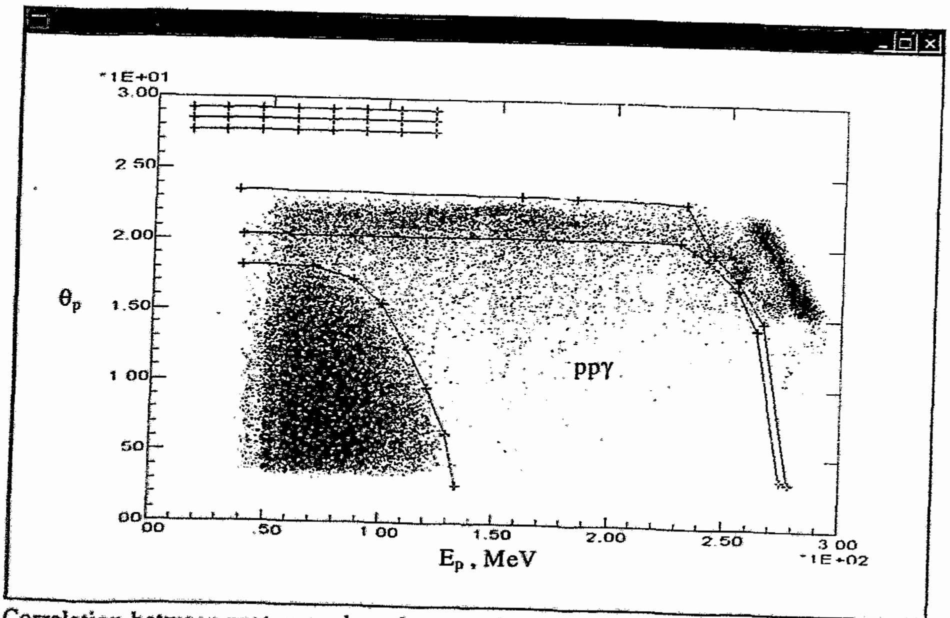

Correlation between proton angle and energy for pp→pγ+X at 310 MeV. Illustration of the selection of the pp→ppγ reaction.

pp→ppγ at 310 MeV

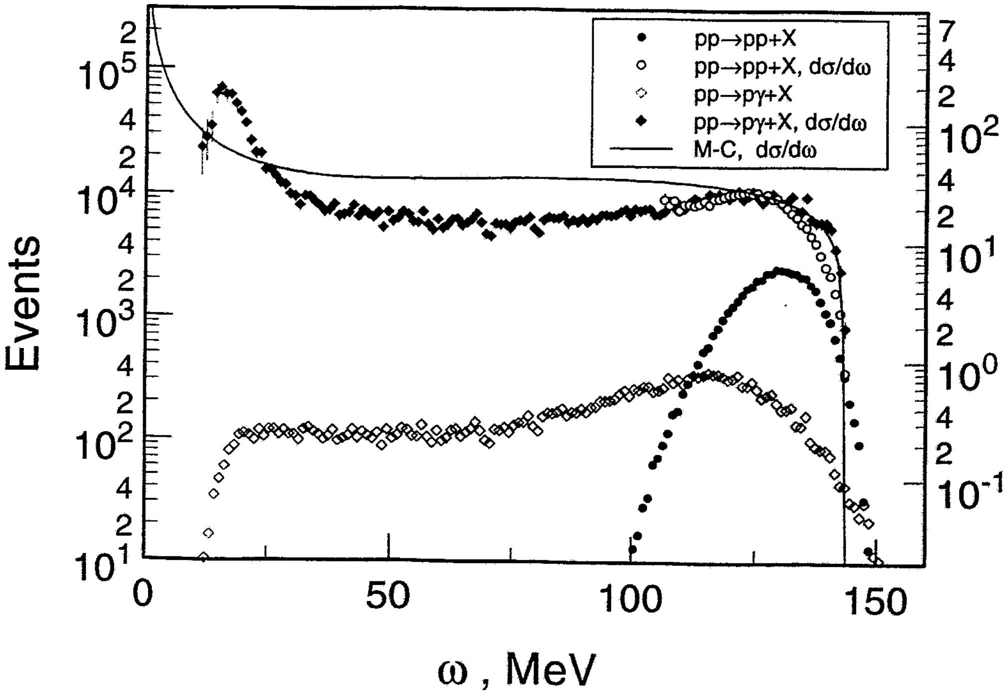

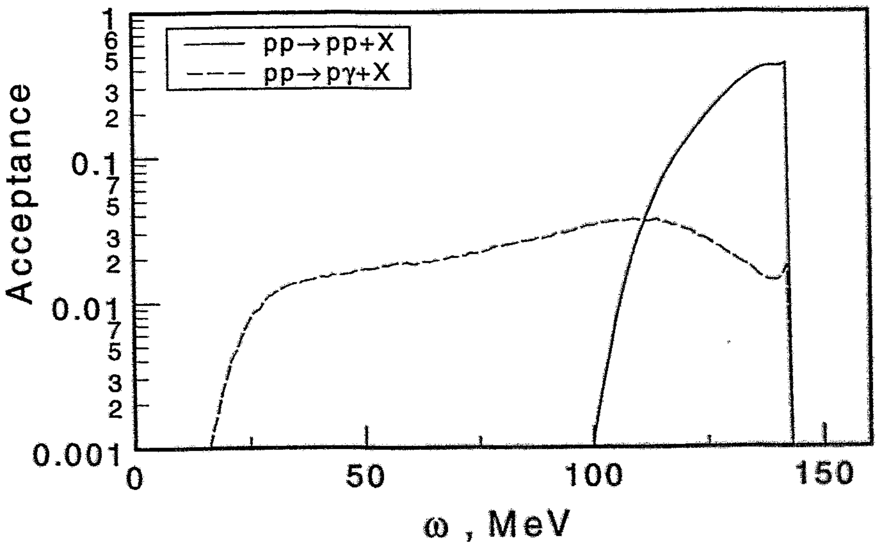

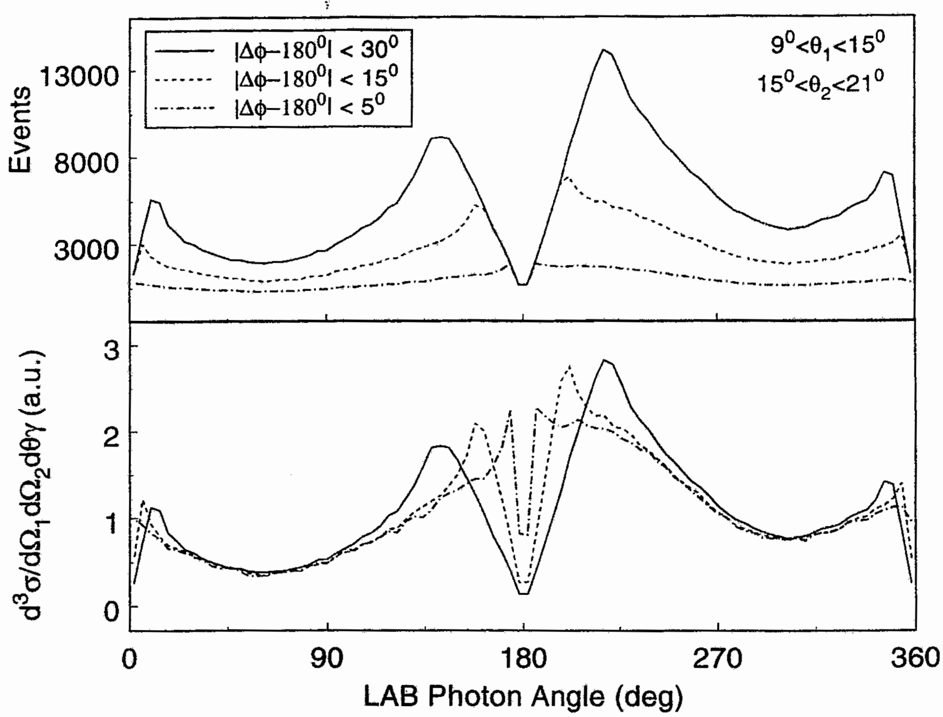

|Δϕ−180°| < 30°
|Δϕ−180°| < 15°
|Δϕ−180°| < 5°
9°<θ1<15°
15°<θ2<21°
Events
13000
8000
3000
d3σ/dΩ1dΩ2dθγ (a.u.)
3
2
1
0
0
90
180
270
360
LAB Photon Angle (deg)

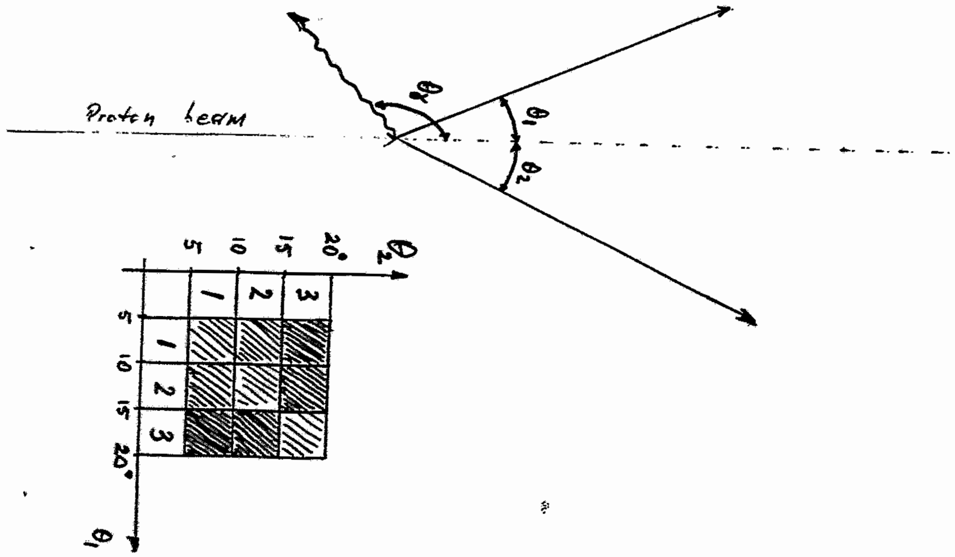

Proton beam
θγ
θ1
θ2

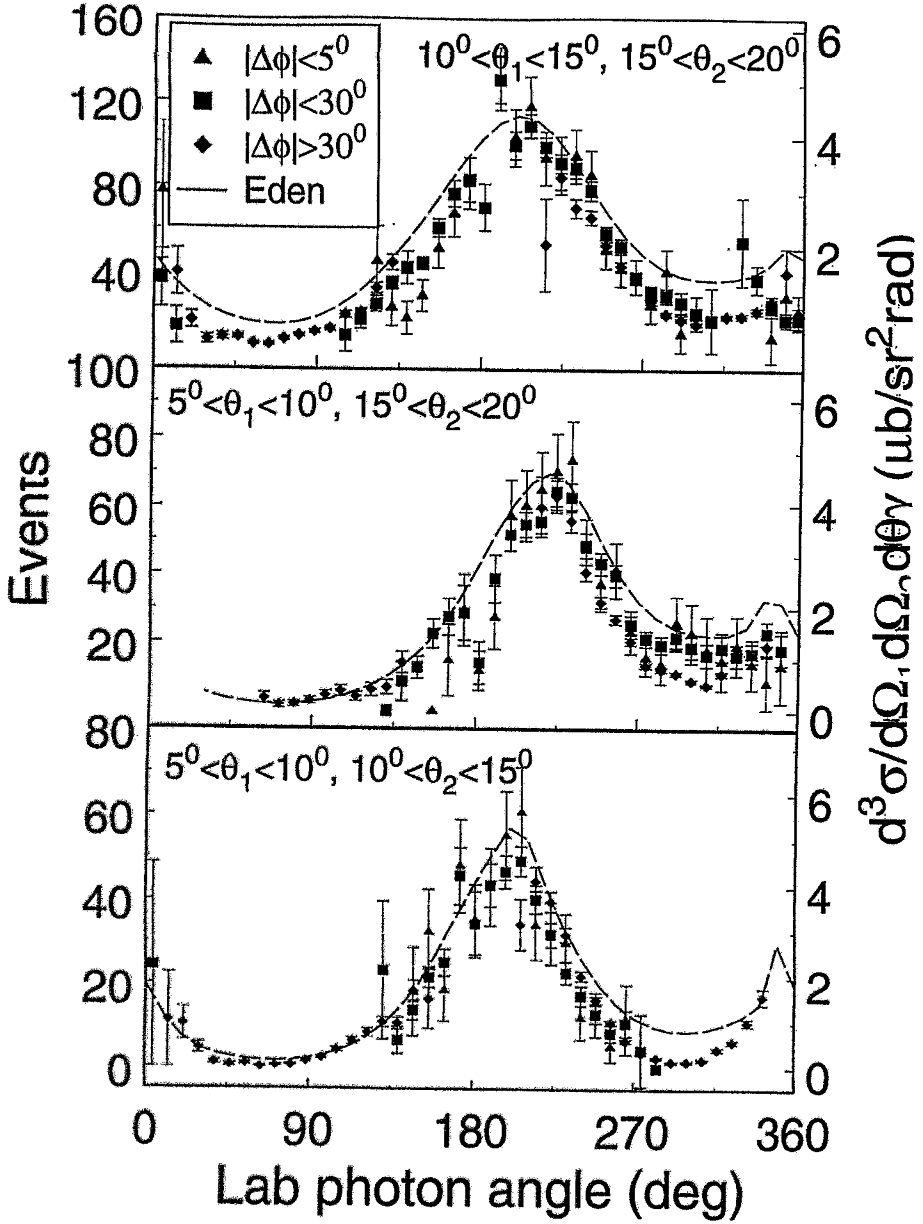
Events
d$^3\sigma$/dΩ_1dΩ_2d$\theta\gamma$ (μb/sr^{2}rad)
Lab photon angle (deg)
|Δφ|<5^0
|Δφ|<30^0
|Δφ|>30^0
Eden
10^0<θ$_1$<15^0, 15^0<θ$_2$<20^0
5^0<θ$_1$<10^0, 15^0<θ$_2$<20^0
5^0<θ$_1$<10^0, 10^0<θ$_2$<15^0

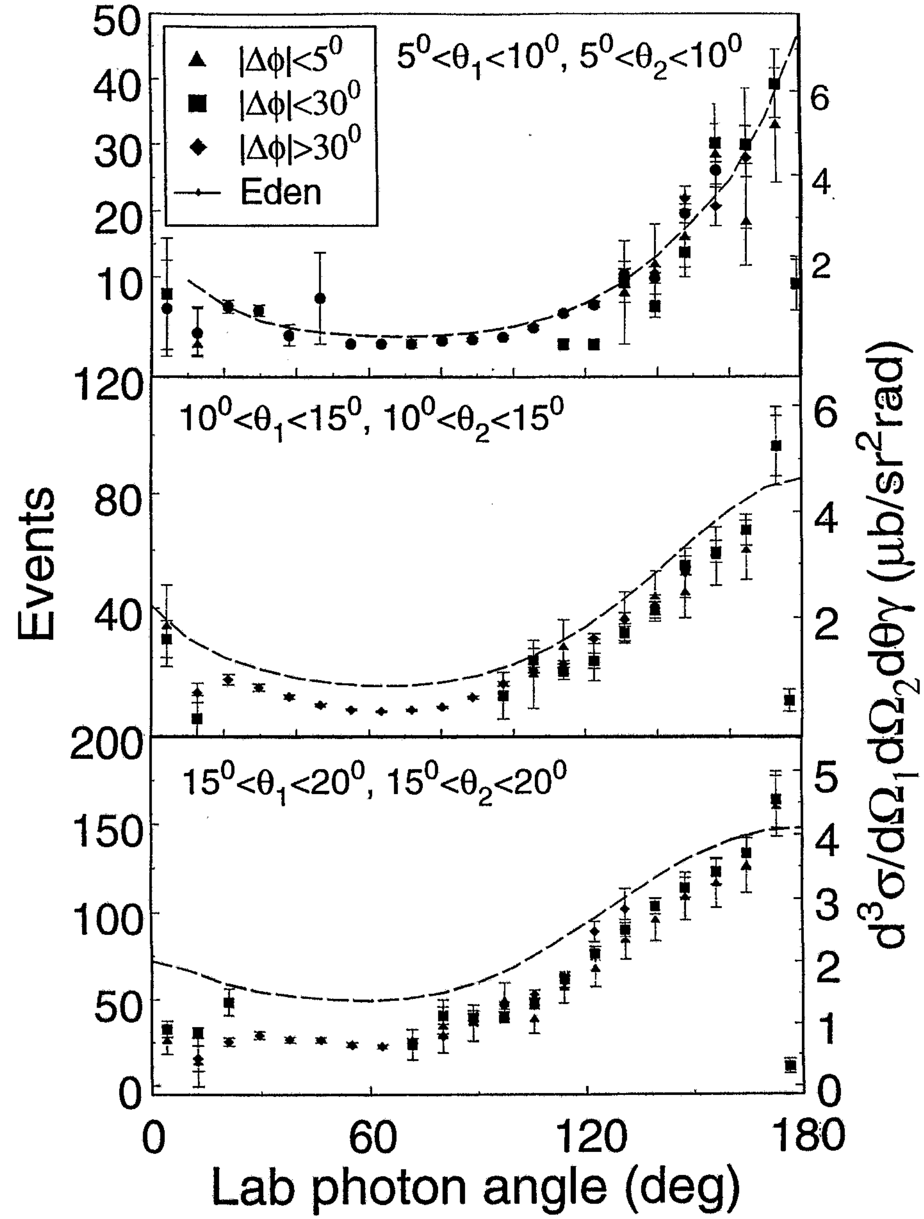
Events
d$^3\sigma$/dΩ_1dΩ_2d$\theta\gamma$ (μb/sr^{2}rad)
Lab photon angle (deg)
|Δφ|<5^0
|Δφ|<30^0
|Δφ|>30^0
Eden
5^0<θ$_1$<10^0, 5^0<θ$_2$<10^0
10^0<θ$_1$<15^0, 10^0<θ$_2$<15^0
15^0<θ$_1$<20^0, 15^0<θ$_2$<20^0

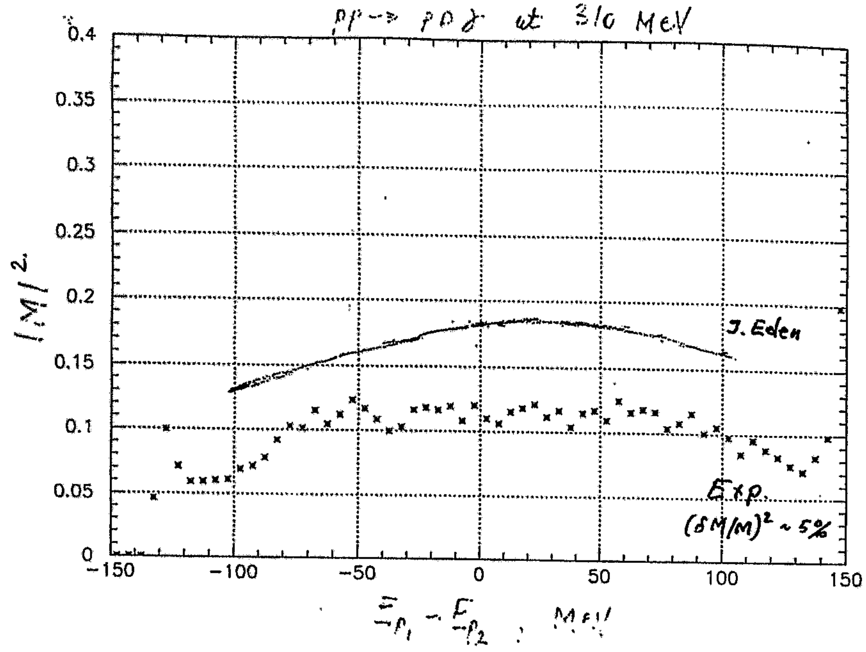

$10^\circ < \theta_1 < 15^\circ$
$15^\circ < \theta_2 < 20^\circ$
$||\Delta\phi| - 180^\circ| < 60^\circ$

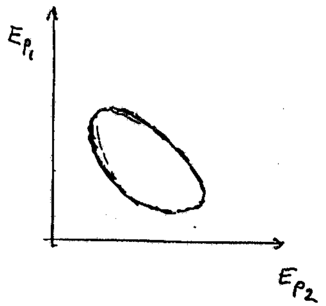

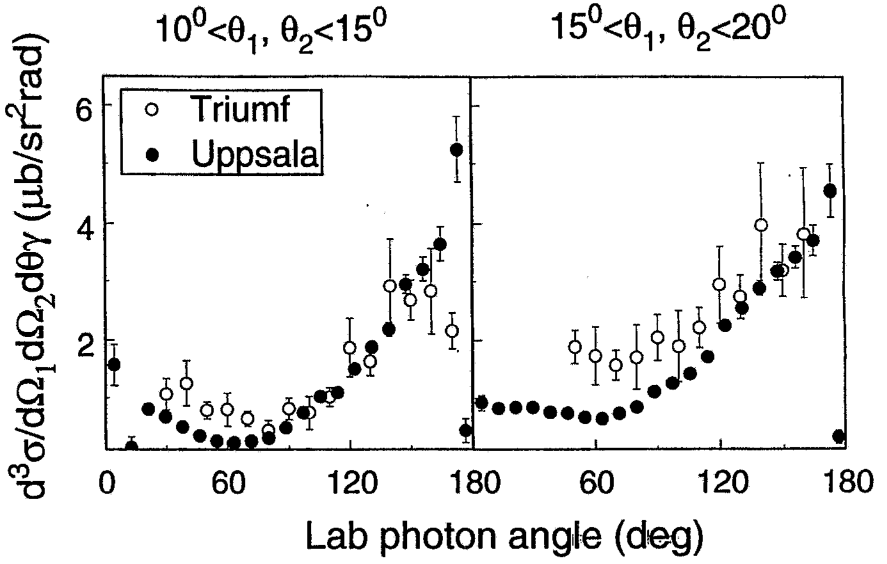

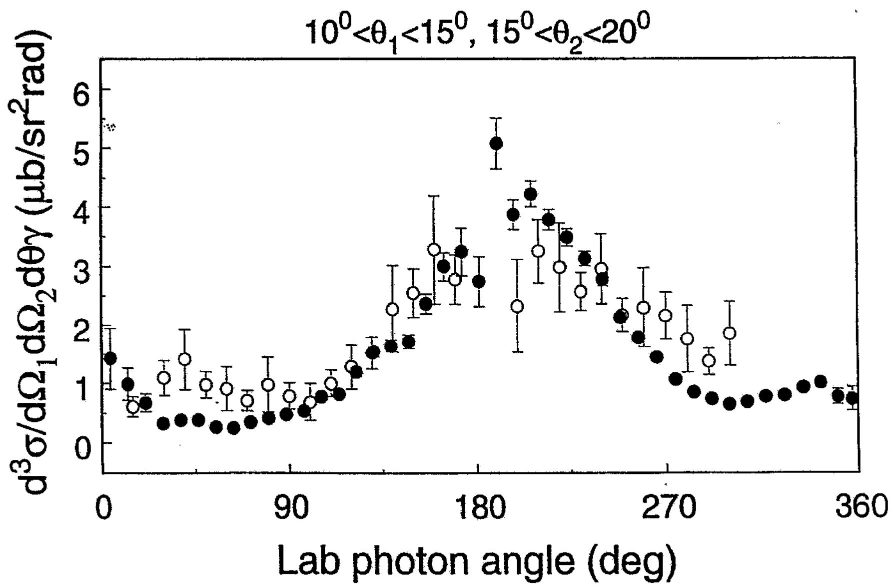

Layout of the WASA 4π-Detector

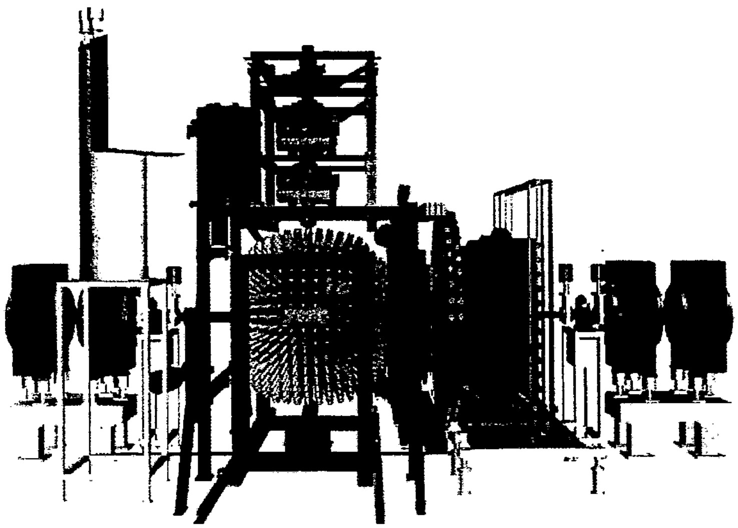

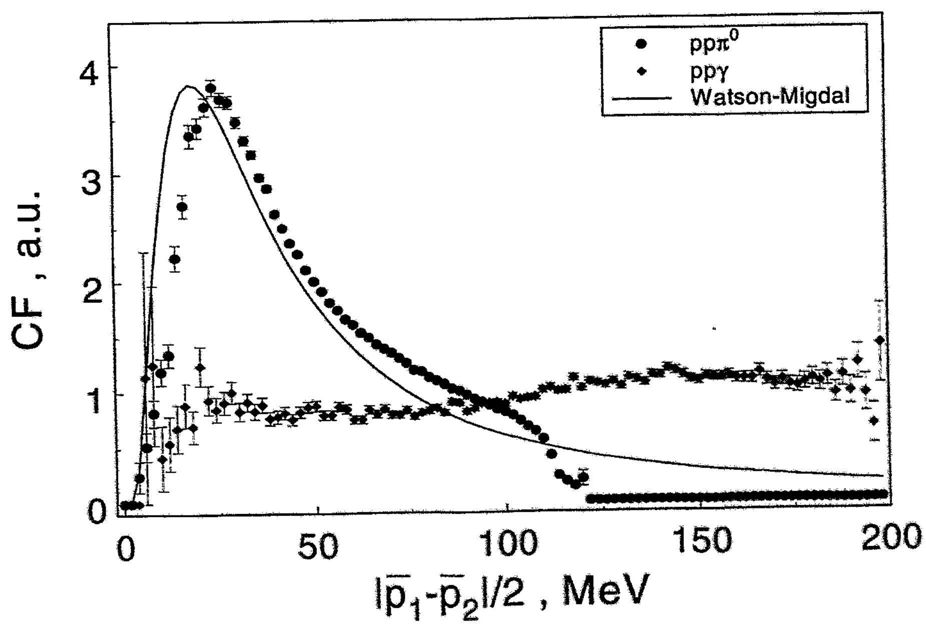

E. Kuhlmann:

Bremsstrahlung experiments at COSY-TOF

Rossendorf, April 16, 1999

Bremsstrahlung Experiments at COSY-TOF

E. Kuhlmann, TU Dresden

for the COSY-TOF collaboration

* Experimental Setup
* Recent Results
* Old Problems Revisited
* Polarization Observables

Bremsstrahlung - a tool to investigate off-shell effects (?)

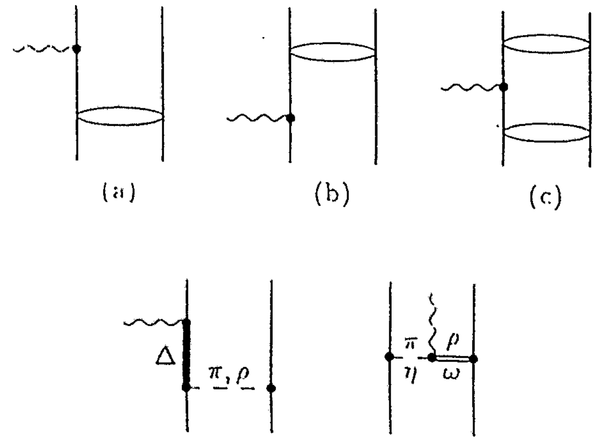

(a) (b) (c) (d) (e)

recent development:

consideration of contact term

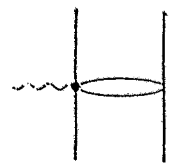

(f)

better: supply hi-quality data !

14.05.98 kph015

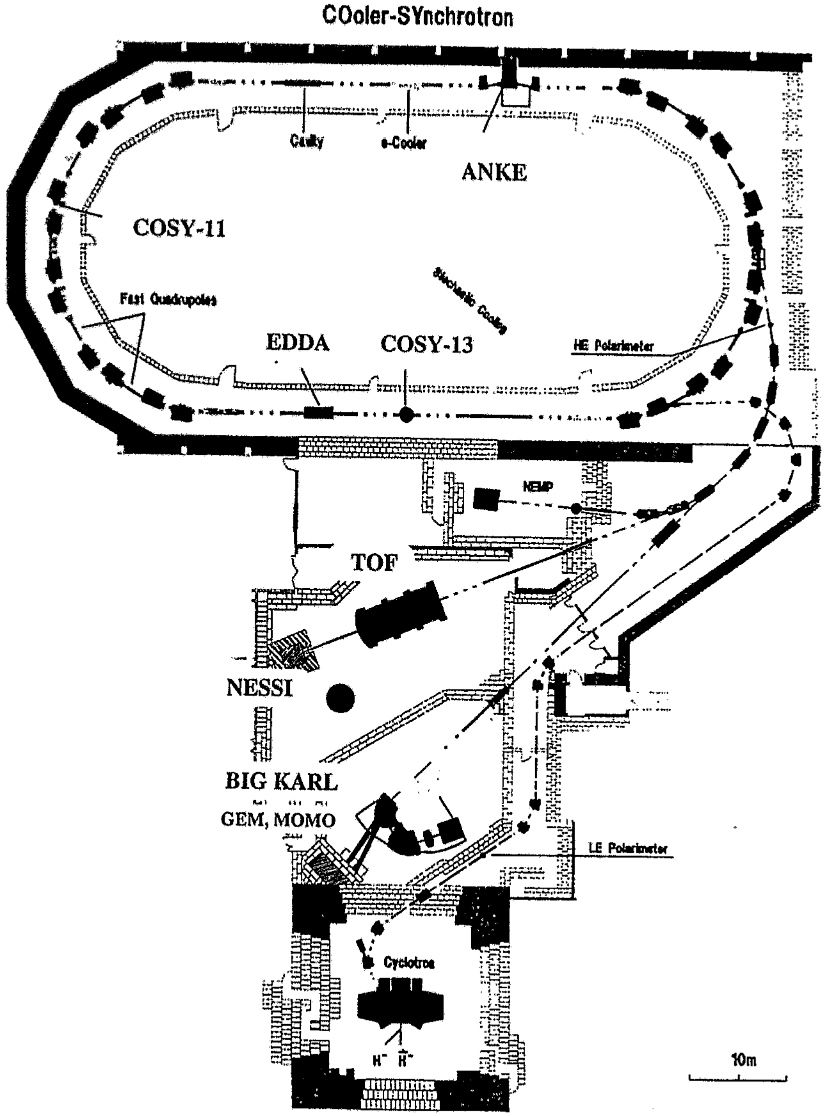

$pp\gamma$ at 797 MeV/c (October '96)

$pn\pi^+$ threshold

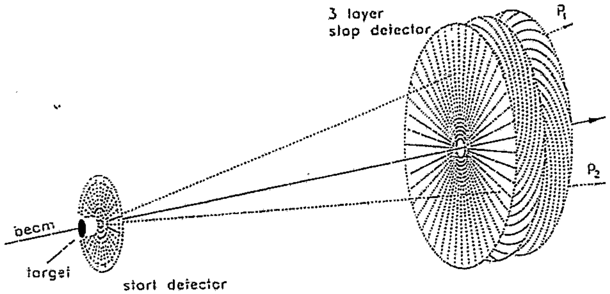

COSY-TOF spectrometer

start-, stop-detector system
+ 3 veto's (≥ 2 mm ϕ_i)

<u>detected:</u>

2 charged particles

<u>reconstructed:</u>

photon via
missing mass
analysis

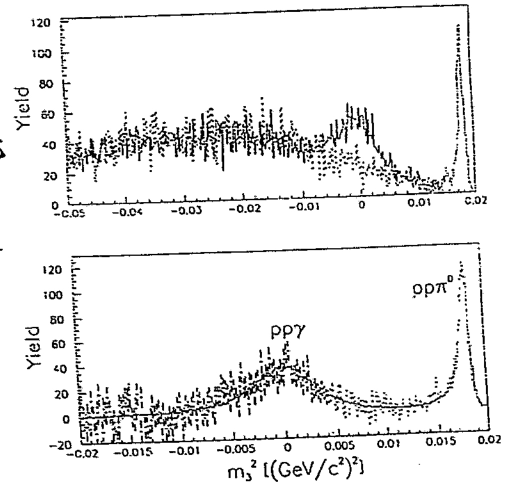

P. Herrmann (thesis); Phys. Lett. B429(98)1

Data analysis accompanied by extensive Monte Carlo simulation

- phase space
- detector response
- $1/3 + \cos^2\Theta_{12}$

cm data

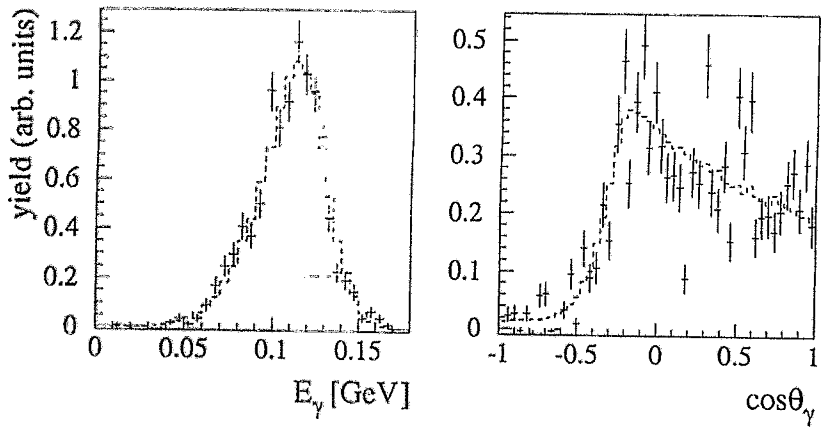

throughout

very good agreement

the weighting factor $1/3 + \cos^2\Theta_{12}$

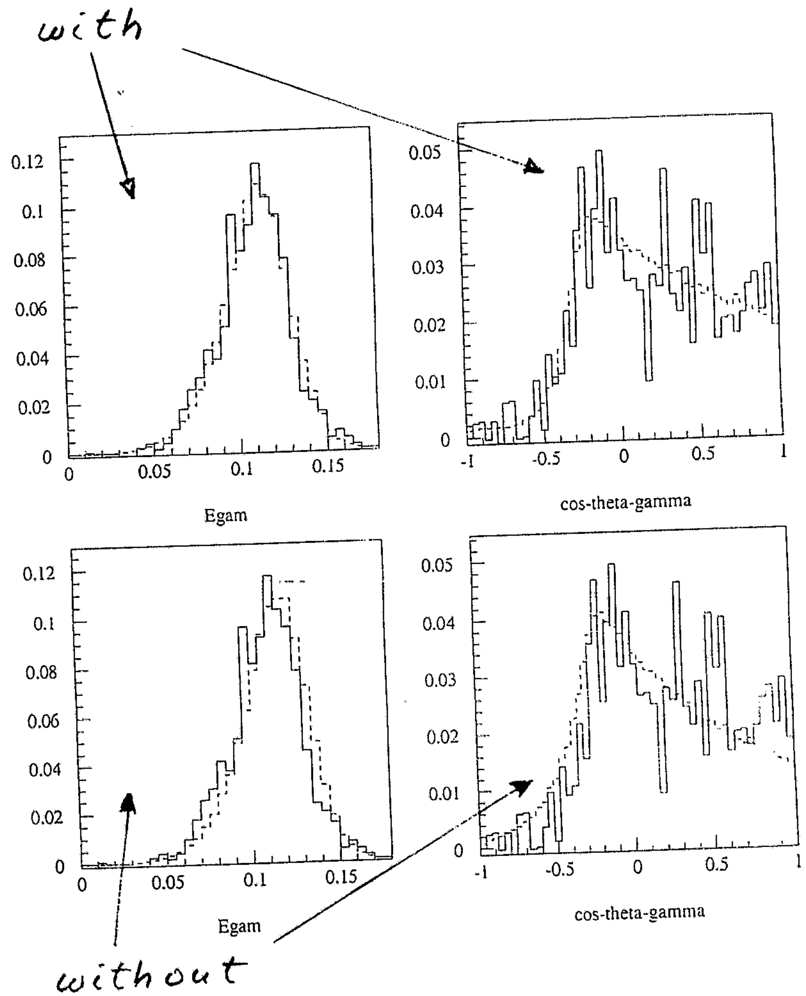

sample of coplanar angular distributions

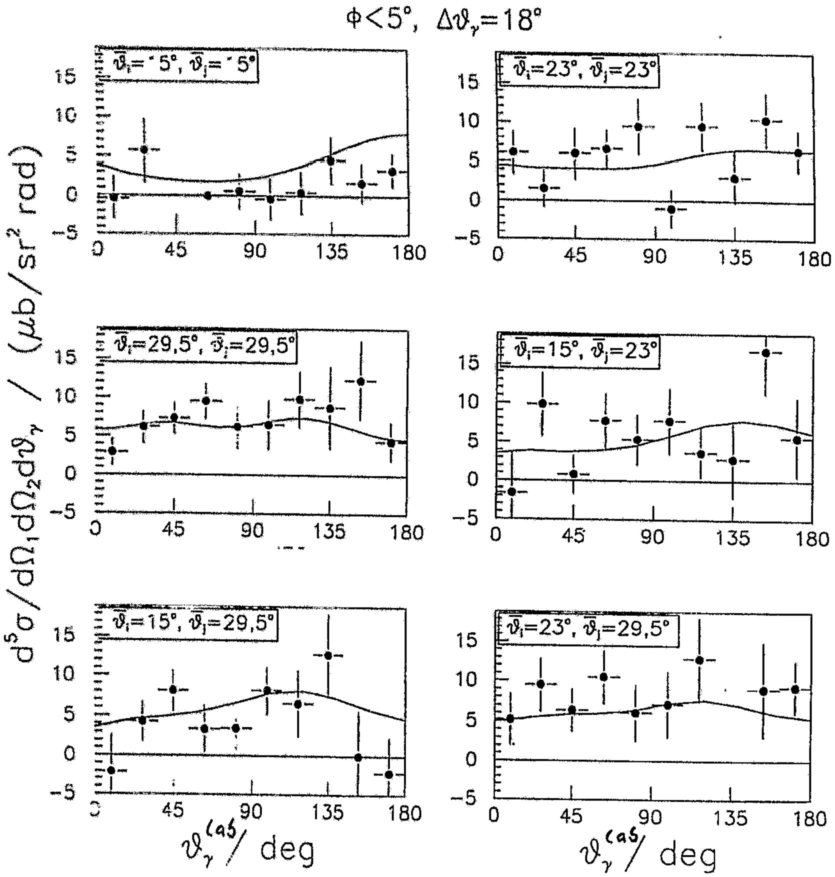

theory: J. Eden et al.,

Phys. Rev. C53 (96) 1102

+priv. communication

PHYSICAL REVIEW C VOLUME 58, NUMBER 2 AUGUST

Meson exchange and Δ isobar currents in proton-proton bremsstrahlung

G. H. Martinus and O. Scholten
Kernfysisch Versneller Instituut, 9747 AA Groningen, The Netherlands

J. A. Tjon
Institute for Theoretical Physics, University of Utrecht, 3508 TA Utrecht, The Netherlands

(Received 13 February 1998)

The contributions from meson exchange and isobar excitation currents to proton-proton bremsstrahlung are discussed within the framework of a relativistic NN interaction. Below the pion-production threshold the Δ isobar is shown to give the dominant contribution to the two-body currents. The nonrelativistic and static limits to these current operators are discussed, and are shown to give a good approximation to the full relativistic meson-exchange current in the considered kinematic region. For the Δ isobar the static limit is a poor approximation. Including, however, also the energy dependence of the Δ propagation yields a reasonable representation of the isobar excitation current. [S0556-2813(98)00708-0]

PACS number(s): 13.40.−f, 14.20.−c, 24.10.−i, 25.10.+s

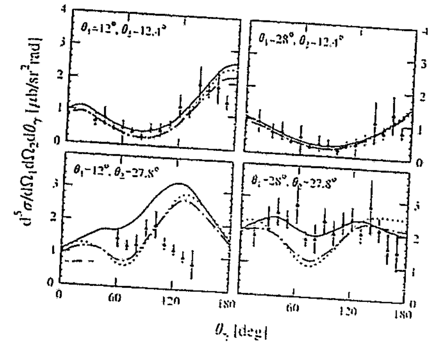

FIG. 10. The cross section at T_{Lab}=280 MeV as a function of photon angle θ_γ at various proton angles: $\theta_1=12°, \theta_2=12.4°$ (top left), $\theta_1=28°, \theta_2=12.4°$ (top right), $\theta_1=12°, \theta_2=27.8°$ (bottom left), and $\theta_1=28°, \theta_2=27.8°$ (bottom right). The solid line is the result of the calculation if both MEC and Δ currents are included, and the dotted line if only the MEC contributions are included, whereas the dot-dashed line is the result of the calculation with only the nucleonic current. The data is from the TRIUMF [6] experiment, with the normalization factor 2/3 for the cross section included. Proton 1 is on the same side of the beam as the photon.

TRIUM × 2/3 is wro

Compilation of 4-fold differential cross sections ("Harvard" geometry)

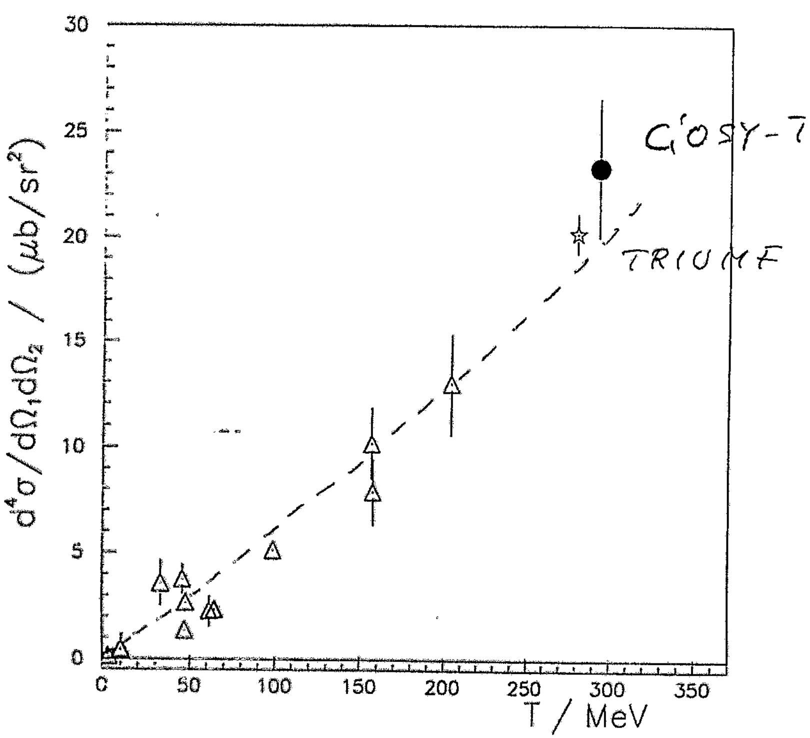

theory: Reid soft-core

G. Schiffrer and D. Drechsel NP A148 (70) 286

old problems revisited:

How to present data of a 3-partic reaction...

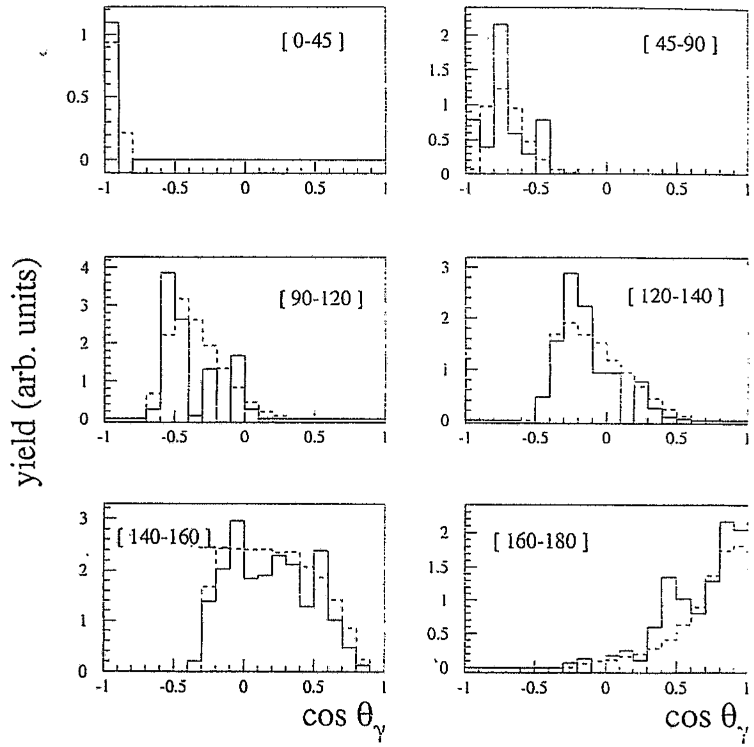

... if taken with a 4π-detector

possible (?) solution: CM-system (always coplanar)

Dalitzplots, FSI and all that

3-Teilchen Kinematik, CM-System

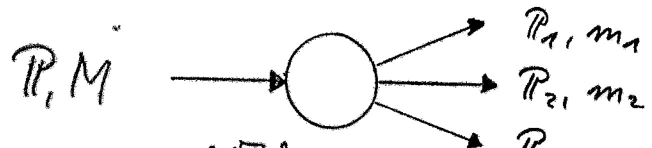

$$\mathbb{P} = \begin{Bmatrix} M \\ 0 \end{Bmatrix} = \begin{Bmatrix} \sqrt{s} \\ 0 \end{Bmatrix}$$

$$s = \mathbb{P}^2 = M^2 = \sum \mathbb{P}_i^{\,2}$$

Def. $$s_{ik} = (\mathbb{P}_i + \mathbb{P}_k)^2 = (\mathbb{P} - \mathbb{P}_j)^2$$
$$= s + m_j^2 - 2E_j\sqrt{s}$$
$$= m_i^2 + m_k^2 + 2E_iE_k - 2|\vec{p}_i|\cdot|\vec{p}_k|\cos\theta_{ik}$$

Relation $$\sum_{perm.} s_{ik} = s + \sum_i m_i^2 = const$$

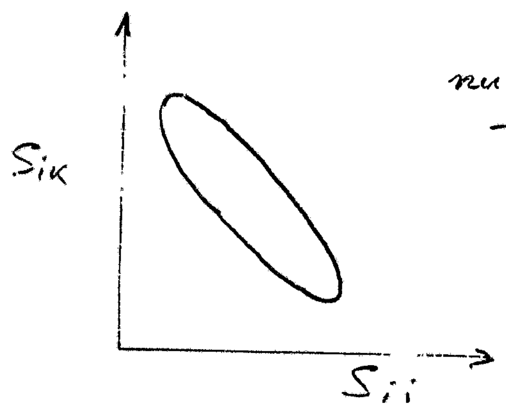

nur Phasenraum
→ Belegung
Konstant

$pp\pi^0$
PLB 356 (95) 8
CELSIUS
300 MeV

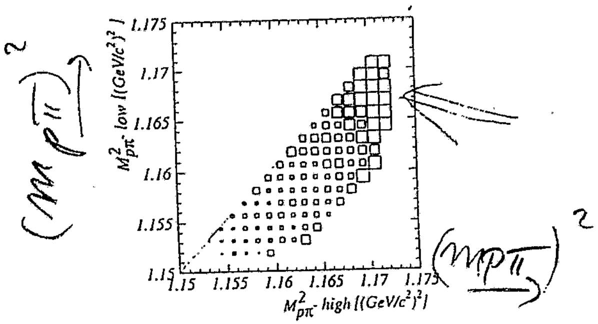

Dalitz plot of events in a plane defined by the squared invariant masses of the pion with each of the two final-state protons. The largest value of invariant masses are plotted along the x-axis. The experimental data are divided by Monte Carlo events generated according to phase space. The uncertainty in each histogram bin is typically 15%.

$pn\pi^+$
PRC 56 (96) 20
IUCF
319 MeV

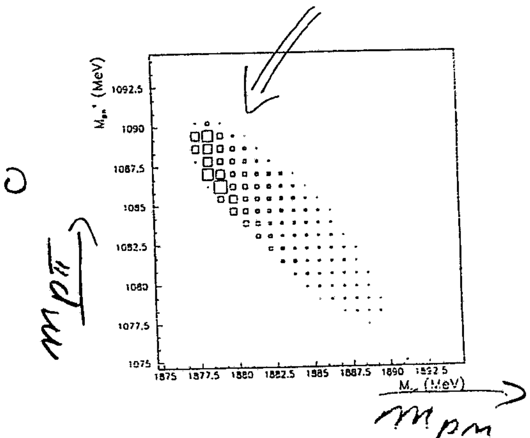

FIG. 19. The Dalitz plot for 319.2 MeV data with phase space acceptance not including FSI. These plots show the invariant mass of the proton-pion pair vs the invariant mass of the proton-neutron pair. All values in the kinematically allowed region are populated in this experiment to some degree. There is a strong enhancement at low M_{pn} and high M_{π^+p}. This would be expected from strong pn final state interactions.

Dalitz plot for $pp\gamma$:

no indications for sizeable FSI-effects

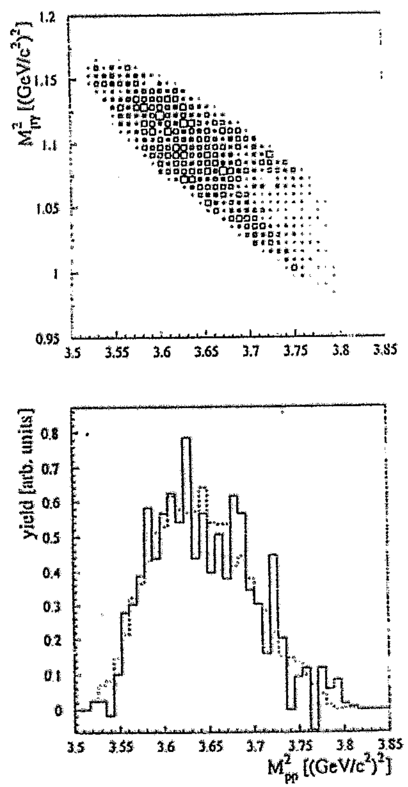

plain phase space effect

or

due to em-transition operator (suppression of $1 \leftrightarrow 3$ transitions)

spin structure in $pp \to pp\gamma$

entrance channel $\quad {}^1S_0, {}^1D_2, \ldots$
$\quad {}^3P_{0,1,2}, {}^3F_{1,2,3}, \ldots$

exit channel $\quad H_S \otimes H_{em}$

H_S : $S \leftrightarrow S$, $T \leftrightarrow T$

H_{em} $\quad \mathcal{E} \quad S \leftrightarrow S, T \leftrightarrow T$

$\quad \mathcal{M} \quad S \leftrightarrow T, T \leftrightarrow T$

at high energy end of photon spectrum

$\mathcal{M} \gg \mathcal{E}$

matrix element for $\mathcal{M}$:

$\langle s' | \mathcal{M}(\vec{k}; \vec{p}'\vec{p}) | s \rangle$

$\propto \left[(-)^s \mu_p f(p', p - \tfrac{k}{2}) + (-)^{s'} \mu_p f(p', p + \tfrac{k}{2}) \right]$

s, s' total spin in entrance; exit channel

$\Rightarrow$ $T \leftrightarrow T$ transitions favored!

impact on spin observables?

(IX) l'9?

Near Future

- begin polarisation studies
  $\vec{p}p \rightarrow pp\gamma$ performed yesterday
- measure $np\gamma$ by use of LD_2-tar
  $pd \rightarrow n + p + p_s + \gamma$

impact of Fermi-motio on missing mass distributio

broadening

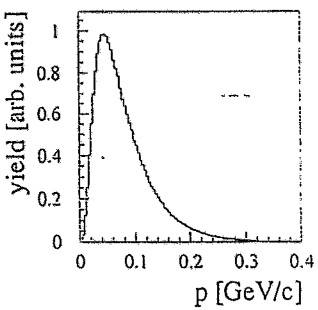

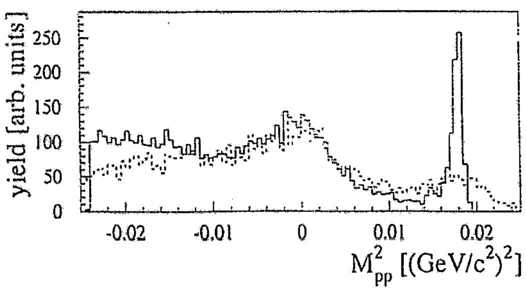

enlarged COSY-TOF spectrome

~ 1π solid angle coverage

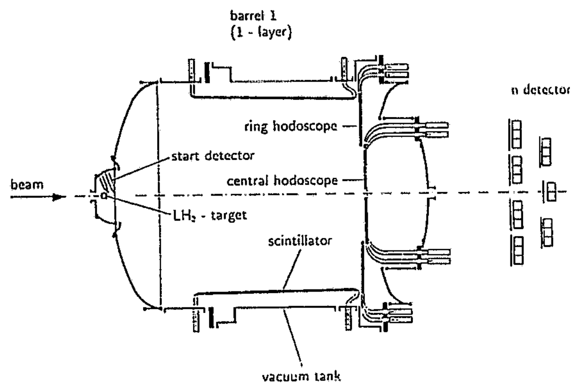

$1^\circ \leq \Theta_p \leq 70^\circ, \quad 0^\circ \leq \Phi_p \leq 360^\circ$

time resolution for barrel elements

measured via pp_{elast}

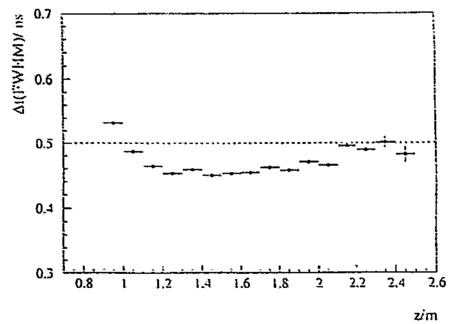

deduced position resolution

$\Delta z(FWHM) \lesssim 5\,cm$

polarization of extracted COSY-beam

$t_{spill} \simeq 10\ s$

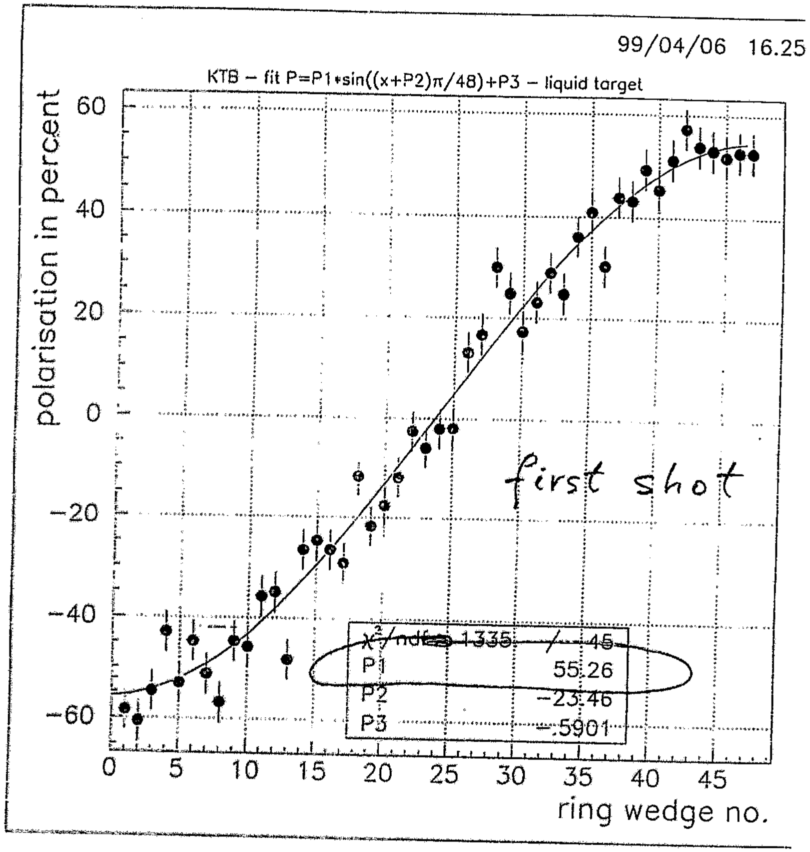

$$P = \frac{1}{A_y} * \frac{N_i^{\uparrow} - N_i^{\downarrow}}{N_i^{\uparrow} + N_i^{\downarrow}}$$

$$N_i^{\uparrow} = \sqrt{L_i^{\uparrow} \cdot R_{i+48}^{\downarrow}} \qquad N_i^{\downarrow} = \sqrt{L_i^{\downarrow} \cdot R_{i+48}^{\uparrow}}$$

(elimination of detector-specific asymmetri

Summary

* COSY delivers (polarized p's)
* COSY-TOF performs well at $\Omega_{LAB} = 1\pi$
* first data on $pp\gamma$ published PL B429 (98) 195
* polarized $pp\gamma$ data on tape

open questions:

in general

presentation of 3-particle differential X-secti.

for COSY

improvement of luminosity

The COSY-TOF collaboration

S. AbdElSamad[e], R. Bilger[g], A. Böhm[c], K.-Th. Brinkmann[c], H. Clement[g], H. Dennert[d], S. Dshemuchadse[f], H. Dutz[b], A. Erhardt[g], W. Eyrich[d], C. Fanara[k], D. Filges[e], A. Filippi[k], H. Freiesleben[c], M. Fritsch[d], R. Geyer[e], U. Goldmann[e], A. Hassan[i], J. Hauffe[d], P. Herrmann[a], D. Hesselbarth[e], P. Jahn[e], B. Jakob[c], K. Kilian[e], H. Koch[a], J. Kress[g], J. Krug[a], E. Kuhlmann[c], S. Marcello[k], S. Marwinski[e], A. Metzger[d], W. Meyer[a], P. Michel[f], K. Möller[f], H. P. Morsch[e], H. Nann[h], B. Naumann[f], L. Naumann[f], A. Raimondo[k], E. Roderburg[e], M. Rogge[e], A. Schamlott[f], P. Schönmeier[c], W. Schroeder[d], M. Schulte-Wissermann[c], M. Steinke[a], F. Stinzing[d], G.Y. Sun[c], J. Wächter[d], G. J. Wagner[g], M. Wagner[d], A. Wilms[a], S. Wirth[d], U. Zielinski[a]

[a]Institut für Experimentalphysik I, Ruhr-Universität Bochum, D-44780 Bochum
[b]Physikalisches Institut, Universität Bonn, D-53115 Bonn
[c]Institut für Kern und Teilchenphysik, Technische Universität Dresden, D-01062 Dresden
[d]Physikalisches Institut, Universität Erlangen-Nürnberg, D-91058 Erlangen
[e]Institut für Kernphysik, Forschungszentrum Jülich, D-52425 Jülich
[f]Institut für Kern- und Hadronenphysik, Forschungszentrum Rossendorf, D-01314 Dresden
[g]Physikalisches Institut, Universität Tübingen, D-72076 Tübingen
[h]IUCF Bloomington, Indiana 47408, USA
[i]Atomic Energy Authority NRC, Kairo, Ägypten
[k]INFN Torino, Italien

thanks to financial support by
BMBF + FZ-Jülich

J. Wambach:

Dileptons and chiral symmetry restoration

LOW-MASS DILEPTONS AND CHIRAL SYMMETRY RESTORATION

J. Wambach

1. Introduction
2. Chiral Symmetry Breaking and its Restoration
3. Dileptons as a Probe
   - 3.a Hadron Gas- vrs. Plasma Rates
   - 3.b Models for in-medium Effects
4. Chiral Symmetry Restoration and Vector Mesons
   - 4.a Weinberg Sum Rules
   - 4.b V-A Mixing
5. Comparison with Data
   - 5.a 'Fireball' Model
   - 5.b Hydrodynamics

Collaborators:

E. Bratkovskaya, M. Buballa, W. Cassing, G. Chanfray, R. Rapp, M. Urban

Relativistic Heavy Ions

RHIC's study hadronic matter under extreme conditions in temperature and density

Facilities:

GSI/SIS	$\sim$ 1 AGeV
CERN/SPS	$\sim$ 20 AGeV
BNL/RHIC	$\sim$ 100 AGeV
CERN/LHC	$\sim$ 10 ATeV

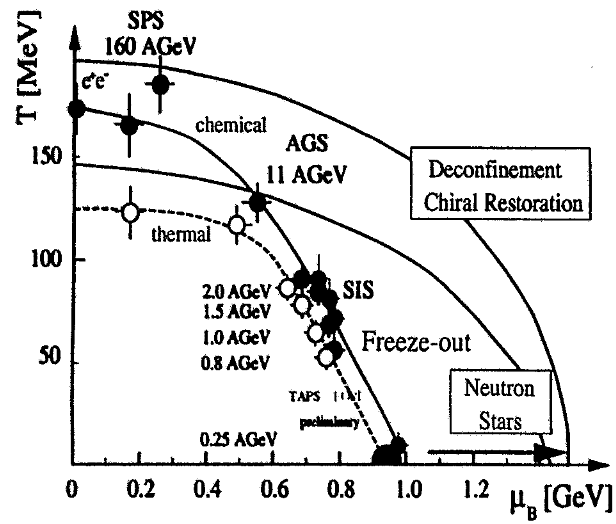

Heavy-Ion Collisions and Dileptons

vector mesons observed in dilepton production of RHIC's

ideal probes of the early stages of the collision

Sources:

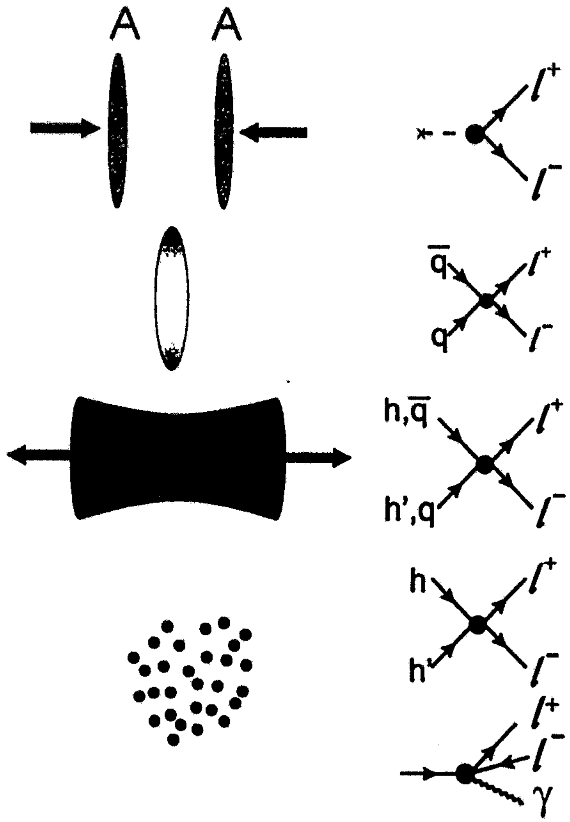

Chiral Symmetry Breaking

chiral symmetry is spontaneously broken in the physical vacuum

$$Q_5^a|0\rangle \neq 0$$

→ Goldstone bosons

$$\langle 0|A_k^\mu(x)|\pi_j(p)\rangle = -i\delta_{jk}F_\pi p^\mu e^{-ipx}$$

→ no parity doublets

$\bar{q}q$-excitations of the QCD vacuum

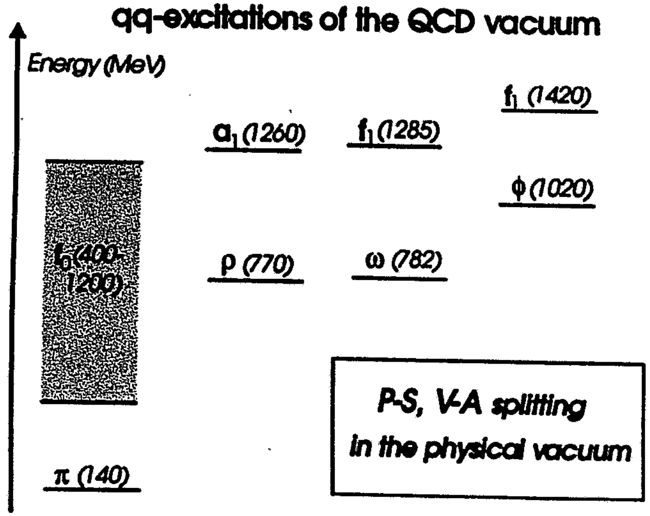

Chiral Symmetry Restoration

consider a hadronic medium in thermal equilibrium

QCD partition function:

$$\mathcal{Z}_{QCD}(T,\mu,V) = \mathrm{Tr}\, e^{-(H_{QCD}-\mu N)/T}$$

free energy density:

$$\mathcal{F}(T,\mu) = -\lim_{V\to\infty}\frac{T}{V}\ln \mathcal{Z}_{QCD}(T,\mu,V)$$

from the Feynman-Hellmann theorem:

$$\langle\bar{q}q\rangle^* = \frac{\partial\mathcal{F}(T,\mu)}{\partial m_q}$$

quark mass m acts like an external magnet !

with the GOR: $(m_\pi^2 F_\pi^2 = -2m\langle\bar{q}q\rangle)$

$$\frac{\langle\bar{q}q\rangle^*}{\langle\bar{q}q\rangle} = 1 - \sum_h \frac{(m\partial/\partial m)\,\delta\mathcal{F}(T,\mu)}{F_\pi^2 m_\pi^2}$$

$$\delta\mathcal{F}(T,\mu) = \mathcal{F}(T,\mu) - \mathcal{F}(0)$$

dilute gas of hadrons : $\delta\mathcal{F}(T,\mu) = \sum_h M_h \rho_h^s(T,\mu)$

$$\frac{\langle\bar{q}q\rangle^*}{\langle\bar{q}q\rangle} = 1 - \sum_h \frac{\Sigma_h \rho_h^s(T,\mu)}{F_\pi^2 m_\pi^2}$$

T,μ small (pions and nucleons only)

$$\frac{\langle\bar{q}q\rangle^*}{\langle\bar{q}q\rangle} \sim 1 - \frac{T^2}{8F_\pi^2} - 0.3\frac{\rho}{\rho_0} + \cdots$$

Chiral Condensate

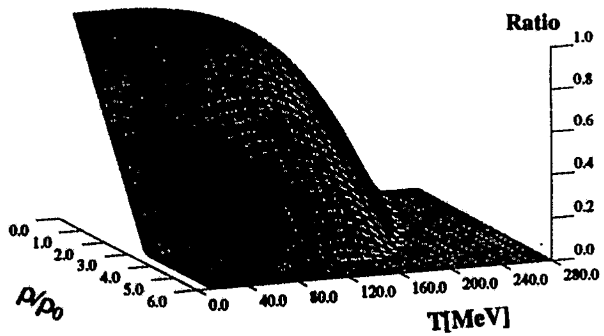

no obvious connection between M_h and $\langle\bar{q}q\rangle^*$!

Initial conditions (currently reached):

$\epsilon > 1$ GeV/fm^3

$T > 150$ MeV

lattice QCD:

EoS

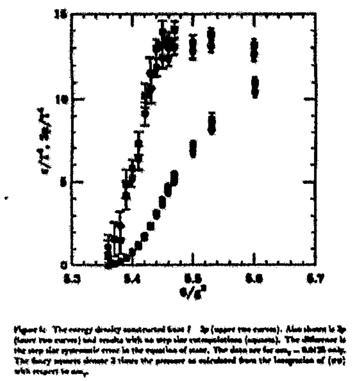

quark condensate

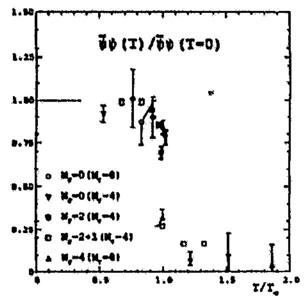

what are the

signatures ?

Schematic View

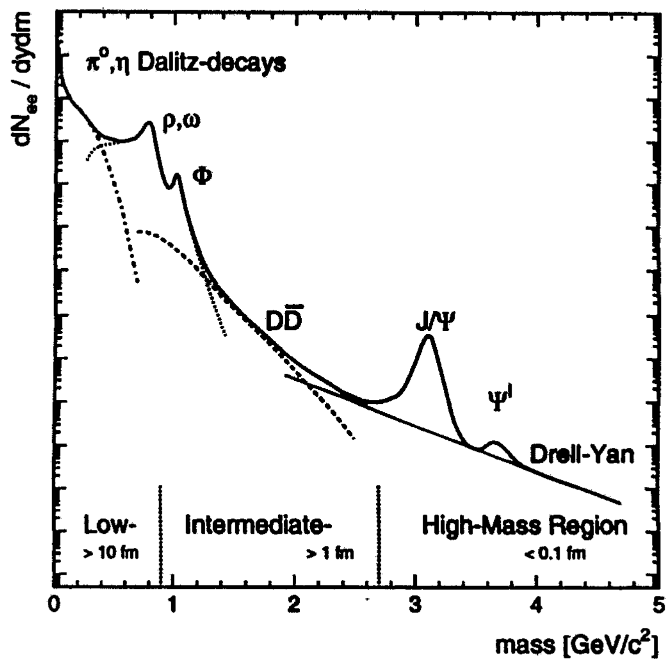

Vector Mesons

- vector mesons $\rho, \omega, \phi, J/\psi$ as resonances in e^+e^- annihilation

$$R(s) = \frac{\sigma(e^+e^- \to \text{hadrons})}{\sigma(e^+e^- \to \mu^+\mu^-)}$$

$$\sigma(e^+e^- \to \mu^+\mu^-) = 4\pi\alpha^2/3s$$

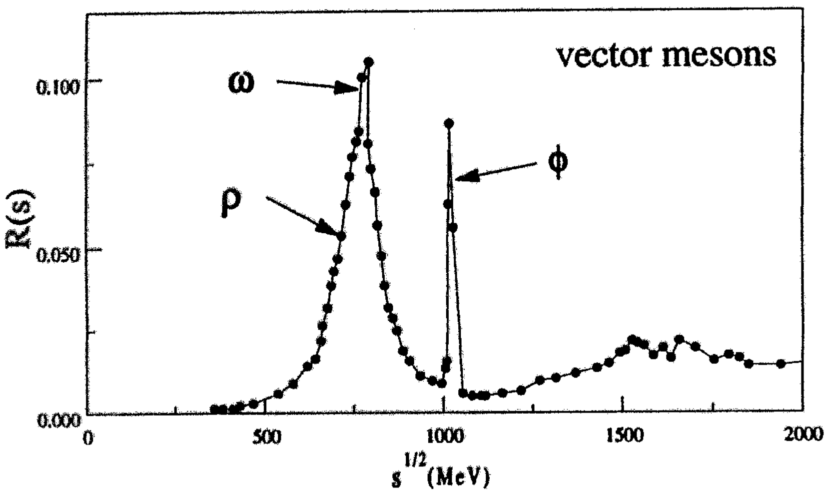

Dilepton Rates

dilepton production from the medium:

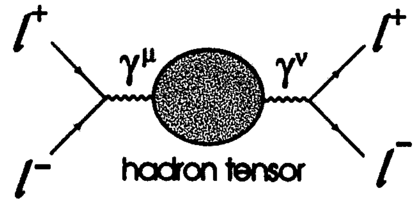

rate: $M^2 \equiv q^2 > 0$

$$\frac{dN_{l^+l^-}}{d^4x\,d^4q} = \frac{dR}{d^4q} = L^{\mu\nu}(q)H_{\mu\nu}(q)$$

lepton tensor:

$$L^{\mu\nu}(q) = -\frac{\alpha^2}{6\pi^3 q^2}\left(g^{\mu\nu} - \frac{q^\mu q^\nu}{q^2}\right)$$

hadron tensor:

$$H_{\mu\nu}(q) = \int d^4x\, e^{-iqx} \ll J_\mu^{em}(x) J_\nu^{em}(0) \gg$$

electromagnetic current: $\sqrt{s} < 2m_c \sim 3\,\mathrm{GeV}$

$$J_\mu^{\rm em} = \frac{2}{3}\bar{u}\gamma_\mu u - \frac{1}{3}\bar{d}\gamma_\mu d - \frac{1}{3}\bar{s}\gamma_\mu s = J_\mu^\rho + J_\mu^\omega + J_\mu^\phi$$

$$J_\mu^\rho = \frac{1}{2}(\bar{u}\gamma_\mu u - \bar{d}\gamma_\mu d)$$

$$J_\mu^\omega = \frac{1}{6}(\bar{u}\gamma_\mu u + \bar{d}\gamma_\mu d)$$

$$J_\mu^\phi = -\frac{1}{3}(\bar{s}\gamma_\mu s)$$

quark gas at finite temperature:

$$\frac{dR}{dM^2} = R^q \frac{\alpha^2}{6\pi^2} M T K_1(M/T)$$

$$R^q = N_c \sum_f e_f^2 = 3(\tfrac{4}{9} + \tfrac{1}{9} + \tfrac{1}{9})$$

resonance gas at finite temperature:

$$\frac{dR}{dM^2} = R^{\rm exp} \frac{\alpha^2}{6\pi^2} M T K_1(M/T)$$

$$R^{\rm exp} = \frac{\sigma(e^+e^- \to \text{hadrons})}{\sigma(e^+e^- \to \mu^+\mu^-)}$$

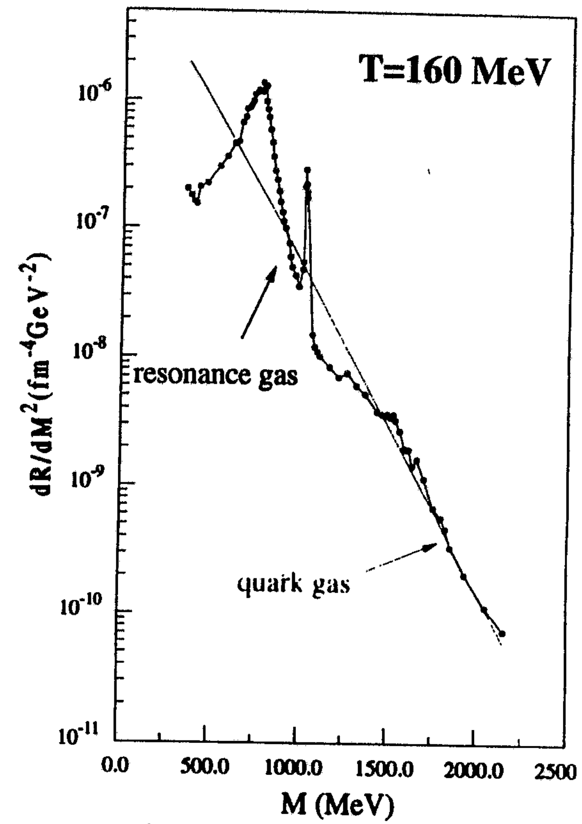

Medium Effects

time-ordered correlation function:

$$\Pi_{\mu\nu}(q) = -i \int d^4x \, e^{iqx} \ll \mathcal{T}(J^{\rm em}_\mu(x), J^{\rm em}_\nu(0)) \gg$$

$$\mathrm{Im}\Pi_{\mu\nu}(q) = -\frac{1}{2}(e^{-\beta q_0}+1)H_{\mu\nu}(q)$$

virial expansion: (low T, small μ)

$$\Pi_{\mu\nu}(q) = \Pi^{0}_{\mu\nu}(q) + \sum_h n_h(T,\mu)\Pi^h_{\mu\nu}(q)$$

$$\Pi_{\mu\nu}(q) = -(g_{\mu\nu} - \frac{q_\mu q_\nu}{q^2})\Pi(q^2)$$

$$R(s) = -\frac{12\pi}{s}\mathrm{Im}\Pi(q^2)$$

dominant contribution from pions and nucleons

$$n_\pi \Pi^\pi_{\mu\nu}(q) = \int \frac{d^3k}{(2\pi)^3} \frac{n(\omega_k)}{2\omega_k} C^\pi_{\mu\nu}(q,k)$$

$$n_N \Pi^N_{\mu\nu}(q) = \int \frac{d^3p}{(2\pi)^3} \frac{m_N}{E_p} \frac{n(E_p)}{2\omega_k} C^N_{\mu\nu}(q,p)$$

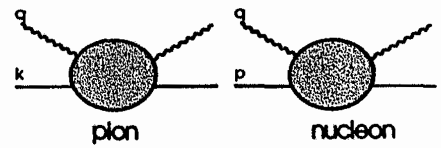

'virtual Compton tensor' of the pion:

$$C_{\mu\nu}(q,k) = -i \int d^4x \, e^{iqx} \langle \pi(\vec{k}) | \mathcal{T}(J^{\rm em}_\mu(x), J^{\rm em}_\nu(0)) | \pi(\vec{k}) \rangle$$

similar expression for the nucleon

- 'chiral reduction formalism':

J.V. Steele et al. PRL (1996), PRD (1997)

$$g^{\mu\nu} C^\pi_{\mu\nu}(q,k) = -\frac{\mathrm{Im}}{F_\pi^2}(2\Pi^\circ_V(q^2) + \underbrace{\Pi^\circ_A((q+k)^2)}_{a_1 \to \pi e^+ e^-} \cdots)$$

vector and avialvector correlators !

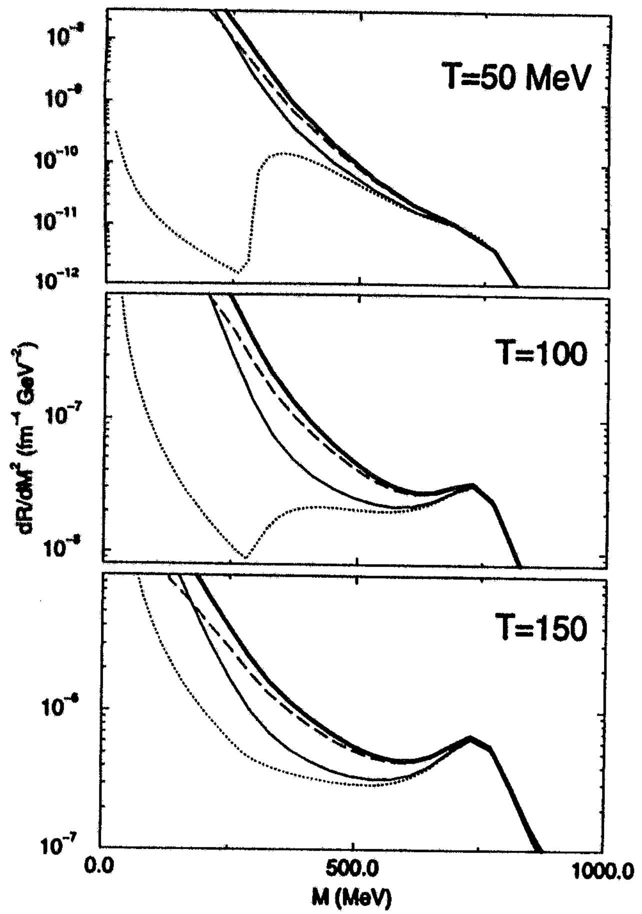

Low-Mass Region

modification of the rho meson in an meson gas

$$\omega, h_1, a_1, K_1, f_1, \pi'$$

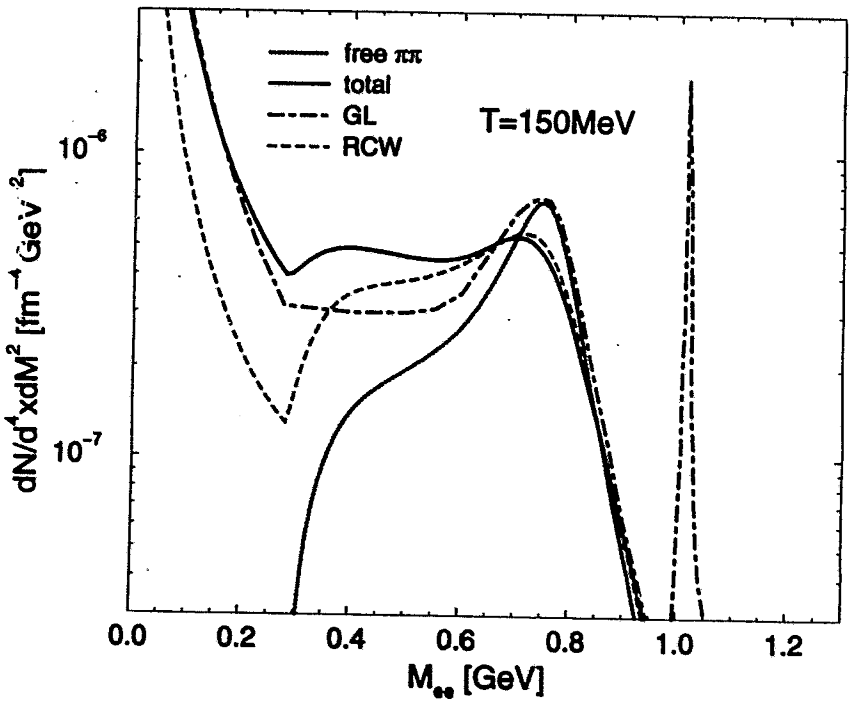

R.Rapp et at. (1999)

- 'chiral dynamics': $(T = 0)$

F. Klingl et al. ZPA (1996), NPA (1997)

'chiral' Lagrangian :

$$\mathcal{L}_{eff}(U, \partial_\mu U; \mathcal{V}_\mu ..; \mathcal{B}..)$$

nucleon Compton tensor:

$$C^N_{\mu\nu} = -i \int d^4x \, e^{iqx} \langle N(\vec{p}) | \mathcal{T}(J^{em}_\mu(x), J^{em}_\nu(0)) | N(\vec{p}) \rangle$$

diagrammatic expansion:

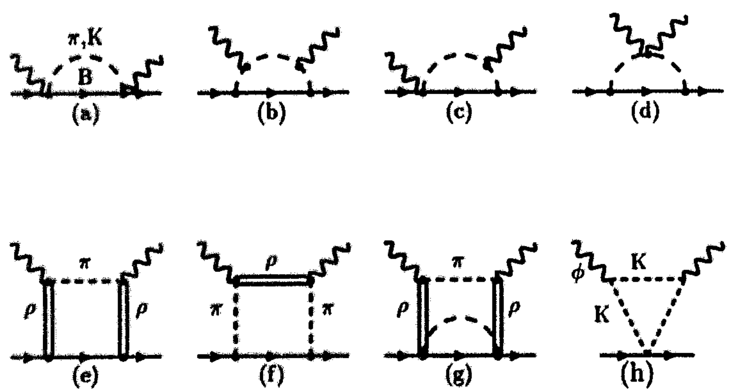

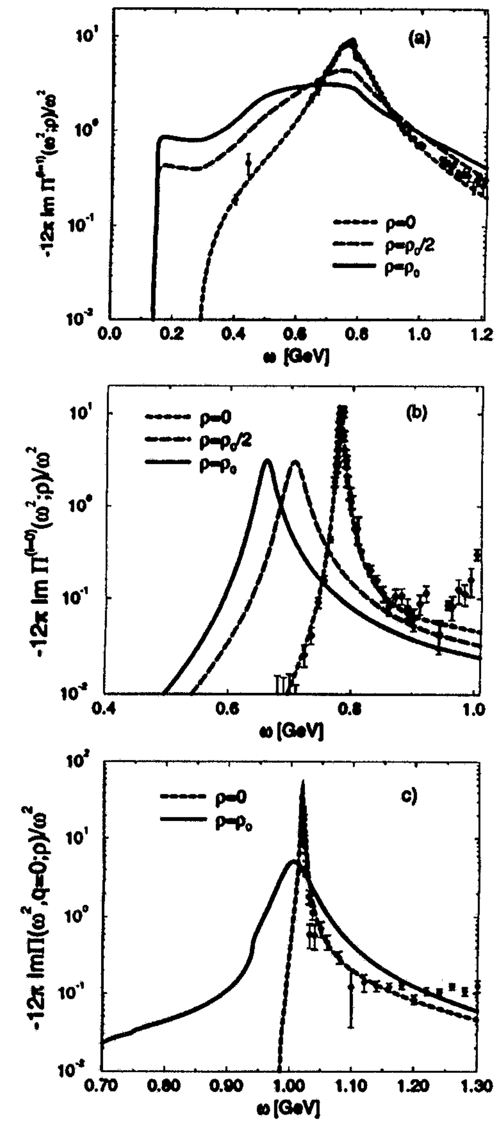

- Vector-Dominance Model (ρ meson)

R. Rapp et al. PRL (1996), NPA (1997)

$$J^V_\mu = \frac{1}{2}(\bar u \gamma_\mu u - \bar d \gamma_\mu d) = \frac{m_\rho^2}{g_\rho}\vec{\rho}_\mu$$

vacuum correlation function:

$$\Pi^{\circ V}_{\mu\nu}(q) = -i\frac{m_\rho^4}{g_\rho^2}\int d^4x\, e^{iqx}\langle 0|\mathcal{T}(\vec{\rho}_\mu(x),\vec{\rho}_\nu(0))|0\rangle = -i\frac{m_\rho^4}{g_\rho^2}D^{\circ\rho}_{\mu\nu}(q)$$

$$D^{\circ\rho}_{\mu\nu}(q) = -(g_{\mu\nu} + \frac{q_\mu q_\nu}{q^2})D^\circ_\rho(q^2) + \frac{q_\mu q_\nu}{q^2 m_\rho^2}$$

$$D^\circ_\rho(q^2) = (q^2 - m_\rho^2 - \Sigma_\rho(q^2))^{-1}$$

effective Lagrangian:

$$\mathcal{L}_{VDM} = \mathcal{L}_\pi + \mathcal{L}_\rho + g_\rho(\vec{\pi}\times\partial^\mu\vec{\pi})\cdot\vec{\rho}_\mu + g_\rho^2(\vec{\rho}^\mu)^2(\vec{\pi})^2$$

Σ_ρ to order g^2:

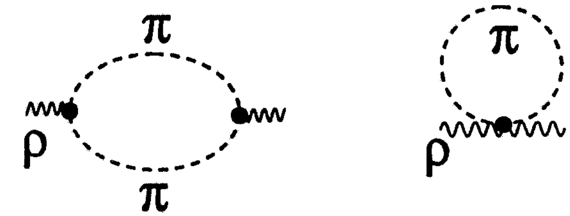

regularization via Pauli-Villars $\Lambda = 1$ GeV

→ covariance and gauge invariance

fits:

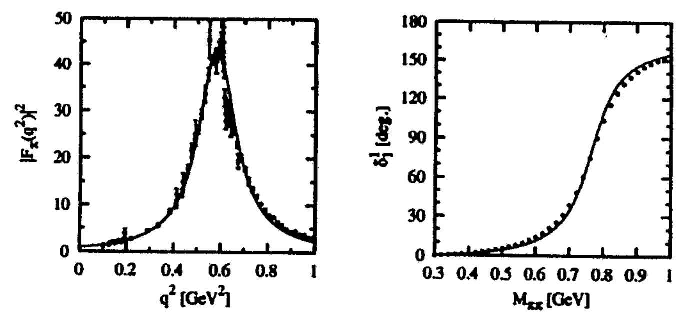

ρ meson in the medium :

$$D^{\rho}_{\mu\nu}(q) = -i \int d^4x\, e^{iqx}\theta(x^0) \ll [\vec{\rho}_\mu(x), \vec{\rho}_\nu(0)] \gg$$

tensor structure: (Lorentz invariance broken)

$$D^{\rho}_{\mu\nu}(q) = D^{L}_{\rho}(\omega,\vec{q})P^{L}_{\mu\nu} + D^{T}_{\rho}(\omega,\vec{q})P^{T}_{\mu\nu}$$

longitudinal transverse

$P^{L,T}_{\mu\nu}$: long (trans) projectors

in-medium selfenergy:

- change of the pion dispersion relation
- direct coupling to N^*-Resonances

rho meson:

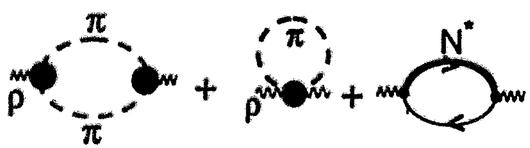

plon:

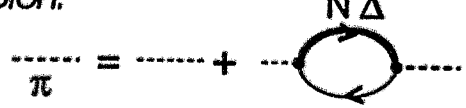

vertex corrections from gauge invariance :

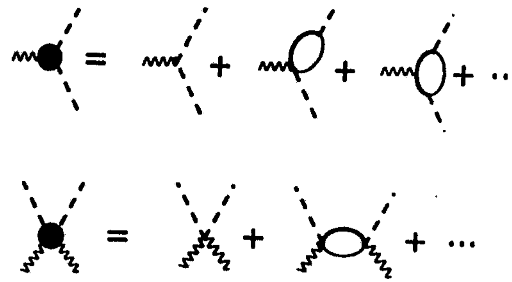

physical processes included:

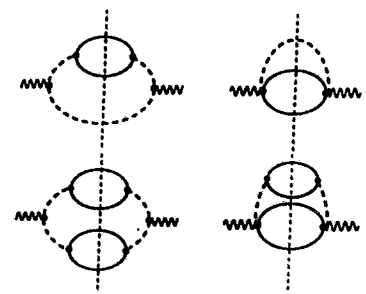

corresponding amplitudes:

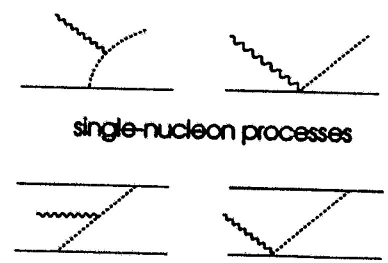

Spectral Functions

-Im $D_\rho(M, q, \rho_B, T)$ [GeV^{-2}]
T=150 MeV

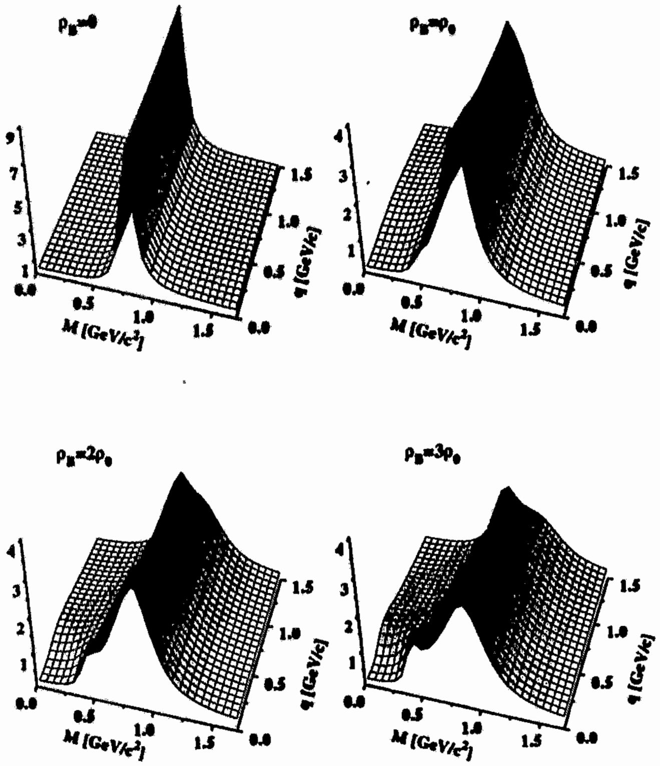

Photoabsorption

- important constraint of the model

total $\gamma-$ absorption cross section :

$$\sigma_\gamma/A = -\frac{1}{\rho}\frac{e^2}{\omega}\epsilon^\mu\epsilon^\nu\frac{m_\rho^4}{g_\rho^2}D^\rho_{\mu\nu}(\omega, |\vec{q}| = \omega)$$

low-density limit:

$$\sigma_\gamma/A \to \sigma_{\gamma P}$$

diagrams:

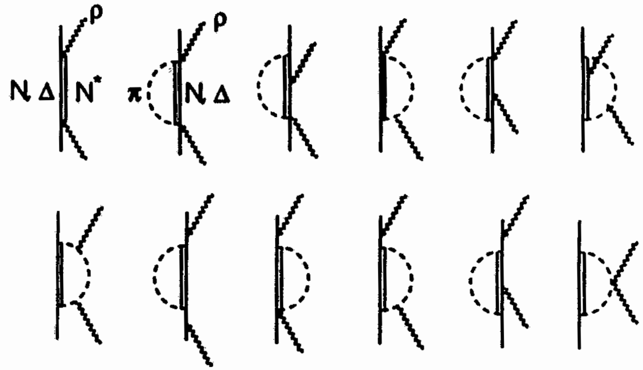

Photoabsorption

proton:

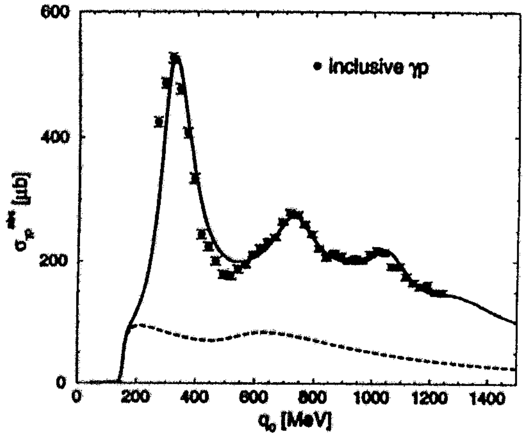

nuclei:

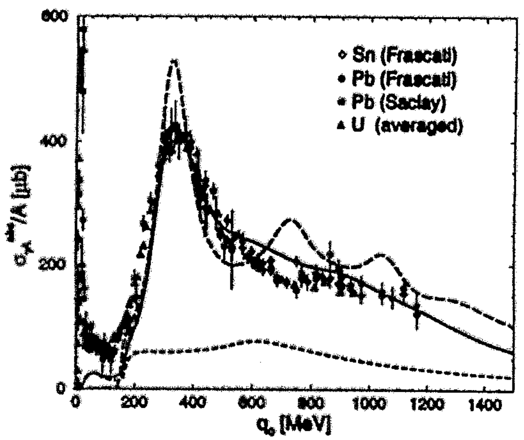

Chiral Symmetry Restoration and Vector Mesons

vector and axialvector currents:

$$\mathcal{V}_k^\mu = \bar\psi\gamma^\mu \frac{\tau_k}{2}\psi; \quad \mathcal{A}_k^\mu = \bar\psi\gamma^\mu\gamma_5\frac{\tau_k}{2}\psi$$

correlators:

$$\Pi_V^{\mu\nu}(q) = -i\int d^4x\, e^{iqx} \ll \mathcal{T}(\mathcal{V}_k^\mu(x), \mathcal{V}_k^\nu(0)) \gg$$

$$\Pi_A^{\mu\nu}(q) = -i\int d^4x\, e^{iqx} \ll \mathcal{T}(\mathcal{A}_k^\mu(x), \mathcal{A}_k^\nu(0)) \gg$$

vacuum:

$$-\frac{1}{\pi}\mathrm{Im}\Pi_V^{\circ\mu\nu}(q) = -(q^2 g^{\mu\nu} - q^\mu q^\nu)\rho_V(q^2)$$

$$-\frac{1}{\pi}\mathrm{Im}\Pi_A^{\circ\mu\nu}(q) = -(q^2 g^{\mu\nu} - q^\mu q^\nu)\rho_A(q^2) + q^\mu q^\nu F_\pi^2\delta(q^2 - m_\pi^2)$$

Spectral Functions

vector: $e^+e^- \to 2n\pi$

axial : $\tau \to (2n+1)\pi + \nu_\tau$

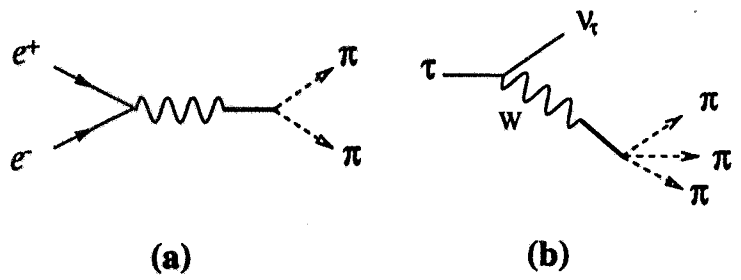

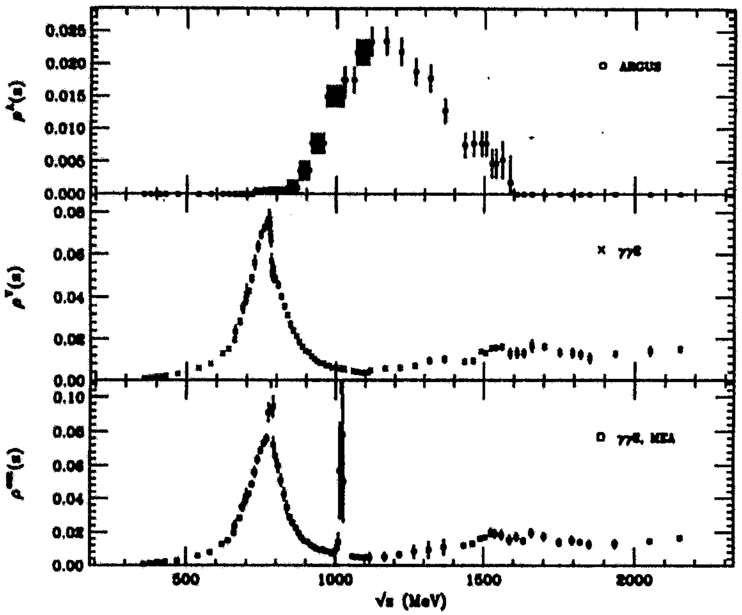

Z. Huang PLB (1997)

Weinberg Sum Rules

In the vector sector chiral symmetry is encoded in Weinberg sum rules

vacuum:

$$\int_0^\infty ds\,(\rho_V(s) - \rho_A(s)) = F_\pi^2 \quad \text{polarizability}$$

$$\int_0^\infty dss\,(\rho_V(s) - \rho_A(s)) = 0 \quad \text{EWSR}$$

pole approximation: (chiral limit)

$$\rho_V(s) = \frac{m_\rho^4}{g_\rho^2}\frac{1}{s}\delta(s - m_\rho^2)$$

$$\rho_A(s) = \frac{m_{a_1}^4}{g_{a_1}^2}\frac{1}{s}\delta(s - m_{a_1}^2)$$

then

$$m_\rho^2 = a g_\rho^2 F_\pi^2; \quad a = \left(1 - \frac{m_\rho^2}{m_{a_1}^2}\right)^{-1}$$

for $m_{a_1} = \sqrt{2} m_\rho$ (a=2 KFSR relation) medium: ($\vec{q}=0$) (J. Kapusta et al. PRD (1994))

$$\int_0^{\infty} \frac{d\omega}{\omega} \left(\mathrm{Im}\Pi_V(\omega) - \mathrm{Im}\Pi_A(\omega)\right) = 0$$
$$\int_0^{\infty} d\omega\omega \left(\mathrm{Im}\Pi_V(\omega) - \mathrm{Im}\Pi_A(\omega)\right) = 0$$

Mixing theorem: (M.Dey et al. PLB (1990))

$$\Pi_V^{\mu\nu}(\omega) = (1-\epsilon)\Pi_V^{\circ\mu\nu}(\omega) + \epsilon\Pi_A^{\circ\mu\nu}(\omega)$$
$$\Pi_A^{\mu\nu}(\omega) = (1-\epsilon)\Pi_A^{\circ\mu\nu}(\omega) + \epsilon\Pi_V^{\circ\mu\nu}(\omega)$$

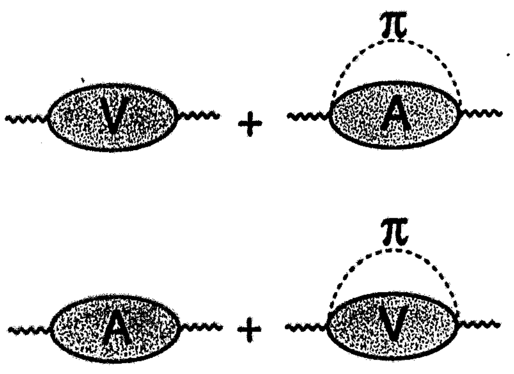

$$\epsilon = \frac{2}{F_\pi^2} \int \frac{d^3k}{(2\pi)^3} \frac{n(\omega_k)}{\omega_k} = \frac{T^2}{6F_\pi^2}$$

pole approximation:

$$-\frac{1}{\pi}\mathrm{Im}\Pi_V(\omega) = \frac{m_\rho^4}{g_\rho^2} Z_\rho \delta(s - m_\rho^{*2})$$
$$\frac{1}{\pi}\mathrm{Im}\Pi_A(\omega) = \frac{m_{a_1}^4}{g_{a_1}^2} Z_{a_1} \delta(s - m_{a_1}^{*2}) + F_\pi^{*2}\omega^2\delta(\omega^2)$$

then

$$\frac{F_\pi^{*2}}{F_\pi^2} = a Z_\rho \left(\frac{m_\rho^2}{m_\rho^{*2}} - \frac{m_\rho^2}{m_{a_1}^{*2}}\right)$$

chiral symmetry restored when $m_\rho^* = m_{a_1}^*$!

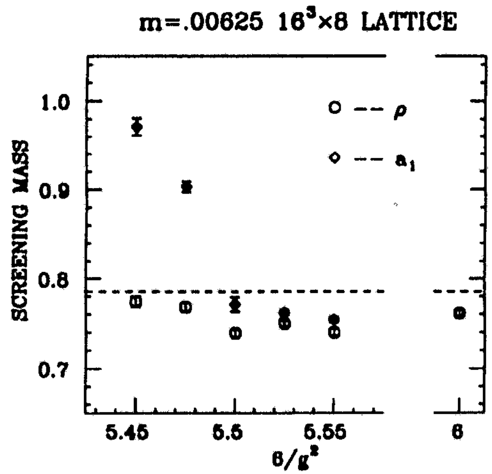

Chiral Restoration and Dileptons

symmetry restoration:

$$\epsilon = 1/2 \rightarrow T_c = \sqrt{3}F_\pi \simeq 160 \text{ MeV}$$

Dilepton rates:

$$\frac{dR}{dM^2} = \frac{\alpha^2}{2\pi^3} M T K_1(M/T) \times [\rho^{em}(M) - \epsilon(\rho_V(M) - \rho_A(M))]$$

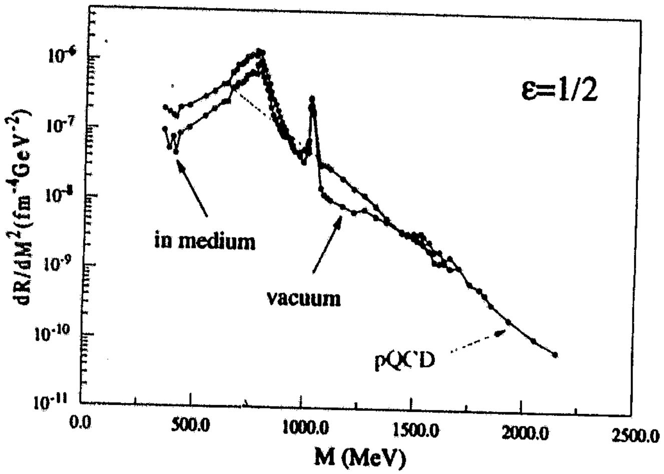

Chiral Restoration and Dileptons

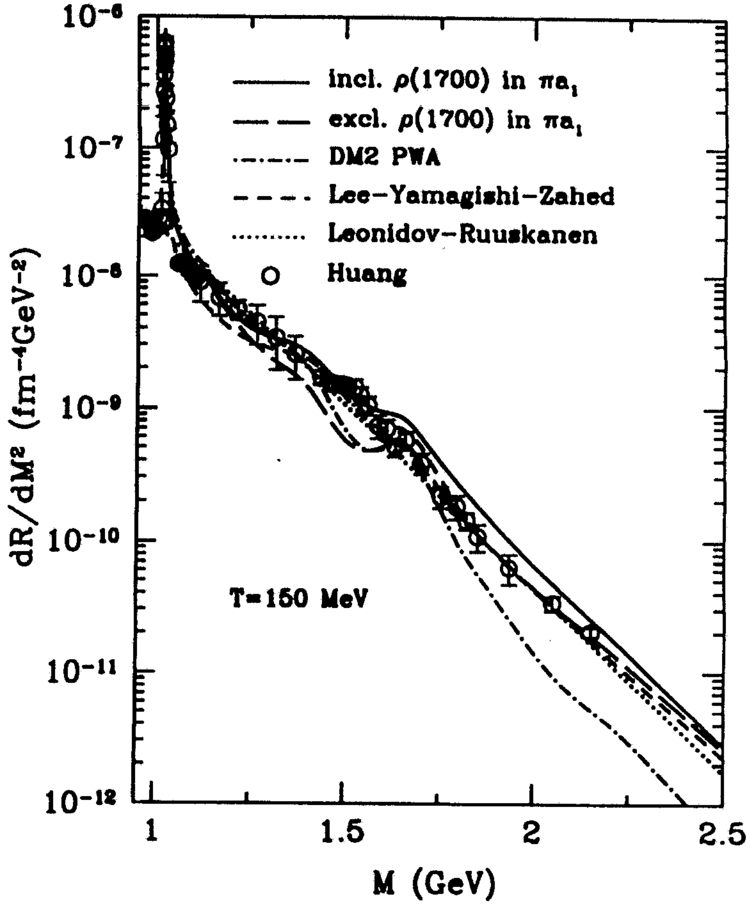

G. Li et al. PRC (1998)

Comparison with Data

local rate: (at given $T(x)$ and $\mu(x)$)

$$\frac{dN_{l^+l^-}}{d^4x d^4q} = L_{\mu\nu}(q)[H^{\mu\nu}_{\rho}(q) + H^{\mu\nu}_{\omega}(q) + H^{\mu\nu}_{\phi}(q) + \cdots]$$

need space-time history of the collision

- homogeneous fire-ball model:
  - isotropic homogeneous expansion
  - initial conditions from transport models
  - cooling curve $T(t)$ from transport models
  - particle abundances from $T(t)$ in equilibrium

    except for pions: $\mu_\pi \simeq 50$ (MeV)

rate:

$$\frac{d^2N}{dMd\eta} = \frac{1}{\Delta\eta}\int_{t_0}^{t_f} dt V(t) \int d^3q \frac{M}{q_0}\frac{dN_{l^+l^-}}{d^4x d^4q}(t) A(M,|\vec{q}|)$$

$A(M,|\vec{q}|)$: detector acceptance (Monte-Carlo)

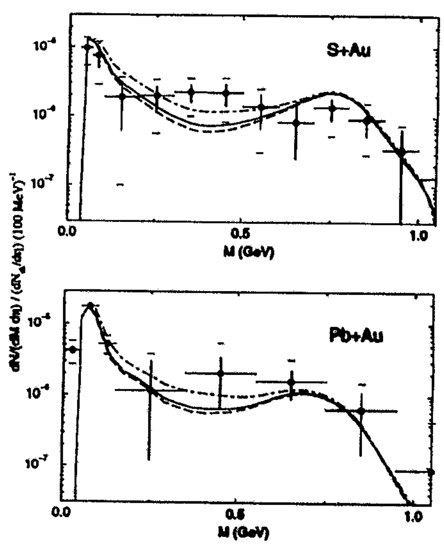

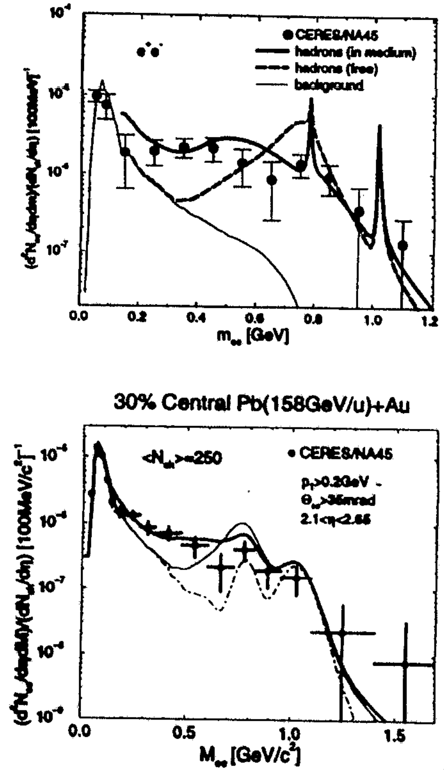

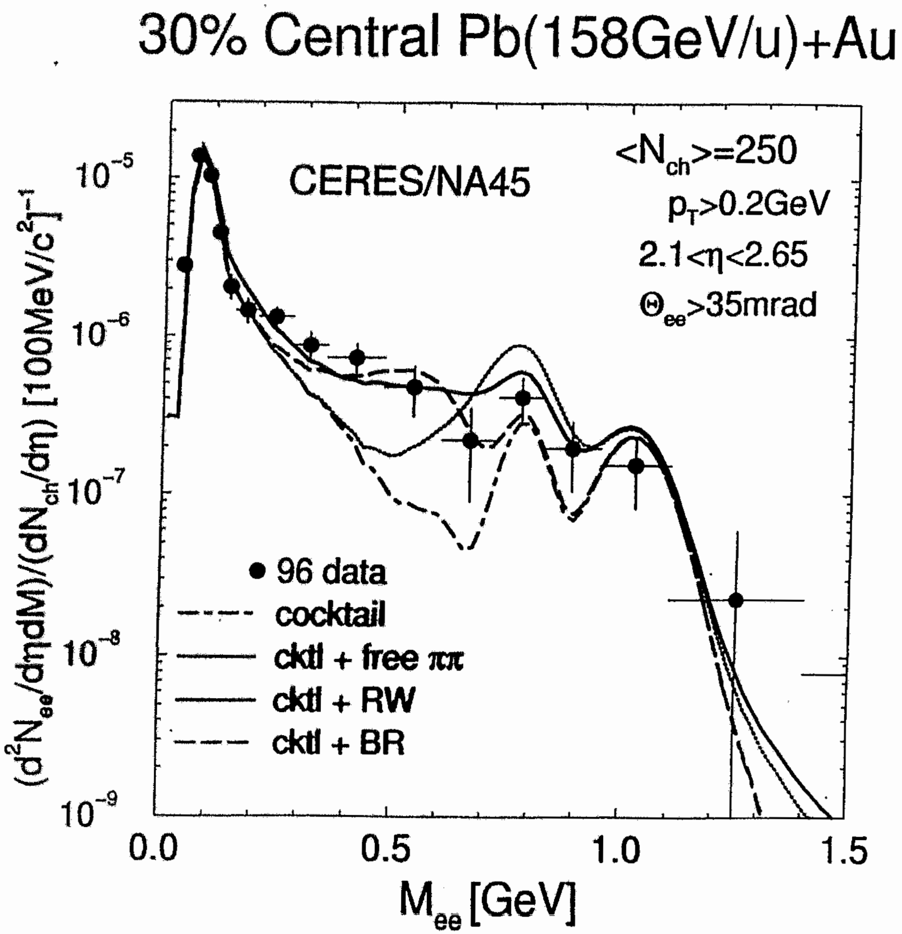
30% Central Pb(158GeV/u)+Au
CERES/NA45
<N_ch>=250
p_T>0.2GeV
2.1<η<2.65
Θ_ee>35mrad
96 data
cocktail
cktl + free ππ
cktl + RW
cktl + BR
(d²N_ee/dηdM)/(dN_ch/dη) [100MeV/c²]⁻¹
M_ee [GeV]

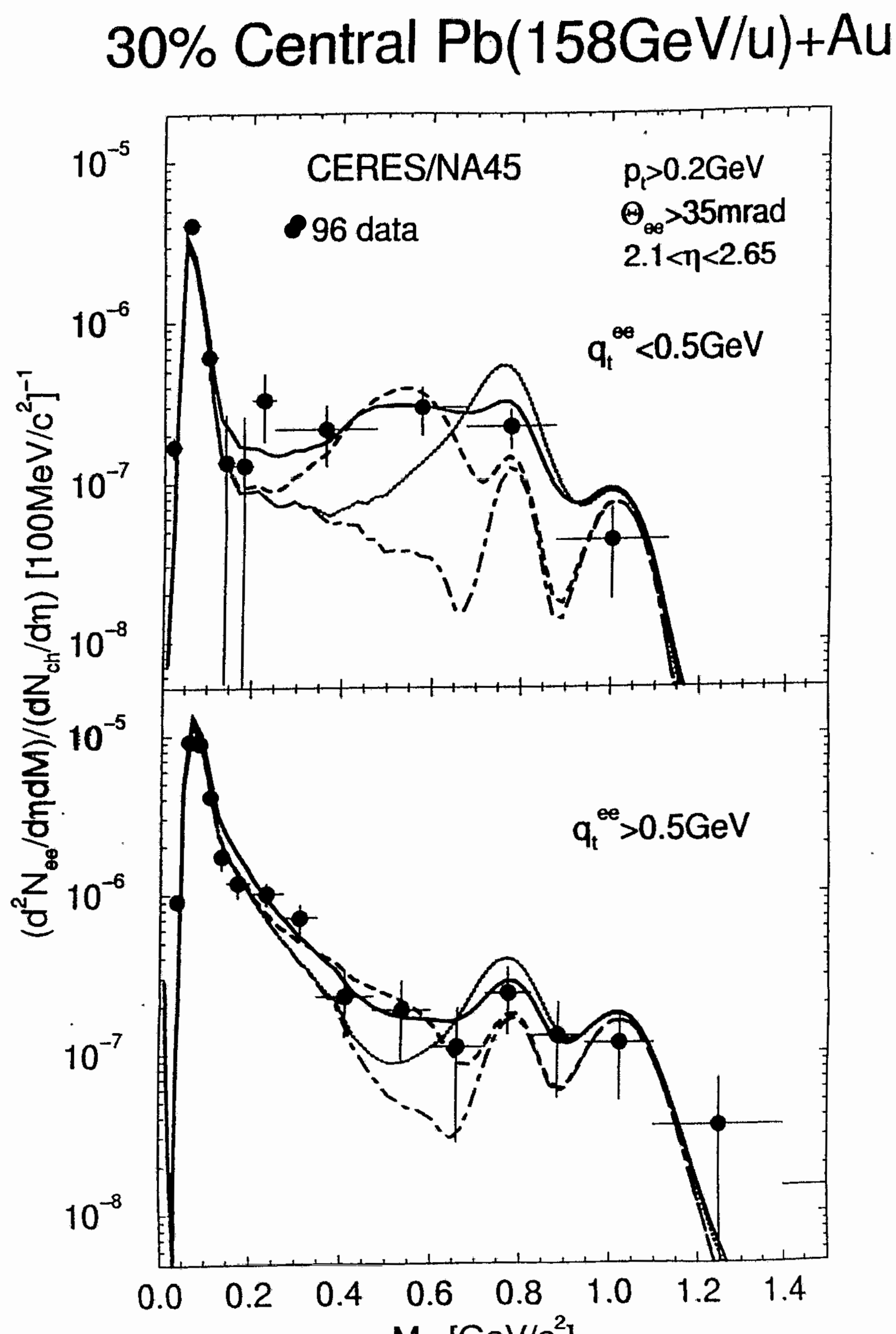
30% Central Pb(158GeV/u)+Au
CERES/NA45
96 data
p_t>0.2GeV
Θ_ee>35mrad
2.1<η<2.65
q_t^ee<0.5GeV
q_t^ee>0.5GeV
(d²N_ee/dηdM)/(dN_ch/dη) [100MeV/c²]⁻¹

CERES/NA45: 30% Central Pb(158GeV/u)+Au

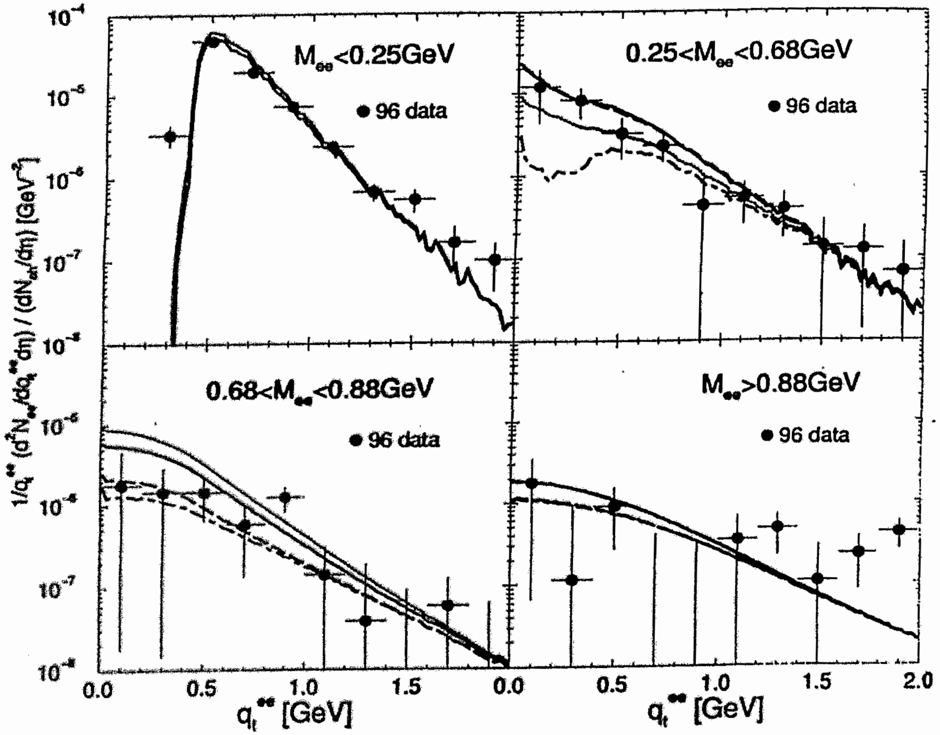

30% Central Pb(158GeV/u)+Au

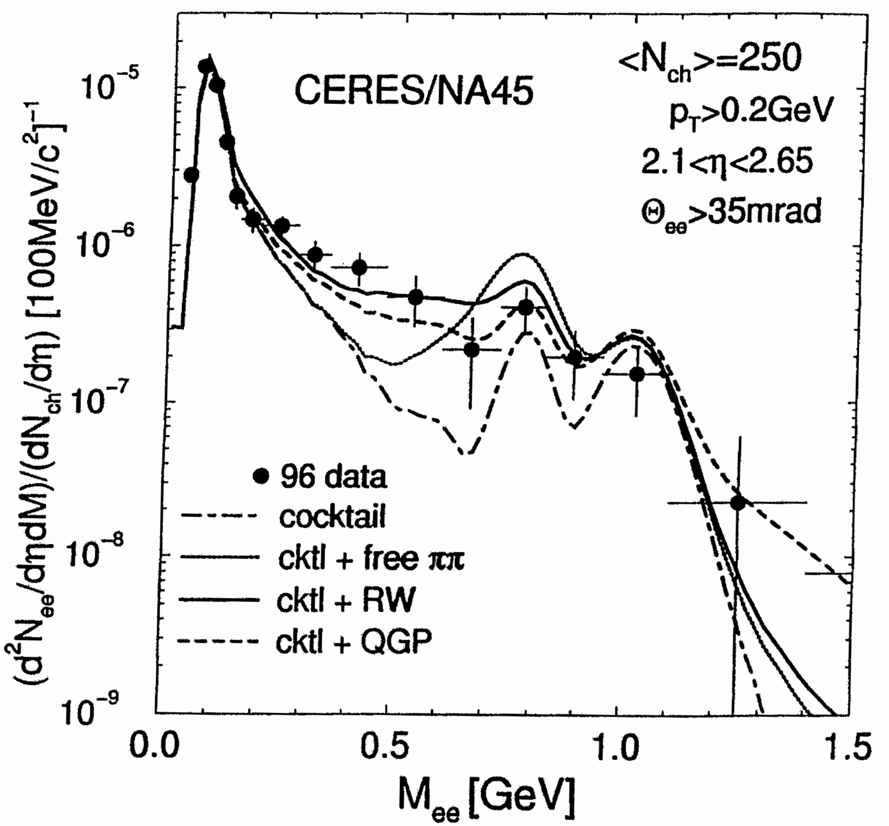

- **hydrodynamics:**

hydrodynamical equations:

$$\partial_\mu T^{\mu\nu}(x) = 0; \quad \partial_\mu j^\mu_{\rm B}(x) = 0$$

energy-momentum tensor:

$$T^{\mu\nu}(x) = [\epsilon(x) + p(x)]u^\mu(x)u^\nu(x) - p(x)g^{\mu\nu}$$

baryon current:

$$j^\mu_{\rm B}(x) = \rho_{\rm B}(x)u^\mu(x)$$

- EoS from hadron gas and partonic gas
- initial conditions from parametrizations of $\rho^i_B, \epsilon^i, u^{\mu i}$
- freeze out condition

rate:

[illegible]

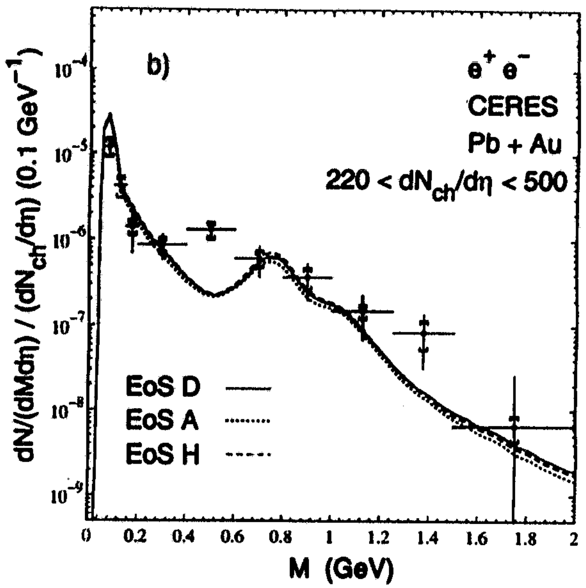

P. Huovinen et al. nucl-th/98

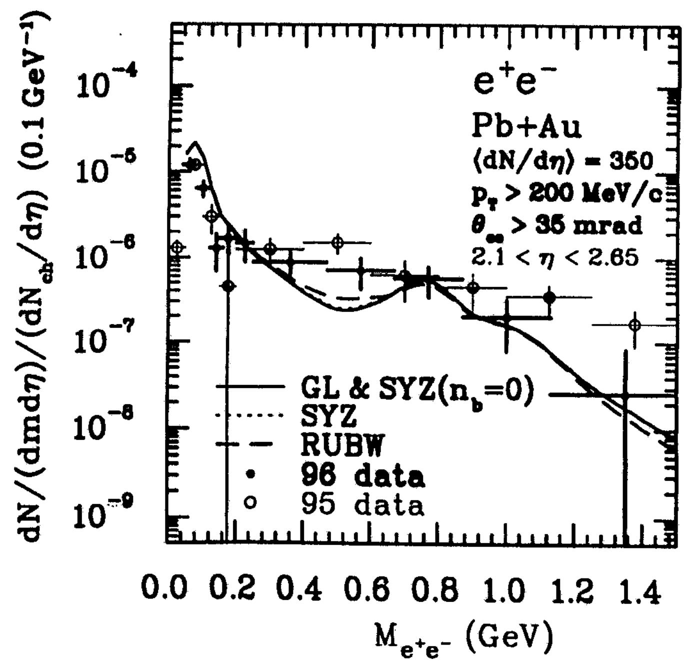

Gy. Wolf:

Vector mesons in nuclear matter

Vector mesons in nuclear matter

Gy. Wolf

QCD Sum Rules

ρ "propagator"

$$\Pi^{\mu\nu}(q) = i \int dx\, e^{iqx} \langle 0| T(\Gamma^\mu(x)\Gamma^\nu(0))|$$

$$\Pi^{\mu\nu} = (g^{\mu\nu} q^2 - q^\mu q^\nu)\, \Pi(q^2)$$

basic idea

Parametrize $\mathrm{Im}\,\Pi$ in the hadronic world

Try to calculate $\mathrm{Re}\,\Pi(q^2)$ ... QCD

Operator Product Expansion

$$\lim_{x \to y} \psi(x)\,\phi(y) = \sum_n C_n(x-y)\; O_n\left(\frac{x+y}{2}\right)$$

C_n: Wilson coefficients; O_n: local operator

d_O : mass dimension of the operator O

$$\lim_{x \to y} C_n(x-y) \sim |x-y|^{d_{O_n} - d_\psi - d_\phi}$$

For small $|x-y|$ (for large p) the sum can be written as an expansion in $|x-y|$ (in $\frac{1}{q^2}$)

in case of QCD

1	$d = 0$
$m\bar{q}q$	$d = 4$
$G^a_{\mu\nu} G_{a\mu\nu}$	$d = 4$
$\bar{q}\,\Gamma_1 q\,\bar{q}\,\Gamma_2 q$	$d = 6$
$m\,\bar{q}\,\sigma_{\mu\nu}\frac{\lambda^a}{2} q\, G^a_{\mu\nu}$	$d = 6$
$f_{abc}\, G^a_{\mu\nu} G^{b\nu\gamma} G^{c\mu}_{\gamma}$	$d = 6$

Apply the operator product expansion to the correlator

$q^\mu q^\nu - q^2 g^{\mu\nu}$ ...

How to calculate?

Go to high momentum q^2 $\Rightarrow$ perturbative QCD

C_1 :

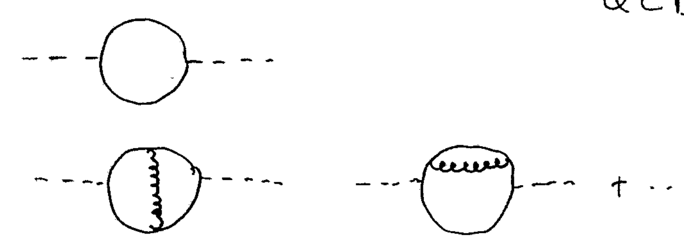

C_q :

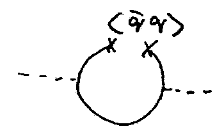

C_G :

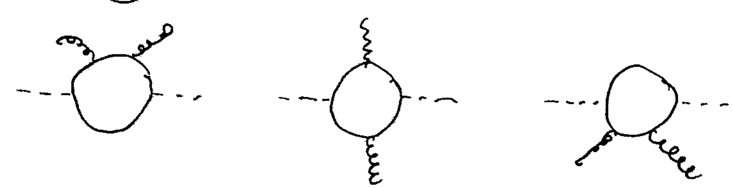

C_{q^2} :

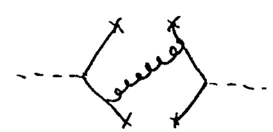

$$\langle O \rangle_\rho = \langle O \rangle_0 + \rho \langle O \rangle_N$$

$$\langle \bar{q}q \rangle_\rho = \langle \bar{q}q \rangle + \frac{\Sigma_{\pi N}}{2\bar{m}} \rho \approx \langle \bar{q}q \rangle_0 \left(1 - 0.3 \frac{\rho}{\rho_0}\right)$$

– Brown - Rho

– Hatsuda - Lee

$$m_\rho \approx \langle \bar{q}q \rangle^{1/3}$$

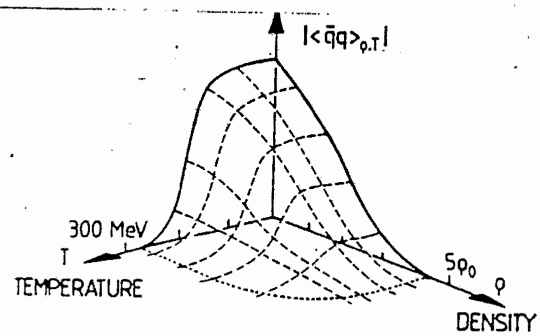

Figure 3: The condensate $\langle \bar{q}q \rangle$ as a function of density ρ and temperature T (adapted from ref.[14]). The density is given in units of nuclear matter density $\rho_o = 0.17\, fm^{-3}$

Weise

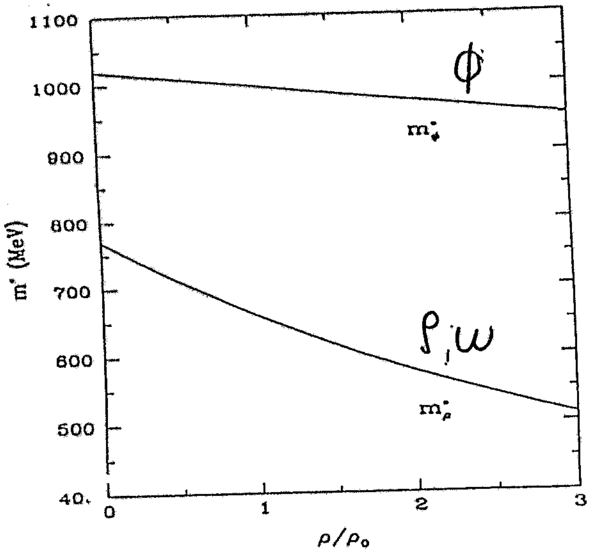

Hatsuda - Lee

Leupold, Mosel

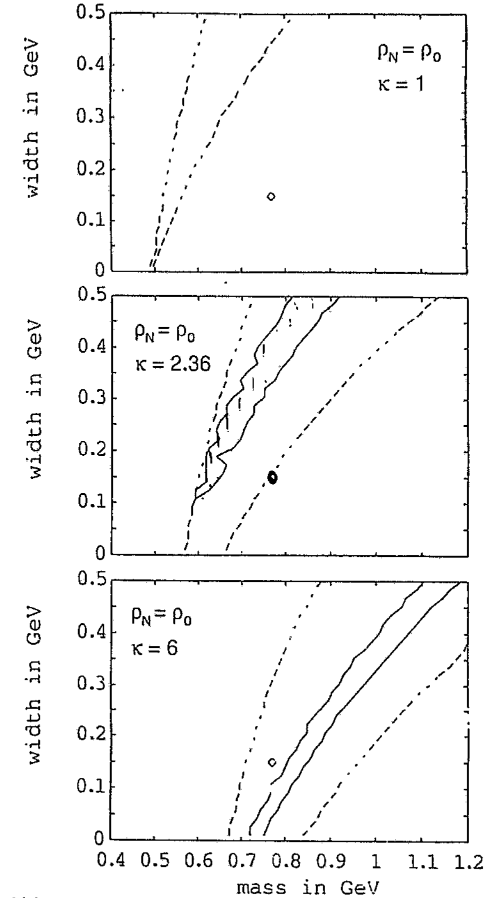

FIG. 2. The width γ over the mass m_ρ for nuclear saturation density ρ_0 and for different values of κ. The full lines border the region of QCD sum rule allowed parameter pairs with $d \leq 0.2\%$ and $\Delta M^2 \geq 0.6\,\mathrm{GeV}^2$, the dashed lines border the allowed region for $d \leq 1\%$ (same ΔM^2). The diamond marks mass and width of the free ρ meson.

Vector meson self energies

$\langle n.m | \mathcal{O} | n.m \rangle = \langle 0 | \mathcal{O} | 0 \rangle + \rho \langle N | \mathcal{O} | N \rangle$

Correlation function („propagator") of a vector meson:

$(q^\mu q^\nu - q^2 g^{\mu\nu}) \, \Pi(q) = i \int d^4x \, e^{iqx} \langle T(V^\mu(x) V^\nu(0)) \rangle$

$\Delta \Pi^{\mu\nu} = i \int d^4x \, e^{iqx} \langle N | T(V^\mu(x) V^\nu(0)) | N \rangle$

LSZ reduction

$T_V(\rho) = -4\pi \left(1 + \frac{m_V}{m_N}\right) \langle NV | NV \rangle$

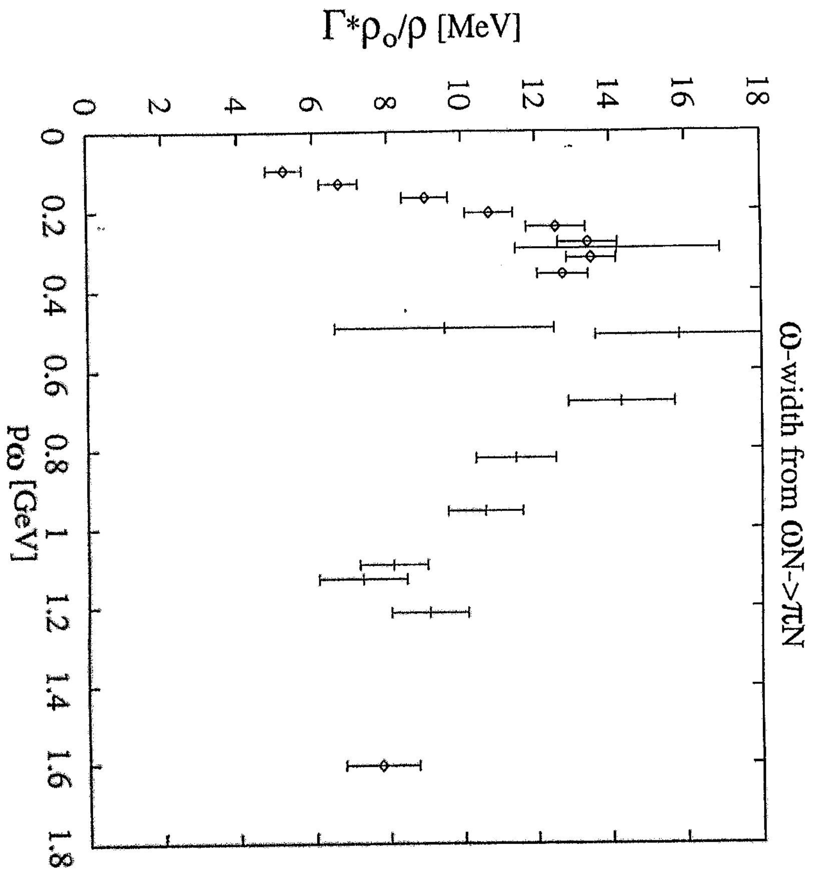

$\Gamma_{coll} = \gamma v \sigma \rho$

$\pi^- p \to \omega n$

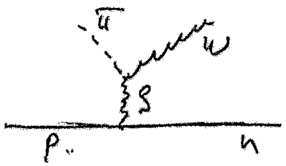

data:

$\sigma \sim p^{*\,2L+1}$

energy dependence and angular distribut does not allow a simple picture

resonance fit:

no reasonable parameters

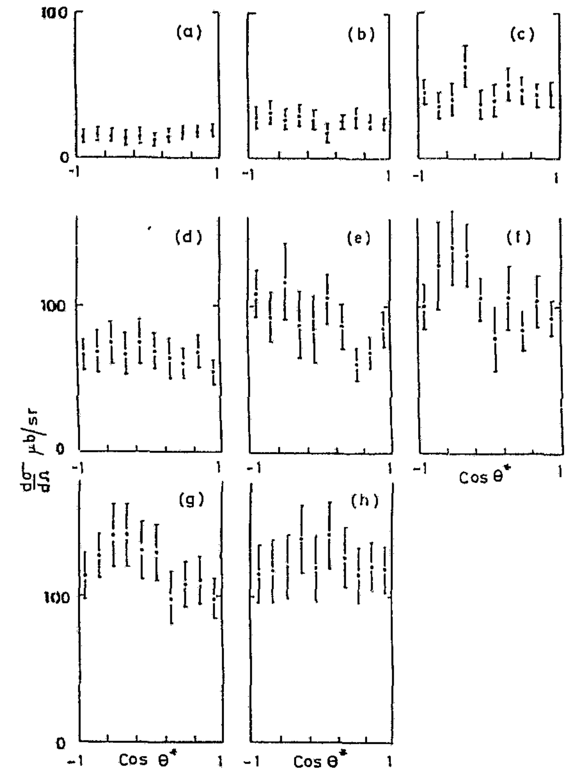

Fig. 3. Detailed differential cross sections in 20 MeV/c steps for 8 intervals of P^*, starting at (a) $40 < P^* < 60$ rising to (h) $180 < P^* < 200$ MeV/c. Any departures from isotropy are clearly small!

Table 1
Production cross sections for the reaction $\pi^- + p \to \omega + n$

P^* range (MeV/c)	Coefficients (μb/sr) C_0	C_1	C_2	σ (μb)	σ/P^* (μb/MeV/c)
40– 60	15.7 ± 1.4	2.2 ± 2.4	2.6 ± 3.3	197 ± 18	3.94 ± 0.36
60– 80	27.0 ± 2.0	−2.4 ± 3.4	1.8 ± 4.3	339 ± 26	4.84 ± 0.37
80–100	45.0 ± 3.1	1.4 ± 4.7	−0.9 ± 6.7	577 ± 40	6.41 ± 0.44
100–120	65.7 ± 3.9	−5.8 ± 5.9	−5.9 ± 8.0	830 ± 50	7.55 ± 0.45
120–140	86.0 ± 5.2	−20.4 ± 8.2	6.4 ± 11.3	1118 ± 71	8.60 ± 0.55
140–160	104.3 ± 5.8	−13.5 ± 9.1	−5.0 ± 11.6	1350 ± 80	9.00 ± 0.53
160–180	119.4 ± 5.8	−14.9 ± 9.1	−15.8 ± 12.6	1510 ± 74	8.88 ± 0.44
180–200	123.6 ± 6.0	1.3 ± 8.5	−9.1 ± 11.3	1560 ± 83	8.21 ± 0.44

Coupled channel approach

measured $\pi N \to VN$, $\pi N \to \pi N$

- Inelasticities

Channels:

πN, ρN, ωN, ηN, $\pi\Delta$ ($K\Lambda$, ...)

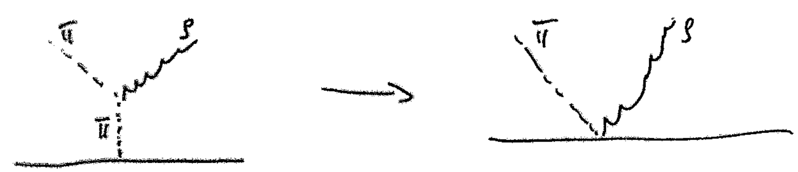

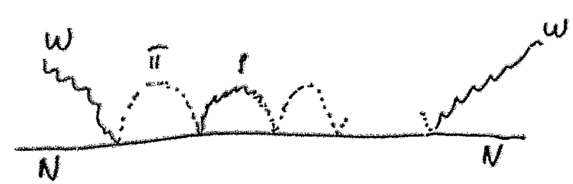

Vector mesons around threshold

ρN : s-wave (relativistic formalism)

ηN : s-wave

πN, $\pi\Delta$: s- and d-wave

η^{SI} (amputated amplitude in the SI chann

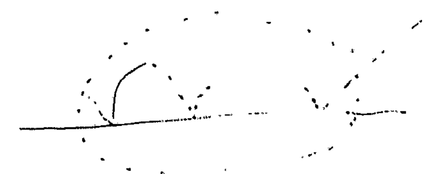

J^{SI} loop function, g^{SI} coupling constants

$$M_{SI} = g_{SI} \left(1 - J_{SI}\, g_{SI}\right)^{-1}$$

fitting : 37 coupling constants

~400 data points

Energy intervall ... 1.45 – 1.8 GeV

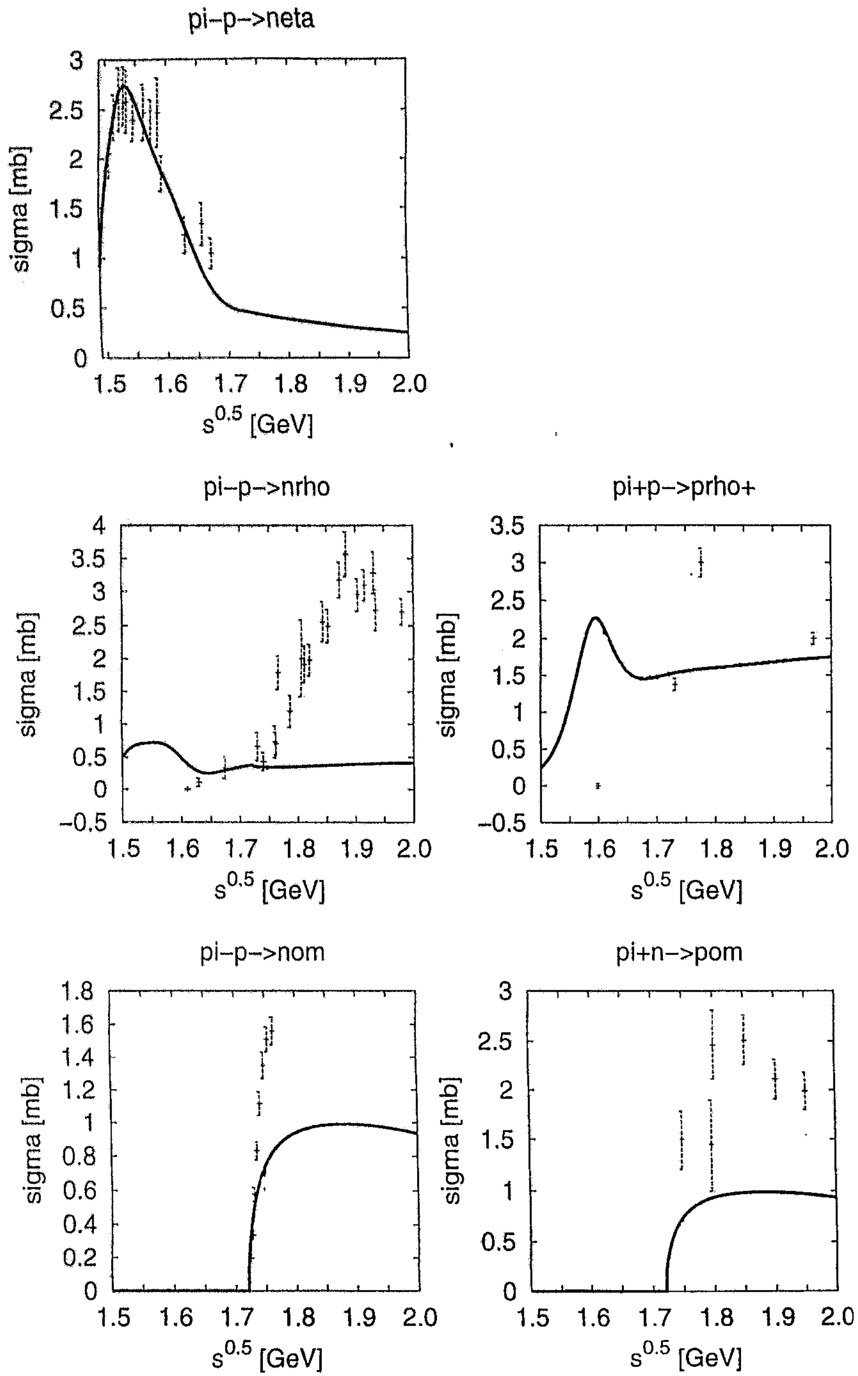

pi−p−>neta
pi−p−>nrho
pi+p−>prho+
pi−p−>nom
pi+n−>pom
sigma [mb]
s^0.5 [GeV]

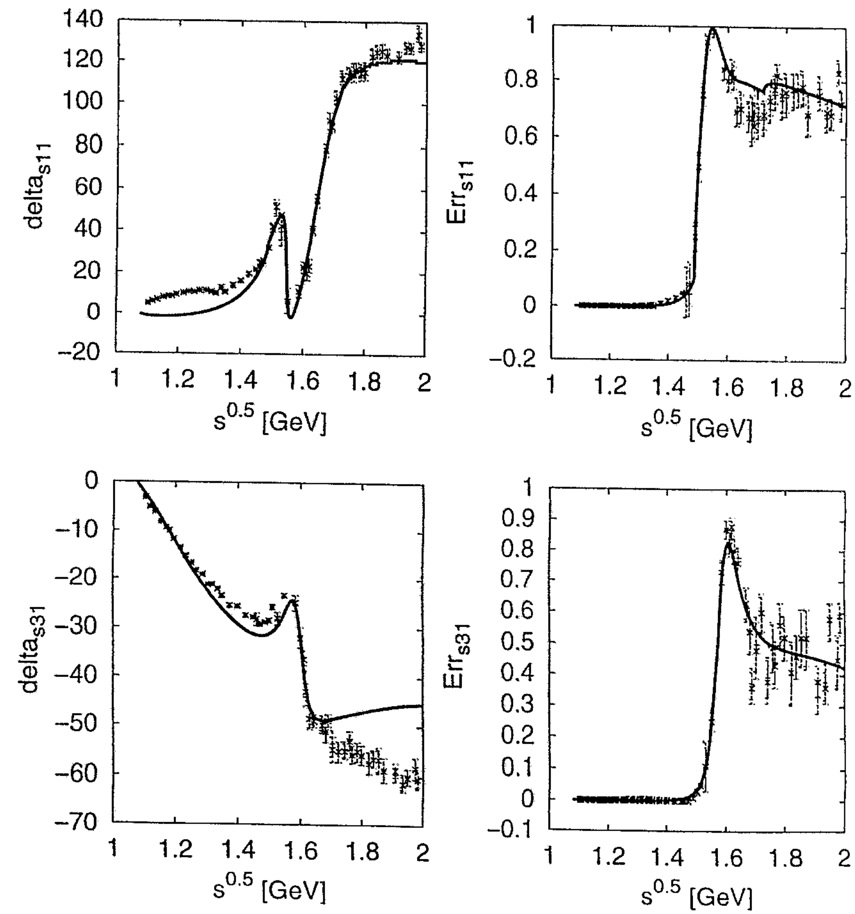

delta_s11
Err_s11
delta_s31
Err_s31
s^0.5 [GeV]

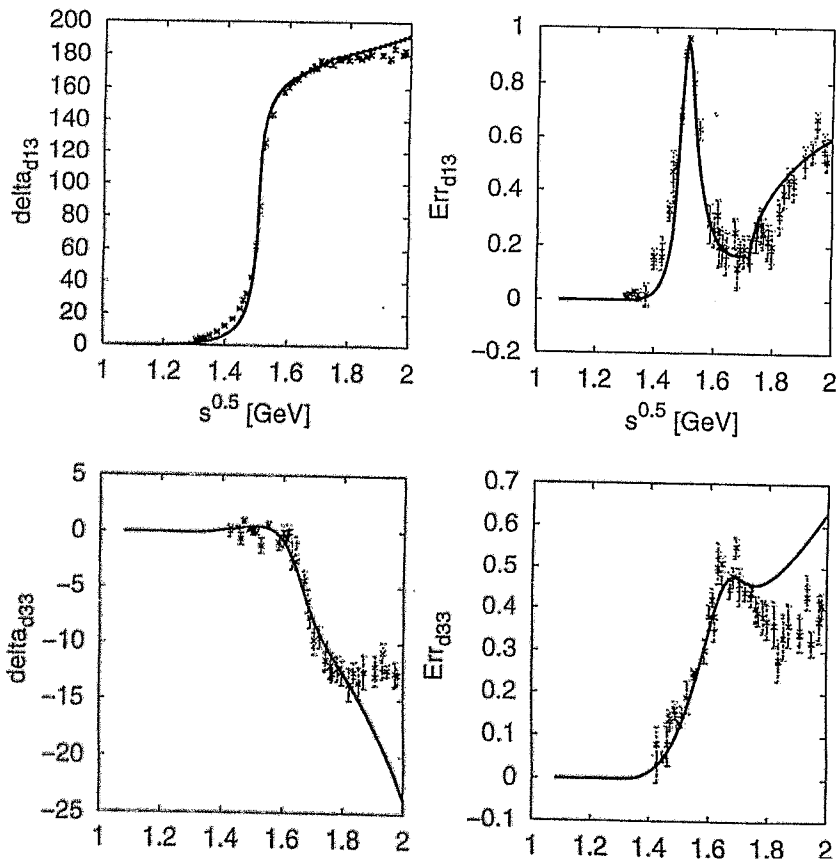
delta_d13
s^0.5 [GeV]
Err_d13
s^0.5 [GeV]
delta_d33
Err_d33

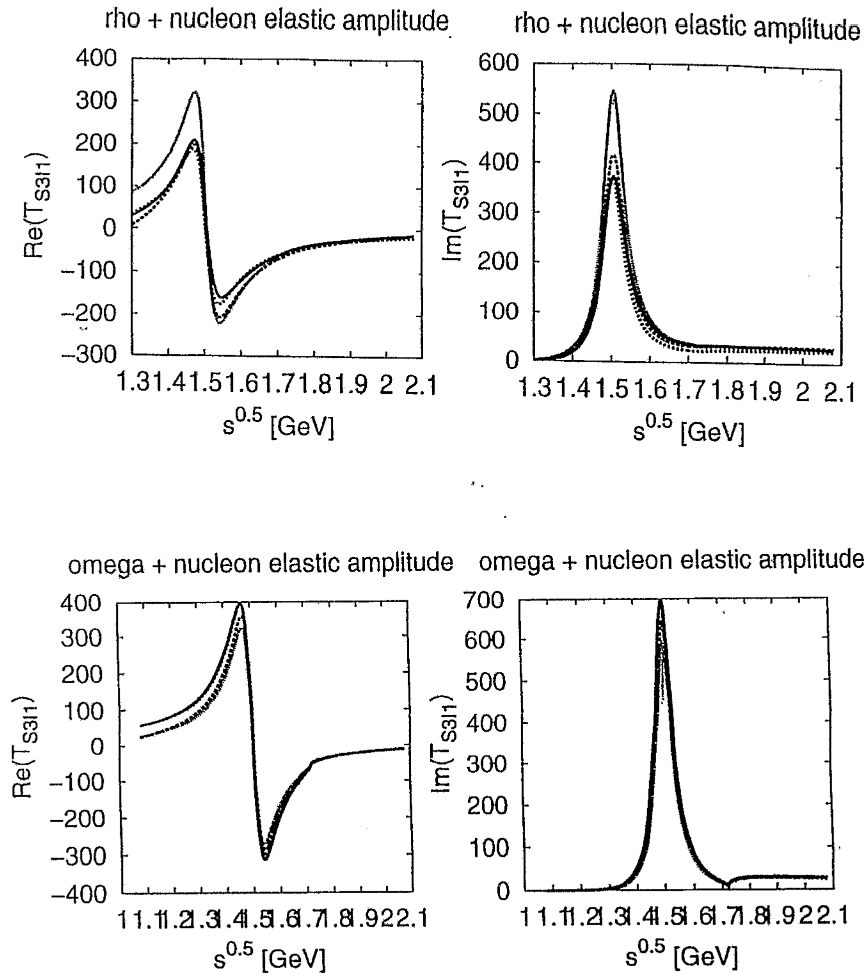
rho + nucleon elastic amplitude
Re(T_S3I1)
s^0.5 [GeV]
rho + nucleon elastic amplitude
Im(T_S3I1)
s^0.5 [GeV]
omega + nucleon elastic amplitude
Re(T_S3I1)
s^0.5 [GeV]
omega + nucleon elastic amplitude
Im(T_S3I1)
s^0.5 [GeV]

preliminary

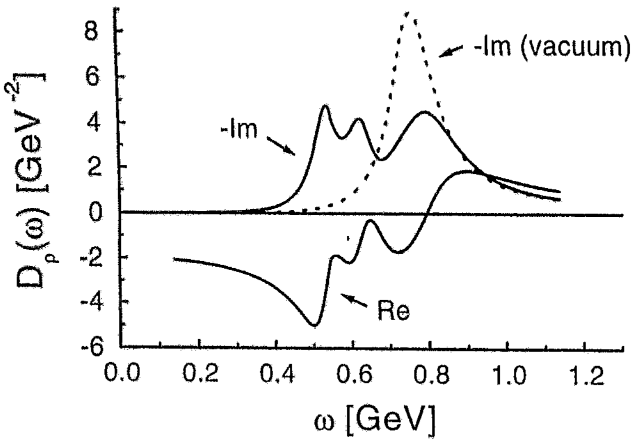

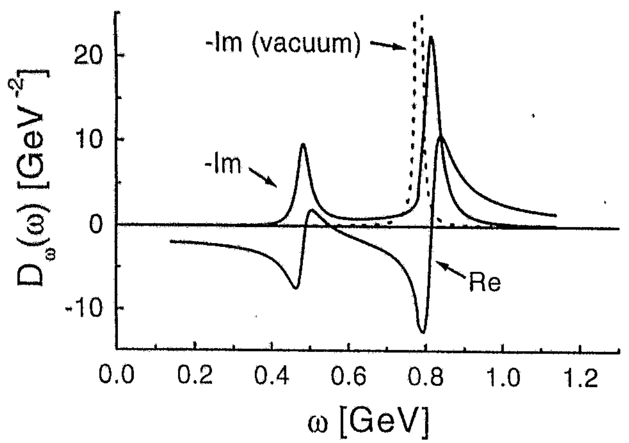

Figure 1: the real and imaginary parts of the ρ and ω propagators in nuclear matter at ρ_0, compared to the imaginary parts in vacuum.

M. Krivoruchenko:

Decay rates for dilepton production in HICs

Dilepton Spectra from Decays of Light Unflavored Mesons

Amand Faessler, C. Fuchs (ITP - Tübingen U.)
M. I. K. (ITEP - Moscow)

M.I. Krivoruchenko

nucl-th/9909024

The invariant mass spectrum of the e^+e^- and $\mu^+\mu^-$ pairs from decays of the light unflavored mesons with masses below the $\varphi(1020)$-meson mass to final states containing along with a dilepton pair one photon, one meson, and two mesons are calculated within the framework of the effective meson theory.

CONTENT:

I. Relation between the decays $\mathcal{M} \to \mathcal{M}'\gamma$ and $\mathcal{M} \to \mathcal{M}'\ell^+\ell^-$

II. Decays of the ρ-, ω-, and φ-mesons to $\ell^+\ell^-$ pairs

III. Meson decays to photons and $\ell^+\ell^-$ pairs

Decay modes $\pi^0 \to \gamma e^+e^-$, $\eta \to \gamma\ell^+\ell^-$, and $\eta' \to \gamma\ell^+\ell^-$
Decay modes $f_0(980) \to \gamma\ell^+\ell^-$ and $a_0^0(980) \to \gamma\ell^+\ell^-$

IV. Meson decays to one meson and a $\ell^+\ell^-$ pair

Decay modes $\omega \to \pi^0 e^+e^-$, $\rho \to \pi e^+e^-$, and $\phi \to \pi^0 e^+e^-$
Decay modes $\omega \to \eta\ell^+\ell^-$, $\rho^0 \to \eta\ell^+\ell^-$, and $\phi \to \eta\ell^+\ell^-$
Decay modes $\eta' \to \omega e^+e^-$ and $\eta' \to \rho^0 e^+e^-$

V. Meson decays to two mesons and $\ell^+\ell^-$ pair

Decay modes $\eta \to \pi^+\pi^-\ell^+\ell^-$ and $\eta' \to \pi^+\pi^-\ell^+\ell^-$
Decay mode $\rho^0 \to \pi^+\pi^-\ell^+\ell^-$
Decay modes $\rho^0 \to \pi^0\pi^0\ell^+\ell^-$, $\omega \to \pi^0\pi^0\ell^+\ell^-$, and $\omega \to \pi^+\pi^-\ell^+\ell^-$
Decay modes $\rho \to \eta\pi e^+e^-$ and $\omega \to \eta\pi^0 e^+e^-$
Decay mode $\rho^+ \to \pi^+\pi^0\ell^+\ell^-$
Decay mode $f_0(980) \to \pi^+\pi^-\ell^+\ell^-$
Decay mode $a_0(980) \to \pi\eta\ell^+\ell^-$

VI. Numerical results:

(a) simulations of the dilepton spectra in heavy-ion collisions
(b) experimental searches of dilepton meson decays

Electromagnetic Radiation off Colliding Hadron Systems.
Dileptons & Bremsstrahlung
Forschungszentrum Rossendorf near Dresden
17|IV-1999

■ Reduction of nucleon masses in nuclei: Walecka model

J.D. Walecka,1974; Chin, 1977.

$$\mathcal{L} = \ \dots \ - g\sigma\bar{\psi}\psi, \quad < \sigma > \sim < \bar{\psi}\psi >$$

$$m_N^* = m_N - g < \sigma >$$

■ Firmer grounds for reduction of nucleon masses on the basis of a partial restoration of chiral symmetry and finite-density QCD sum rules:

Drukarev and Levin, 1988.

$$\frac{< \bar{q}q >_\rho}{< \bar{q}q >} = 1 - \frac{\rho}{f_\pi^2\mu^2}\{\Sigma_{\pi N} + m\frac{d}{dm}(\frac{E(\rho)}{A})\}$$

■ The change of the meson properties:

C. Amadi and G.E. Brown, 1993;
Hatsuda, Suomi and Kuwabara, 1996.

$$m_V^* = m_V(1 - \alpha\frac{\rho}{\rho_0}), \qquad \alpha \approx 0.18$$

■ The investigations in the Nambu-Jona-Lasinio model provide an evidence for reduction of nucleon and meson masses at finite density and temperature:

Maruyama, Tsushima and A. Faessler, 1991.

■ Reduction of the corresponding life times of resonances:

Herrmann, Friman and Nörenberg, 1993.
Rapp, Chanfray and Wambach, 1997.

$$\Gamma^{tot} = \Gamma^{vac} + \Gamma^{coll}, \quad \Gamma^{coll} = \rho\sigma v$$

■ Brown-Rho scaling:

Brown and Rho, 1991.

$$\frac{m_N^*}{m_N} = \frac{m_\rho^*}{m_\rho} = \frac{m_\omega^*}{m_\omega} = \ldots$$

■ DISPERSION THEORY (Eletsky, Ioffe)

$m_V^* \approx m_V$

RESONANCE BROADENING

V. Weisskopf

Physikalische Zeitschrift 34, 1 (1933)

hydrogen atom in gas:

length free path: $\ell_f = 1/n\sigma$

$$N(\ell) = N(0)exp(-\ell/\ell_f), \quad \ell = vt \quad \Rightarrow \quad N(t) = N(0)exp(-n\sigma vt)$$

$$|\Psi(t)|^2 = |\Psi(0)|^2 exp(-\Gamma t)$$

total width: $\Gamma = \Gamma_{vac} + \Gamma_{coll}$

where Γ_{vac} = natural line width (= vacuum width of the atomic energy level) and

$$\boxed{\Gamma_{coll} = n\sigma v.}$$

in agreement with the uncertainty relation:

$$\Delta E \gtrsim \frac{1}{\Delta t} \sim \frac{v}{\ell_f} = n\sigma v = \Gamma_{coll}$$

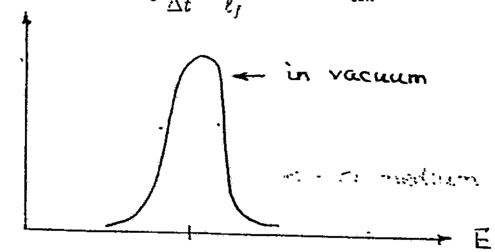

The shift of atomic energy levels and broadening of the atomic lines are observed experimentally in gases

SOBELMAN, TH. OF ATOMIC SPECTRA 1963.

MORE ABOUT SHIFT OF THE ATOMIC ENERGY LEVELS AND BROADENING OF THE SPECTRAL LINES

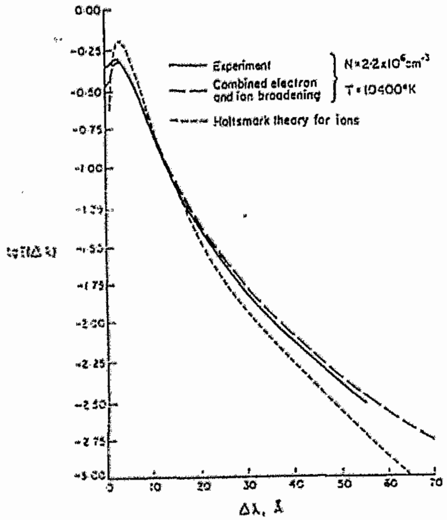

Fig. 57. Comparison of calculated and experimental contours of the line H_β.

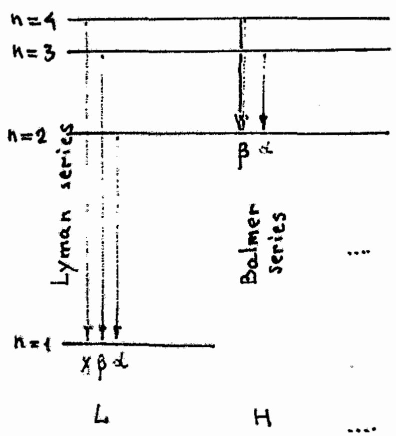

$\gamma \equiv \Gamma_{coll} + \dots$

TABLE 90. CALCULATED AND EXPERIMENTAL VALUES OF γ AND Δ FOR He I LINES

Line		C_4, 10^{-15} cm^4/sec	N, 10^{17} cm^{-3}	T, °K	Experiment (Å)		Griem, Kolb, Baranger, Oertel (Å)		Formulas (39.33), (39.34) (Å)	
λ, Å	Transition				γ	Δ	γ	Δ	γ	Δ
5016	2^1S-3^1P	−1334	1.65	25,000	13	−4.8	14.5	−6	14.4	−4.7
4713	2^3P-4^3S	1250	1.3	20,000	14	6	15.2	8.9	15	5.7
4713	2^3P-4^3S	1250	0.25	30,000	3	1.5	2.8	1.4	3	1.1
3889	2^3S-3^3P	264	1.5	25,000	4.5	1.2	4.2	1.1	5.4	1
3889	2^3S-3^3P	264	0.25	30,000	0.74	0.25	0.68	0.15	0.9	0.17
3188	2^3S-4^3P	2600	1.5	30,000	13.4	4.1	12.6	3.8	14.4	2.6
5048	2^1P-4^1S	2405	0.25	30,000	4.2	2.1	4.6	2.3	4.6	2.0
4121	2^3P-5^3S	6410	0.25	30,000	6.2	2.8	6.6	3	6.2	2.8

Dilepton spectra measured by

- CERES and HELIOS-3 Collaborations at CERN SPS (high energies)

Agakichiev et al., Phys. Rev. Lett. 75 (1995) 1272;
Drees, Nucl. Phys. A610 (1996) 536c;
M. Masera, Nucl. Phys. A590 (1995) 93c.

Experiments found a significant enhancement of the low-energy dilepton yield below the ρ and ω peaks.

Current theoretical models interpret this by the scenario of a significant reduction of the ρ-meson mass in dense medium.

Dilepton spectra obtained by the

- DLS Collaboration at the BEVALAC (energies around 1 A GeV)

R.J. Porter et al., Phys. Rev. Lett. 79 (1997) 1229.

cannot be reproduced by present transport calculations: There remains a discrepancy by a factor 2 to 3

Cassing and Bratkovskaya, Phys. Rep. 308 (1999) 65.

- HADES experiment at GSI, Germany

MOTIVATION FOR OUR INVESTIGATIONS:

To draw serious physical conclusions, one needs to eliminate first possible trivial explanations, like those connected to the existence of the nondirect decay modes of light unflavored mesons.

THE ENHANCED PRODUCTION OF DILEPTONS
IN THE LOW- AND INTERMEDIATE MASS CONTINUUM

$$\frac{\textit{integral of measured data}}{\textit{integral of expected yield from hadronic sources}} = \begin{cases} 1.40 \pm 0.1 & NA38 \\ 2.43 \pm 0.42 & HELIOS-3 \\ 5.0 \pm 2.7 & CERES \\ 2 \div 3 & DLS^{*)} \end{cases}$$

*) for $0.15 < M_{ee} < 0.4$ GeV

CERES data can be explained by broadening and dropping vector meson masses

DLS data **cannot**

CLASSIFICATION OF DILEPTON MODES

V = ρ, ω, ϕ
P = π, η, η'
S = $f_0(980), a_0(980)$

(i) $V -> e^+ e^-$
(ii) $P -> \gamma e^+ e^-$ $S -> \gamma e^+ e^-$
(iii) $V -> Pe^+ e^-$ $P -> Ve^+ e^-$
(iv) $V -> PPe^+ e^-$ $P -> PPe^+ e^-$ $S -> PPe^+ e^-$

OUTLINE OF THE TALK:

I. M —> $M'\gamma^*$ AND M —> $M'e^+e^-$

II. $f_0(980)$ —> γe^+e^-

III. ρ^0 —> $\pi^+\pi^- e^+e^-$

IV. NUMERICAL RESULTS FOR ALL DECAY MODES

RELATION BETWEEN DECAYS $\mathcal{M} \to \mathcal{M}'\gamma*$ and $\mathcal{M} \to \mathcal{M}'e^+e^-$

$\mathcal{M}$ is a meson, $\mathcal{M}'$ is a one- or two-meson state (or even a photon)

The decay $\mathcal{M} \to \mathcal{M}'e^+e^-$ proceeds through two steps: $\mathcal{M} \to \mathcal{M}'\gamma^*$ and $\gamma^* \to e^+e^-$:

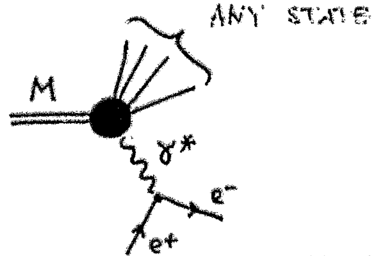

The matrix element of the physical process $\mathcal{M} \to \mathcal{M}'\gamma$ for a real photon γ has the form

$$\mathfrak{M} = \mathfrak{M}_\mu \varepsilon^*_\mu(k)$$

▲ $\varepsilon^*_\mu(k)$ is a photon polarization vector.

A consequence of the gauge invariance:

$$\mathfrak{M}_\mu k_\mu = 0$$

The decay rate $\mathcal{M} \to \mathcal{M}'\gamma^*$ can formally be calculated as

$$d\Gamma(\mathcal{M} \to \mathcal{M}'\gamma^*) = \frac{1}{2\sqrt{s}} \sum_f \overline{\mathfrak{M}_\mu \mathfrak{M}_\nu^*}(-g_{\mu\nu}) \frac{(2\pi)^4}{(2\pi)^{3n+3}} d\Phi_{n+1}$$

▲ $\sqrt{s} = m_{\mathcal{M}}$ is the mass of the decaying meson

▲ n is the number of mesons in the state $\mathcal{M}'$

The limit $M^2 \to 0$ gives the decay rate for the physical process $\mathcal{M} \to \mathcal{M}'\gamma$

The phase space

$$d\Phi_k(\sqrt{s}, m_1, ..., m_k) = \prod_{i=1}^{k} \frac{d\mathbf{p}_i}{2E_i} \delta^4(P - \sum_{i=1}^{k} p_i). \qquad (**)$$

▲ P is a four-momentum of the meson $\mathcal{M}$, $P^2 = s$, p_i are momenta of particles in the final state, including the virtual photon γ^*

The decay rate for the process $\mathcal{M} \to \mathcal{M}'e^+e^-$ is given by

$$d\Gamma(\mathcal{M} \to \mathcal{M}'e^+e^-) = \frac{1}{2\sqrt{s}} \sum_f \overline{\mathfrak{M}_\mu \mathfrak{M}_{\bar\mu}^* j_\mu j_{\bar\mu}^*} \frac{1}{M^4} \frac{(2\pi)^4}{(2\pi)^{3n+6}} d\Phi_{n+2}$$

▲ j_μ is the lepton current, the term $1/M^4$ comes from the photon propagator

The value $\Gamma(\mathcal{M} \to \mathcal{M}'e^+e^-)$ can related to the decay rates $\Gamma(\mathcal{M} \to \mathcal{M}'\gamma^*)$ and $\Gamma(\gamma^* \to e^-e^-)$. The width of a virtual photon γ^* :

$$M\Gamma(\gamma^* \to e^+e^-) = \frac{\alpha}{3}(M^2 + 2m^2)\sqrt{1 - \frac{4m^2}{M^2}}$$

The expression for product of the two dilepton currents, summed up over the final states of the e^-e^- pair, has the form

$$\boxed{\sum_f \overline{j_\mu j_{\bar\mu}^*} = \frac{16\pi\alpha}{3}(M^2 + 2m^2)(-g_{\mu\nu} + \frac{k_\mu k_\nu}{M^2})}$$

▲ k is the total momentum of the pair

Factorization of the n-body invariant phase space:

$$d\Phi_k(\sqrt{s}, m_1, ..., m_k) = d\Phi_{k-1}(\sqrt{s}, m_1, ..., m_{k-2}, M) dM^2 d\Phi_2(M, m_{k-1}, m_k)$$

It can be proved using the unity decomposition

$$1 = \int d^4q dM^2 \delta(q^2 - M^2) \delta^4(q - p_{k-1} - p_k)$$

into Eq.(**).

- The two-body phase space:

$$\Phi_2(\sqrt{s}, m_1, m_2) = \frac{\pi p^*(\sqrt{s}, m_1, m_2)}{\sqrt{s}}$$

- The particle momentum in the c. m. frame:

$$p^*(\sqrt{s}, m_1, m_2) = \frac{\sqrt{(s-(m_1+m_2)^2)(s-(m_1-m_2)^2)}}{2\sqrt{s}}$$

The decay width becomes

$$d\Gamma(\mathcal{M} \to \mathcal{M}' e^+ e^-) = d\Gamma(\mathcal{M} \to \mathcal{M}'\gamma^*) M\Gamma(\gamma^* \to e^+ e^-) \frac{dM^2}{\pi M^4}.$$

In what follows, we work with the matrix elements of the processes $\mathcal{M} \to \mathcal{M}'\gamma^*$.

Decay mode $f_0(980) \longrightarrow \gamma\, e^- e^+$

The isoscalar $f_0(980)$-meson: $I^G(J^{PC}) = 0^+(0^{++})$

The effective vertex for the S —> $\gamma\gamma^*$ decay has the form

$$\delta\mathcal{L}_{S\gamma\gamma} = f_{S\gamma\gamma} F_{\tau\mu} F_{\tau\mu} S$$

where $F_{\mu\nu} = \partial_\nu A_\mu - \partial_\mu A_\nu$.

The matrix element for the process S —> $\gamma\gamma^*$ is given by

$$\mathfrak{M} = -i f_{S\gamma\gamma} F_{S\gamma\gamma}(M^2)(g_{\tau\sigma}k_{1\lambda} - g_{\tau\lambda}k_{1\sigma})(g_{\mu\sigma}k_\lambda - g_{\mu\lambda}k_\sigma)\varepsilon^*_\tau(k_1)\varepsilon^*_\mu(k).$$

Here, k_1 is real ($k_1^2 = 0$), and k is the virtual photon momentum ($k^2 = M^2$).

- $F_{S\gamma\gamma}(t)$ is transition form factor of the decay S —> $\gamma\gamma^*$.

The square of the matrix element summed up over the photon polarizations can easily be found to be

$$\sum_f |\mathfrak{M}|^2 = 8 s p^{*2}(\sqrt{s}, 0, M),$$

with $\sqrt{s} = m_S$ the scalar meson mass.

$$p^*(\sqrt{s}, m_1, m_2) = \frac{1}{2\sqrt{s}}\sqrt{(s-(m_1+m_2)^2)(s-(m_1-m_2$$

The width of the S —> γ^* e⁺e⁻ decay can be written as follows

$$\frac{d\Gamma(S \to \gamma e^+ e^-)}{\Gamma(S \to \gamma\gamma)} = 2\frac{p^{*3}(\sqrt{s},0,M)}{p^{*3}(\sqrt{s},0,0)} \left|F_{S\gamma\gamma}(M^2)\right|^2 M\Gamma(\gamma^* \to e^+e^-)\frac{dM^2}{\pi M^4}.$$

- The transition form factor $F_{S\gamma\gamma}(t)$ depends on the nature of the scalar meson S.

The asymptotics of the form factor according to the quark counting rules:

$\sim 1/t$ for a 2-quark model

$\sim 1/t^2$ for a 4-quark MIT bag model

$\sim 1/t^4$ for a $K\bar{K}$ molecular model

In the SND experiment at the VEPP-2M e⁺e⁻ collider (Novosibirsk) the branching ratio $\phi \to \pi^0\eta^0\gamma$ was measured

M.N. Achasov et al. (SND Collaboration), Phys. Lett. 440B (1998) 442

It goes mainly through the $\phi \to f_0\gamma$ decay mode.

4-quark MIT bag nature of the f_0-meson

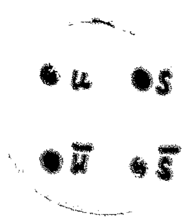

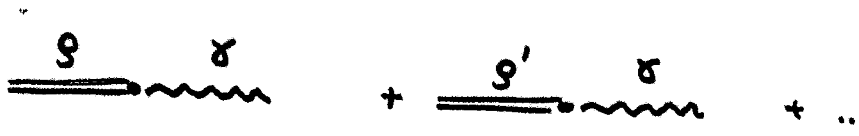

■ VMD model: Contributions from ground-state and excited vector mesons with masses m_i

$$F_{S\gamma\gamma}(t) = \sum_i \frac{c_i m_i^2}{m_i^2 - t}.$$

The normalization condition

$$F_{S\gamma\gamma}(t) = 1$$

and the asymptotic condition

$$F_{S\gamma\gamma}(t) \sim 1/t^2 \quad \text{at} \quad t \to \infty$$

give constraints to the residues c_i:

$$1 = \sum_i c_i,$$
$$0 = \sum_i c_i m_i^2.$$

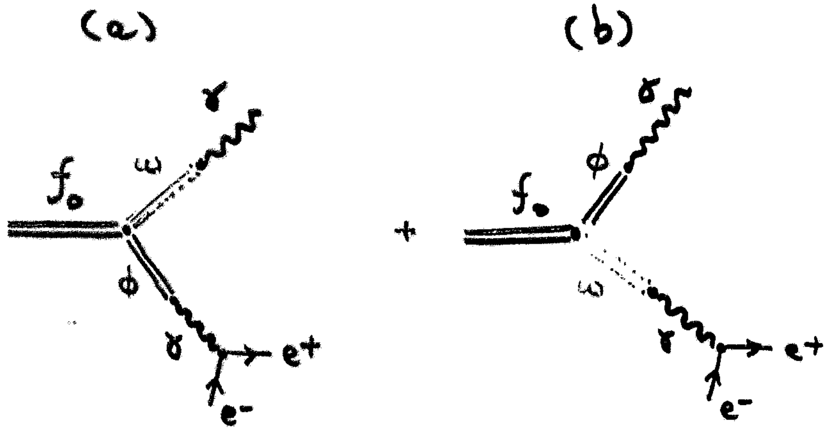

$\frac{t}{m_\omega^2 - 0}$ $\frac{m_\omega^2}{f_\omega}$ $\frac{t}{m_\phi^2 - t}$ [illegible] $\frac{m_\phi^2}{f_\phi}$ (α)

$\frac{1}{m_\omega^2 - t}$ $\frac{m_\omega^2}{g_\omega}$ $\frac{1}{m_\phi^2 - 0}$ $\frac{m_\phi^2}{g_\phi}$ (β)

At least three vector mesons should be considered to fit the asymptotic behavior:

$$F_{f_0\gamma\gamma}(t) \sim \frac{m_\omega^2}{m_\omega^2 - t} + \frac{m_\phi^2}{m_\phi^2 - t} + c_X \frac{m_X^2}{m_X^2 - t}.$$

The resulting form factor is given by

$$F_{f_0\gamma\gamma}(t) = \frac{m_\omega^2 m_\phi^2 m_X^2 (1 + Ct)}{(m_\omega^2 - t)(m_\phi^2 - t)(m_X^2 - t)}$$

where

$$C = -\frac{m_\omega^2 (m_X^2 - m_\omega^2) + m_\phi^2 (m_X^2 - m_\phi^2)}{m_\omega^2 m_\phi^2 (2m_X^2 - m_\omega^2 - m_\phi^2)}.$$

finally: $m_V^2 \to m_V^2 - i m_V \Gamma_V$

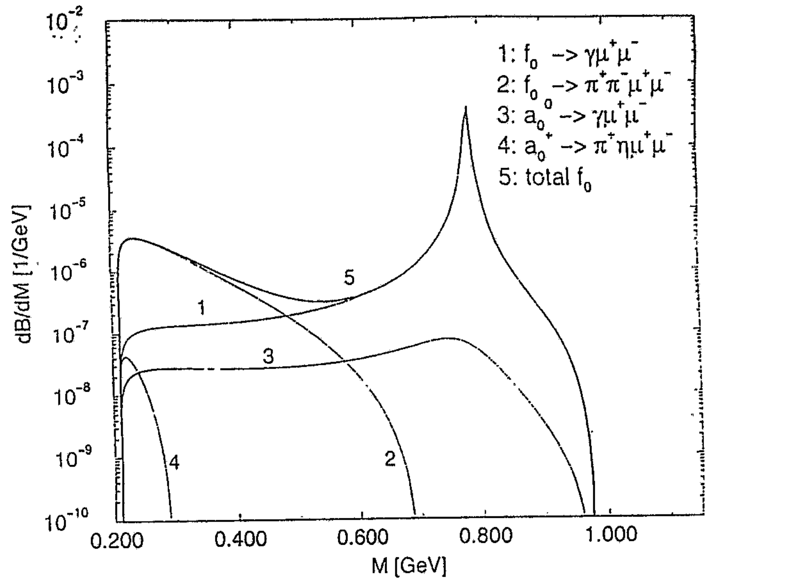

FIG. 24. The differential branching ratios for the $f_0(980)$- and $a_0(980)$-mesons into the $\mu^+\mu^-$ channels versus the invariant mass, M, of the dilepton pairs. The solid curve No. 5 gives the total $\mu^+\mu^-$ ratio of the f_0 -meson decays. The structures in the f_0, $a_0 \to \gamma\mu^+\mu^-$ decay modes are connected to the ω- and ρ-mesons contributions to transition form factors of the f_0- and a_0-mesons.

SPECIFIC EXAMPLE: DECAY MODE $\rho^0 \to \pi^+\pi^-e^+e^-$

MOTIVATION:

$Br^{exp}(\rho^0 \to \pi^0\gamma) = (7.9 \pm 2.0) \times 10^{-4}$

$Br^{exp}(\rho^0 \to \pi^+\pi^-\gamma) = (9.9 \pm 1.6) \times 10^{-3}$

The decay mode $\rho^0 \to \pi^+\pi^-e^+e^-$ gives an important (if not a dominant) contribution to the dilepton spectrum of the ρ^0-meson decays.

The diagrams contributing to the decay $\rho^0 \to \pi^+\pi^-\gamma^*$:

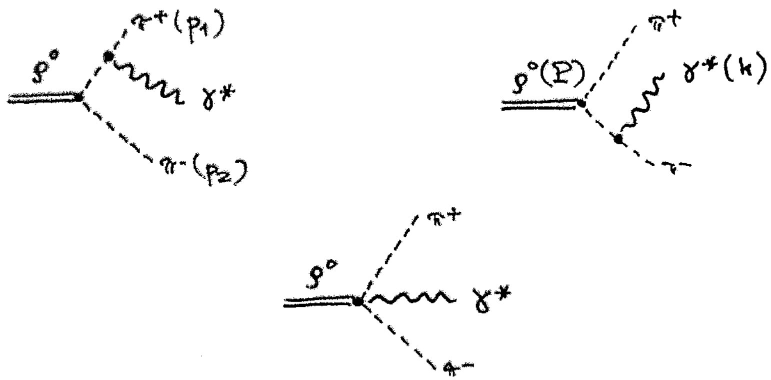

The matrix element of the process $\rho^0 \to \pi^+\pi^-\gamma^*$:

$$\mathfrak{M} = -ie f_{\rho\pi\pi} F_\pi(k^2)\epsilon_\tau(P)\mathfrak{M}_{\tau\mu}\epsilon^*_\mu(k)$$

[illegible]

$$\begin{aligned}\mathfrak{M}_{\tau\mu} &= (p_1 - p_2)_\tau \left[\frac{(2p_1+k)_\mu}{(p_1+k)^2-\mu^2} - \frac{(2p_2+k)_\mu}{(p_2+k)^2-\mu^2}\right] \\ &+ k_\tau \left[\frac{(2p_1+k)_\mu}{(p_1+k)^2-\mu^2} + \frac{(2p_2+k)_\mu}{(p_2+k)^2-\mu^2}\right] \\ &- 2g_{\tau\mu}.\end{aligned}$$

$$\boxed{\begin{aligned}\mathfrak{M}_{\tau\mu}k_\mu &= 0, \\ \mathfrak{M}_{\tau\mu}P_\tau &= 0.\end{aligned}}$$

The square of the matrix element summed up over the photon polarizations, averaged over the initial ρ-meson polarizations and over directions of the pion momenta in the c. m. frame of the two pions:

$$\begin{aligned}\mathfrak{R} &\equiv \int \frac{d\Omega_{12}}{4\pi}\mathfrak{M}_{\tau\mu}\mathfrak{M}^*_{\tilde{\tau}\tilde{\mu}}\frac{1}{3}\left(-g_{\tau\tilde{\tau}} + \frac{P_\tau P_{\tilde{\tau}}}{s}\right)(-g_{\mu\tilde{\mu}}) \\ &= \frac{2}{3B_\pi^2}\left(4B_\pi^2 + (M^2-4\mu^2)(s-4\mu^2)F(\xi)\right. \\ &\left.+((s-4\mu^2)(M^2-4\mu^2+2s_{12}) + 2s_{12}M^2)L(\xi)\right)\end{aligned}$$

▲ $s = P^2 = m_\rho^2,\ s_{12} = (p_1+p_2)^2$,

$$\begin{aligned}F(\xi) &= \frac{1}{1-\xi^2}, \\ L(\xi) &= \frac{1}{2\xi}\ln\left(\frac{1+\xi}{1-\xi}\right)\end{aligned}$$

********* and *********

$$\begin{aligned}\xi &= \frac{2}{B_\pi}\sqrt{\frac{s}{s_{12}}}p^*(\sqrt{s_{12}},\mu,\mu)p^*(\sqrt{s},\sqrt{s_{12}},M), \\ B_\pi &= \frac{1}{2}(s+M^2-s_{12}).\end{aligned}$$

The decay rate $\Gamma(\rho^0 \to \pi^+\pi^-\gamma^*)$ takes the form

$$\boxed{\Gamma(\rho^0 \to \pi^+\pi^-\gamma^*) = \frac{\alpha}{16\pi^2 s}f^2_{\rho\pi\pi}|F_\pi(M^2)|^2\int_{4\mu^2}^{(\sqrt{s}-M)^2}\mathfrak{R}\,\frac{p^*(\sqrt{s},\sqrt{s_{12}},M)p^*(\sqrt{s_{12}},\mu,\mu)}{\sqrt{s_{12}}}ds_{12}.}$$

The dilepton spectrum is given by

$$d\Gamma(\rho^0 \to \pi^+\pi^-e^+e^-) = \Gamma(\rho^0 \to \pi^+\pi^-\gamma^*)(M)\Gamma(\gamma^* \to e^+e^-)\frac{dM^2}{\pi M^4}.$$

BRANCHING RATIOS FOR RADIATIVE MESON DECAYS

Decay mode	B^{th}	B^{exp}
→ $\rho^{\pm} \to \pi^{\pm}\pi^{0}\gamma^{*)}$	4.0×10^{-3}	
→ $\rho^{0} \to \pi^{+}\pi^{-}\gamma^{*)}$	1.2×10^{-2}	$(0.99 \pm 0.16) \times 10^{-2}$
→ $\rho^{0} \to \pi^{0}\pi^{0}\gamma$	1.2×10^{-5}	
→ $\rho^{0} \to \pi^{0}\eta\gamma$	3.8×10^{-10}	
→ $\omega \to \pi^{+}\pi^{-}\gamma^{*)}$	3.2×10^{-4}	$< 3.6 \times 10^{-3}$
→ $\omega \to \pi^{0}\pi^{0}\gamma$	3.1×10^{-5}	$(7.2 \pm 2.5) \times 10^{-5}$
→ $\omega \to \pi^{0}\eta\gamma$	2.1×10^{-7}	
$\eta \to \pi^{+}\pi^{-}\gamma$	6.9×10^{-2}	$(4.78 \pm 0.12) \times 10^{-2}$
$\eta' \to \pi^{+}\pi^{-}\gamma$	2.5×10^{-1}	$(2.8 \pm 0.4) \times 10^{-1}$
→ $f_0 \to \pi^{+}\pi^{-}\gamma^{*)}$	1.1×10^{-2}	
→ $a_0^{\pm} \to \pi^{\pm}\eta\gamma^{*)}$	2.4×10^{-3}	

*) for photon energies above 50 MeV

→ in agreement with calculations
A. Bramon, A. Grau, G. Pancheri
Phys. Lett. **283B** (1992) 416

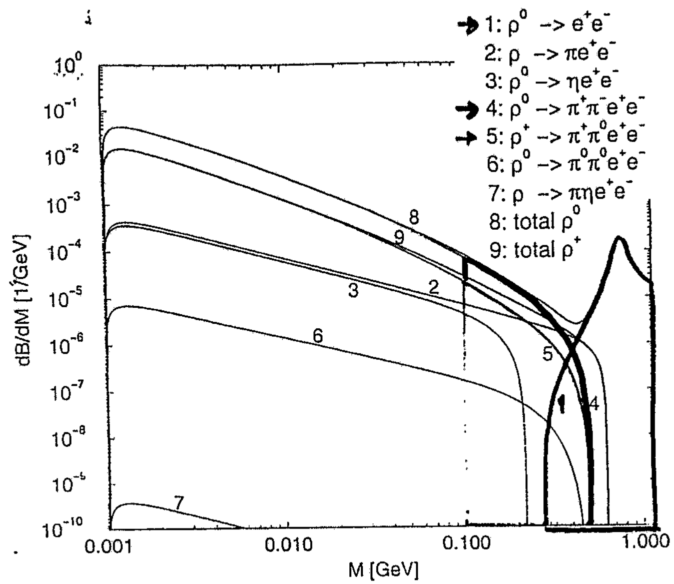

FIG. 15. The differential branching ratios for the ρ-meson decays into the e^+e^- channels as functions of the invariant mass, M, of the dilepton pairs. The solid curves (8 and 9) are the total ratios for the ρ^0- and $\rho^{\pm}$-mesons.

$$\frac{B(\rho^{\pm} \to \pi^{\pm}\pi^{0} e^+e^-) + B(\rho^{0} \to \pi^{+}\pi^{-} e^+e^-)}{B(\rho^{0} \to e^+e^-)} \approx 1/3$$

for $M \geq 100$ MeV

BRANCHING RATIOS FOR RADIATIVE MESON DECAYS

Decay mode	B^{th}	B^{exp}
→ $\rho^{\pm} \rightarrow \pi^{\pm}\pi^{0}\gamma^{*)}$	4.0×10^{-3}	
→ $\rho^{0} \rightarrow \pi^{+}\pi^{-}\gamma^{*)}$	1.2×10^{-2}	$(0.99 \pm 0.16) \times 10^{-2}$
→ $\rho^{0} \rightarrow \pi^{0}\pi^{0}\gamma$	1.2×10^{-5}	
→ $\rho^{0} \rightarrow \pi^{0}\eta\gamma$	3.8×10^{-10}	
→ $\omega \rightarrow \pi^{+}\pi^{-}\gamma^{*)}$	3.2×10^{-4}	$< 3.6 \times 10^{-3}$
→ $\omega \rightarrow \pi^{0}\pi^{0}\gamma$	3.1×10^{-5}	$(7.2 \pm 2.5) \times 10^{-5}$
→ $\omega \rightarrow \pi^{0}\eta\gamma$	2.1×10^{-7}	
$\eta \rightarrow \pi^{+}\pi^{-}\gamma$	6.9×10^{-2}	$(4.78 \pm 0.12) \times 10^{-2}$
$\eta' \rightarrow \pi^{+}\pi^{-}\gamma$	2.5×10^{-1}	$(2.8 \pm 0.4) \times 10^{-1}$
→ $f_0 \rightarrow \pi^{+}\pi^{-}\gamma^{*)}$	1.1×10^{-2}	
→ $a_0^{\pm} \rightarrow \pi^{\pm}\eta\gamma^{*)}$	2.4×10^{-3}	

*) for photon energies above 50 MeV

→ in agreement with calculations
A. Bramon, A. Grau, G. Pancheri
Phys. Lett. **283B** (1992) 416

INTEGRAL BRANCHING RATIOS FOR UNFLAVORED MESON DECAYS TO e^+e^- AND $\mu^+\mu^-$ CHANNELS

Decay mode	$B^{th}_{e^-e^-}$	$B^{exp}_{e^-e^-}$	$B^{th}_{\mu^-\mu^-}$	$B^{exp}_{\mu^-\mu^-}$
$\rho^0 \rightarrow \ell^+\ell^-$	input	$(4.48 \pm 0.22) \times 10^{-5}$	input	$(4.60 \pm 0.28) \times 10^{-5}$
$\rho \rightarrow \pi\ell^+\ell^-$	4.1×10^{-6}		4.6×10^{-7}	
$\rho^0 \rightarrow \eta\ell^+\ell^-$	2.7×10^{-6}		7.0×10^{-11}	
$\rho^{\pm} \rightarrow \pi^{\pm}\pi^{0}\ell^+\ell^-$	[illegible]		1.8×10^{-7}	
$\rho^0 \rightarrow \pi^+\pi^-\ell^+\ell^-$	[illegible]		6.7×10^{-7}	
$\rho^0 \rightarrow \pi^0\pi^0\ell^+\ell^-$	7.5×10^{-8}		2.4×10^{-9}	
$\rho \rightarrow \pi\eta\ell^+\ell^-$	1.9×10^{-12}			
$\omega \rightarrow \ell^+\ell^-$	input	$(7.15 \pm 0.19) \times 10^{-5}$	input	$(7.15 \pm 0.19) \times 10^{-5}$
$\omega \rightarrow \pi^0\ell^+\ell^-$	7.9×10^{-4}	$(5.9 \pm 1.9) \times 10^{-4}$	9.2×10^{-5}	$(9.6 \pm 2.3) \times 10^{-5}$
$\omega \rightarrow \eta\ell^+\ell^-$	6.0×10^{-6}		1.8×10^{-9}	
$\omega \rightarrow \pi^+\pi^-\ell^+\ell^-$	3.9×10^{-6}		2.9×10^{-8}	
$\omega \rightarrow \pi^0\pi^0\ell^+\ell^-$	2.0×10^{-7}		7.4×10^{-9}	
$\omega \rightarrow \pi^0\eta\ell^+\ell^-$	8.7×10^{-10}			
$\phi \rightarrow \ell^+\ell^-$	input	$(3.00 \pm 0.06) \times 10^{-4}$	input	$(2.48 \pm 0.34) \times 10^{-4}$
$\phi \rightarrow \pi^0\ell^+\ell^-$	1.6×10^{-5}		4.8×10^{-6}	
$\phi \rightarrow \eta\ell^+\ell^-$	1.1×10^{-4}	$(1.4 \pm 0.7) \times 10^{-4}$	6.8×10^{-6}	
$\eta \rightarrow \gamma\ell^+\ell^-$	6.5×10^{-3}	$(4.9 \pm 1.1) \times 10^{-3}$	3.0×10^{-4}	$(3.1 \pm 0.4) \times 10^{-4}$
$\eta \rightarrow \pi^+\pi^-\ell^+\ell^-$	3.6×10^{-4}	$(1.3 {}^{+1.2}_{-0.8}) \times 10^{-3}$	1.2×10^{-8}	
$\eta' \rightarrow \gamma\ell^+\ell^-$	4.2×10^{-4}		8.1×10^{-5}	$(1.04 \pm 0.26) \times 10^{-4}$
$\eta' \rightarrow \omega\ell^+\ell^-$	2.0×10^{-4}			
$\eta' \rightarrow \pi^+\pi^-\ell^+\ell^-$	1.8×10^{-3}		2.0×10^{-5}	
$f_0 \rightarrow \gamma\ell^+\ell^-$	2.2×10^{-7}		2.8×10^{-8}	
$f_0 \rightarrow \pi^+\pi^-\ell^+\ell^-$	1.4×10^{-4}		4.1×10^{-7}	
$a_0^0 \rightarrow \gamma\ell^+\ell^-$	6.0×10^{-8}		7.4×10^{-9}	
$a_0 \rightarrow \pi\eta\ell^+\ell^-$	4.0×10^{-5}		1.4×10^{-9}	
$\pi^0 \rightarrow \gamma\ell^+\ell^-$	1.18×10^{-2}	$(1.198 \pm 0.032) \times 10^{-2}$		

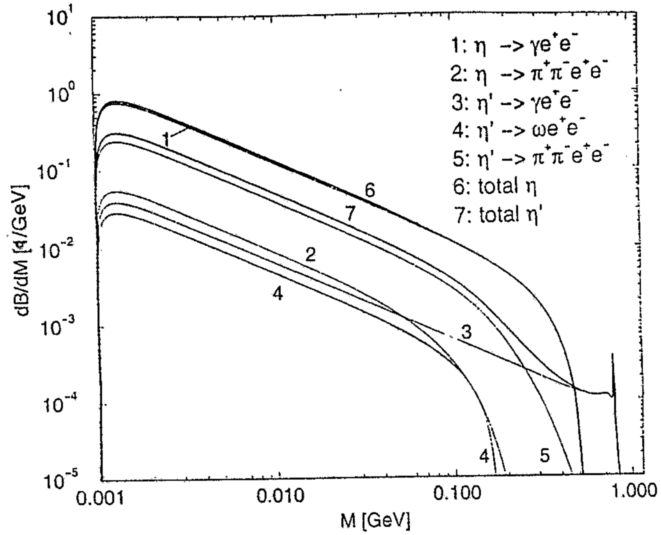

FIG. 21. The differential branching ratios for the η- and η'-mesons decaying into the e^+e^- channels versus the invariant mass, M, of the dilepton pairs. The solid curves (6 and 7) give the total ratios. The narrow structure in the $\eta' \to \gamma e^+ e^-$ decay is connected to the ω-meson contribution to the $\eta' \to \gamma\gamma^*$ transition form factor (see Eq.(IV.5)).

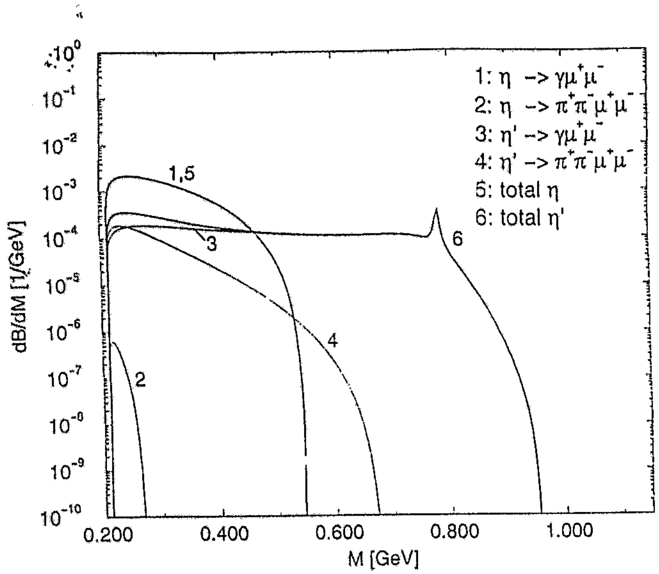

FIG. 22. The differential branching ratios for the η- and η'-mesons decays into the $\mu^+\mu^-$ channels versus the invariant mass, M, of the dilepton pairs. The solid curves give the total ratios. The narrow structure in the $\eta' \to \gamma\mu^+\mu^-$ decay is connected to the ω-meson contribution to the $\eta' \to \gamma\gamma^*$ transition form factor.

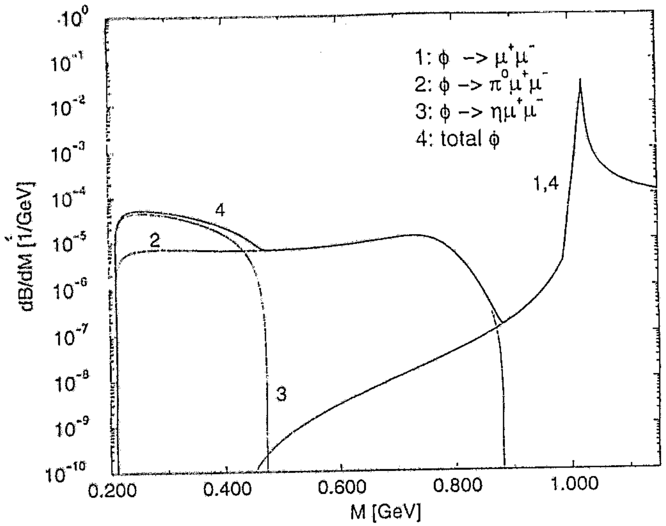

FIG. 20. The differential branching ratios for the ϕ- mesons decaying into the $\mu^+\mu^-$ channels versus the invariant mass, M, of the dilepton pairs. The solid curve gives the total ratio of the $\mu^+\mu^-$ modes.

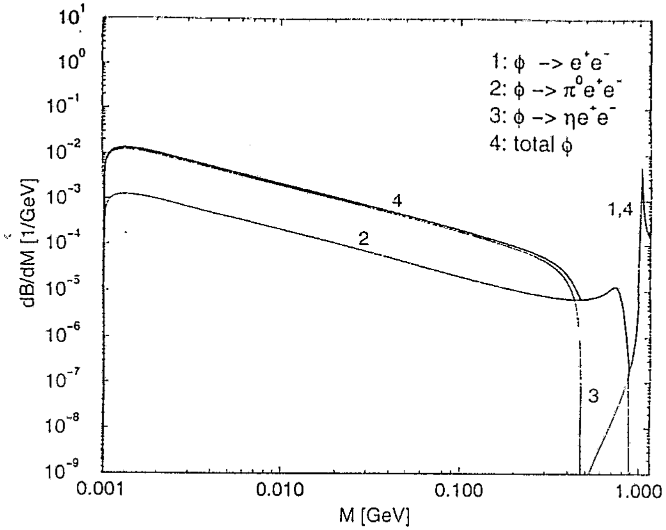

FIG. 19. The differential branching ratios for the ϕ-meson decays into the e^+e^- channels versus the invariant mass, M, of the dilepton pairs.

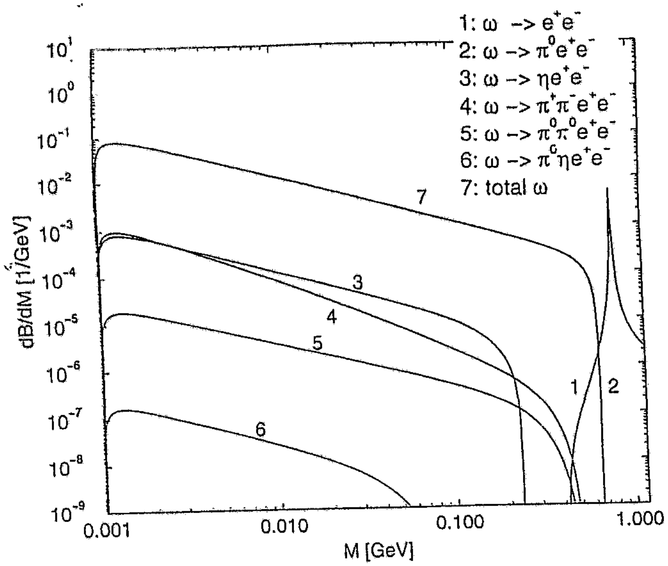

FIG. 17. The differential branching ratios for the ω-meson decays into the e^+e^- channels as functions of the invariant mass, M, of the dilepton pairs. The solid curve is the total ratio. The background is dominated through the πe^+e^- Dalitz decay.

$$dB \sim \Gamma(M \to M'\gamma^*) \frac{dM}{M}$$

1: $\Gamma(M \to M'\gamma^*) \sim$ constant at $2m_e \lesssim M$

$$\Rightarrow \frac{d}{d\log M} \log \frac{dB}{dM} \approx -1$$

2: $\Gamma(M \to M'\gamma^*) \sim \log^3\left(\frac{1}{M}\right)$ at $2m_e \lesssim M$

$$\Rightarrow \left| \frac{d}{d\log M} \log \frac{dB}{dM} \right| \gtrsim 1$$

/ bremsstrahlung /

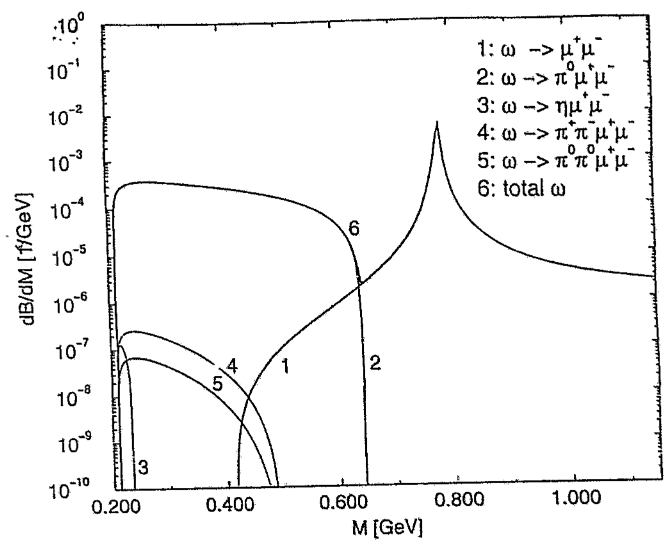

FIG. 18. The differential branching ratios for the ω-meson decays into the $\mu^+\mu^-$ channels as functions of the invariant mass, M, of the dilepton pairs. The solid curve is the total ratio.

$pp \to pp e^+e^-$

$pp e^+e^- \pi^0$

$pp e^+e^- \pi^+\pi^-$

....

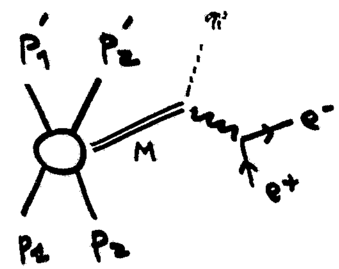

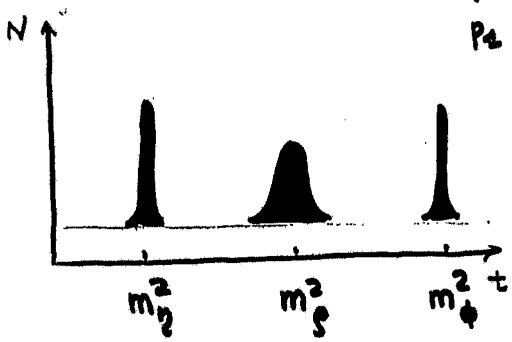

$$t = (p_1 + p_2 - p_1' - p_2')^2$$

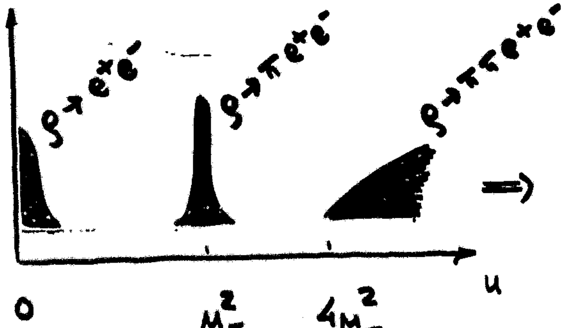

$$\Longrightarrow \frac{d^2B}{dM\,ds_{12}}$$

$$u = (p_1 + p_2 - p_1' - p_2' - k_{e^+} - k_{e^-})^2$$

$$u = s_{12} = (q_1 + q_2)^2$$

CONCLUSION

1. BRANCHING RATIOS TO DILEPTON CHANNELS ARE CALCULATED:

   $M \to e^+e^-$, γe^+e^-, $M e^+e^-$, $MM e^+e^-$

2. $$\frac{B(\rho \to \pi\pi e^+e^-)}{B(\rho^0 \to e^+e^-)} \sim 1/3 \quad \text{at } M > 100\ M$$

3. EXCESS OF DILEPTONS AT M < 500 MeV IN HIC SEEMS TO BE NOT CONNECTED TO NEGLECTION OF MESON DECAY CHANNELS

4. RESULTS REPRESENT INTREST FOR:

   (i) HIC (HIGH ENERGIES)

   (ii) $\pi N \to NN e^+e^- + \dots$

   (iii) $\gamma N \to N e^+e^- + \dots$

   (iv) SEARCHES OF DILEPTON DECAY OF MESONS

F. Dohrmann:

The HADES project

The HADES Project

- Motivation
- Concept and Status
- HADES in 1999/2000
- Summary

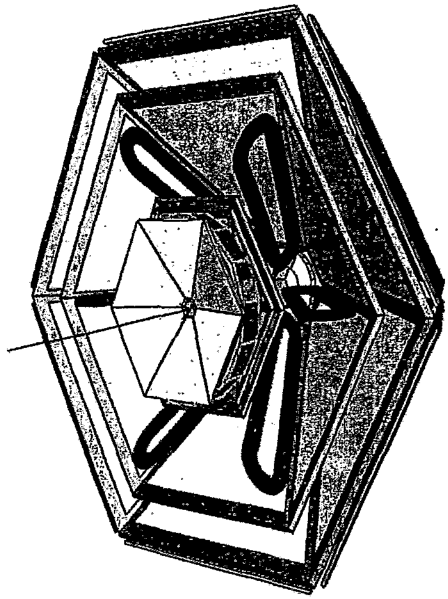

Frank Dohrmann, FZ Rossendorf, Institut f. Kern- u. Hadronenphysik

Electromagnetic Radiation off Colliding Hadron Systems: Dileptons & Bremsstrahlung
Miniworkshop, Forschungszentrum Rossendorf, Dresden, April 16-17, 1999

Collisions of Hadrons and Nuclei

- Production of Mesons at SIS Darmstadt
  - Kaons K^+,K^- (with strangeness) — KaoS, FOPI
  - Light vector mesons ρ, ω, φ (Decay → e^+e^- Dileptons) — <u>HADES</u>

  ➨ Modification of effective mass m* of mesons in nuclear matter ?

  ➨ *Hypothesis*: chiral symmetry is partially restored in ***hot*** and ***dense*** nuclear matter

- Important for description of nuclear matter under extreme conditions, i.e. early universe, neutron stars

Light Vector Mesons

$\rho, \omega, \Phi \longrightarrow e^+e^-$

Meson	Mass (MeV)	Width (MeV)	ct(fm)	dom. Decay	e^+e^- BR
ρ	768	152	1.3	$\pi^+\pi^-$	4.4×10^{-5}
ω	782	8.43	23.4	$\pi^+\pi^-\pi^0$	7.2×10^{-5}
Φ	1019	4.43	44.4	K^+K^-	3.1×10^{-4}

Vector mesons in nuclear matter

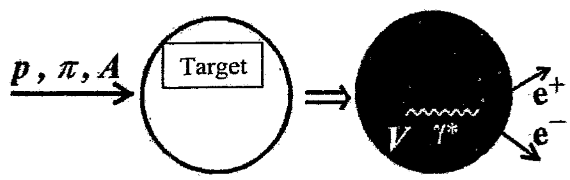

Dilepton Spectra: Calculation by C. Ernst et al., Univ. Frankfurt a.M.

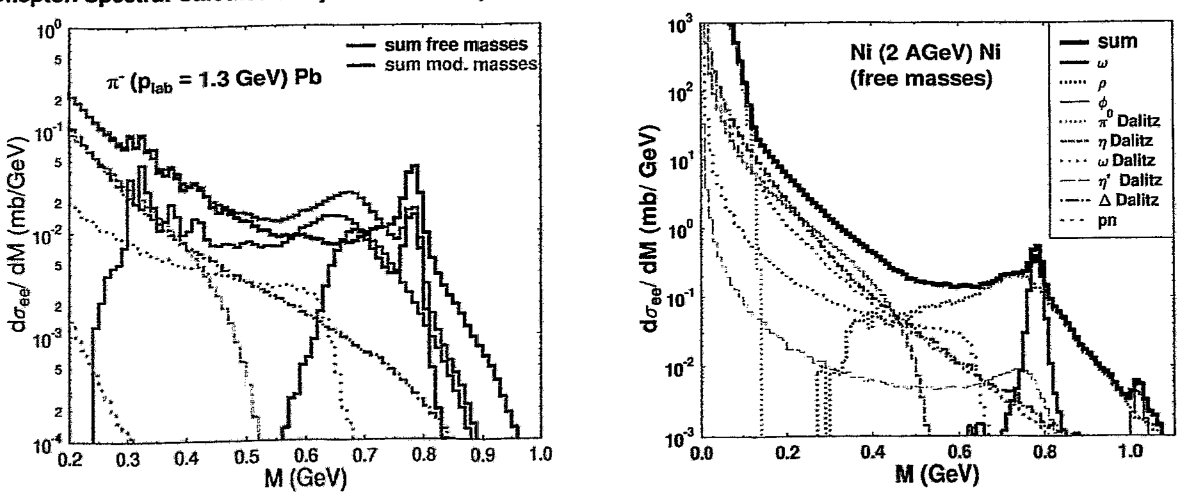

➨Experiments with HADES at SIS/GSI

Results of DLS Experiment

- Data by DLS collaboration
  Porter et al. PRL **79** (1997)1229,
  Wilson et al. PRC **57(4)** (1998) 1865
- — Transport calculation (HSD model)
  Bratkovskaya, Ko, PL **B445** (1999) 265
  - ✎ most recent attempt to describe DLS data
  - ✎ underpredicts data by a factor of 3 in the invariant mass region 0.2 GeV/c² < M_{ee} < 0.5 GeV/c² regardless of using bare meson masses or in-medium masses of mesons.
  - ✎ all earlier attempts failed as well
  - ↳ Situation should be clarified by new data from HADES very soon

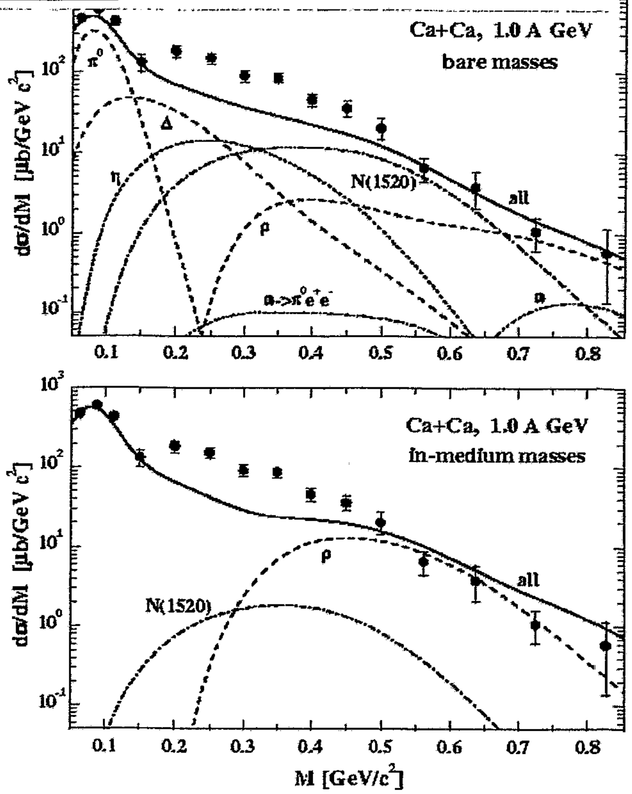

Results of DLS Experiment

- Unexplained high rates of Dielectrons in nuclear collisions
- Increased η strength would contradict TAPS results:
  - ➡ Dalitz decay of η meson cannot explain dielectrons rates as measured by DLS for invariant masses from 0.15 < M_{inv}/GeV < 0.55
- ✎ *New measurements with HADES even with incomplete setup*

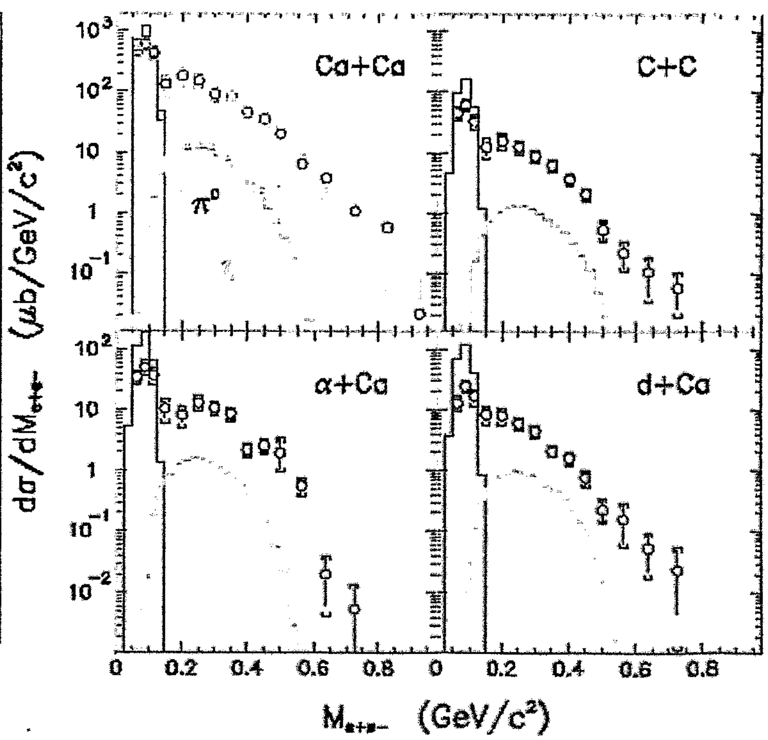

TAPS R. Holzmann et al, PRC 56(1997)R2920,

DLS data: Porter et al. PRL 79(1997)1229, Wilson et al. PRC 57(4) (1998) 1865

Key Parameters of HADES

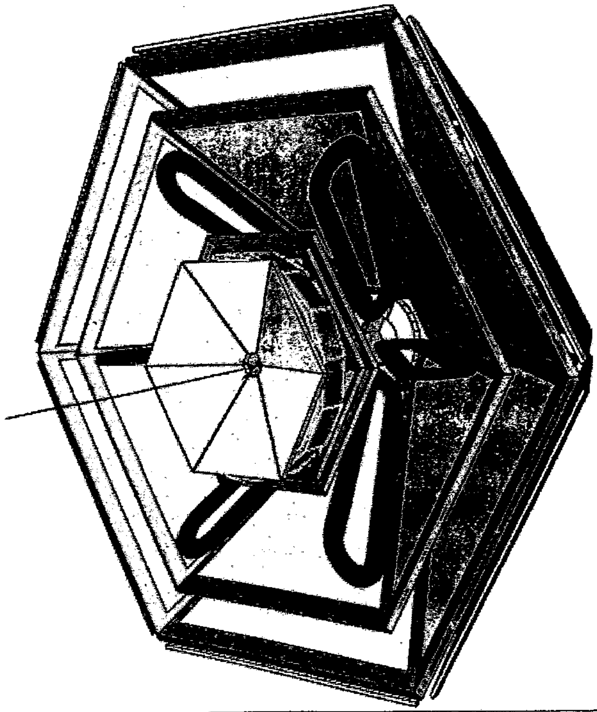

Parameter (2.Generation)

- Large acceptance for Lepton pairs $\varepsilon_{pair} \sim 40\ \%$
- Capable of high rates (R ~ 10^6 s^{-1} and high multiplicities
- High resolution spectrometer
  - Resolution for reconstructed invariant masses comparable to width of free ω meson **(ΔM/M ~ 1 % (σ))**
- Signal to background S/B > 1 for invariant masses up to $M_{ee} \sim 1\ GeV/c^2$
- High granularity to study heaviest systems (U+U, 1 AGeV)

High Acceptance DiEelectron Spectrometer

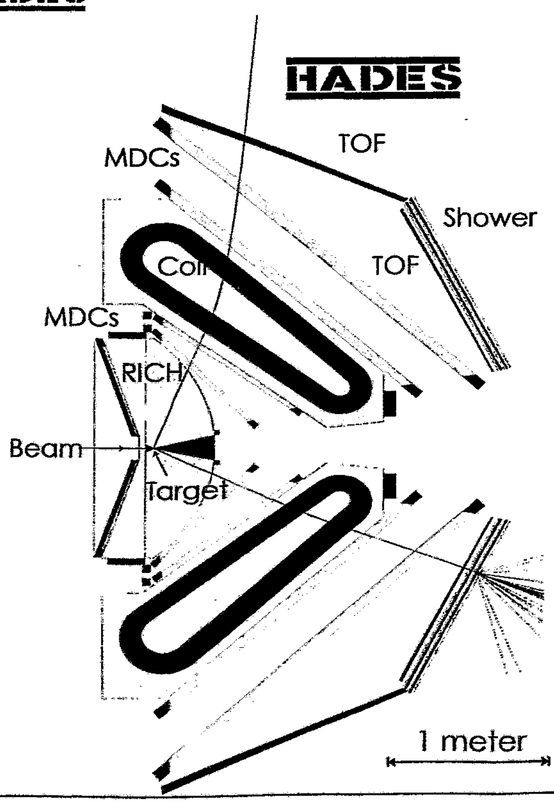

Geometry

6 sectors form hexagonal pyramid

- 2π in ϕ
- 18° < ϑ < 85°

Dilepton Identification

- RICH
  - Radiator: C_4F_{10}
  - Spherical VUV mirror
  - Photon detector: CsI photocathode
- META
  - TOF Plastic scintillator wall
  - Lead shower detector

Track Reconstruction

- Superconducting Toroid (6 coils)
  - $B_{max} = 0.7$ T,
  - $B\rho$ = 0.34 Tm
- MDC (Multiwire Drift Chamber)
  - Low Z of wire material (Al)
  - 4 layers with high granularity, i.e. small drift cells (≈ 1 cm diameter).

In total ~ 100.000 channels

e^+e^- Identification with RICH

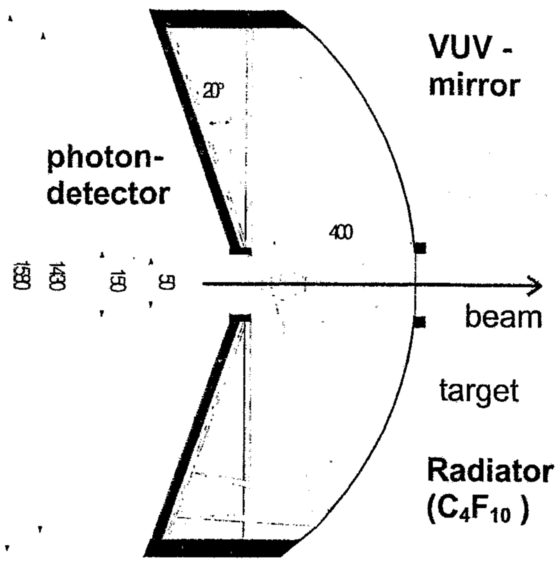

- **Ring Imaging Cherenkov**
  $\cos\theta_c = 1/\beta \cdot n(\lambda)$
  $N = N_0 \cdot l_{rad} \cdot 1/\gamma_t^2$ (l_{rad} = 40 cm)
  ↳ N_0 = 80 - 150 cm^{-1}
- **Radiator** (hadr. blind)
  $3 \sim \gamma_{had} < \gamma_t < \gamma_{lep}$
  C_4F_{10} : γ_t = 18.3
  ΔE = 350 MeV/event (200 ch.p.)
- **VUV mirror**
  Poly-C substr. (2 mm) **x/X < 2%** Al + MgF_2 coating **R > 80%**
- **Photon detector** (MWPC)
  CsI - cath.
  CaF_2 window

Mirror Segments for RICH

MDC Design Parameters

	A [mm]	B [mm]	C [mm]	a [mm]
I	139.21	767.38	839.19	5
II	205.00	905.00	1049.27	6
III	310.43	1804.80	2139.05	12
IV	345.46	2224.05	2689.04	14

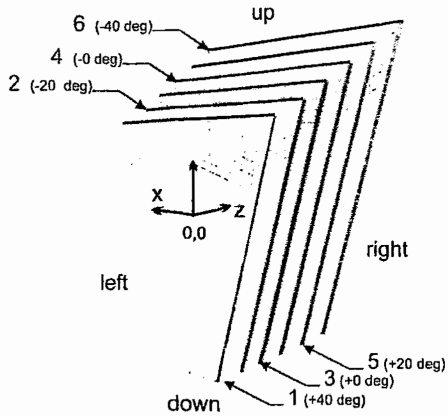

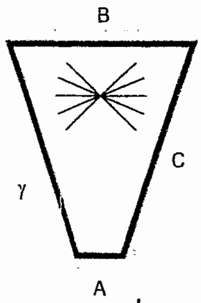

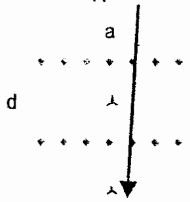

- 24 conceptually identical modules in 4 different geometries
- 6 drift cell layers
  - stereo angles + 40, − 20, + 0, − 0, + 20, − 40 deg
- Maximum drift path: 5 up to 14 mm
- Cathode wires: 80 µm bare Aluminum
- Potential wires: 80 and 100 µm bare Aluminum
- Sense wires: 20 µm Tungsten/Au
- Counting Gas: He/i-C_4H_{10}

✎ Position resolution from prototype tests σ ~ 80 µm

Full System Test MDC Typ II

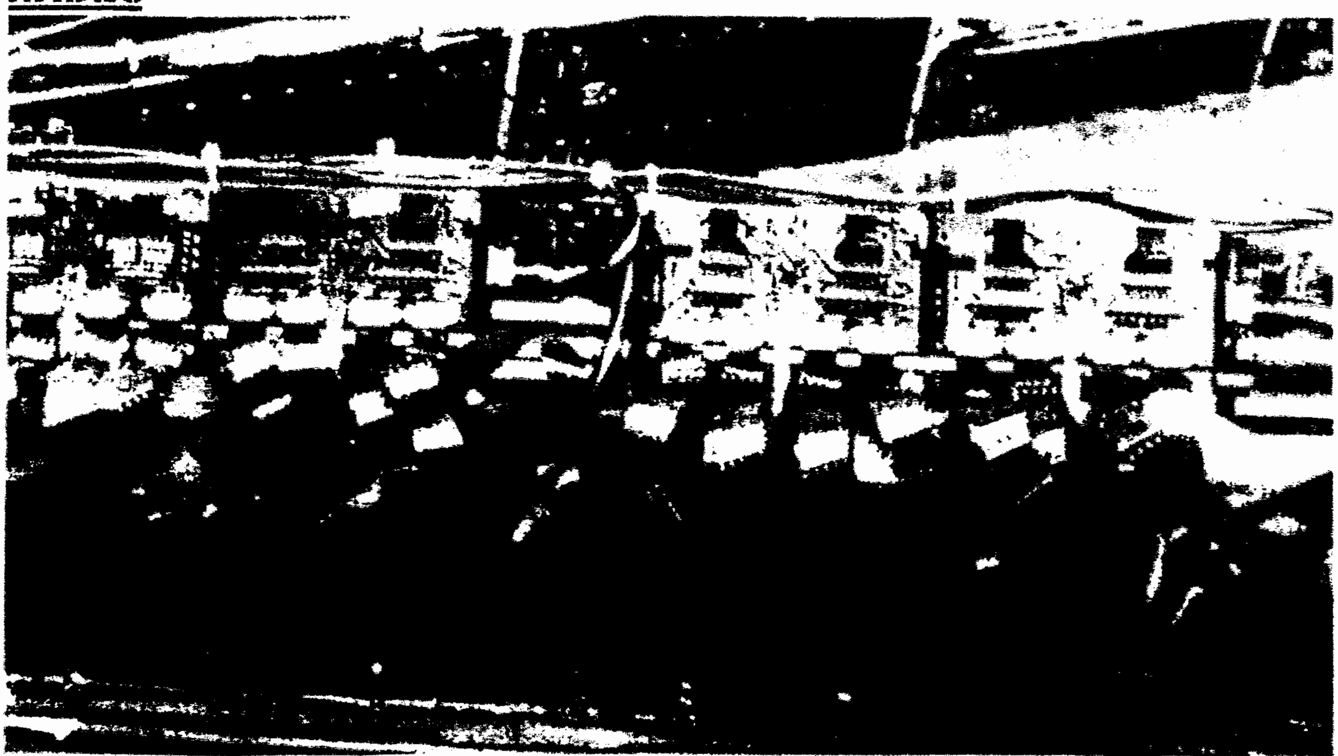

Size of MDC Frames

MDC I

MDC III

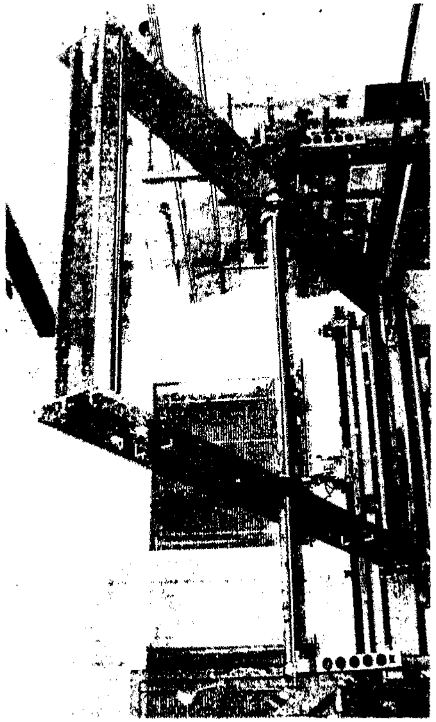

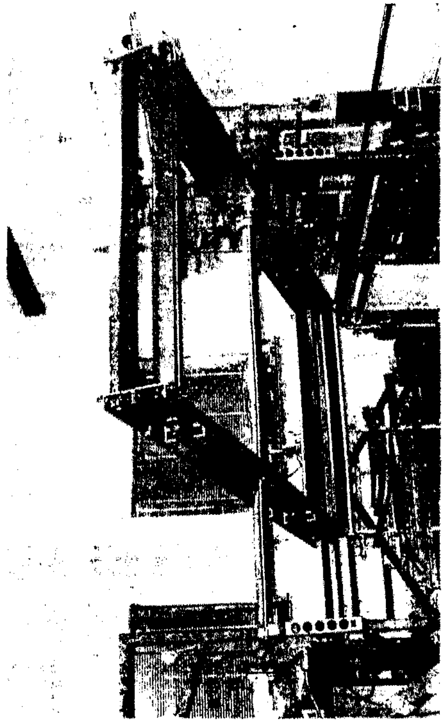

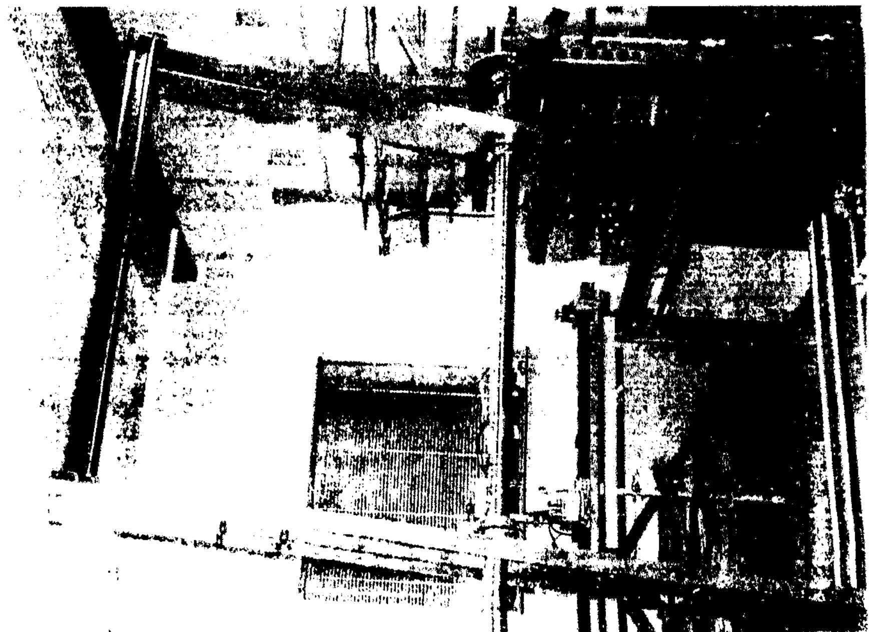

e^+e^- Identification Shower-Detector

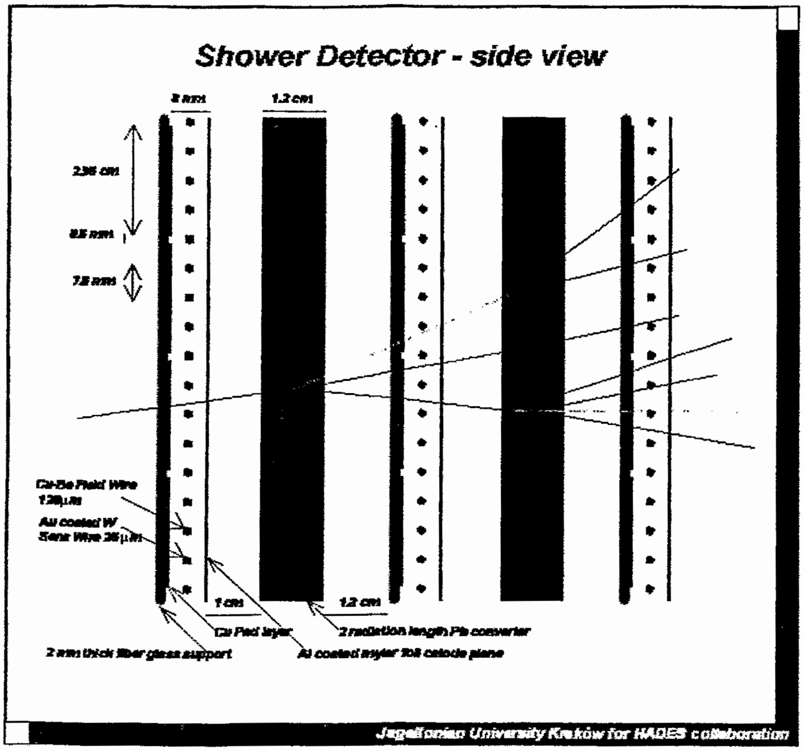

- **E.m. shower-Detektor**
  - 20 m²
- **Wire chambers**
  - *self quenching streamer mode*
  - Signal not $\propto \Delta E$
- **Pad readout**
  - Pad multiplicity before and after lead converter
  - e^+,e^- identification

Pre-Shower Detector

evt # 1349

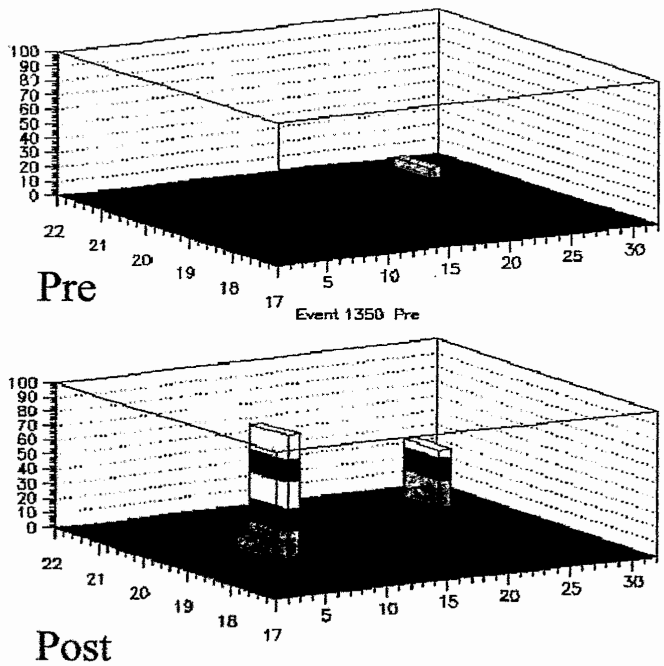

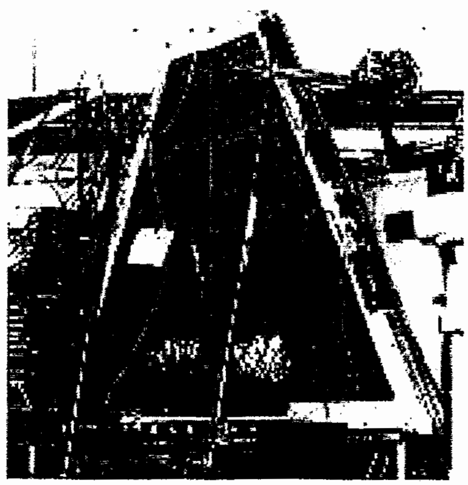

Electron Identification in RICH & TOF for U + Pb 1AGeV

TOF particle velocity distribution

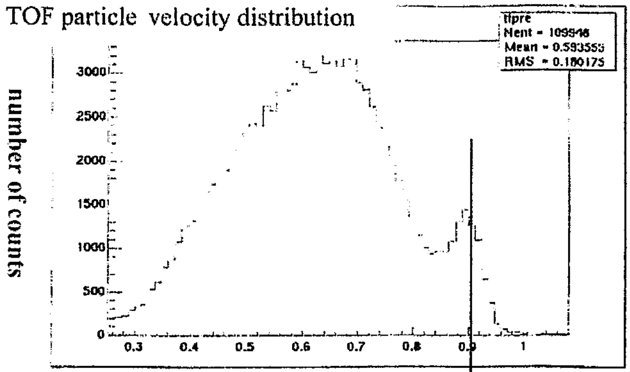

TOF particle velocity distribution for events with correlated ring

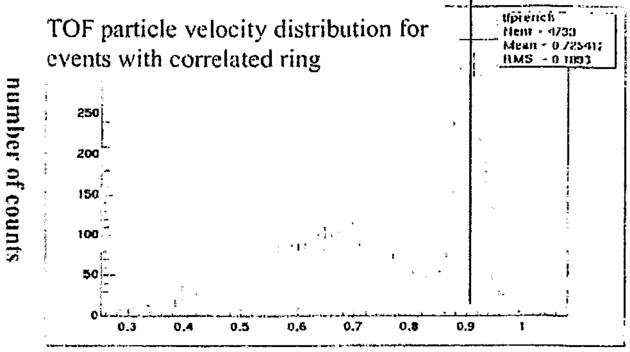

TOF & RICH track polar and azimuthal correlation

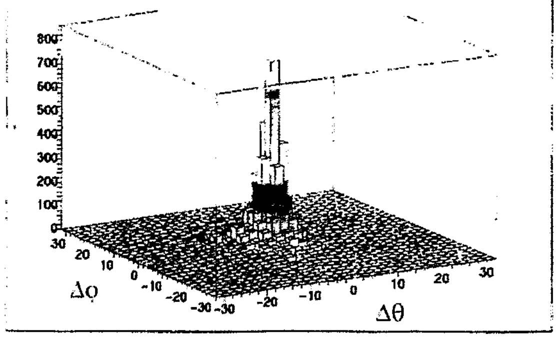

- Straight line trajectory and target emission assumed
- polar and azimuthal angular matching window $\Delta\theta \,.\, \Delta\phi \approx 8^{\circ}$

Beamtime Dec. 1998: TOF

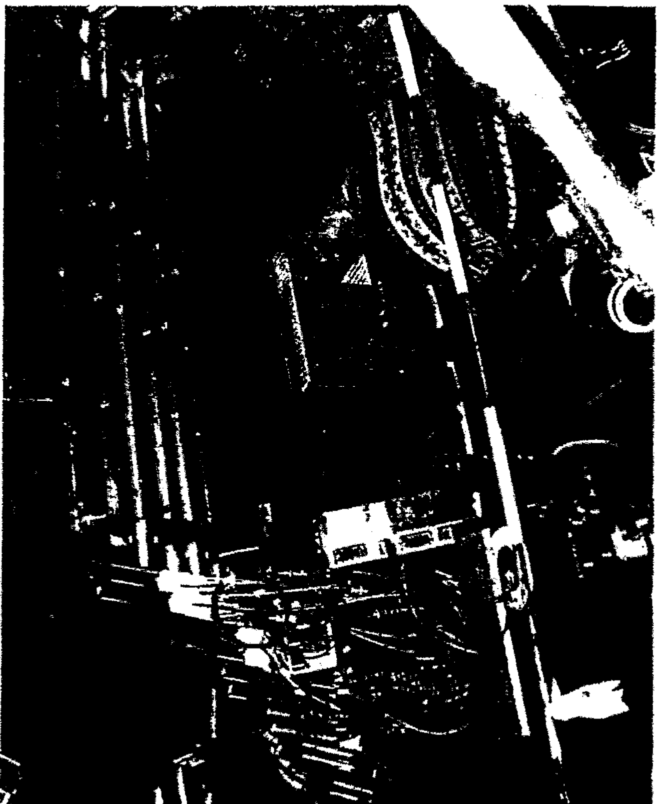

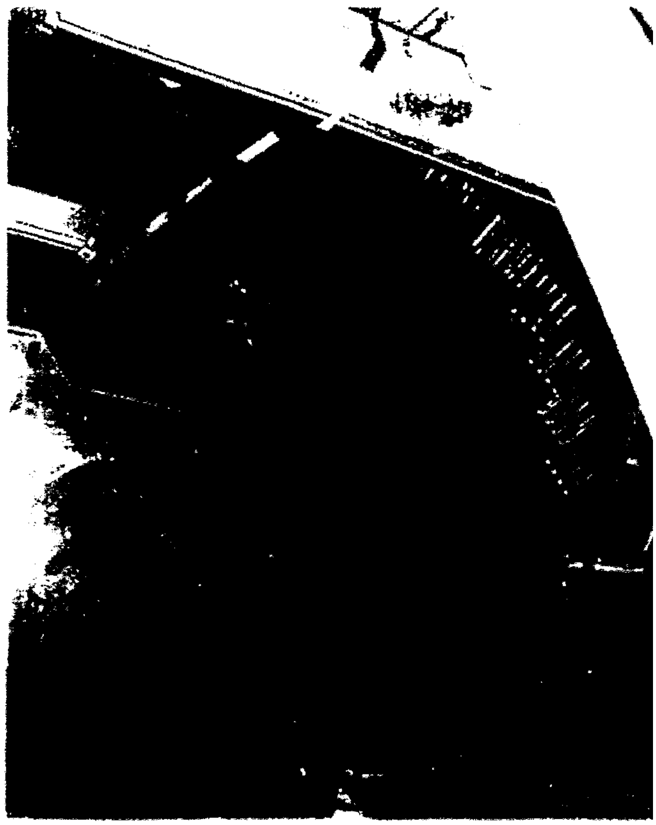

Magnet

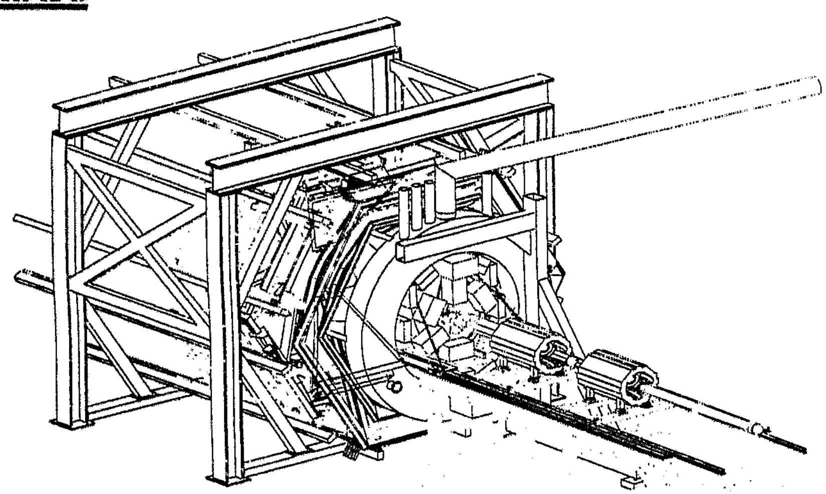

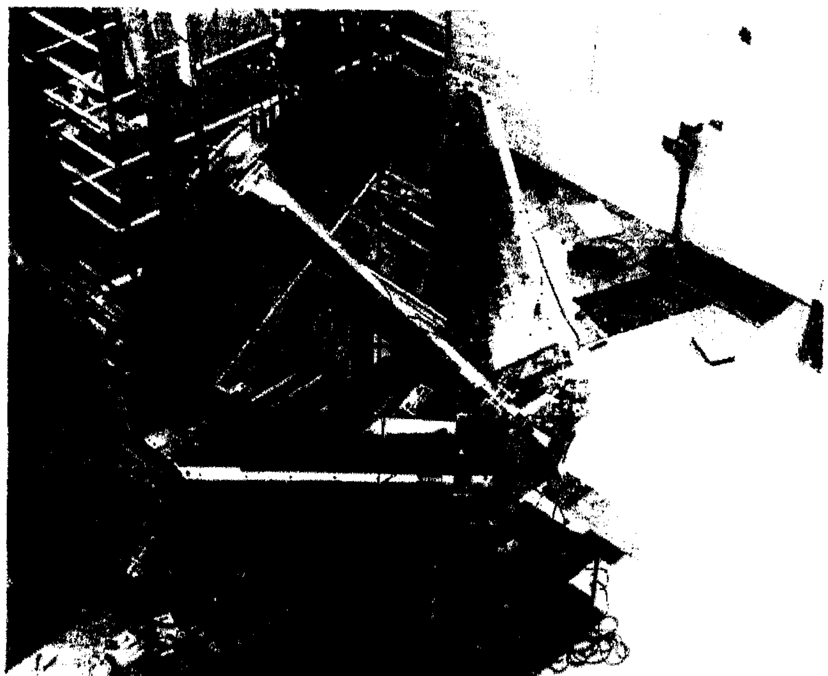

F.Dohrmann, FZ Rossendorf

Scheme Hades Simulation

HADES simulation software (Nov. 98)

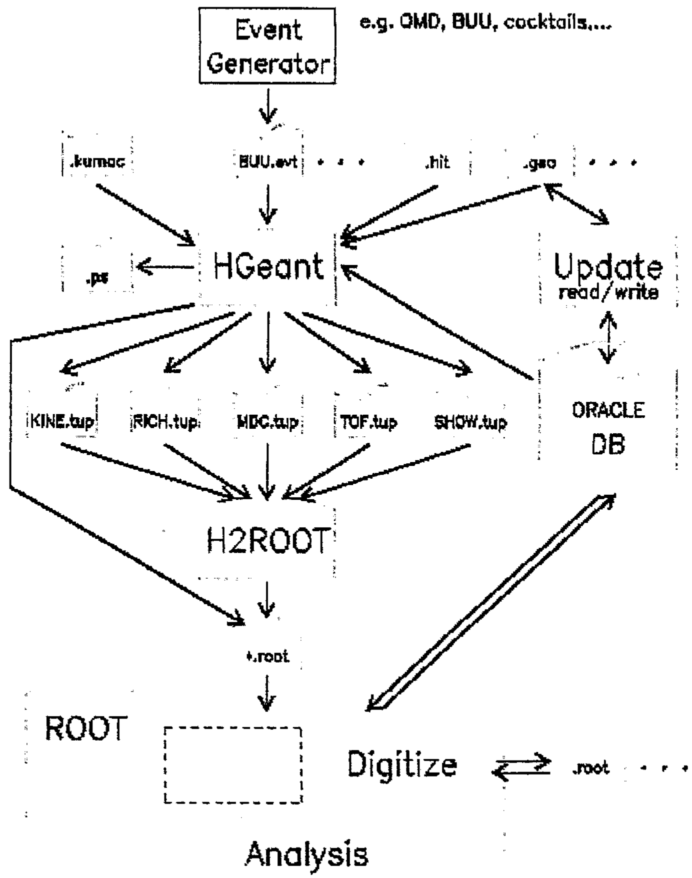

Experiments with HADES

Sim.: Au + Au , E = 1 AGeV

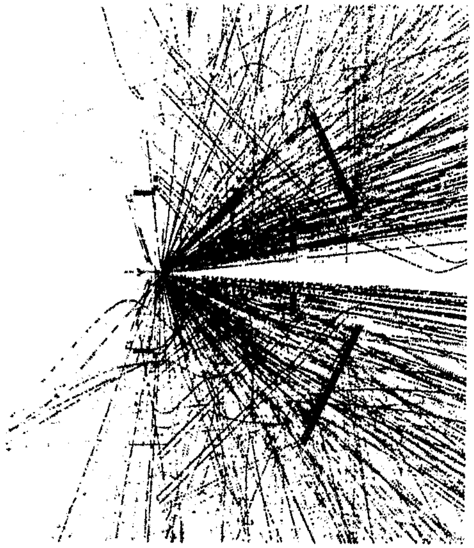

- **2-3** ρ_0
- **High Multiplicity**
  200 charged hadrons &
  20 photons (π^0-decays)
  ↳ high granularity
  ↳ very good track reconstruction
- **Suspression of hadr. & EM backgr.**
  "hadron-blind" trigger
  ↳ "fast" **RICH**
  ↳ Z < 10 material

$\pi^- + p \rightarrow \omega + n$

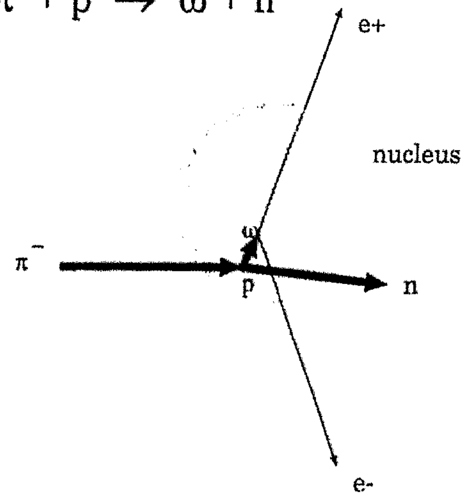

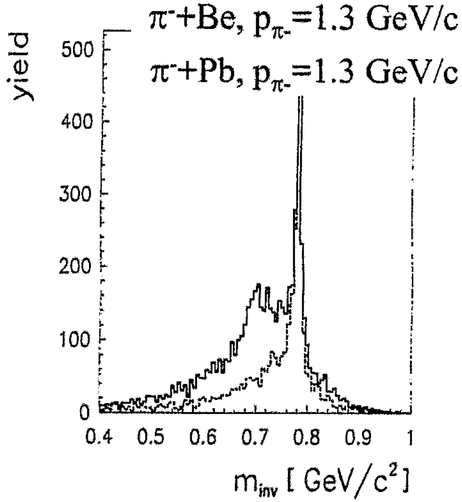

- ~1 ρ_0 -> normal nucl. density
- large WQ

•simulation: W. Schön et al., Act. Phys.Pol. B27(1996) 2959)

Beam in HADES Cave

First Au-beam in Hades Cave

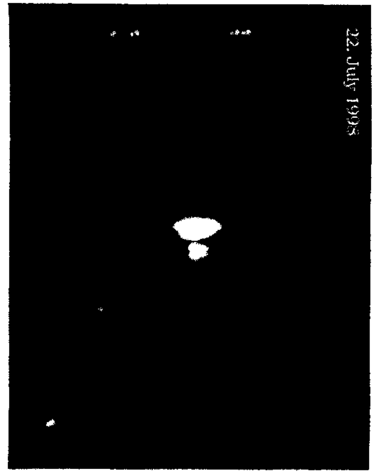

Secondary π-beam

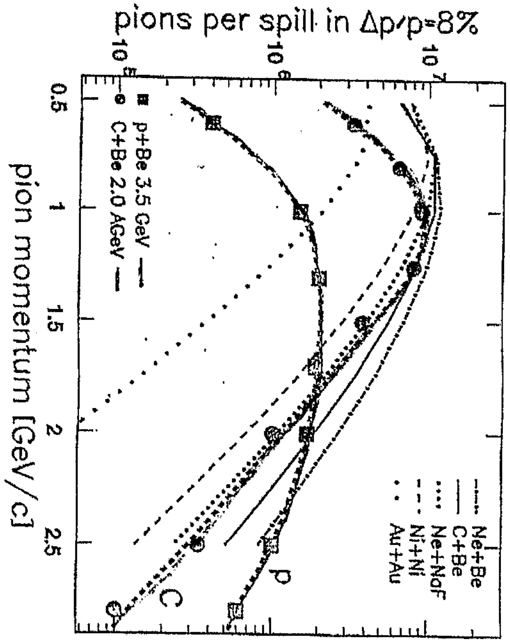

Data: π^--beam September 1998

Institut für Kern- und Hadronenphysik

F. Dohrmann, FZ Rossendorf

FZR

Summary and Outlook

- High resolution dilepton spectroscopy in 0.1- 2 AGeV range is of fundamental interest
- New data with high resolution is expected to test DLS data
- π,p, and A-beams available at GSI
- Experiments at $1\rho_0$ as well as $2\text{-}3\rho_0$ possible

- HADES starts in 1999 with pp collisions
  - elastic scattering
  - dielectrons
    - **100 MeV/c² < M_{ee} < 500 MeV/c²**
    - **η-Dalitz and Δ-Dalitz**
- Full acceptance and high resolution will be reached 1999/2000
- in 2000: invariant masses up to 1AGeV, C+C, Ca+Ca, Au+Au

The HADES Collaboration

- **Bratislava (SAS, PI)**
- **Catania (INFN/LNS)**
- **Clermont-Ferrand (Univ.)**
- **Cracow (Univ.)**
- **Darmstadt (GSI)**
- **Dubna (LHE/JINR)**
- **Frankfurt (Univ.)**
- **Giessen (Univ.)**
- **Milano (INFN, Univ.)**
- **Moscow (ITEP,MEPhI)**
- **Munich (Tech. Univ.)**
- **Nicosia (Univ.)**
- **Orsay IPN, (Univ.)**
- **Rez (CAS, NPI)**
- **Rossendorf (FZ)**
- **Santiago de Compostela (Univ.)**
- **Valencia (Univ.)**

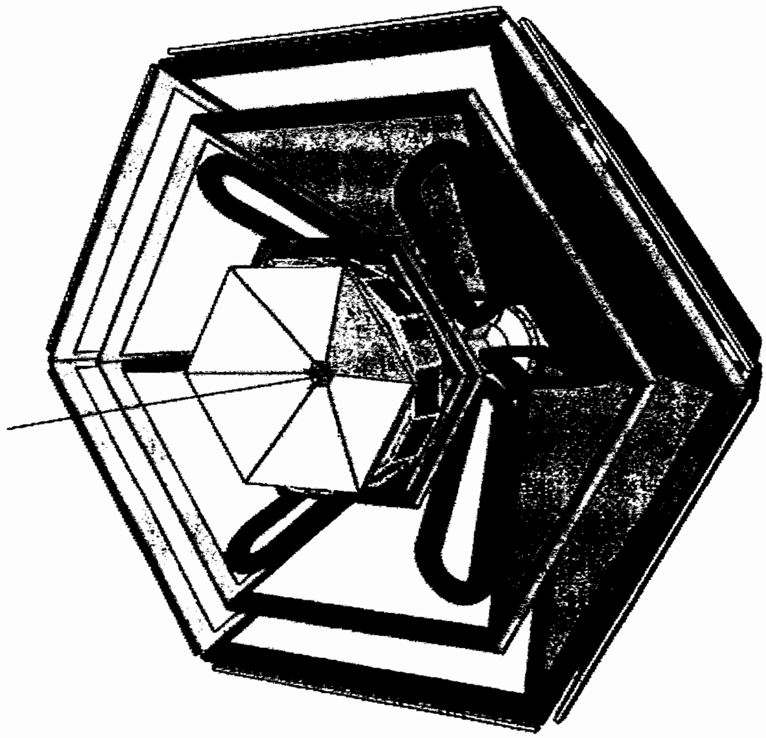

P. Tlusty:

Status of the HADES–ToF

TOF DETECTOR FOR HADES

P. Tlustý

Nuclear Physics Institute of the Academy of Sciences of Czech Republic,
Řež, Czech Republic

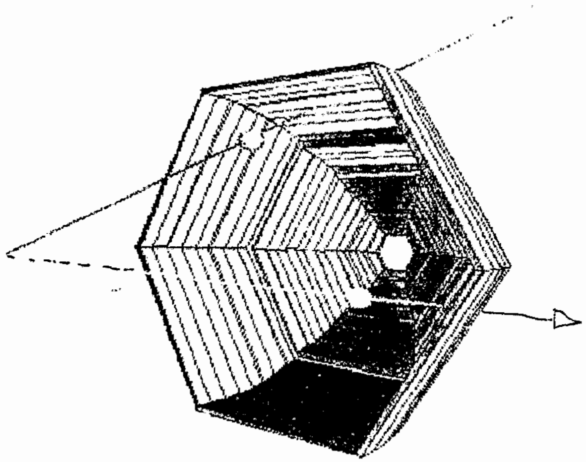

Institute of Physics of the Slovak Academy of Sciences, Bratislava
INFN-LNS of the National Institute of Nuclear Physics,Catania
Gesselschaft für Schwerionenforschung, Darmstadt
INFN-University Milano, Milano
Institute of Theoretical and Experimental Physics, Moscow
Nuclear Physics Institute of the Academy of Sciences of Czech Republic,
Řež

Specification of the TOF detector:

Purpose:

- **trigger:**
  - **multiplicity of charged particles to select central collisions**
  - **velocity of particles to select di-lepton candidates**
- **analysis:**
  - **velocity for electron identification**
  - **position for tracking**
  - **multiplicity for impact parameter determination**
  - **other ?**

HADES: the Time Of Flight wall

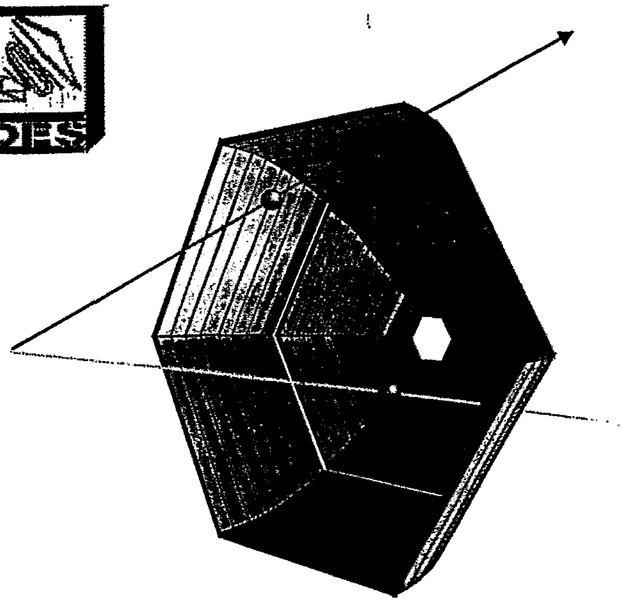

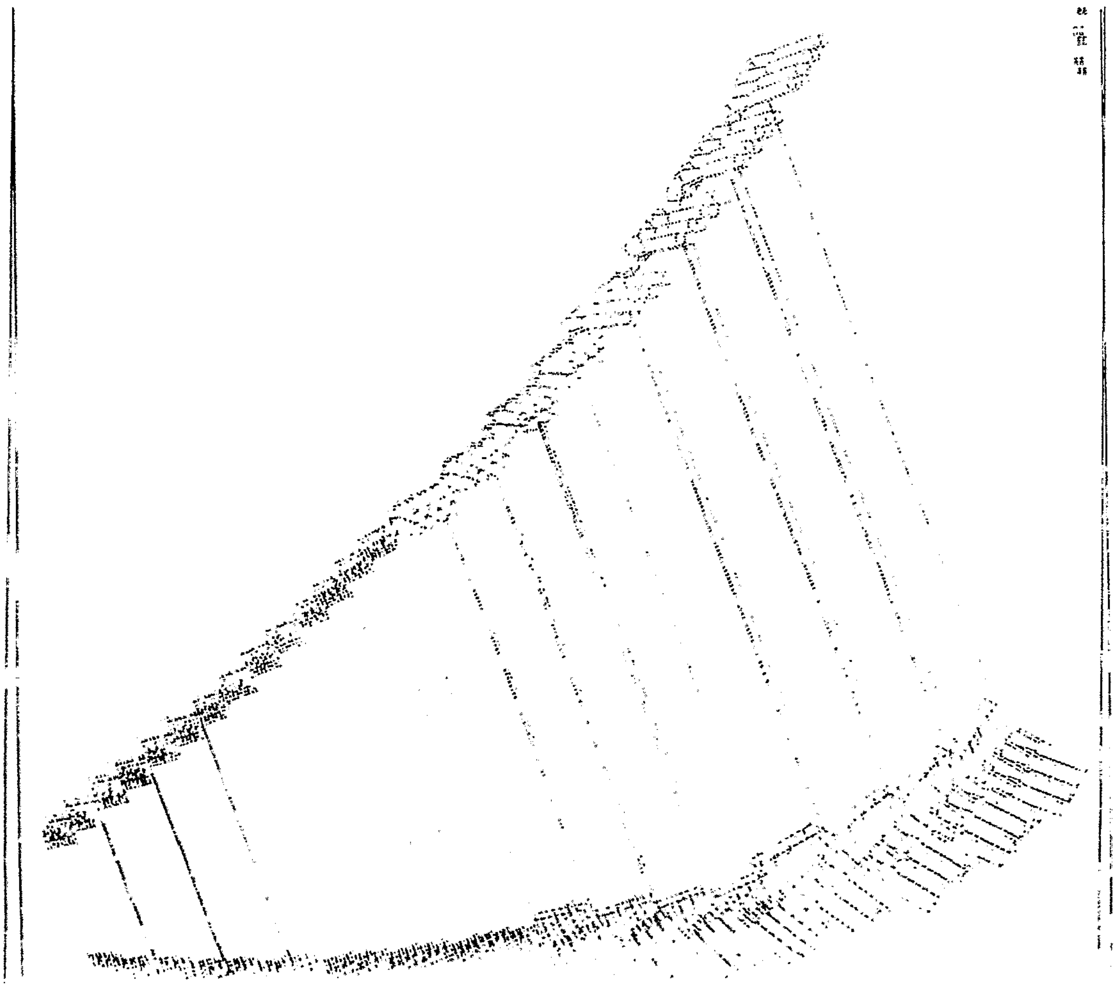

HADES

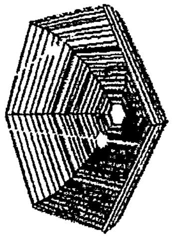

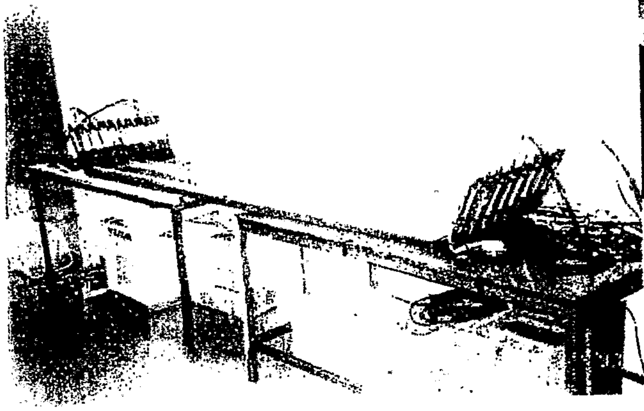

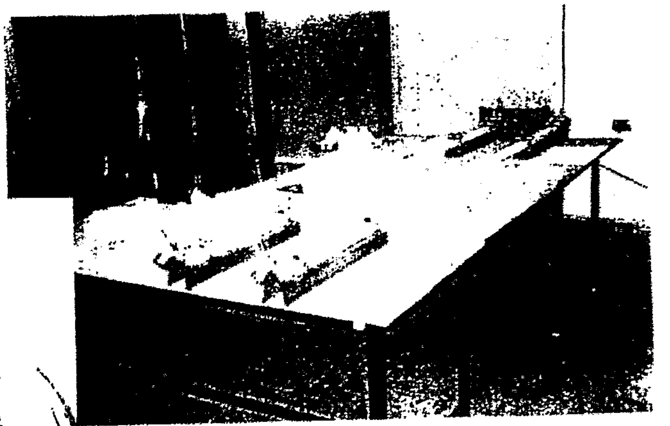

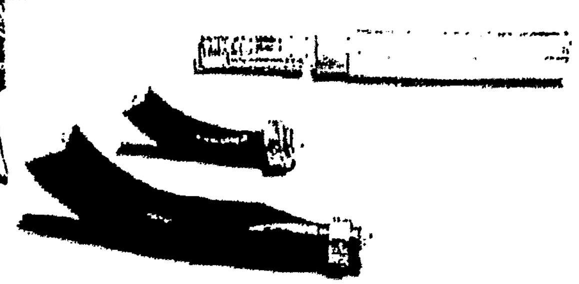

HADES

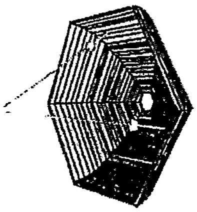

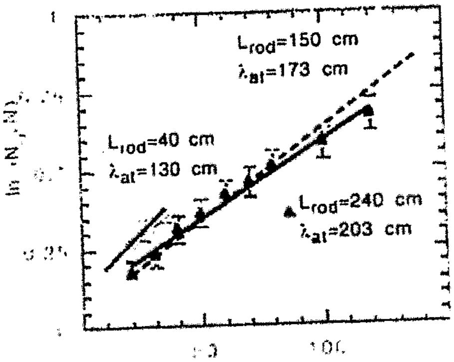
L_rod=150 cm
λ_at=173 cm
L_rod=40 cm
λ_at=130 cm
L_rod=240 cm
λ_at=203 cm

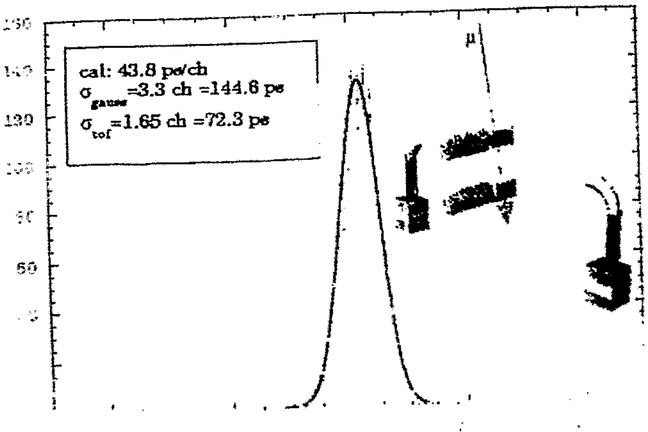
cal: 43.8 ps/ch
σ_gauss=3.3 ch =144.6 ps
σ_tof=1.65 ch =72.3 ps
μ

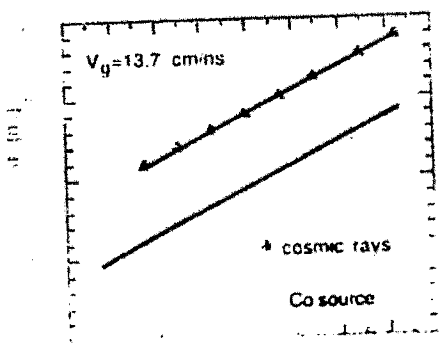
V_g=13.7 cm/ns
cosmic rays
Co source

Time-of-Flight 2

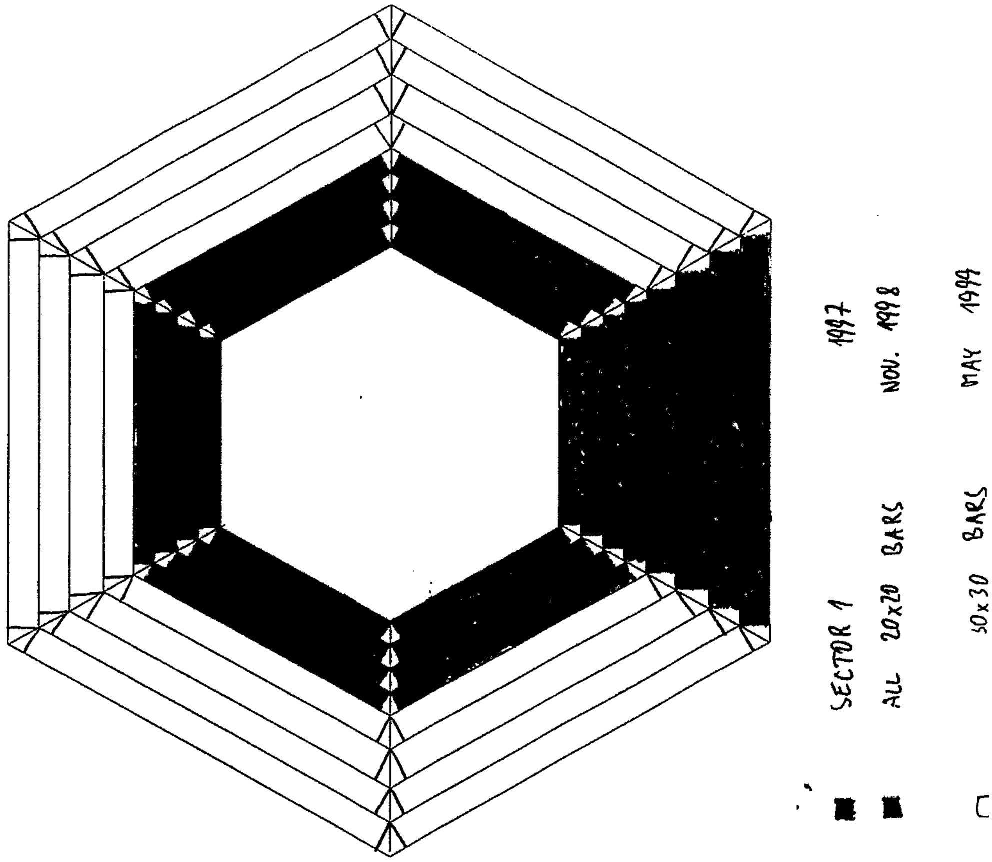

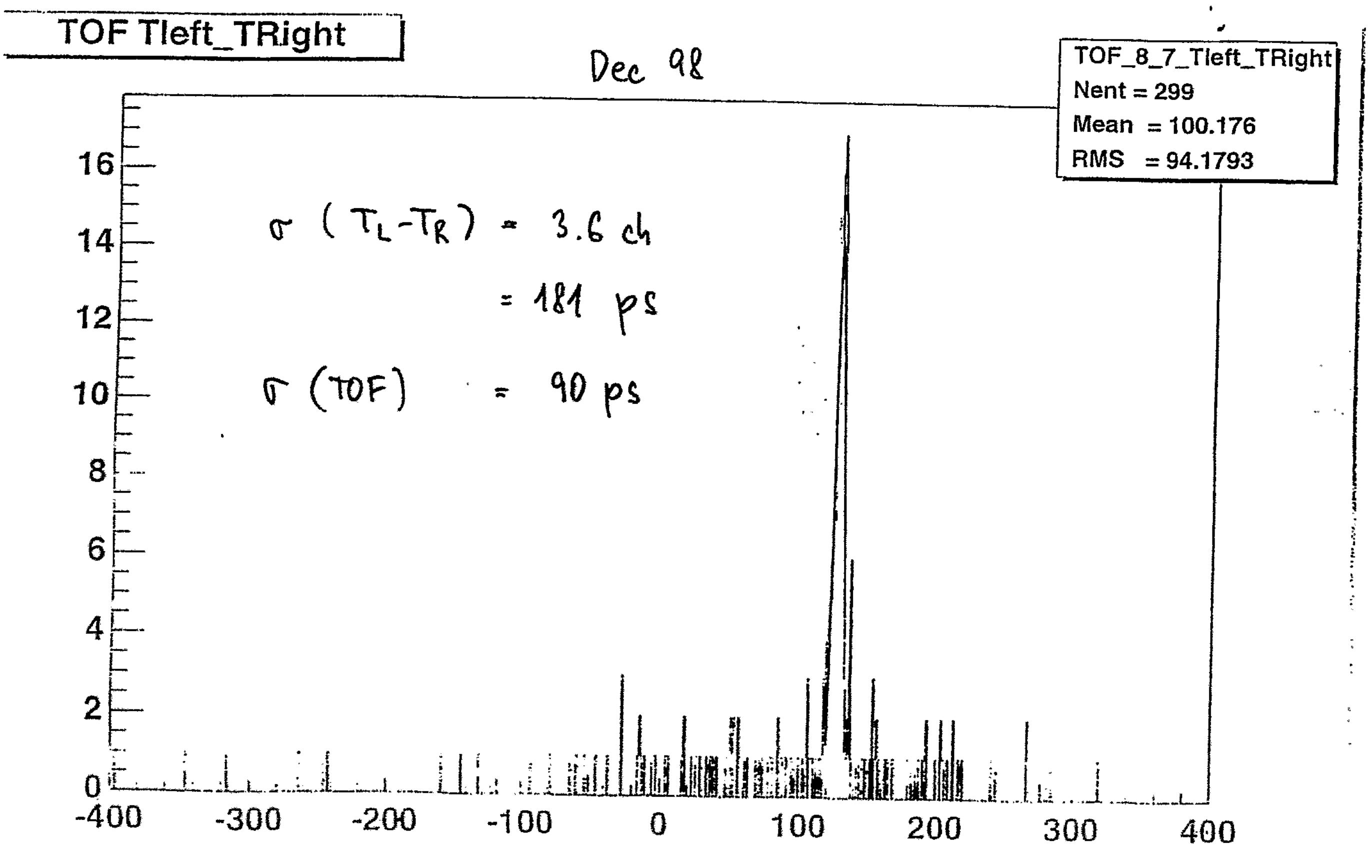

Time-of-Flight 2

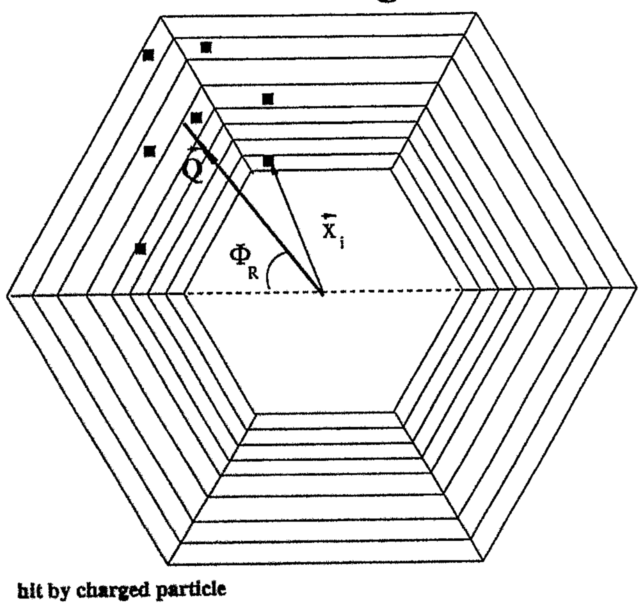

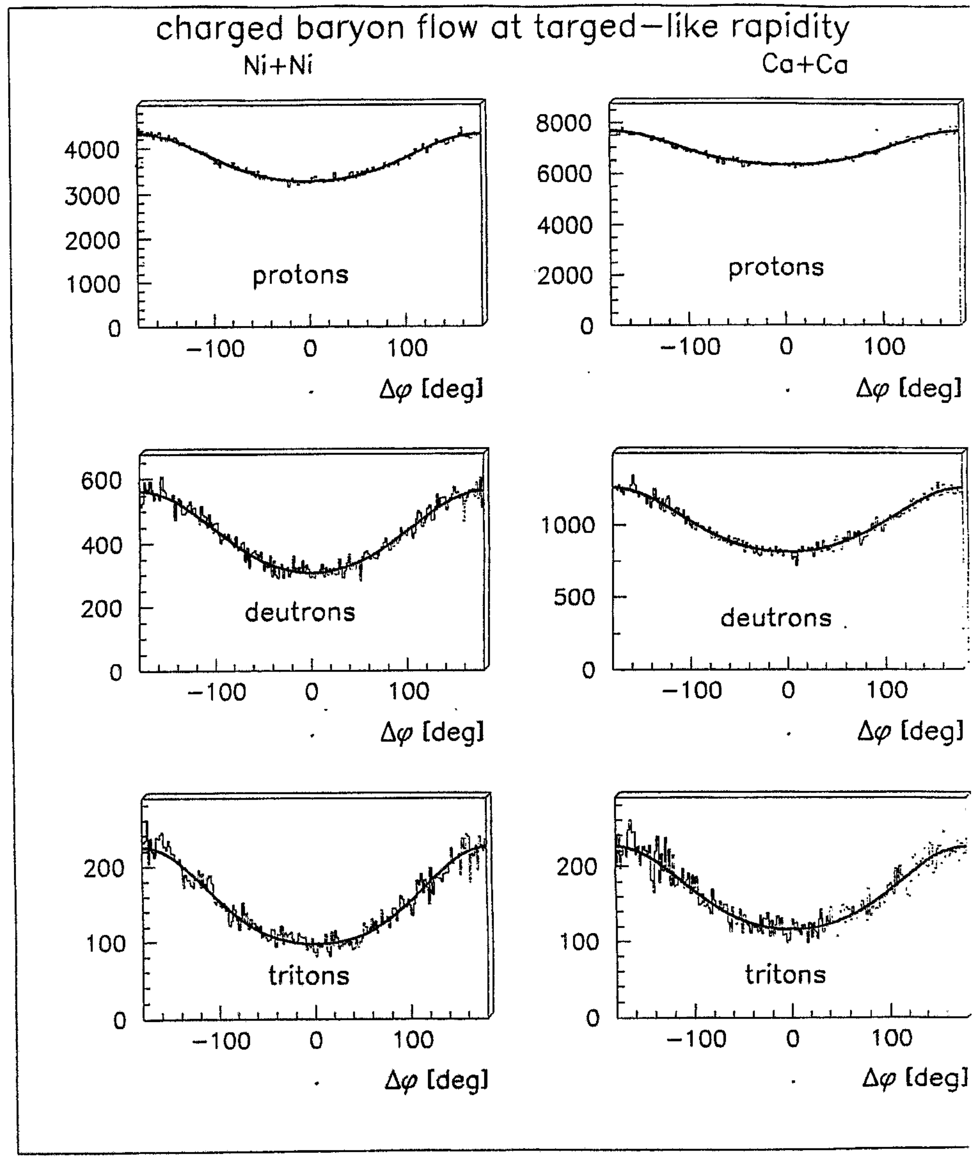

Reaction plane:

$\vec{Q} = \Sigma_{i=1}^{N} \omega_i \vec{p}_t^i$

error of reaction plane determination in semi-central region:

$\sigma = 33^o$ Au+Au 0.8 A GeV

$\sigma = 46^o$ Ni+Ni 2 A GeV

$\sigma = 52^o$ Ca+Ca 2 A GeV

dilepton angular distribution according to the reaction plane $N(\varphi)$,

$\varphi = \phi_{e^+e^-} - \phi_R$

$N(\varphi) = \frac{N_0}{2\pi}\,(\,1 + 2v_1 cos(\varphi) + 2v_2 cos(2\varphi)\,)$

Simulation of anisotropic emission of η and π^0 from Ca+Ca 2 A GeV:

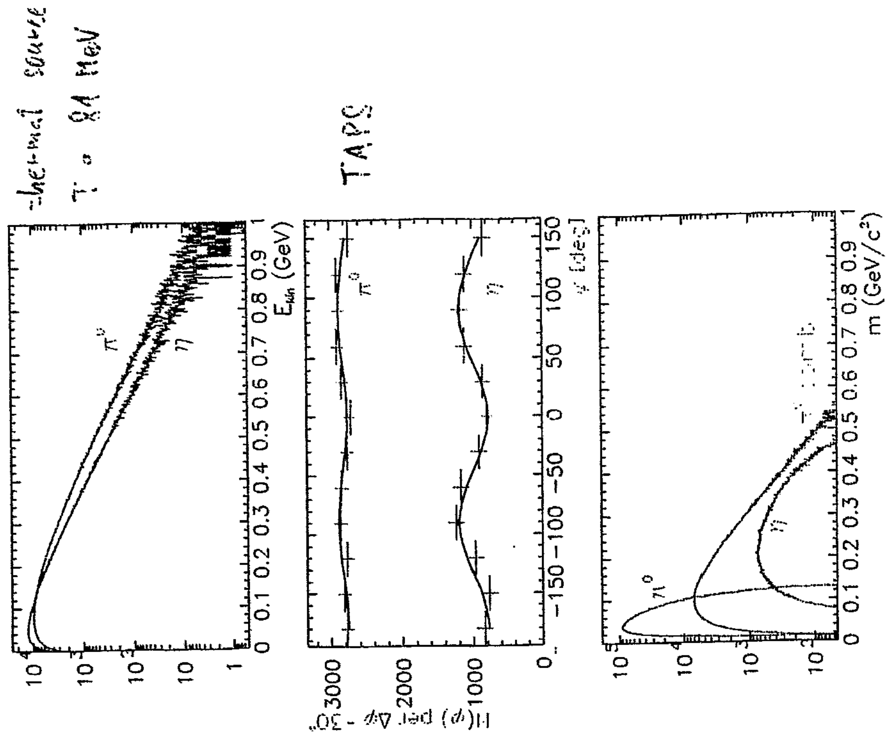

GEANT simulation:

Au + Au 1 AGeV

10^8 ions/s,

5s extraction time,

segmented target (1%)

5000 ρ's, 1000 ω's and 100 φ's per day

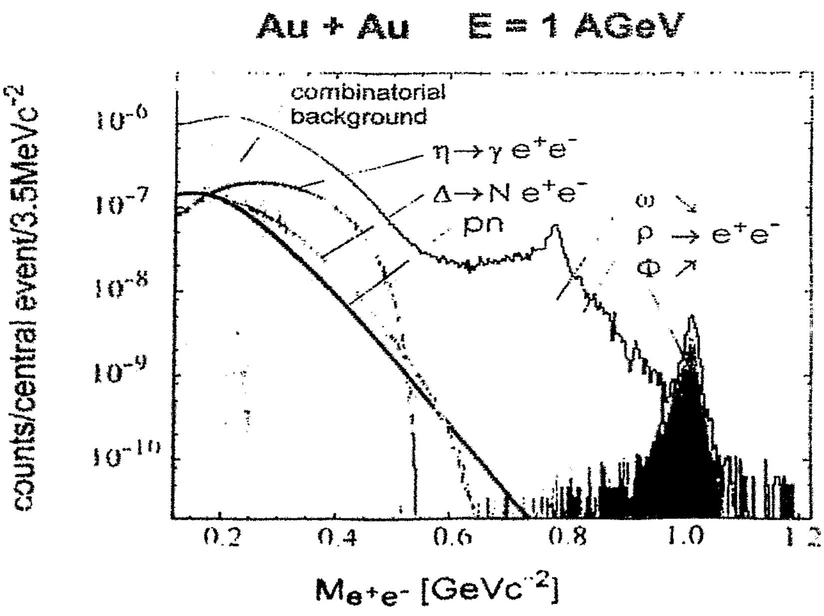

Azimuthal anisotropy of dileptons from η Dalitz decay:

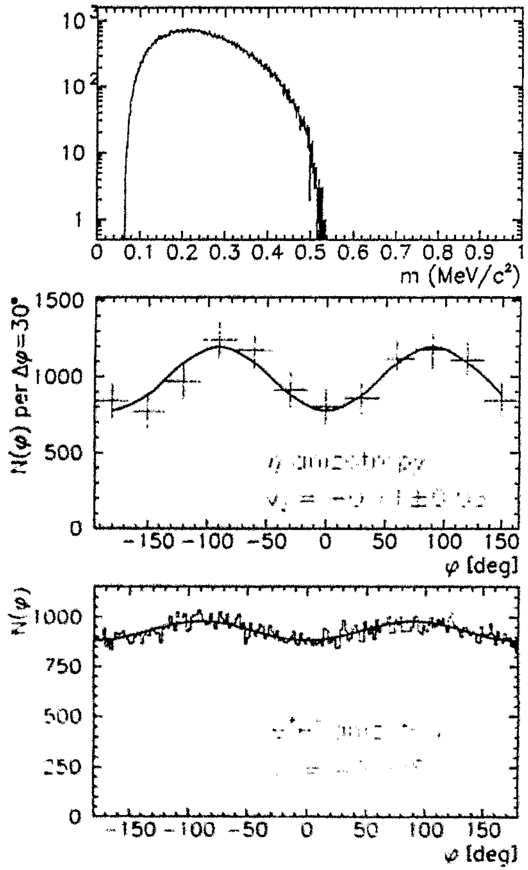

Azimuthal anisotropy of combinatorial background from π Dalitz decay:

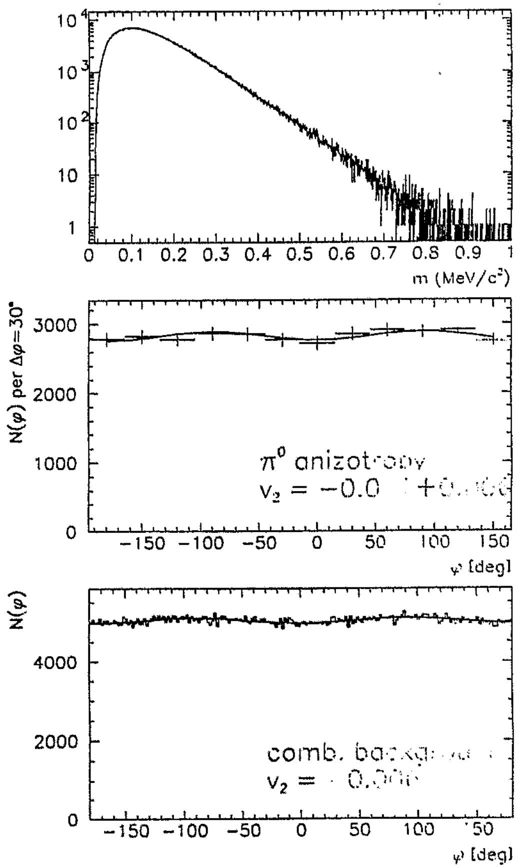

Simulation of azimuthal dependence of ω production:

- semi-central $^{197}Au + ^{197}Au$ collisions at 2 AGeV

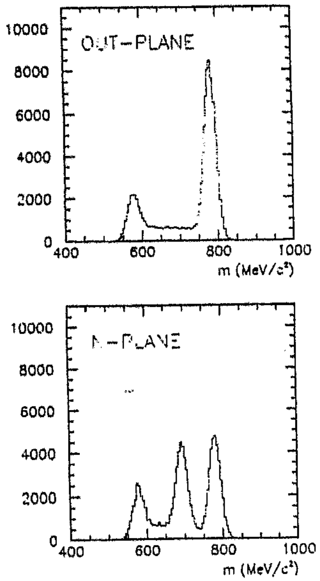

- thermal source of ω meson with T = 81 MeV in centre of compressed zone with radius 3.3 fm and baryon density of $2\rho_0$

- mass shifts given by Brown-Rho scaling

- expected resolution of HADES included

R. Holzmann:

Fist experiments with HADES: e^+e^- production in pp and AA collisions

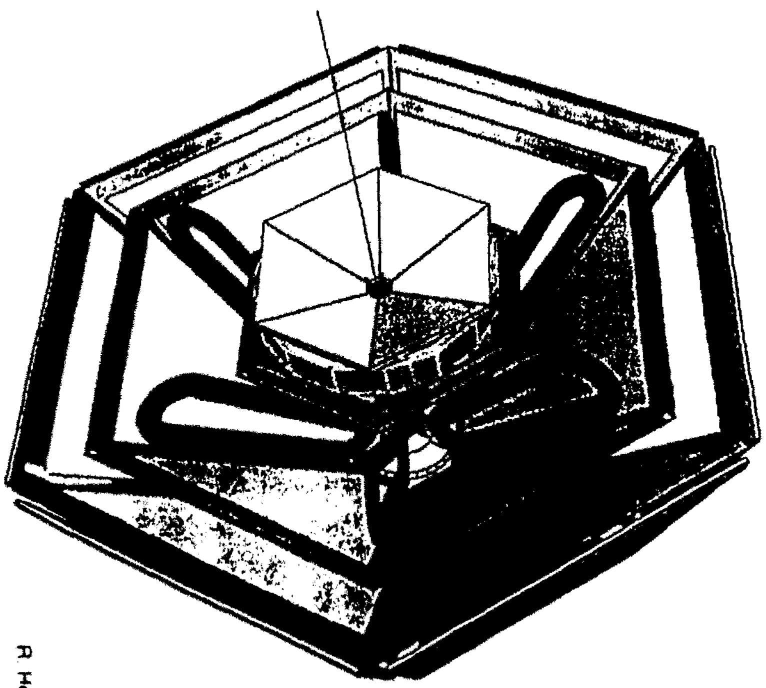

Artist view

R. Holzmann, GSI Darmstadt

HADES

First Physics with HADES:

e^+e^- Production in p+p, p+A and A+A

Romain Holzmann, GSI Darmstadt

- **Status of HADES in 1999/2000**
  1. 2 sectors only: reduced acceptance !
  2. 3 MDC planes only: reduced resolution !
  3. TOF not fully equipped: reduced multi-hit capability !
  4. 2^{nd} and 3^{rd} level triggers not yet optimized: reduced online selectivity !

- **Experimental program in 1999/2000:**
  1. commissioning of the setup: p+p elastics, various A+A
  2. disentangle e^+e^- cocktail: p+p and p+A
  3. check on DLS results: do light A+A systems
  4. see first signals of ω and ϕ in p+A and A+A

Acceptance for 2 sectors

HADES

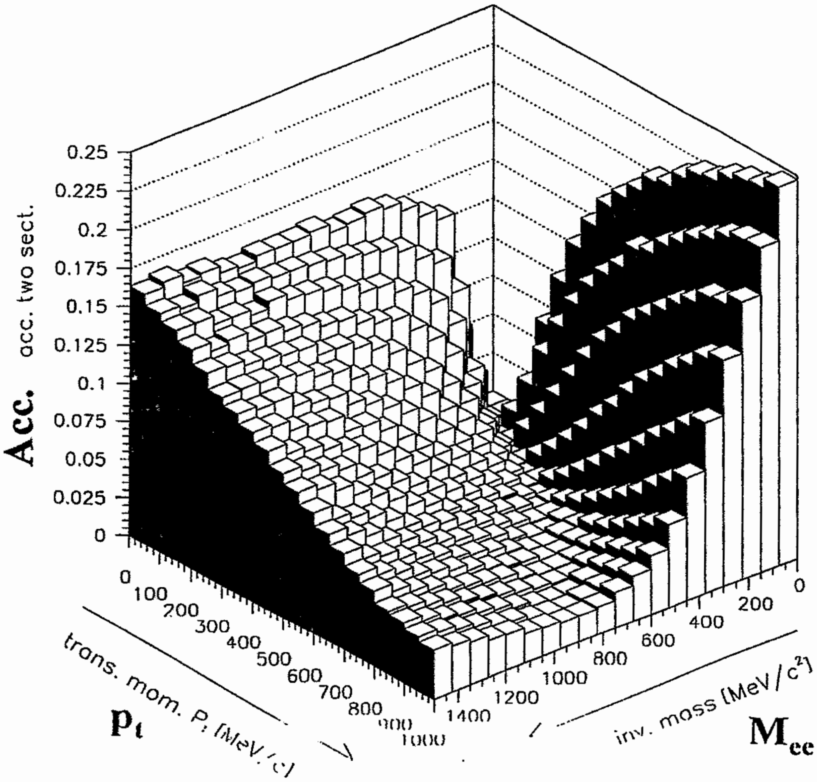

- **Results :**

✓ Acc. > 10%

✓ no holes for:
$M_{inv} > 0.2$ GeV/c²
$p_t > 0.2$ GeV/c

>10 fold improvement over DLS !!!

R.Holzmann, GSI Darmstadt

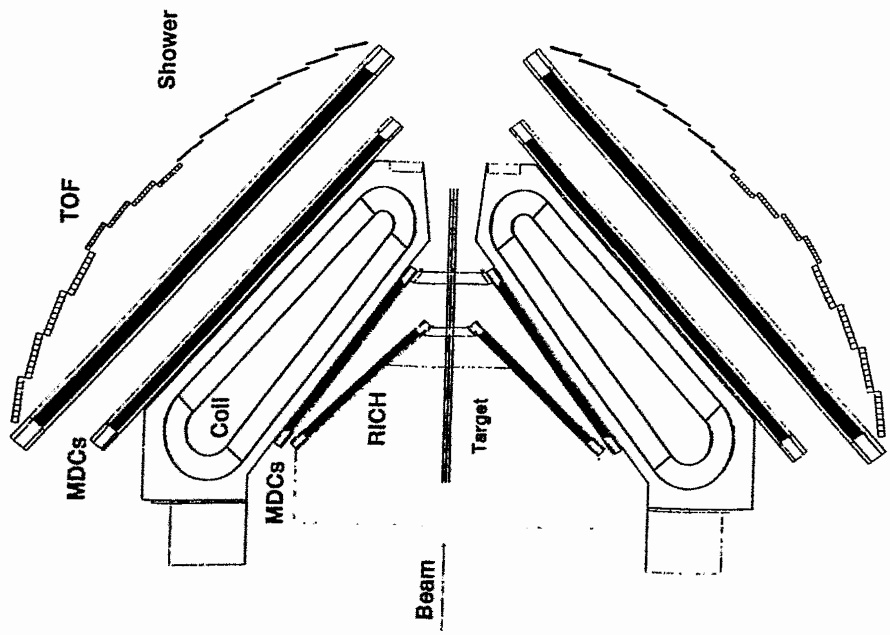

Generic acceptance

Schicker et al.,
NIM A380
(1996) 586

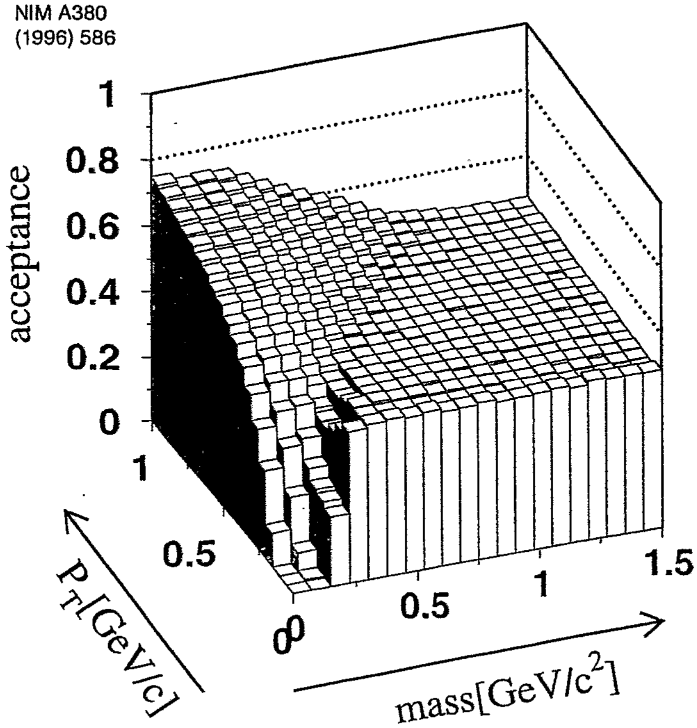

- **Results :**
  - cutoff : p_{e+} > 0.1 GeV/c
  - flat : M_{inv} > 0.6 GeV/c^2

- **Requirements**
  - identification & momentum measurement

0.1 Gev/c < p_{e+} < 1.5 GeV/c

R.Holzmann, GSI Darmstadt

Simulated Momentum Resolution for 2,3,4 MDC planes

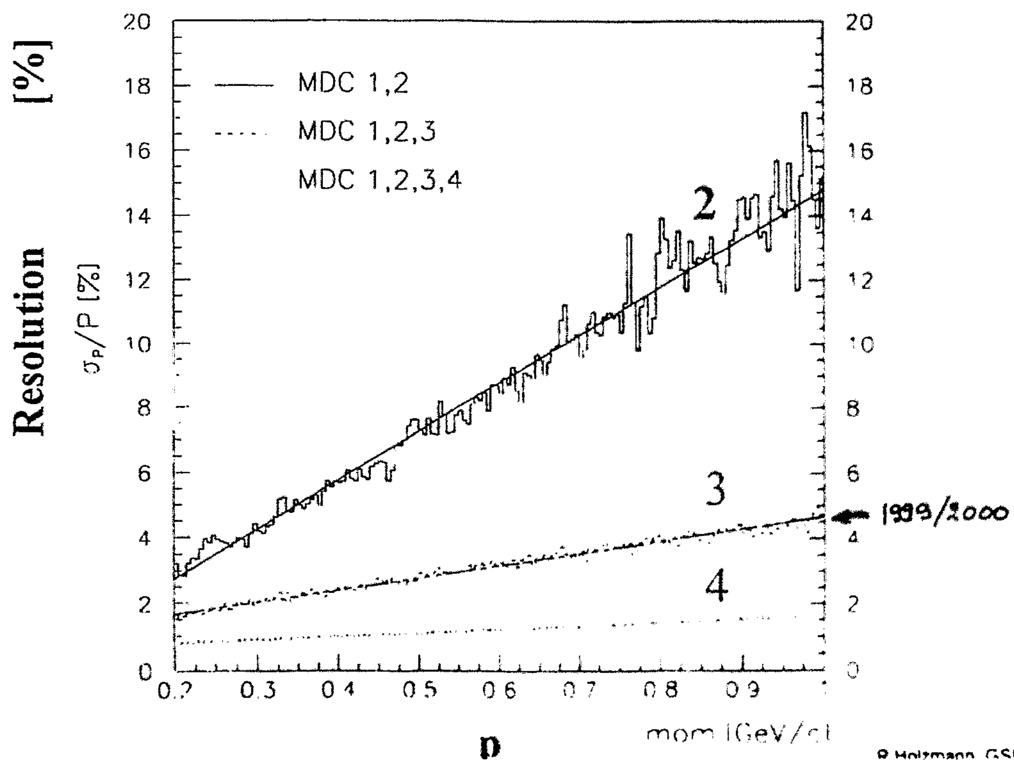

R.Holzmann, GSI Darmstadt

DLS @ Bevalac :

$\frac{\Delta m}{m} = 10\%\ \sigma$

$\varepsilon = 0.5\%$

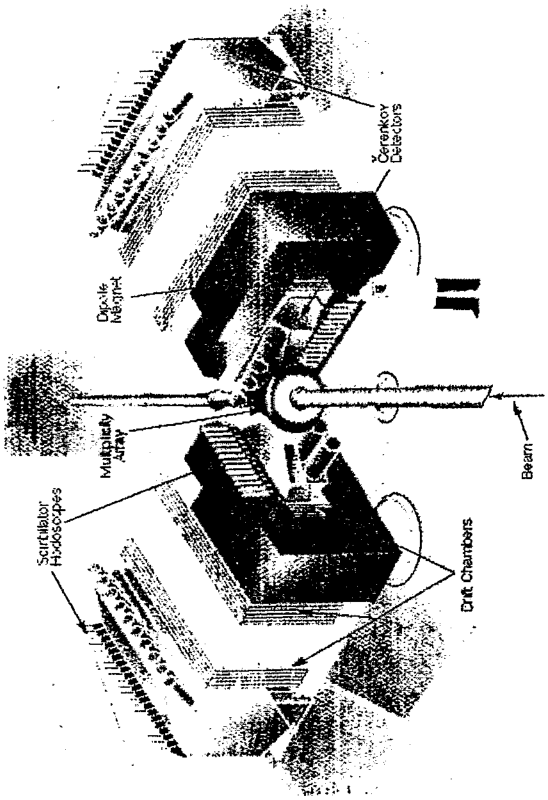

DiLepton Spectrometer

1986-88 :	p-Be	4.9, 2.1, 1.0 GeV
1988-89 :	Ca-Ca	2.1, 1.0 A·GeV
	Nb-Nb	1.0 A·GeV
1990-92 :	p-p, p-d	4.9, 2.1, 1.9, 1.5, 1.25, 1.0 GeV
1992 :	Ca-Ca	1.0 A·GeV
1993 :	α-Ca, d-Ca, C-C	1.0 A·GeV

π / p - separation

HADES

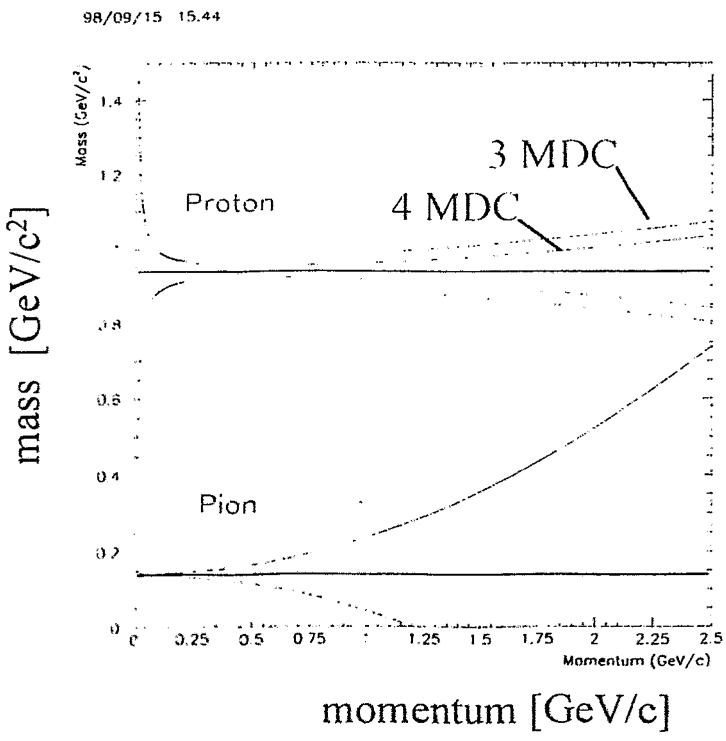

π / p - separation with TOF

Δt = 100 ps (σ)

for :

- Δp/p ~ 1 % (4 MDC planes)
- Δp/p ~ 3 % (3 MDC planes)

e^+e^- Yield from pp reactions

HADES

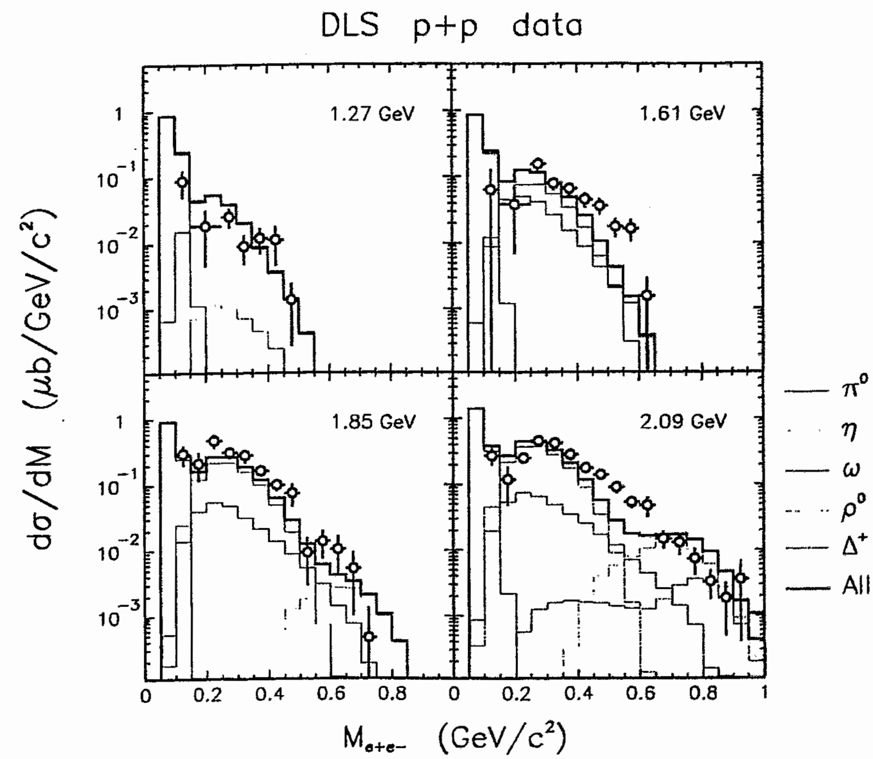

Data:
W.K. Wilson et al.,
PRC 57 (1998) 1865

Calculation:
R. Holzmann

R.Holzmann, GSI Darmstadt

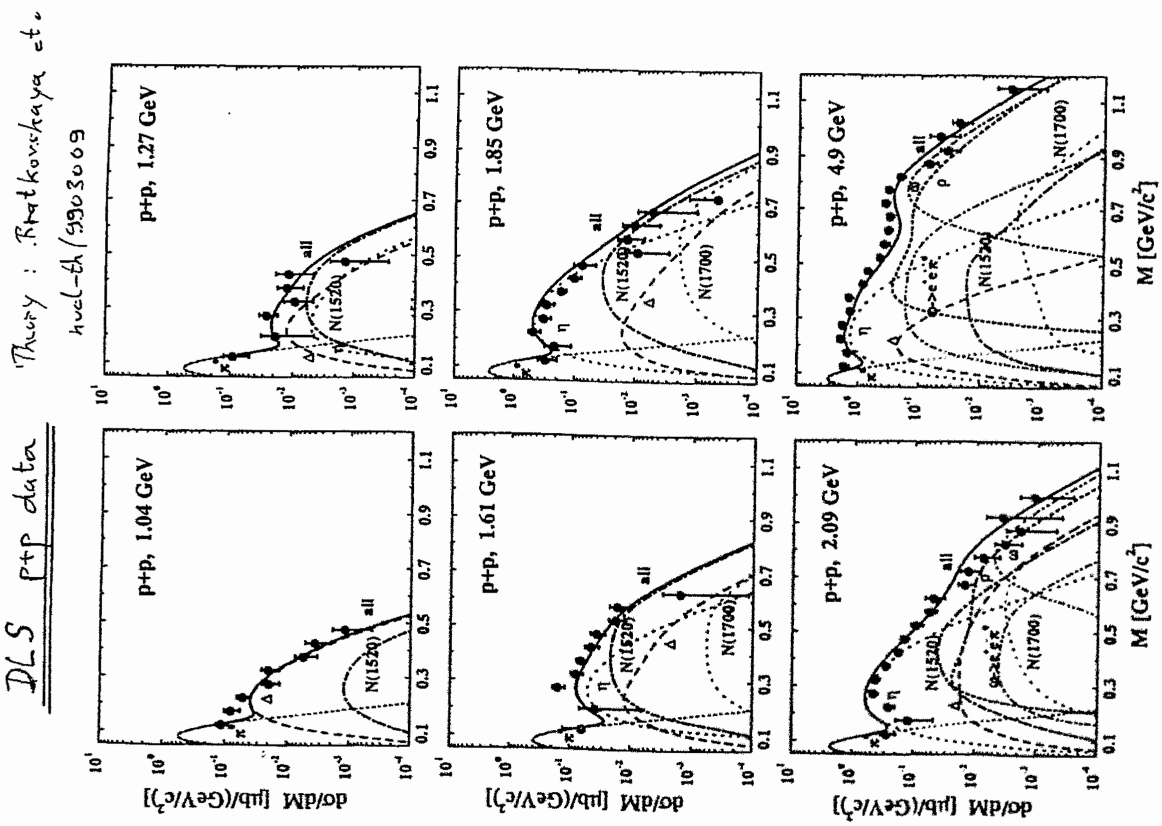

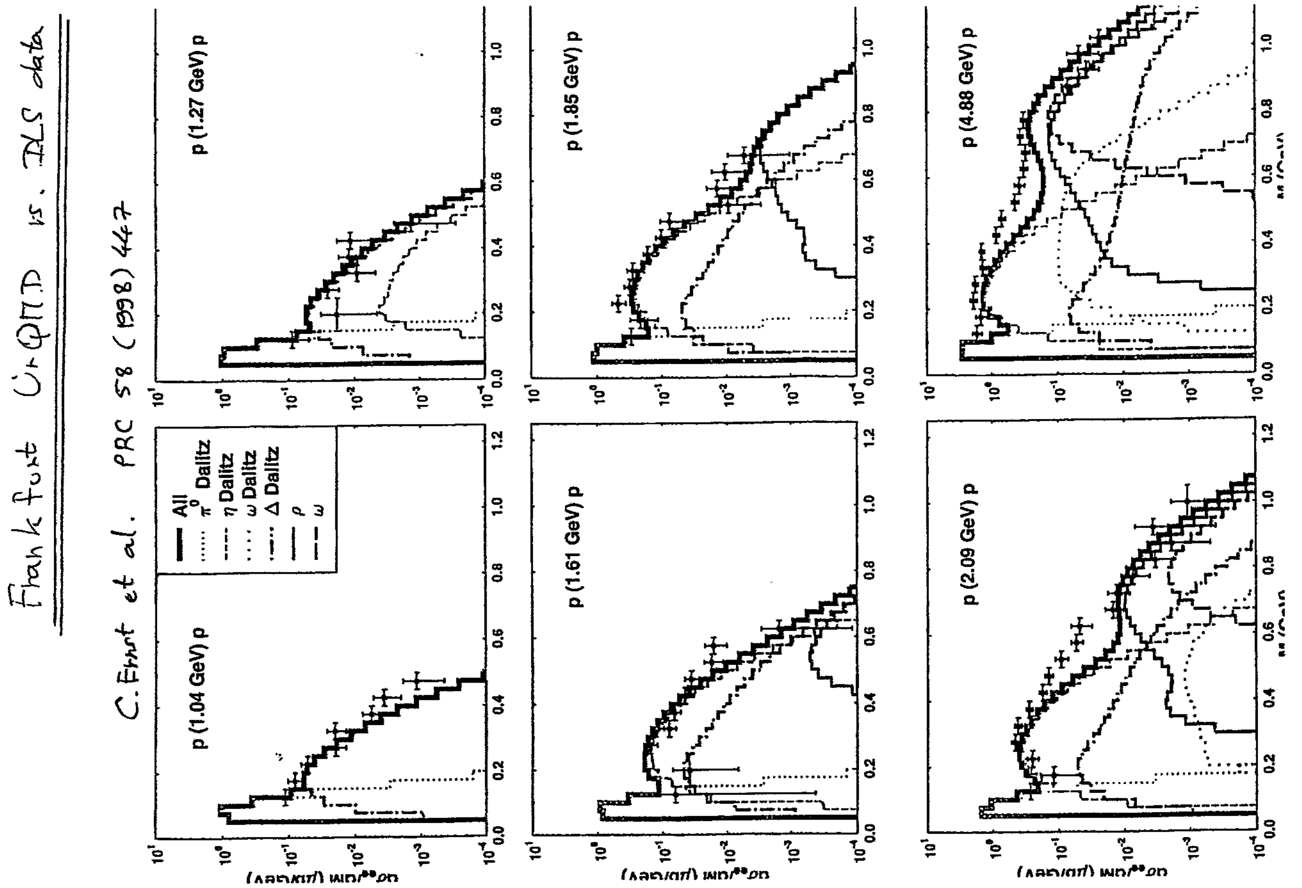

$pp \to pp\, m \hookrightarrow e^+e^-(X)$

M_{miss} M_{inv}

$\varepsilon(pp e^+e^-) \approx 5-15\,\%$ für 6 sectors

Exclusive η-Production in pp Reactions

HADES

6 sectors, full resolution:

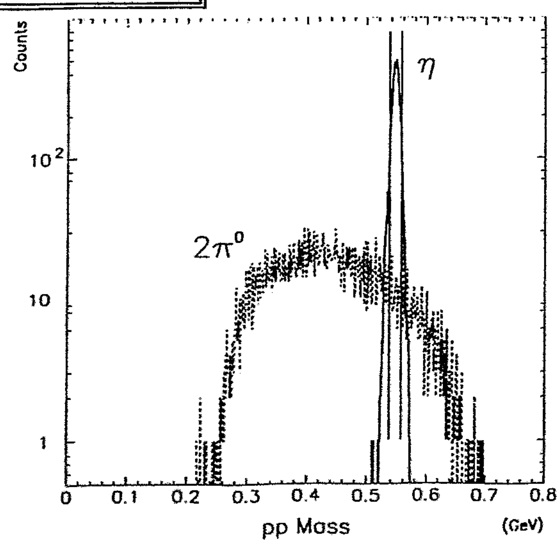

Missing-mass distribution from pp momentum analysis

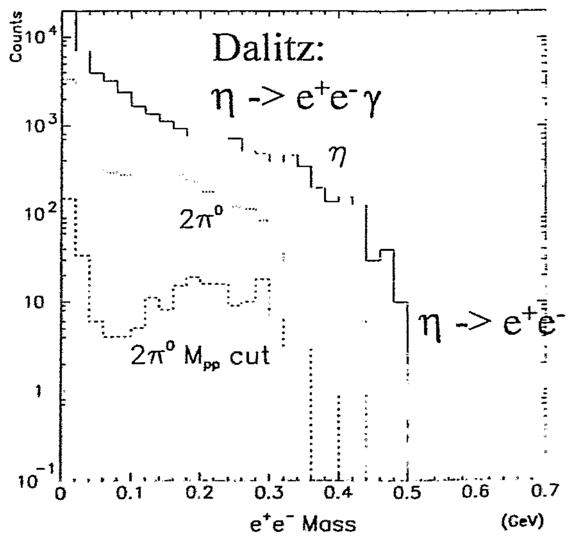

Expected di-electron spectra for 4 days of beam (10^8 protons/s^{-1})

η from pp with reduced setup

HADES

2 sectors, 3 MDC planes only:

→ $\mathcal{E}(ppe^+e^-) \simeq 0.5-1.5\%$

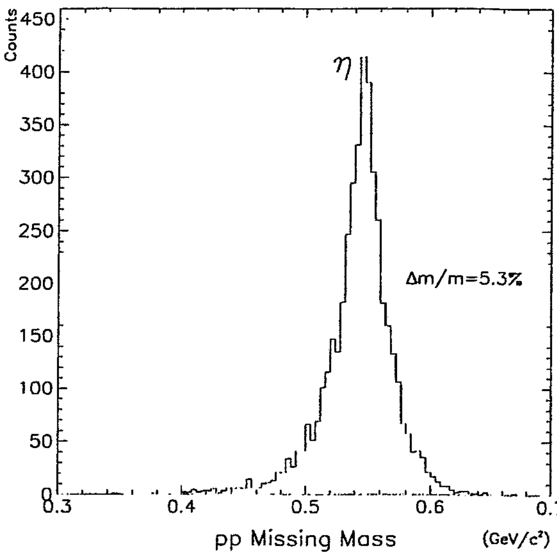

Missing mass distribution from pp momentum analysis

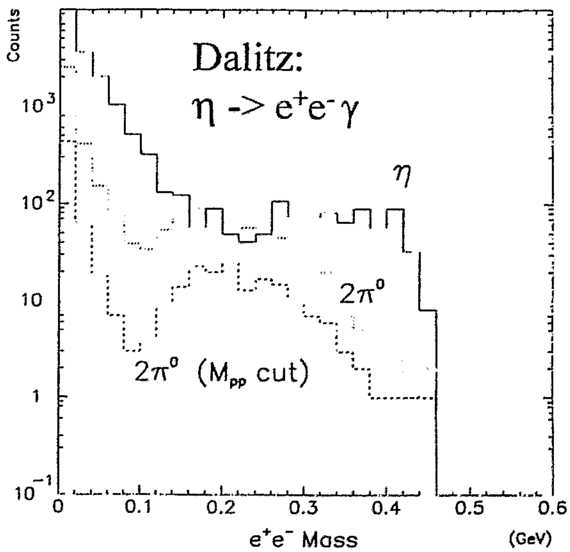

Expected di-electron spectra for 4 days of beam (10^8 protons/s^{-1})

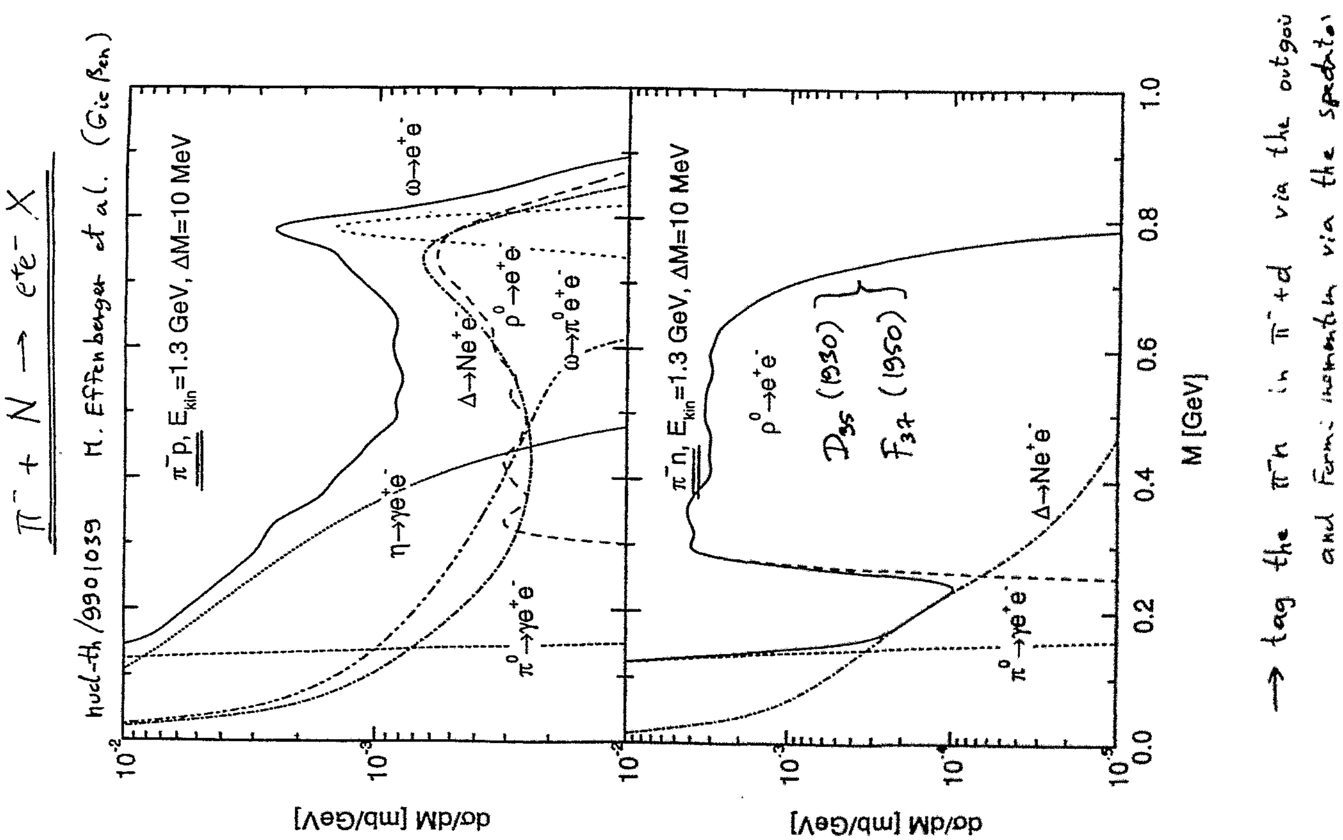

R. J. Porter et al. DLS Collaboration

preprint nucl-ex/9703001 March 97

→ PRL 79 (1997) 1229

Figure 1.

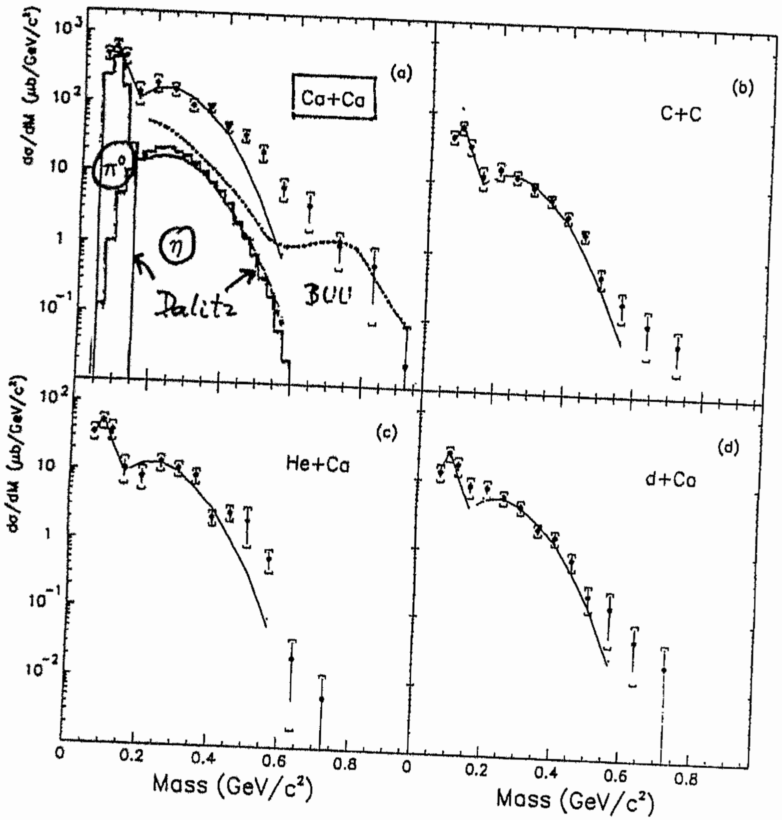

Factor 10 higher cross section !

Comparison with DLS Data

π⁰ and η strongly constrained by TAPS γγ data !

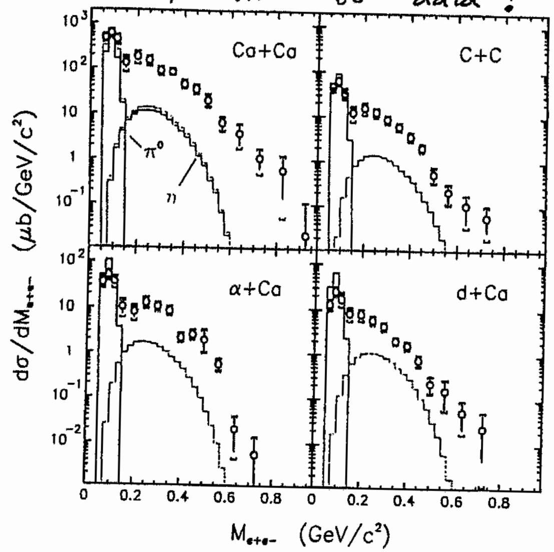

R. Holzmann et al., Phys. Rev. C56 (1997) R2920.

The η Dalitz-decay contribution does not exhaust the observed di-electron yields in the mass range $M_{e^+e^-}$ = 0.15–0.55 GeV !

Need :
- $\Delta \to N e^+e^-$
- $\rho N \to \rho N e^+e^-$
- + ... ?

Di-Electrons @ 1 AGeV: Theory (1)

HADES

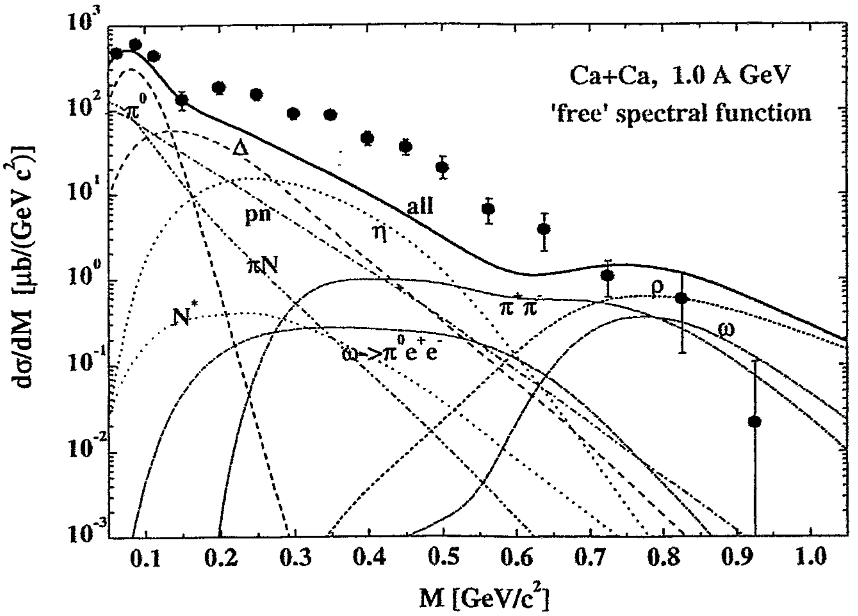

Data:
R.J. Porter et al.,
PRL 79 (1997) 1229

Calculation:
E.L. Bratkovskaya et al.,
NP A609 (1998) 168

theor. distribution folded with exper. resolution ($\Delta M/M \sim 10\%$)

R. Holzmann, GSI Darmstadt

BUU calculation
W. Cassing et al.

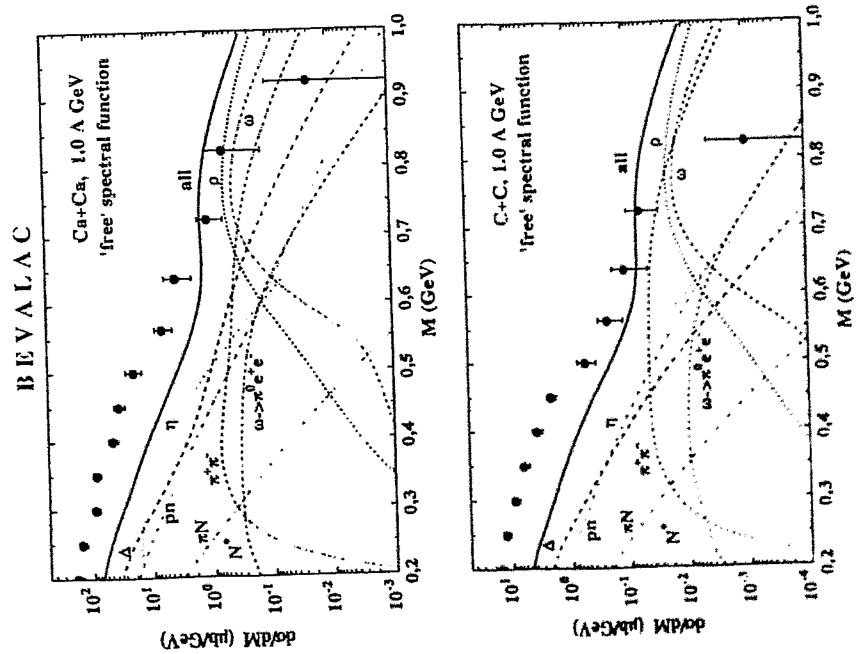

Di-Electrons @ 1 AGeV: Theory (2)

HADES

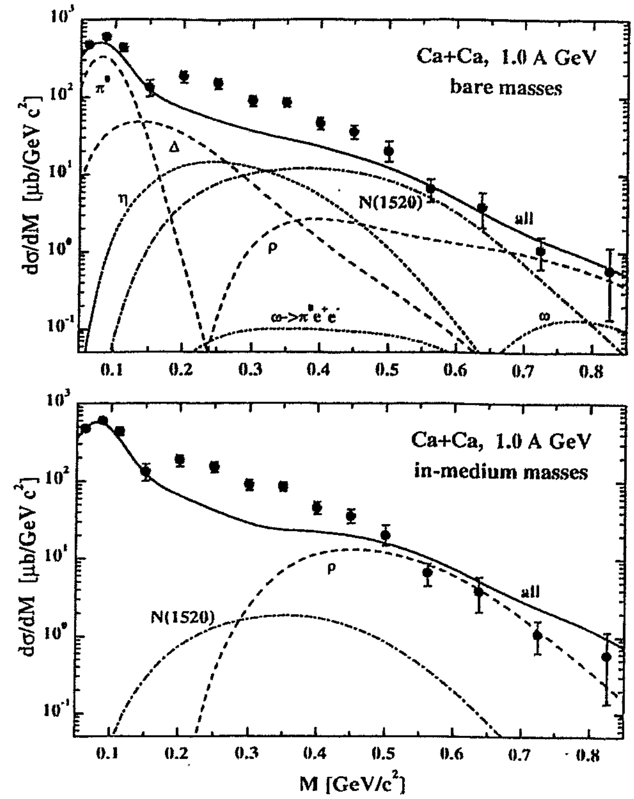

Data:
R.J. Porter et al.,
PRL 79 (1997) 1229

Calculation:
E.L. Bratkovskaya
and C. M. Ko,
PL B445 (1999) 265

theor. distr. folded with experimental resolution ($\Delta M/M \sim 10\%$)

R. Holzmann, GSI Darmstadt

Frankfurt UrQMD does not reproduce e^+e^- yield in A+A.

C. Ernst et al. PRC 58 (1998) 447

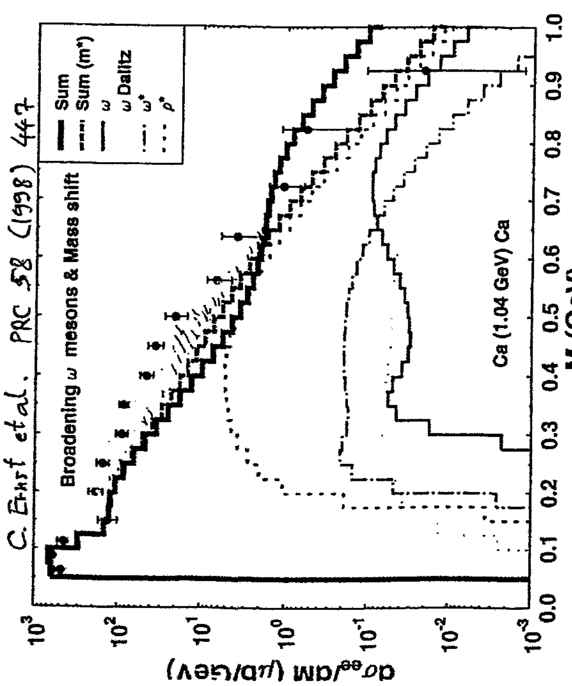

UrQMD

C. Ernst et al. PRC 58 (1998) 447

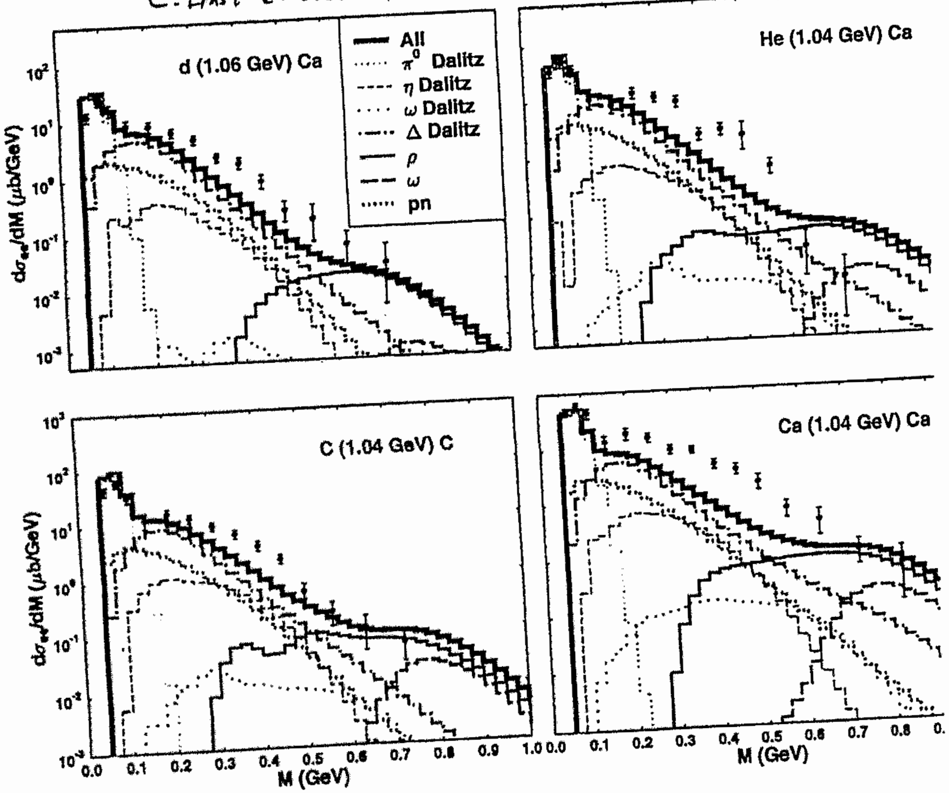

Frankfurt UrQMD p+d calculation

C. Ernst et al. PRC 58 (1998) 447

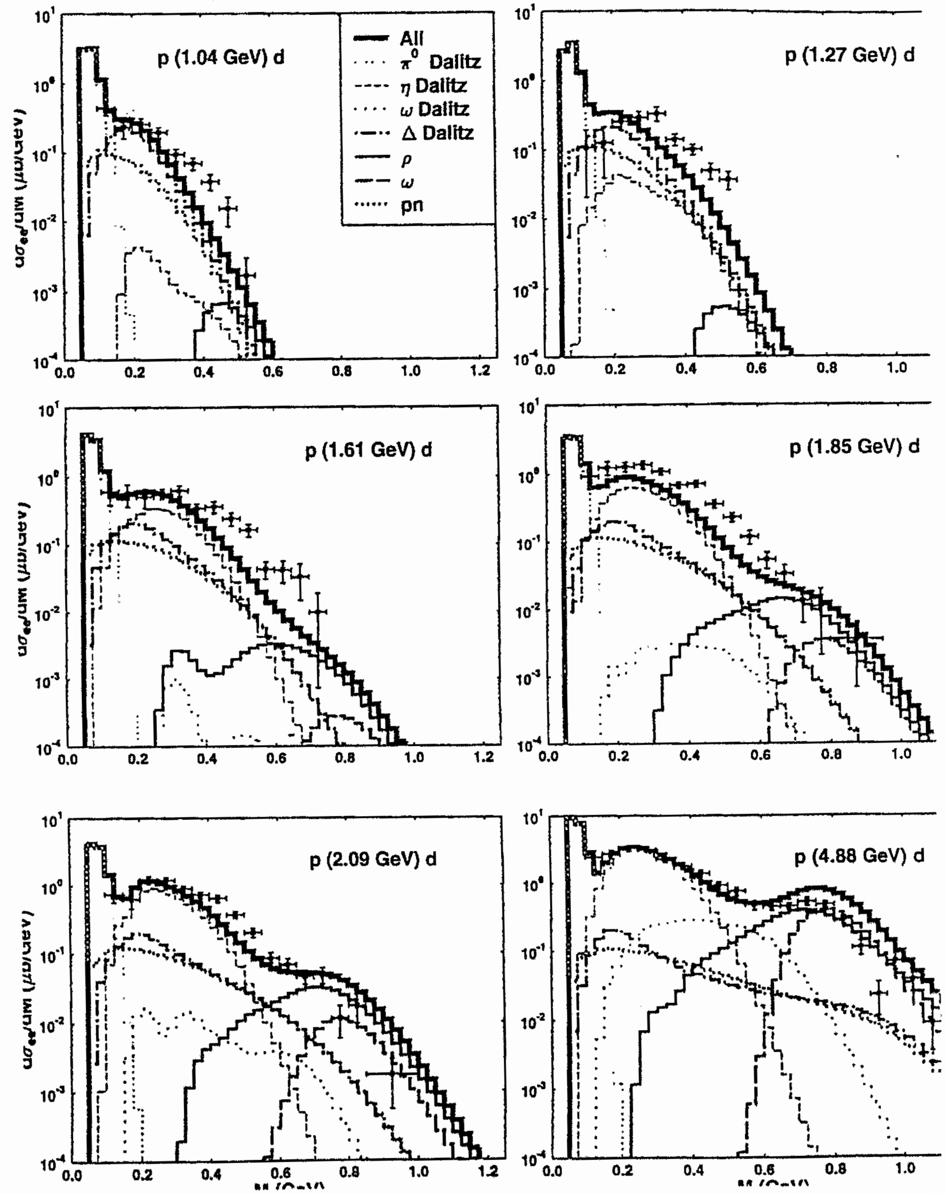

thermal source at mid rapidity for 1 AGeV A+A :

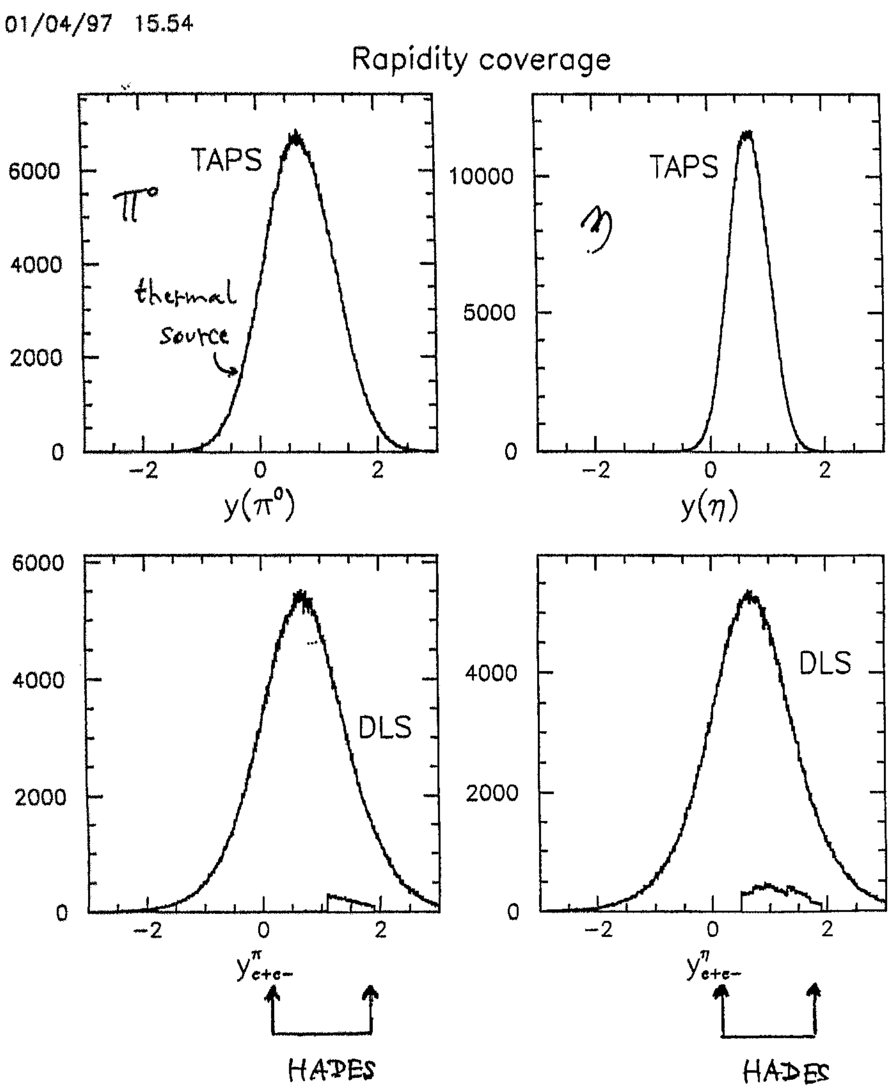

π^0 and η Anisotropies

Evidence of non-isotropic angular distributions from

- π^+, π^- data (Nagamyia et al, Sandoval et al., Pelte et al.)
- BUU calculations (e.g. E. Bratkowskaya et al.)

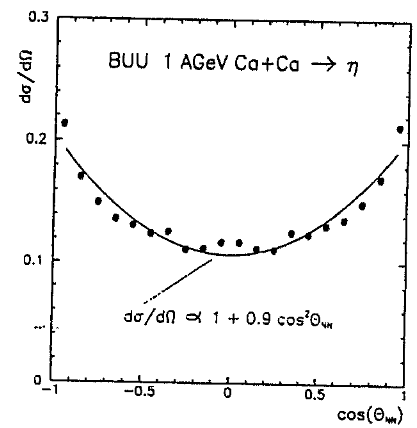

Assuming $A_2 \simeq 0.9$ in extrapolation of cross section to 4π

- $\sigma(\pi^0)$ increases by 25 %
- $\sigma(\eta)$ increases by 18 %

Di-electrons @ 2 AGeV

HADES

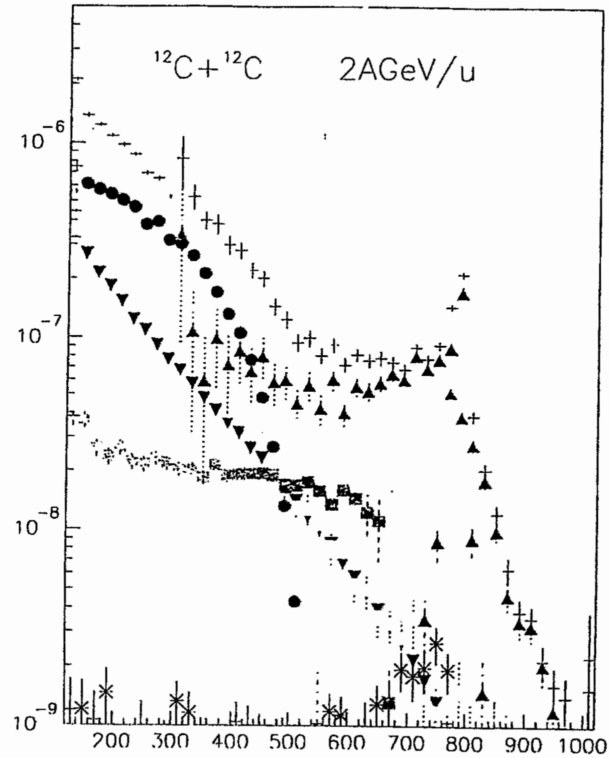

UrQMD calculation
(C. Ernst 1998)

not folded with exp. resolution ($\Delta M/M \sim 1\%$)

Rates:

acceptance of a 2 sector setup

Pion Anisotropies :

800 A·MeV Ar+KCl

Nagamiya et al

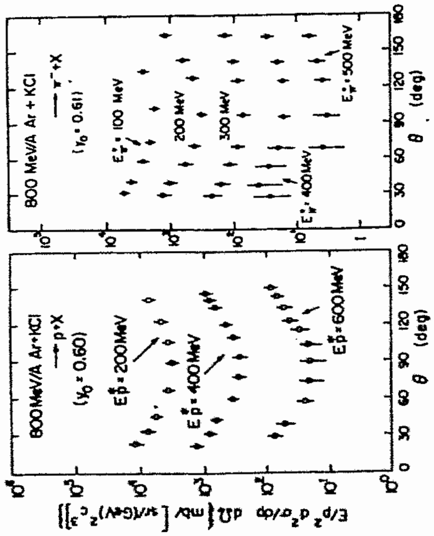

1.0 A·GeV Au+Au

FOPI (Pelte et al.)

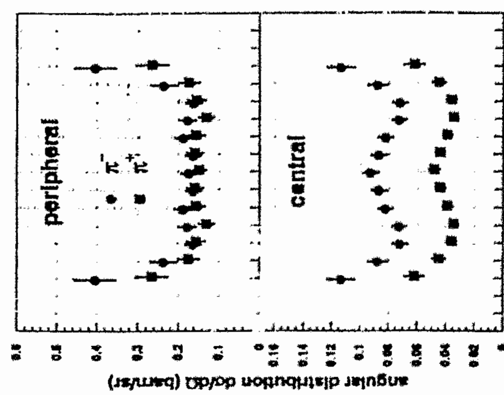

1.8 A·GeV Ar+KCl

Brockmann et al.

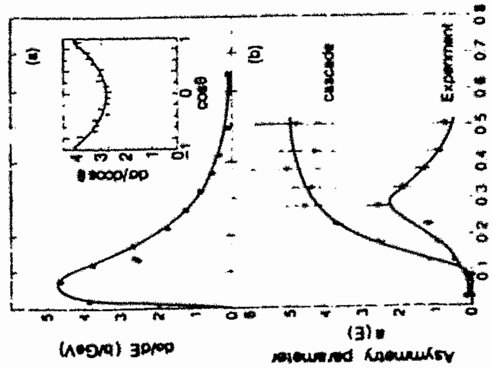

Di-electrons @ 2 AGeV

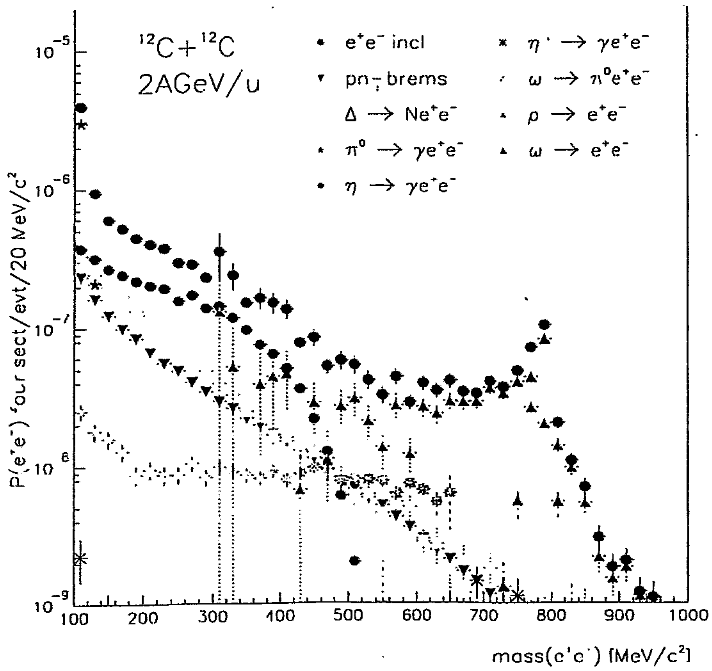

UrQMD calculation

(C. Ernst 1998)

not folded with experimental resolution

($\Delta M/M \sim 1\%$)

Meson m_t Scaling

1. Experimental results :

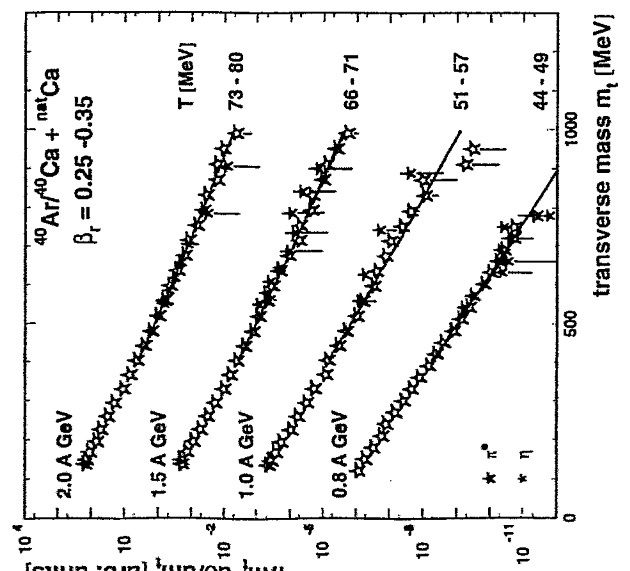

m_t scaling is observed in all systems at all beam energies.

2. BUU predictions (E. Bratkovskaya et al.) :

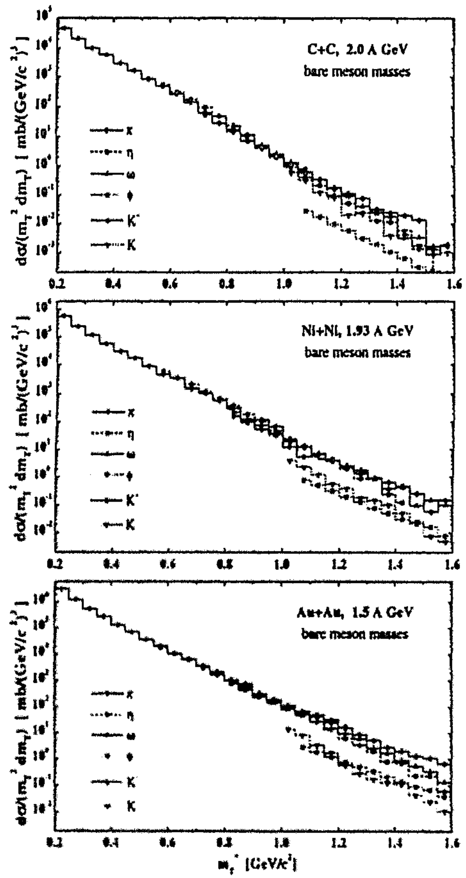

Fig. 1

Scaling expected for heavier mesons too !

3. What do we expect for the ω ?

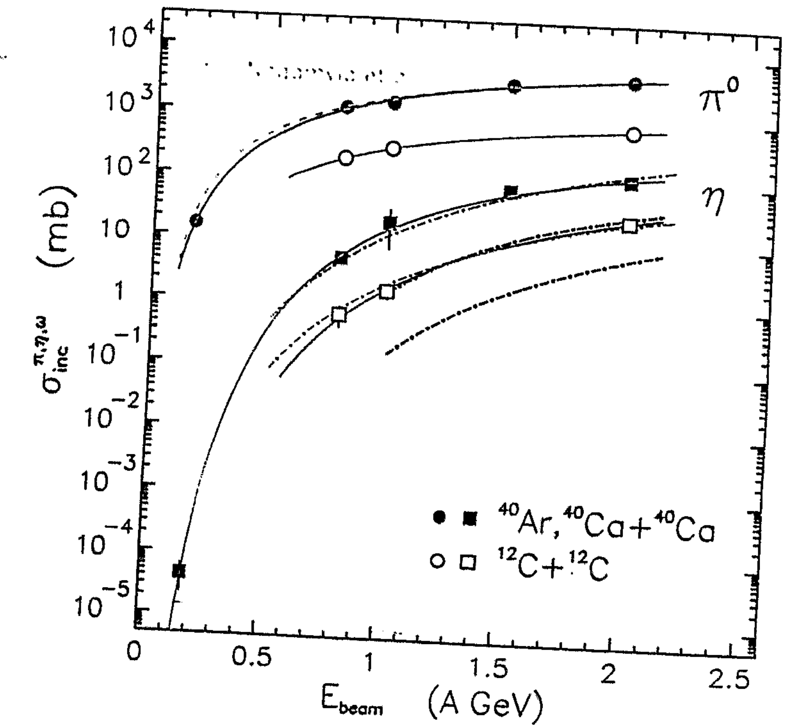

Unfortunately, no clear ω signal in TAPS data.
but HADES should see it, unless...

A First Physics Program

HADES

Properties of vector mesons in the medium

$$\rho, \omega, \phi \Rightarrow \gamma^* \Rightarrow e^+ + e^-$$

A list of topics for 1999/2000 :

- **Cocktail of free mesons**

  ↳ η and Δ production in p + p and p + A

- **Di-electron enhancement (DLS !) in HI collisions for 200 MeV/c² < M_{inv} < 600 MeV/c²**

  ↳ **C + C, Ca + Ca, (Au + Au)**

- **Hunting for vector mesons in nuclei**

  ↳ ω and ϕ production in p + A and A + A

R.Holzmann, GSI Darmstadt

R. Schicker:

Dalitz decay measurements with HADES

[illegible]

1) Form factors

2) Dalitz decay $\omega \to \pi^0 e^+ e^-$

3) Dalitz decay $\phi \to \pi^0 e^+ e^-$

4) Conclusions

april 17, 99

R. Schicker

Vector dominance model (VDM)

- the electromagnetic interaction of hädrons is governed by their couplings to vector mesons (Sakurai 69)

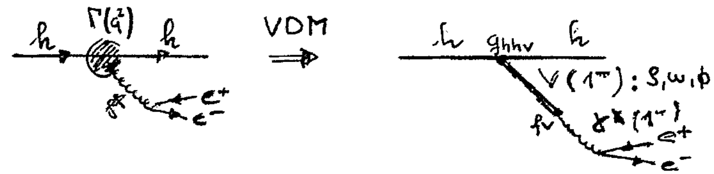

- Landsberg: $V \to P e^+ e^-$ (Phys. Rep 128, 198.

$$\frac{1}{\Gamma(V \to P\gamma)} \times \frac{d\Gamma(V \to P e^+ e^-)}{dq^2} = \frac{\alpha}{3\pi} \left\{1 - \frac{4m_e^2}{q^2}\right\}^{1/2} \left\{1 + 2\frac{m_e^2}{q^2}\right\} \times$$

$$\times \frac{1}{q^2} \times \left[\left(1 + \frac{q^2}{m_V^2 - m_P^2}\right)^2 - \frac{4 m_V^2 q^2}{(m_V^2 - m_P^2)^2}\right]^{3/2} \times \left|\frac{f_{VP}(q^2)}{f_{VP}(0)}\right|^2$$

$$= [QED] \times |F_{VP}(q^2)|^2$$

$$F_{VP}(q^2) = \frac{\sum_V \frac{g_{VP\gamma}}{2g_V} \times \frac{m_V^2}{m_V^2 - q^2 - i\Gamma_V m_V}}{\sum_V \frac{g_{VP\gamma}}{2g_V}}$$

$q^2 \to 0$: $F_{VP}(q^2) \to 0$
selection rules g_{VPV}

if transition dominated by one V: $|F_{VP}(q^2)|^2 = \frac{m_V^4}{(m_V^2 - q^2)^2 + \Gamma_V^2 \ldots}$

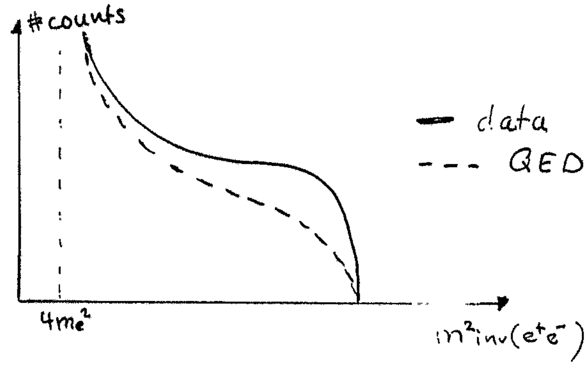

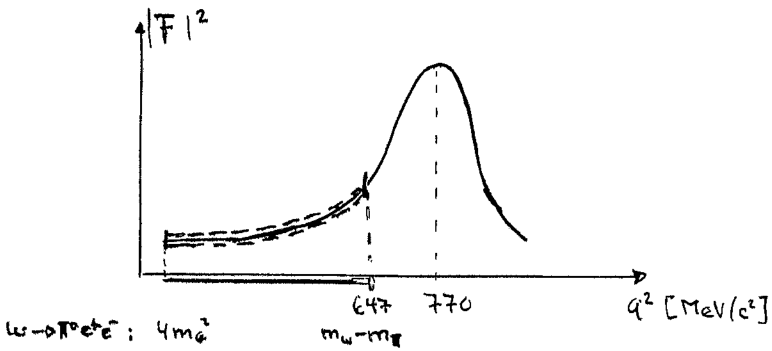

- form factor $q^2 < 0$

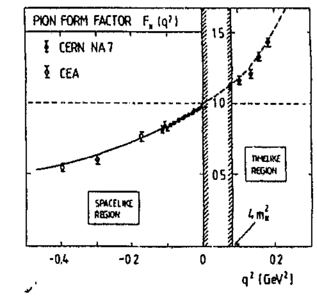

FIG. 1.3. Pion form factor in the space-like region with $q^2 < 0$ from Amendolia *et al.* (1984*a*,*b*). Its extrapolation to the time-like region is shown to the right. The curve is obtained with an improved ρ meson dominance fit (Brown *et al.* 1986).

- form factor $q^2 > 0$

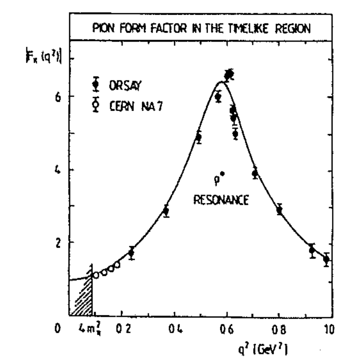

FIG. 1.5. Pion form factor in the time-like region. The experimental data are taken from Quenzer *et al.* (1978) and Amendolia *et al.* (1984*a*). The curve is obtained with a modified ρ meson dominance model (Brown *et al.* 1986).

Dalitz decay $\omega \to \pi^0 e^+e^-$

- ω - Dalitz decay contributes substantially to e^+e^- spectra at SIS, SPS, RHIC and LHC energies

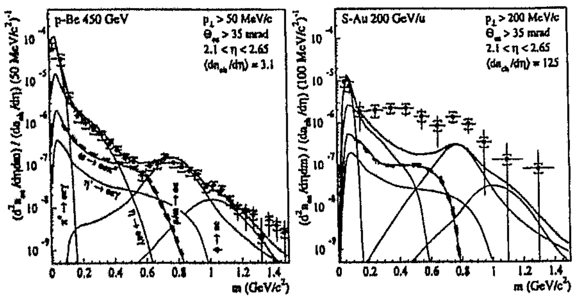

Figure 1. Mass spectra of inclusive e^+e^--pairs in 450 GeV p-Be (left) and S-Au (right) collisions showing the data (full circles) and the various contributions from hadron decays. Systematic (brackets) and statistical errors (bars) are plotted independently of each other. The shaded region indicates the systematic error on the summed contributions.

CERES da QUARK'9

- test of VDM for hadron structure

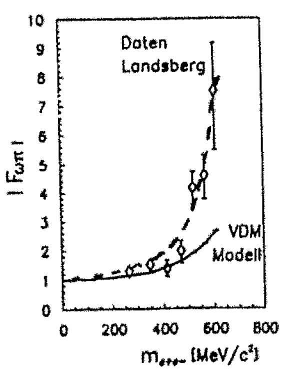

Experimental measurement of energy ...

1) $\pi^- p \to n\omega \to n\pi^0 e^+e^- \to \underline{n}\ \underline{\gamma\gamma}\ \underline{e^+e^-}$

2) $pp \to pp\omega \to$

1) energy-momentum conservation:

a) measure $\gamma\gamma e^+e^-$: HADES + elmag. cal.

b) measure $n e^+e^-$: HADES + LAND

↳ b) has larger acceptance (HADES report R.

How to measure neutron?

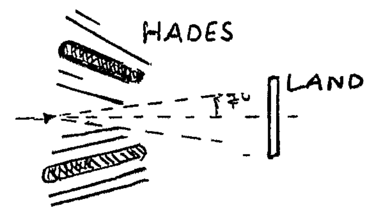

$\pi^- p \to n\omega$ is threshold process:

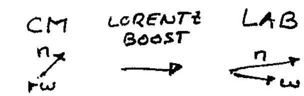

very close to threshold: neutron cone

increasing pion momentum

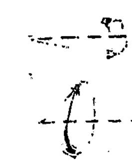

number produced omegas (and measured)

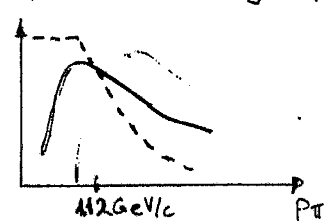

Eff (neutron)

I_{π^-}

Pionenintensitaet HADES Target

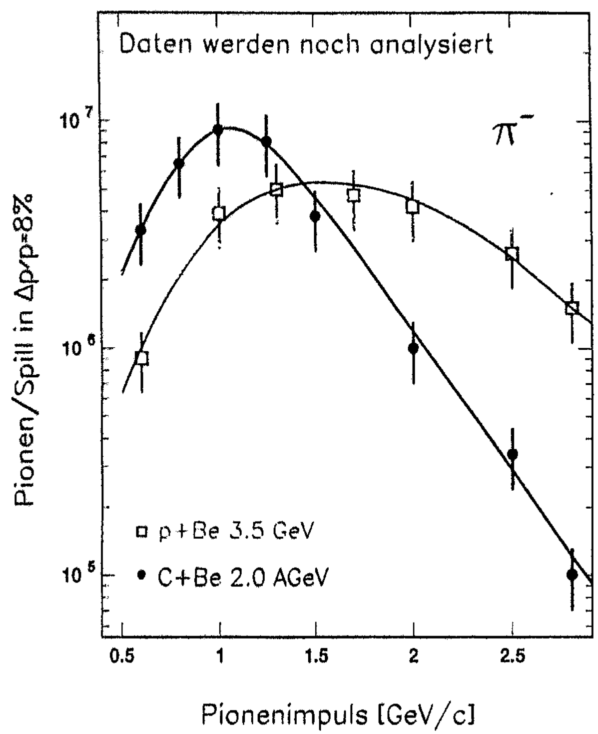

$$\pi^- p \rightarrow n \underbrace{X}$$
$$\rightarrow n\ e^+e^-\gamma$$

$$p_0 = p_{beam} + p_{targ}$$
$$p_X = p_0 - p_N$$
$$p_Y = p_0 - p_N - p_{e^+} - p_{e^-}$$

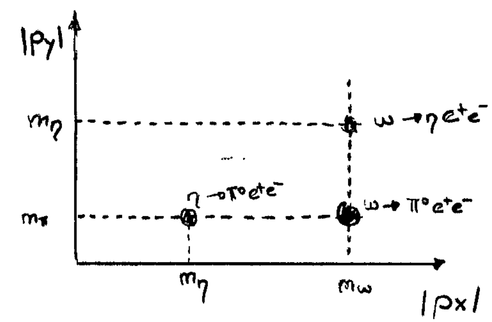

Background

$\pi^- p \rightarrow \underbrace{n e^+ e^-}_{meas.} X$

a) $\rho \rightarrow \pi^0 e^+ e^-$ (not known)

$BR(\rho \rightarrow \pi^0 e^+ e^-) = BR(\rho \rightarrow \pi^0 \gamma) * C, \quad C = \frac{\Gamma(\omega \rightarrow \pi^0 e^+ e^-)}{\Gamma(\omega \rightarrow \pi^0 \gamma)} \sim 7.5 \times 1$

$BR(\rho \rightarrow \pi^0 e^+ e^-) \approx 5 \times 10^{-6} \sim 0.01 \times BR(\omega \rightarrow \pi^0 e^+ e^-)$

b) $\rho \rightarrow e^+ e^-$

$\pi^- p \rightarrow \rho n \rightarrow e^+ e^- n$

$BR(\rho^0 \rightarrow e^+ e^-) \sim \frac{1}{14} \times BR(\omega \rightarrow \pi^0 e^+ e^-)$

c) multi

$\pi^- p \rightarrow n \pi^0 \pi^0 \rightarrow n \gamma_1 e_1^+ e_1^- \gamma_2 e_2^+ e_2^- \xrightarrow{Acc} n e^+ e^-$

$\xrightarrow{Acc} n e^+ e^+$

$\rightarrow n e^- e^-$

Rates of signal and background

	react./spill	react./wk	BR(e⁺e⁻)	react.(e⁺e⁻)/wk
signal $\pi^- P \rightarrow \omega N$	3.5×10^3	4.2×10^8	$6. \times 10^{-4}$	2.5×10^5
background $\pi^- P \rightarrow 2\pi_0 N$	4.4×10^3	5.3×10^8	1.4×10^{-4}	7.5×10^4
background $\pi^- P \rightarrow \rho N$	3.5×10^3	4.2×10^8	4.4×10^{-5}	1.8×10^4

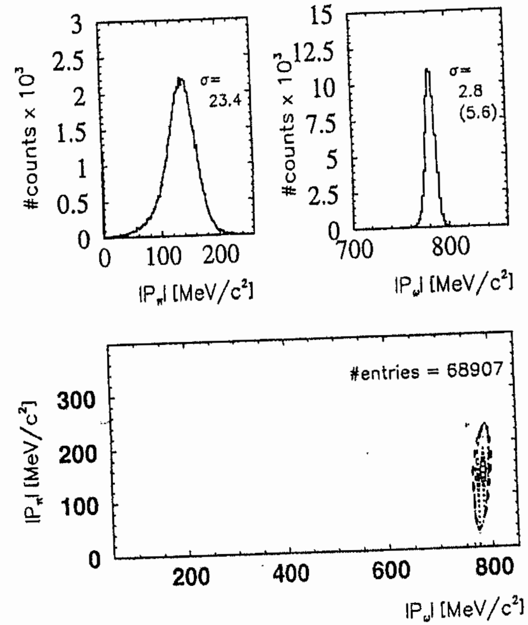

Figure 5: $|P_\omega|$ and $|P_{\pi_0}|$ single distributions (top) and correlation (bottom) for the ω-Dalitz decay if neutron is measured.

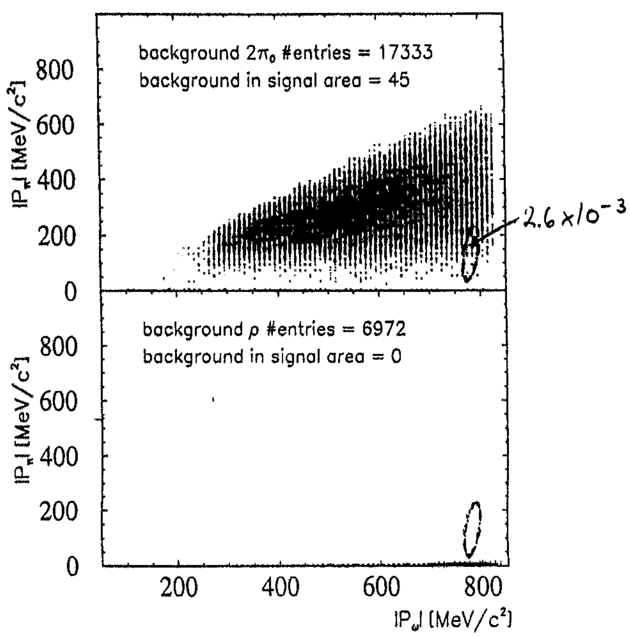

Figure 6: $|P_\omega|$- $|P_{\pi_0}|$ correlation for the $2\pi_0$ background (top) and direct ρ-decay (bottom). The dashed line represents the signal area.

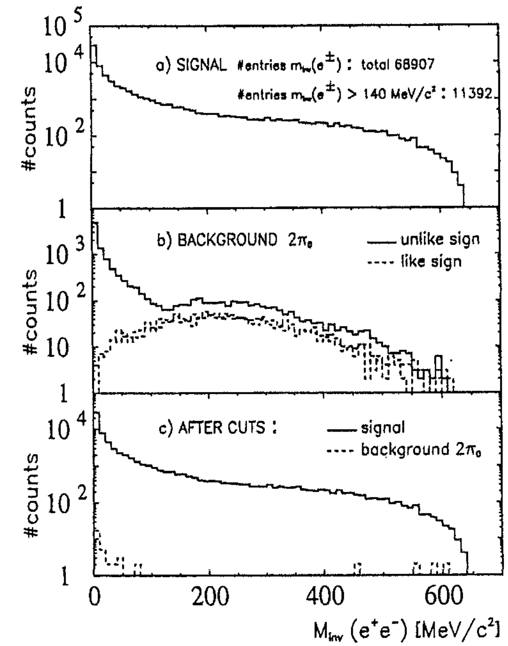

Figure 7: Dielectron invariant mass spectra without cuts for signal (top) and $2\pi_0$ background (center). The bottom part shows the mass spectra for signal and background after the signal area condition has been applied.

VDM form factor Landsberg data –
HADES data

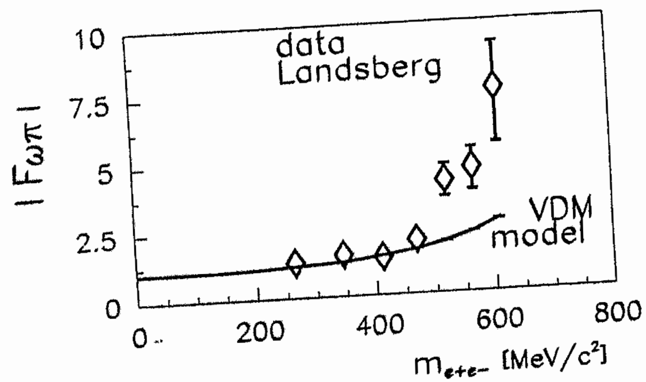

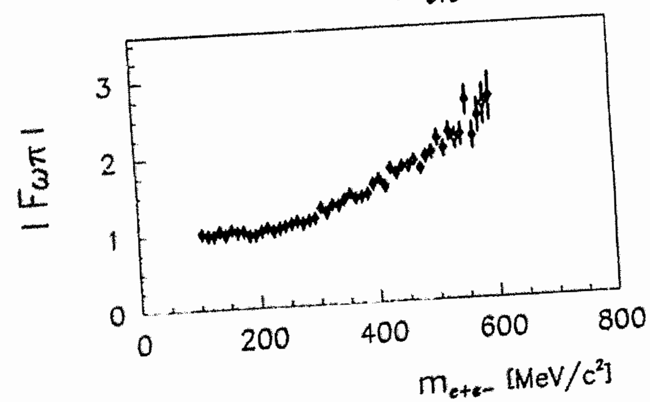

Dalitz decay ϕ

– $BR(\phi \to \pi^0 e^+e^-)$ = not known ($< 1.2 \times 10^{-4}$)

– ϕ-Dalitz decay has more phase space than ω-Dal

– $m_{e^+e^-}^{max} = m_V - m_{\pi^0}$ = 647 MeV/c² ω-Dalit
= 885 MeV/c² ϕ-Dalit

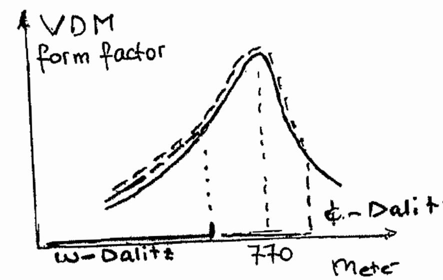

but:

$$n(\phi\text{-Dalitz}) = n(\omega\text{-Dalitz}) \times \underbrace{\frac{\sigma_{\pi p \to n\phi}}{\sigma_{\pi p \to n\omega}}}_{\% 80} \times \underbrace{\frac{BR(\phi \to \pi^0 e^+e^-)}{BR(\omega \to \pi^0 e^+e^-)}}_{\% 50} \times$$

$$n(\phi\text{-Dalitz}) = 2.5 \times 10^5 / 80 \times 50 \times .6 = 40$$

very hard measurement !!!
within HADES design parameters

[illegible] production in pp → ppϕ

- space charge limit proton beam $= 5 \times 10^{11}$/spill
- How much proton beam can HADES take ??
- Landolt – Börnstein

$pp \to 2$ prong 44 mb at $p_{Lab} = 2.8$ GeV/c
$\to 4$ prong 7 mb $= 4.0$ GeV/c
$\to 6$ prong .1 mb $= 4.0$ GeV/c

} $\langle m \rangle \sim 2.5$

↑ 50X ↓

$\langle m \rangle_{Au+Au} \sim 100$.

- double hit probability in HADES:
10^8/s Au+Au $\hat{=}$ 5×10^9/s protons

[illegible]

open question:

1) How to make 1st level trigger ?
(start detector doesn't work at 2×10^{10} protons/sp.
2) Does 1st level trigger reduce to 10^5/s ?
3) pp elastic ??

How to make 1st level trigger [illegible]

- at $p_{Lab} = 3.5$ GeV/c: ($\sqrt{s} = 2.930$)

$\sigma_{pp \to pp\phi} = \sigma_{pp \to pp\omega} \times \frac{\phi}{\omega} = .08\ \text{mb} \times 4 \times 10^{-3} = .3\ \mu b$
$\sigma_{pp \to pp\pi^+\pi^-} = \sim 2.5$ m
$\sigma_{pp \to pp\pi^0} = \sim 3.0$ m.

- $pp \to pp\phi$ is threshold reaction
"little" above threshold → protons are forward pe[illegible]
$\sqrt{s} - \sqrt{s_0} \sim 35$ MeV

→ 1st level trigger [illegible]
– protons [illegible]
[illegible]

- $pp \to pp\pi^0$
- $pp \to pp\pi^+\pi^-$

} protons go to larger polar angles → no trigger (low eff.)

$pp\pi^0$: $\sqrt{s} - \sqrt{s_0} \sim 920$ MeV
$pp\pi^+\pi^-$: $\sqrt{s} - \sqrt{s_0} \sim 775$ MeV

- $p_p = 3.5$ GeV/c

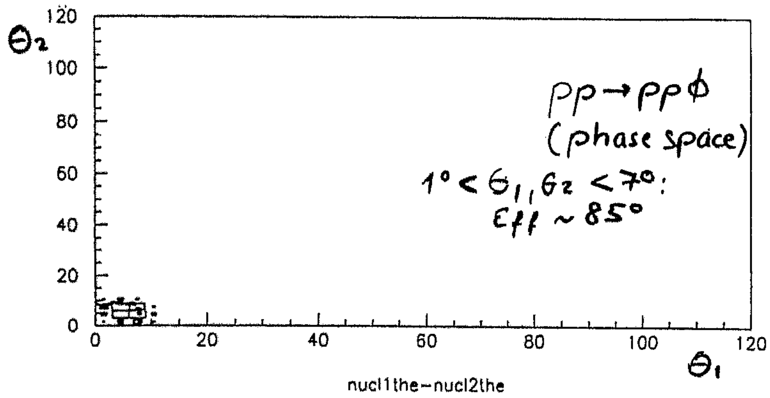

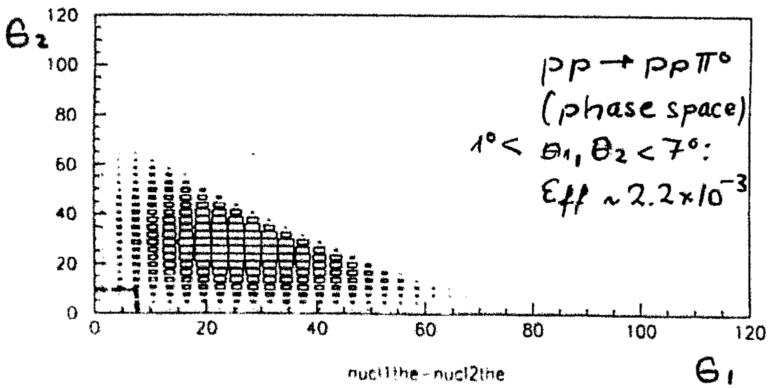

- $pp \rightarrow pp\, 2\pi$: Eff $\sim 2.8 \times 10^{-3}$

- additional: Mult = 2 in HADES TOF wall

$$X = \frac{R_p^\phi}{R_\pi^\phi} = \frac{I_p}{I_\pi} \times \frac{\sigma_{pp \rightarrow pp\phi}}{\sigma_{\pi p \rightarrow n\phi}} = \frac{2 \times 10^{10}}{.6 \times 10^7} \times \frac{.0003}{.025}$$

$$X = 40$$

VDM form factor $\phi \rightarrow \pi^0 e^+ e^-$ (stat. of 1600 de

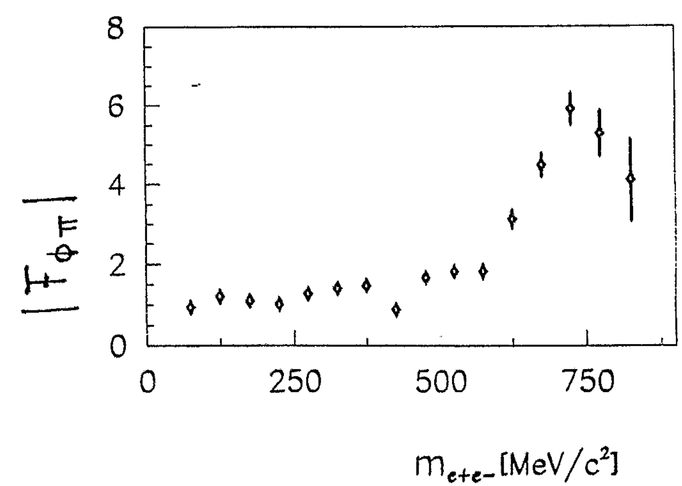

Conclusions

- pion beam at GSI can be used to produce $4. \times 10^8$ tagged omegas/week by measuring neutron with LAND.
- HADES + LAND can measure 2.5×10^5 ω-Dalitz
- $S/B > 10$

- the measurement of the ϕ-Dalitz may be feasible with the proton beam at GSI

W. Koenig:

ω meson spectroscopy at HADES in πA reactions

ω Spectroscopy at HADES in π – A reactions

work started by: Arnold Schröter
work done by: Walter Schön
work presented by: W. K.

Menu:

- Introduction & Motivation
- Why π^-
- ω in medium
- ω in HADES (e^+e^-)
- "Background"
- Summary

'Microscopic' and 'macroscopic' view of π induced ,recoilless' ω production

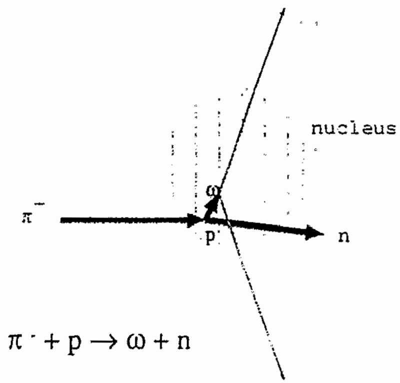

$\pi^- + p \rightarrow \omega + n$

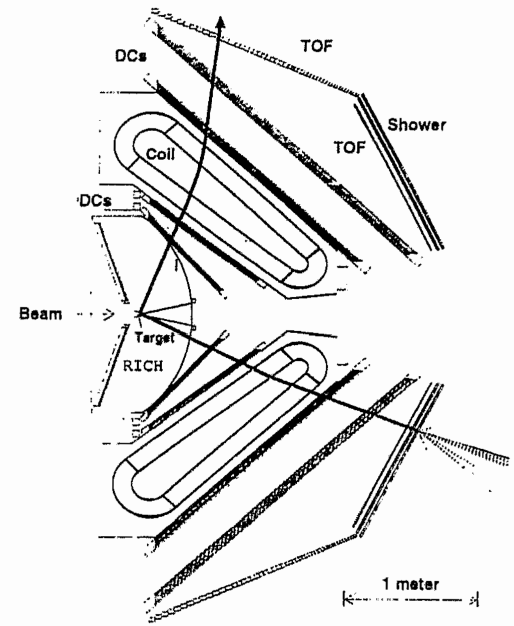

HADES setup

Motivation

Restoration of chiral symmetry

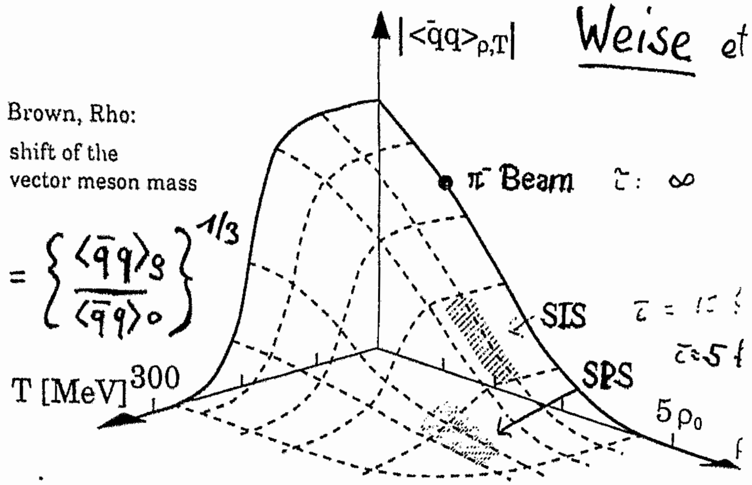

$$\frac{M(\rho)}{M(0)} = \left\{ \frac{\langle \bar{q}q \rangle_\rho}{\langle \bar{q}q \rangle_0} \right\}^{1/3}$$

Candidates

ρ $\tau = 1.3$ fm/c
$\Gamma = 152$ MeV/c^2 *short lived!*

ω $\tau = 23.4$ fm/c
$\Gamma = 8.4$ MeV/c^2 *small width!*

φ $\tau = 44.4$ fm/c
$\Gamma = 4.4$ MeV/c^2

Comparison of Pion and Proton Induced Meson Production

	π^- - beam				p - beam			
meson	$p_{\pi^-}^{optimum}$ [GeV/c]	$\sigma_{\pi^- p \to n\, meson}$ [mb]	$\sigma_{\pi^- p \to n \pi^0}$ [mb]	π^0 / meson	$p_p^{optimum}$ [GeV/c]	$\sigma_{pp \to pp\, meson}$ [mb]	$\sigma_{pp \to pp \pi^0}$ [mb]	[redacted]
η	0.76	2.70	6.80	2.5	3.20	0.24	3.5	
ω	1.40	2.50	2.50	1.0	5.46	0.15	2.8	
ρ	1.41	3.60	2.50	0.7	5.46	0.10	2.8	
η′	1.60	0.10	2.10	21.0				
φ	2.00	0.03	1.00	33.3		≤ 0.001		

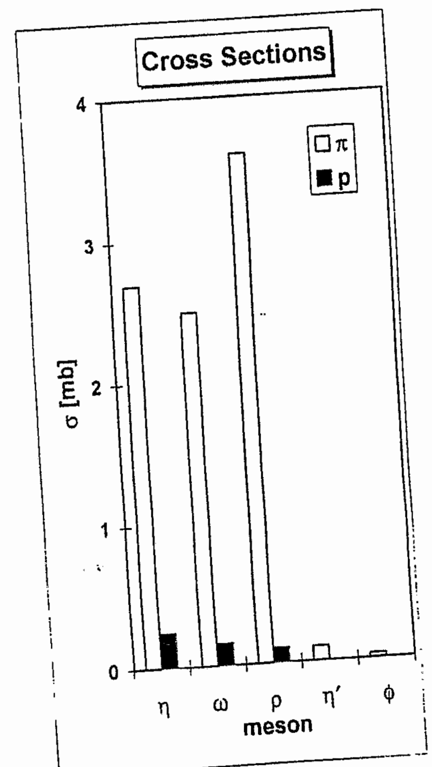

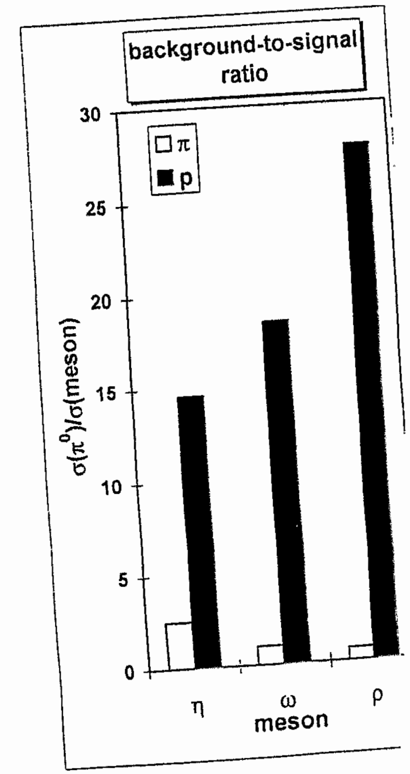

Momentum distribution of ω's

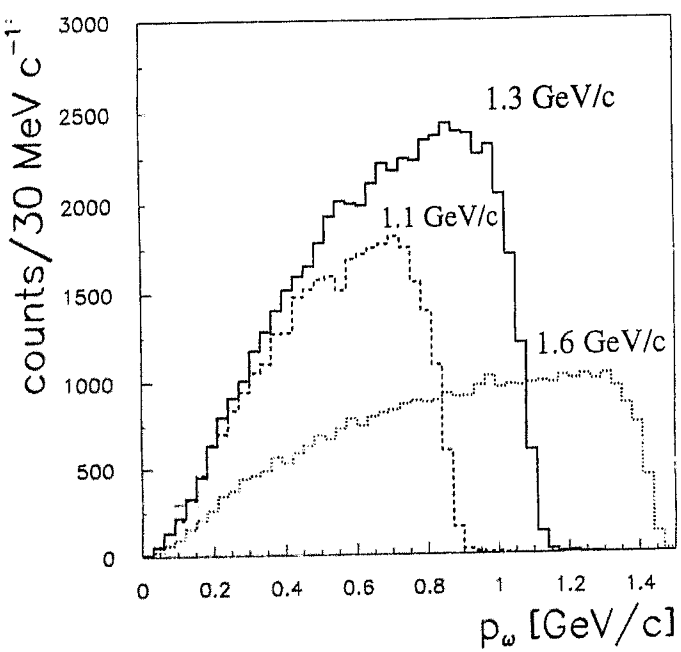

Highest yield of low momentum ω's for incident π's with $p_\pi = 1.3$ GeV/c

Meson production thresholds and π beam intensities

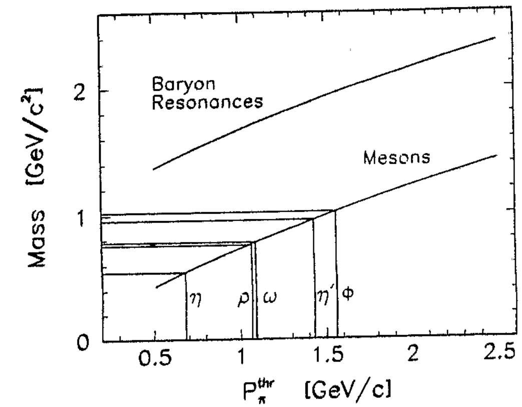

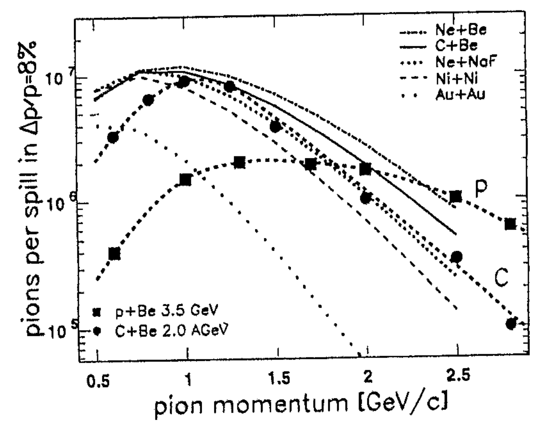

expected ω rates

$\pi^- \rightarrow {}^{208}Pb$

$10^7\ \pi^-$/spill @ 1.5 GeV/c
duty factor 20%

target:
20% interaction length
= 3.4 cm
π^- energy loss: 0.07 GeV
π^- multiple scattering:
$\langle\theta\rangle$=1.4°

$\pi^-+p \rightarrow n+\omega$	ω rate [1/s]	e^+e^- rate [1/shift]	ratio [%]
all ω's	39290	31683	100,0
$p_\omega \leq$ 300 MeV/c	4125	3326	10,5
detected ω's	206	166	0,5
optimized target position (+20 cm)	825	665	2,1
decay inside Pb	446	360	1,1

1 shift = 8 hours

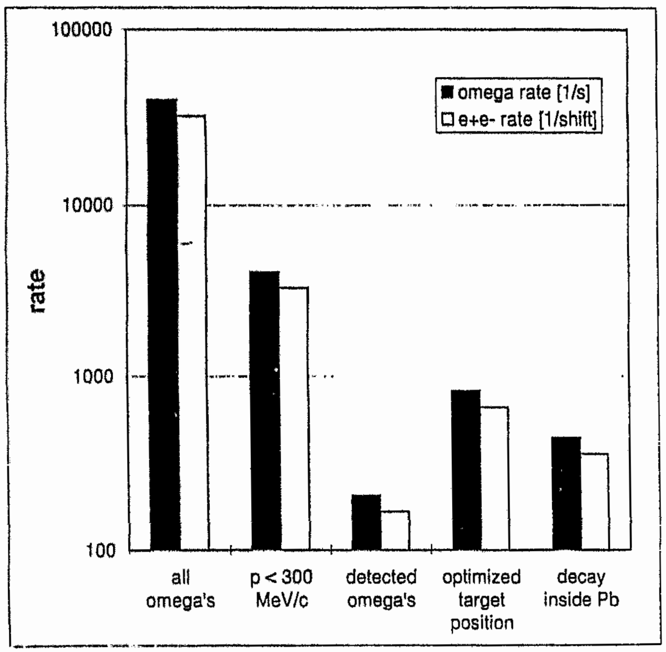

Saclay Sept. 95

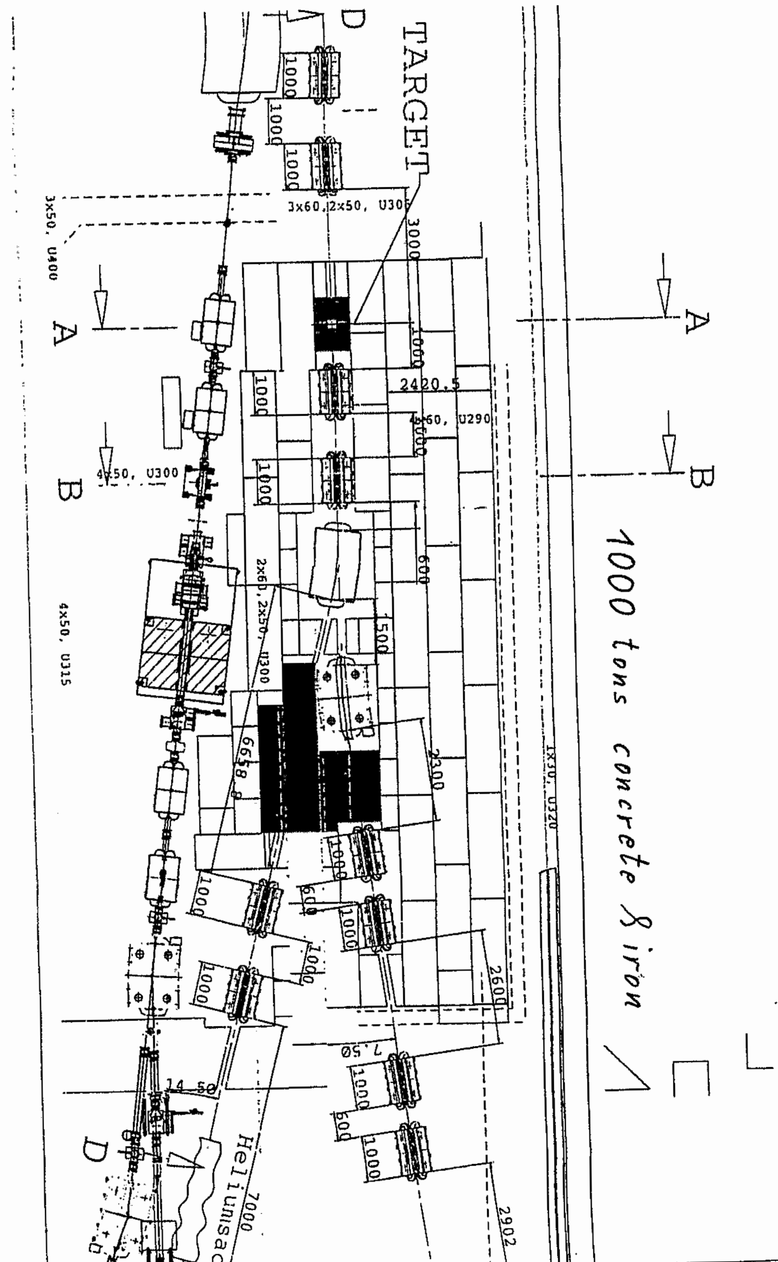

e^+e^- Pairs -
Opening Angle Distribution

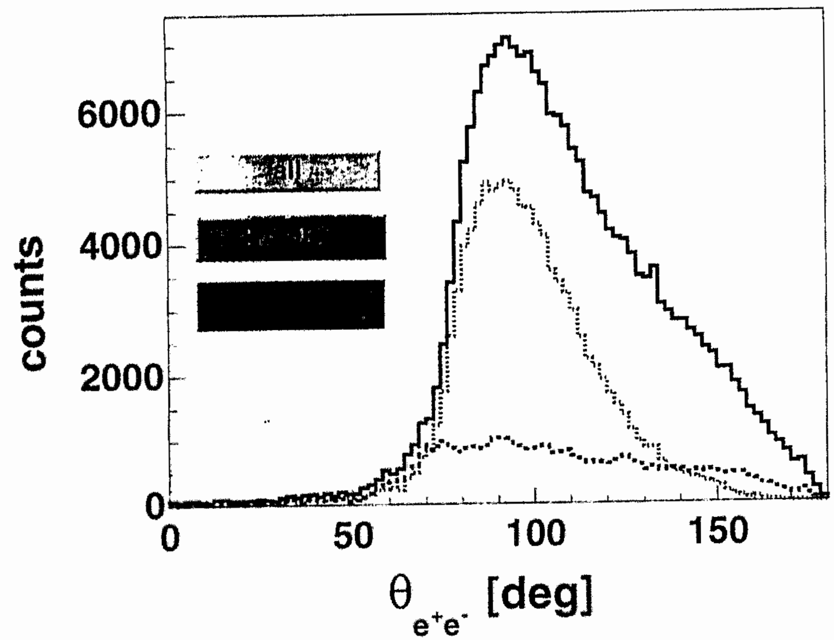

Spatial distribution of ρ, ω production in a Pb nucleus

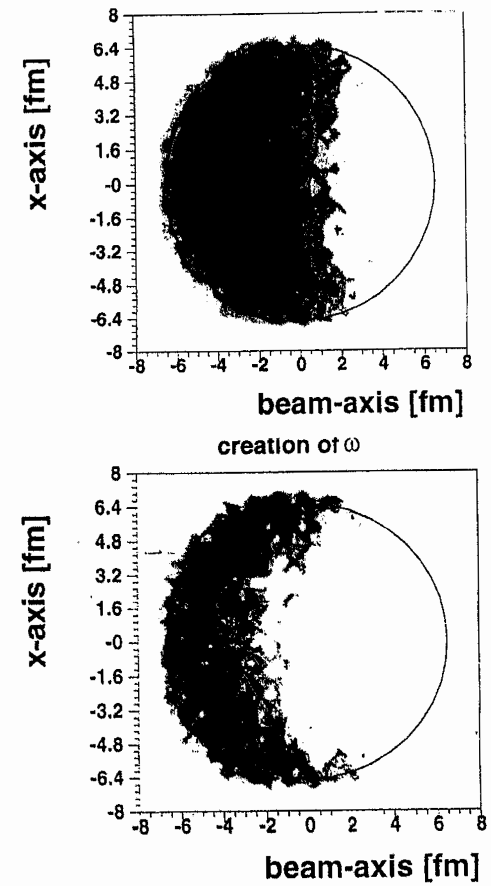

Walter Schoen, TU Muenchen

Spatial distribution of ω creation and decay

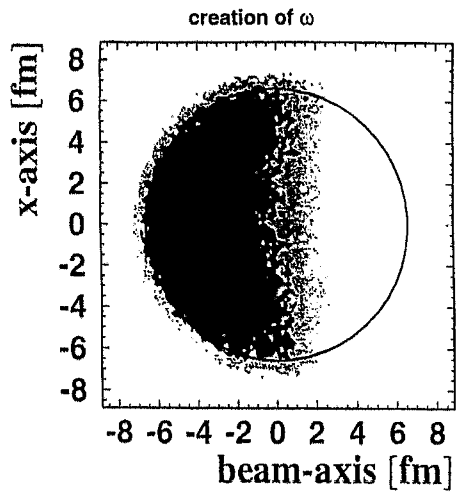

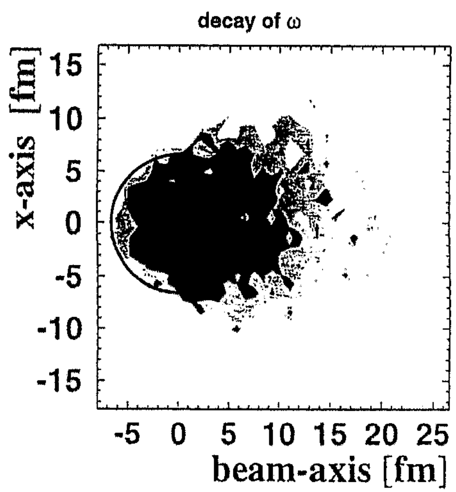

In medium particle width:

total decay width:

⇒ free decay

⇒ absorption detailed balance: $\Gamma \sim 65\ MeV$ $\pi^+ n \to \omega p$, $\pi^- p \to \omega n$, $\pi^0\, n,p \to \omega$

⇒ elastic and inelastic scattering

⇒ **decay of the system:** particle in medium (finite size effect) $\Gamma \sim 50\ MeV$

Decay probability depends on density.

⇒ No exponential decay nor lorentzian mass distribution

Elastic scattering requires quantum mechanical calculation: Add amplitudes.

It is **not** allowed to deduces lifetimes or width's from **elastic scattering** cross sections. (see Hydrogen atom)

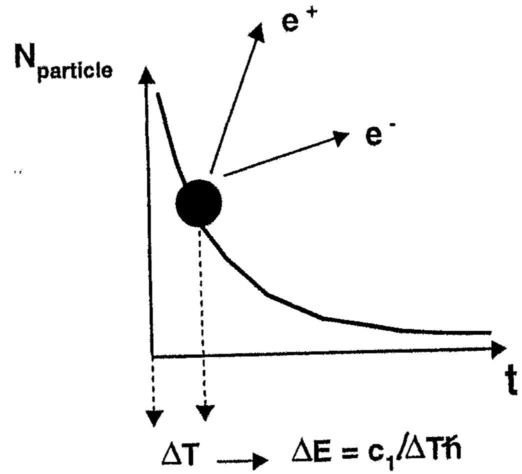
N particle
e +
e -
t
ΔT → ΔE = c1/ΔTħ

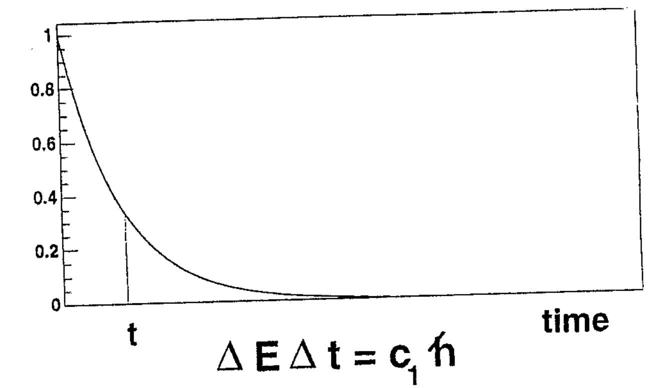
1
0.8
0.6
0.4
0.2
0
t
time
Δ E Δ t = c1 ħ

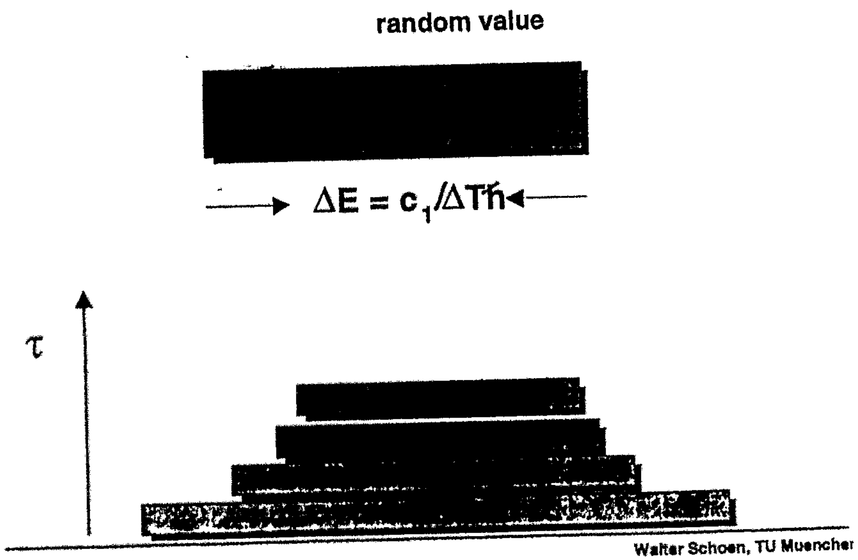
random value
→ ΔE = c1/ΔTħ ←
τ
Walter Schoen, TU Muencher

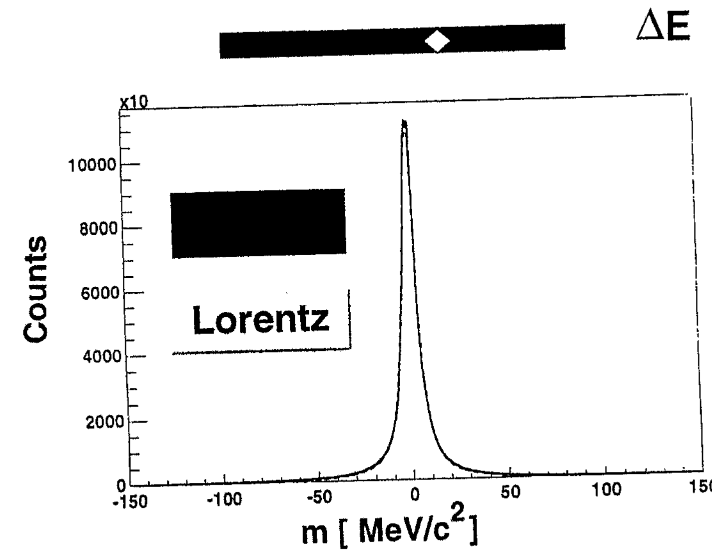
ΔE
x10
10000
8000
6000
4000
2000
0
Counts
Lorentz
-150
-100
-50
0
50
100
150
m [MeV/c2]

Medium Modifications:

- Finit Nuclear Matter
- Collision Broadening
- Mass Shift

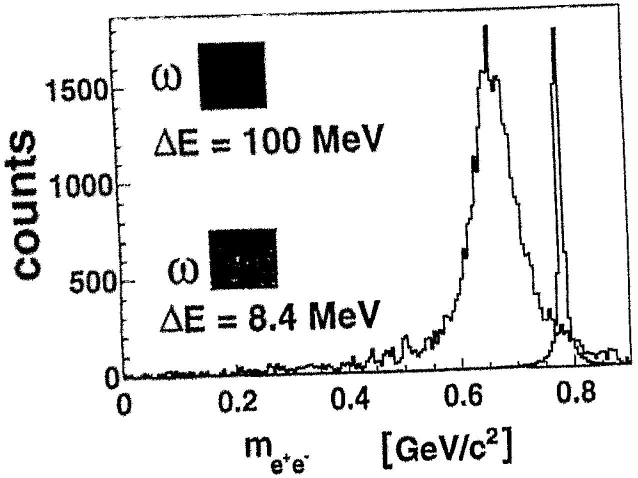

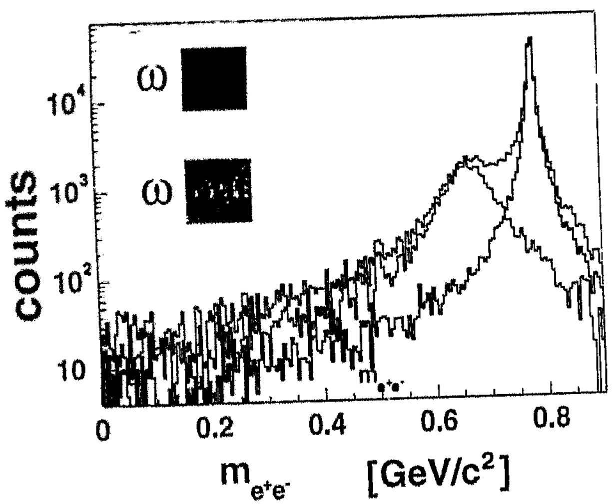

Walter Schoen, TU Muencher

Rho Meson Contribution

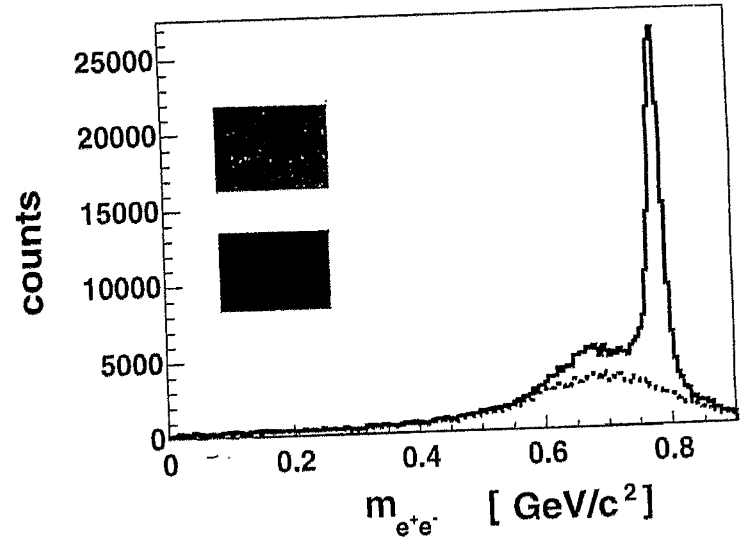

ρ treated somewhat carelessly (just mass s:

HADES Experiment - 10 day s

p_{π^-} = 1.3 GeV/c

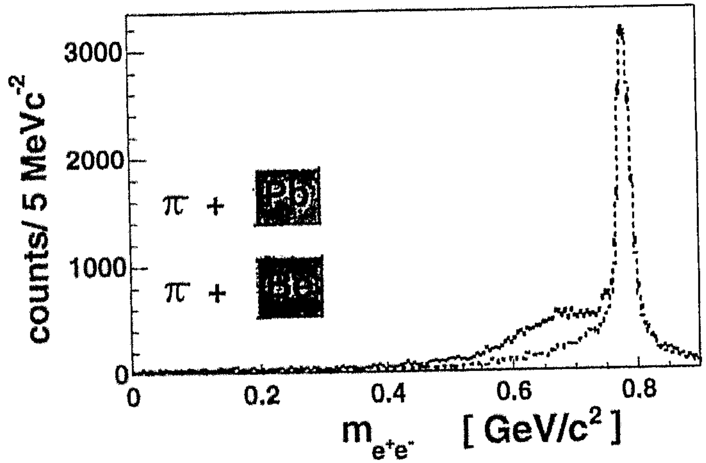

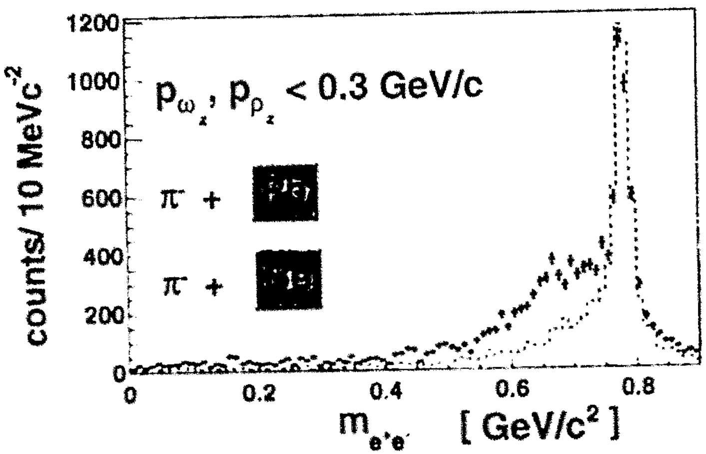

Background contributions (combinatorial background)

e^+e^- combinations from different π^0

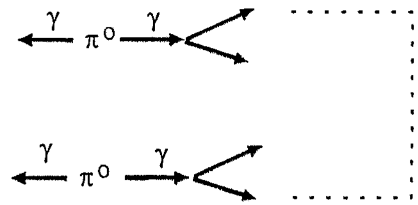

$\pi^- + p \rightarrow \pi^0 + \pi^0 + n$

≈1.4 mb

$\pi^- + p \rightarrow \pi^0 + \pi^0 + \pi^0 + n$

≈0.5 mb

⇒ combinatorial background neglegible at m_ω

including detection & reconstruction efficiency with HADES:

2500 ω's (p<0.8 GeV/c)

in 1 week

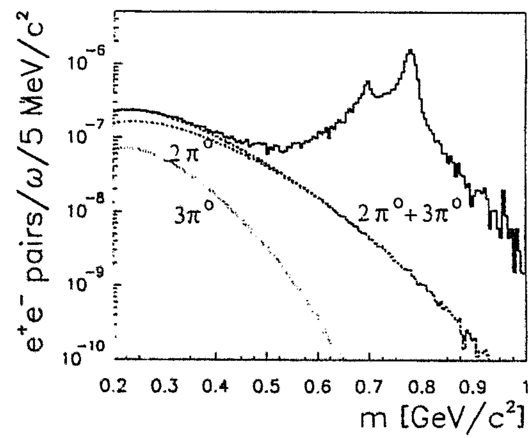

The full cocktail including baryon resonance's
(M. Effenberger et. al., Gießen)

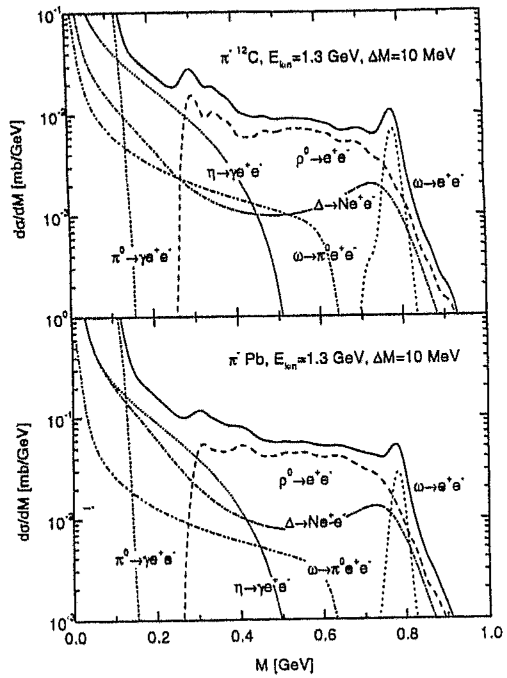

Figure 1: The dilepton invariant mass spectrum for π^-C (upper part) and π^-Pb (lower part) at a kinetic energy of $E_{kin} = 1.3$ GeV calculated without collisional broadening and with vacuum masses for the vector mesons employing a mass resolution $\Delta M = 10\,\text{MeV}$. Fluctuations in the curves are caused by low statistics.

The elementary π-p and π-n reactions
(M. Effenberger et. al., Gießen)

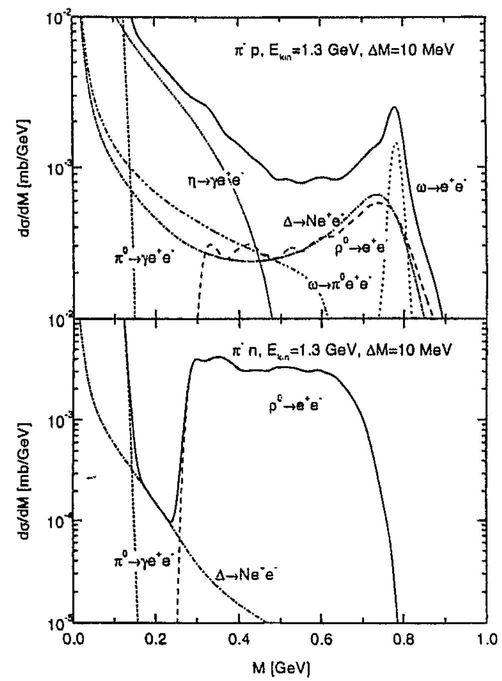

Figure 2: The dilepton invariant mass spectrum for π^-p (upper part) and π^-n (lower part) at a kinetic energy of $E_{kin} = 1.3$ GeV employing a mass resolution of $\Delta M = 10\,\text{MeV}$.

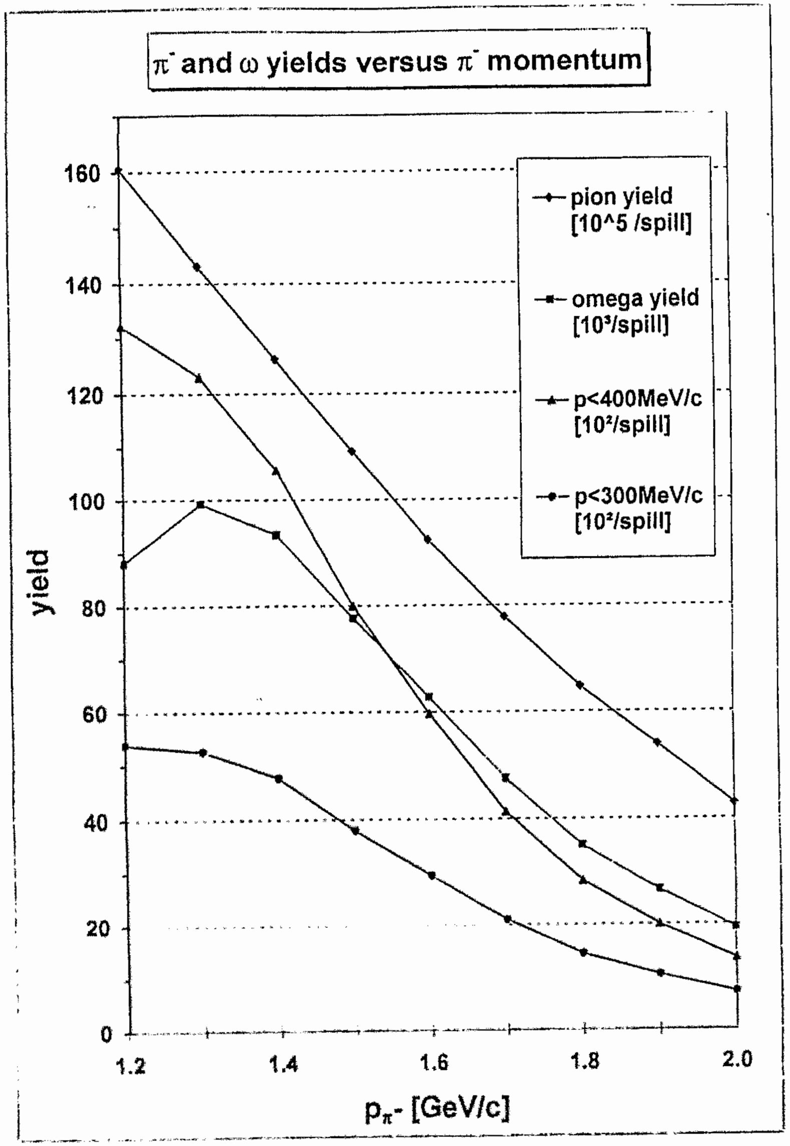

$\pi^- + A$

$p_{\pi^-} = 1.3$ GeV/c

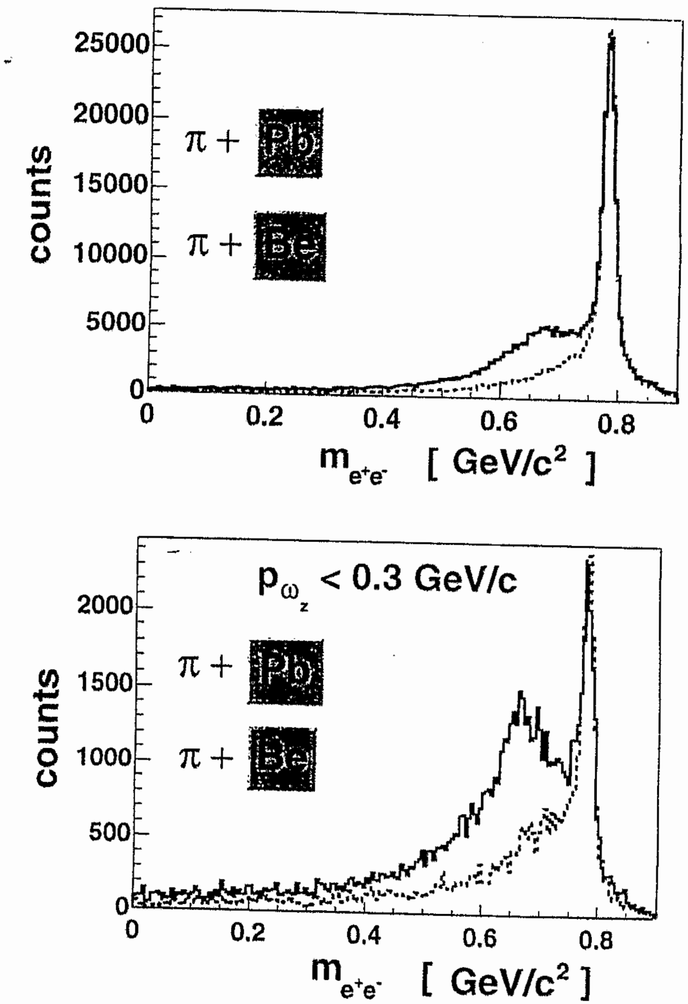

Walter Schoen, TU Muenche

Summary

- if one does not understand $\pi - A$ reactions why measure or calculate Au + Au @ 2 - 200 AGeV ?
- $\pi - p \Leftrightarrow \pi - d \Leftrightarrow \pi - Be \Leftrightarrow \pi - Pb$ might provide insight in medium effect.
- Life is not easy, any way.